



HAL
open science

Development, characterization and experimental validation of metallophthalocyanines based microsensors devoted to monocyclic aromatic hydrocarbon monitoring in air

Abhishek Kumar

► To cite this version:

Abhishek Kumar. Development, characterization and experimental validation of metallophthalocyanines based microsensors devoted to monocyclic aromatic hydrocarbon monitoring in air. Other. Université Blaise Pascal - Clermont-Ferrand II, 2015. English. NNT : 2015CLF22635 . tel-01308196

HAL Id: tel-01308196

<https://theses.hal.science/tel-01308196>

Submitted on 27 Apr 2016

HAL is a multi-disciplinary open access archive for the deposit and dissemination of scientific research documents, whether they are published or not. The documents may come from teaching and research institutions in France or abroad, or from public or private research centers.

L'archive ouverte pluridisciplinaire **HAL**, est destinée au dépôt et à la diffusion de documents scientifiques de niveau recherche, publiés ou non, émanant des établissements d'enseignement et de recherche français ou étrangers, des laboratoires publics ou privés.

N° d'ordre : D.U. 2635

EDSPIC : 729

UNIVERSITE BLAISE PASCAL-CLERMONT II

ECOLE DOCTORALE

SCIENCES POUR L'INGENIEUR DE CLERMONT-FERRAND

Thèse

Présentée Par

Abhishek KUMAR

Pour obtenir le grade de

DOCTEUR D'UNIVERSITÉ

Spécialité: Matériaux et Composants pour l'Electronique

**Development, characterization and experimental
validation of metallophthalocyanines based microsensors
devoted to monocyclic aromatic hydrocarbon monitoring
in air**

Soutenue publiquement le 7 Décembre 2015 devant le jury

Messieurs	Alain PAULY	Président du jury
	Eduard LLOBET	Rapporteur
	Mohamed CHEHIMI	Rapporteur
	Klaus SCHIERBAUM	Examineur
	Jérôme BRUNET	Co-director
Mesdames	Christelle VARENNE	Director

To my father Jay Kumar

**(यह पीएचडी मेरे पिता जय कुमार के अथक प्रयाश के द्वारा मुझे इस
शैक्षणिक मुकाम पर पहुंचाने के लिए समर्पित है)**

*It is a good morning exercise for a research scientist to discard a pet hypothesis every day
before breakfast. It keeps him young*

Acknowledgment

I have many people to acknowledge for their contribution and support throughout my PhD experience both professionally and personally. I am afraid that these lines wouldn't make justice they actually deserve, but I will try my best.

First acknowledgment must go to my supervisors Christelle Varenne and Jérôme Brunet. The results of this thesis would not have been possible without their support and guidance. Their enthusiasm and ability to find solutions to all aspects of sensors research make them a fantastic supervisors and role models for a young scientist. I am truly grateful to Christelle, I have learned a lot from you. Heartiest thanks to you for all the scientific discussions, your suggestions in my experimentation and writing and most of all managing my thesis in an excellent manner. I express my profound thanks to Jérôme. Since the last three years, you are a guide cum friend, with whom I learned the basics of scientific thinking, planning and implementing my ideas in a focused manner. Many thanks to you for the long discussions we always had starting from scientific things like sensors results or theoretical interpretations to discussing weird French sayings and French cuisine.

Amadou, you are amazing, it was a great pleasure working with you. Your positivity and patience towards research always inspired me. Thank you very much for long discussions and especially your great help in benzene sensing experiments and characterizations of my samples. I have no words to express for the helps received from you on a personal level starting from managing my French speaking loyer M. Brunel to all my administrative paper works.

I would like to thank Prof. Alain Pauly. Despite his busy schedule, we had many useful conversations on my work. Yours ideas about temperature corrections, molecular interactions and in general about phthalocyanines were very helpful.

I would like to thank Christine Robert-Goumet for allowing me to carry out SEM characterizations of my samples. Equally, I thank Malika EL-Ghozzi and Joel Cellier from the department of chemistry for doing XRD characterization of my sample.

I acknowledge the head of EDSPI Françoise Palladian for organizing different SPI and OSP modules and annual doctoral functions. These programs greatly helped me in widening my knowledge beside my actual research topic.

I would like to acknowledge other members of Institut Pascal including Françoise Bohaud, Evelyne Gil, Christine Tucart, Michel Dhôme, Pascal Dugat, Laurent Malaterre, Lionel Suty and Yamina Andre for arranging all my scientific missions, managing administrative papers and their kind professional gestures.

I would like to acknowledge EuNetAir-COST Action TD1105 for their collaborations with my lab and providing me a fellowship to attend summer schools in Barcelona and Saarbrücken.

On a personal side, there are many people, both friends and family, whom I would like to thank for their continued friendship and support over the last few years. There are too many to name everyone here but particular thanks to Vaibhav. You are a great friend. Thanks for your support and company since our college days. I never felt homesick because of your company despite living away from my country in the last 5 years. I also thank Jitendra, Hemath, Siwani, Vijetha, Valeria, Juliene, Alexandra, Juliette, Joa, Kabilan for their great company, which made my life full of pleasure in the last three years.

Special thanks to Mom and Dad for their love, support and encouragement not just during my PhD but for the last 25 years. Thanks to my sister Rubi and her husband for a great personal support. I thank a lot to my grand mom and uncle Vijay for their inspirations and encouragement during all these years.

Table of content

INTRODUCTION.....	6
Chapter 1: Air pollution: properties, metrology and sensor-system strategy.....	10
1. General Context of Air pollution.....	30
1.1. Classification of Air pollution.....	31
1.2. International environmental agencies.....	34
1.3. Definition of emission guidelines.....	36
1.4. Nature of pollutants.....	38
1.5. Trends in monitored air pollutants.....	40
2. Focus on Volatile Organic Compounds.....	41
2.1. Definitions, major components and emissions distribution.....	41
2.2. BTX as target gases.....	44
2.2.1. Physical and chemical properties of BTX.....	44
2.2.2. Sources of emission and exposure.....	45
2.2.3. Health effects of BTX exposure.....	46
2.2.4. International guidelines for BTX emissions.....	48
3. BTX monitoring: normalized protocol and limitations.....	51
3.1. Protocols of monitoring.....	51
3.2. Limitations of normative monitoring methods.....	52
3.3. Interest of sensor development.....	52
4. Gas sensors.....	54
4.1. Technical definitions and working principles.....	54
4.2. Metrological requirements.....	55
4.3. Gas sensor technologies for BTX detection.....	57
4.3.1. Optical sensors.....	58
4.3.2. Electrochemical gas sensors.....	59
4.3.3. Conductimetric gas sensors.....	59
4.3.4. Acoustic gas sensors.....	61
5. Strategy of research.....	64
5.1. Global approach.....	64
5.2. Phthalocyanines as investigated materials.....	65
5.2.1. Generalities.....	65

5.2.2.	Molecular structure and thin film arrangements.....	66
5.2.3.	Chemical properties.....	68
5.2.4.	Electronic properties and gas sensing applications	70
5.3.	Choice of transducing mode.....	73
5.4.	Phthalocyanines based QCM sensors for BTX detection: previous studies.....	74
	References	76

Chapter 2: Experimental and characterization techniques.....72

1.	Sample elaboration.....	93
1.1.	Materials.....	93
1.2.	Transducing mode	94
1.3.	Processing.....	96
2.	Physical and chemical characterizations of materials	99
2.1.	UV-Vis absorption	99
2.2.	Fourier Transform Infrared spectroscopy.....	100
2.3.	X-Ray Diffraction.....	101
2.4.	Scanning Electron Microscopy (SEM).....	103
3.	Generation of BTX vapor.....	104
3.1.	Evaporation method for toluene and xylenes vapor generation	104
3.2.	Permeation method for benzene vapor generation	107
4.	Experimental setup for sensor calibration	108
4.1.	General overview	108
4.2.	Exposure chamber	108
4.3.	Gas dilution unit.....	109
4.4.	Automation.....	110
5.	Experimental sensor response	112
5.1.	Raw sensor data.....	112
5.2.	Temperature corrections.....	113
	Reference.....	99

Chapter 3: Relevance of phthalocyanines as sensitive materials for BTX detection.....102

1.	Choice of phthalocyanines and sensing strategy	122
2.	Optical spectroscopic characterizations of materials.....	125

2.1.	UV-Vis spectra of phthalocyanines.....	125
2.2.	FT-IR spectra of phthalocyanines	128
3.	General sensor responses to BTX.....	131
3.1.	Unsubstituted phthalocyanines.....	131
3.2.	Substituted phthalocyanines	135
3.3.	Bis-phthalocyanine.....	139
4.	Effect of thin layer organizations on BTX sensing behavior	141
4.1.	Structural characterization of layers by X-Ray Diffraction.....	141
4.2.	Morphological characterization of layers by Scanning Electron Microscopy.....	145
4.3.	Discussion	148
4.4.	Effects of layer thickness on sensitivity	150
5.	Gas/material interactions at molecular scale	152
5.1.	Non-covalent forces acting between phthalocyanines and BTX.....	152
5.1.1.	Electrostatic forces based interactions.....	152
5.1.2.	Dispersion forces based interactions	154
5.1.3.	Electrostatic and dispersion forces based interactions.....	154
5.2.	Interactions on unsubstituted metallophthalocyanines	155
5.3.	Interactions on substituted metallophthalocyanines.....	156
5.4.	Case of LuPc ₂	159
	Conclusion.....	160
	References	162

Chapter 4: Sensing properties of ttb-CuPc coated QCMs toward BTX gases..... 150

1.	Investigation of sensor characteristics: general approach	170
2.	Sensing performances of ttb-CuPc coated QCM sensors.....	172
2.1.	General sensing behavior towards benzene, toluene and xylenes	172
2.2.	Response and recovery times	174
2.3.	Sensitivity and repeatability	176
2.4.	Effects of gas exposure history.....	180
2.5.	Resolution.....	183
2.6.	Selectivity.....	185
2.7.	Limit of detection	188
3.	Interpretation and modeling of sensor behavior	192
3.1.	Sorption mechanisms on metallophthalocyanine thin layers	192

3.2.	Adsorption model of BTX on ttb-CuPc thin layers.....	193
3.3.	Role of diffusion.....	198
3.3.1.	Effect of thickness: case of ttb-CuPc.....	198
3.3.2.	Influence of tert-butyl group on adsorption: intercomparison with CuPc.....	201
4.	Ageing of the ttb-CuPc sensor layer.....	203
	Conclusion.....	206
	References	208

Chapter 5: Ongoing activities and perspective.....197

1.	On-going activities focused on sensing performance improvements	216
2.	Sensitivity enhancement: development of CNT/ttb-CuPc hybrid materials.....	218
2.1.	Raw and functionalized carbon nanotubes: generalities.....	218
2.2.	Non-Covalent functionalization of carbon nanotubes by phthalocyanines macrocycles	221
2.3.	Preliminary results of ttb-CuPc/CNT hybrid based QCM toward BTX.....	222
2.3.1.	Sensor development.....	222
2.3.2.	Characterization of hybrid sensing material.....	223
2.3.3.	Sensing potentialities: case of toluene.....	226
3.	Selectivity enhancement: strategy for discriminated measurements of BTX.....	229
3.1.	Sensing strategy: general description	229
3.2.	Relevance of TPD for BTX discrimination.....	230
3.3.	Ongoing activities and expected results	230
	References	233

Conclusion.....238

INTRODUCTION

Air pollution is a serious concern at a global scale affecting every component of the biosphere directly or indirectly. The adverse consequences of air pollution on human health are also undeniable. In 2014, 7 million people died at premature age because of atmospheric pollution in the world as recently report by the World Health Organization and a newly paper in Nature by J. Lelieveld et al. If the emission levels remain with the same trend, this figure will double at the horizon 2050. Among the different air contaminants originated from anthropogenic activities, Volatile Organic Compounds namely VOCs have attracted a special attention in the last 3 decades especially in the field of indoor air quality control. Among this extended family of gaseous pollutants, Benzene, Toluene and Xylenes namely BTX exhibit highly lethal consequences on human health in short-term, intermediate-term and long-term. In a recent report from the International Agency for Research on Cancer (IARC), benzene was declared as a potential carcinogen to human which undoubtedly cause leukemia. Based on the well-established effects of these gaseous pollutants on human health, international health organizations, environmental protection agencies as well as local authorities have defined guidelines and recommendations values of exposure at different working spaces to ensure the health protection of public and workers. Some of these emission guidelines are even included into national, European and International legislation. In order to make benefit to each citizen's their right to be informed about the quality of the air they breathe and to react to any violation of emission guidelines, continuous monitoring of these pollutants is mandatory.

Despite the high level of performance of the normative methods commonly used to monitor BTX concentration in air, their required implementation in a fixed air quality stations as well as their bulky, complex and expensive operation are the main drawbacks. Therefore, such equipment's are not conceivable to ensure real time measurements of pollutants on a

wide scale or personal exposure monitoring. In contrast, miniaturized and mobile sensing devices available at competitive price able to perform real-time measurements of gaseous pollutants in common public spaces, confined indoor household environments, passenger compartments and major industrial sites should be highly attractive. Thus, the works realized in the context of this PhD aims to develop, characterize and validate an original gas microsensor system able to accurately measure the concentration of BTX compounds at levels below the emissions guidelines. This goal is also in agreement with the scientific field and skills of *Chemical Sensors System and Microsystems* team at Institute Pascal where this PhD took place.

To realize a sensing device for BTX gases, the selection of the sensing material and an appropriate transducer remains a key task to address. Ideally, sensing materials must be able to recognize the targeted pollutants even at very low concentrations without involving interaction with interfering species. Based on their physical and chemical properties as well as their commercial availability, their processability and their structural similarity with the target aromatic gases, metallophthalocyanines were selected as sensing molecules. The possibility to change the nature of central metal atoms or the type of peripheral ligands grafted on phthalocyanine macrocycle is a great advantage to tailor the material and to modulate the sensing performances according the defined specifications in this thesis using up to date characterization tools, intercomparative analysis of sensors performances and already established principles of molecular interaction to find the optimized sensing material. Taking into consideration the predicted interaction which can occur between aromatic hydrocarbons and metallophthalocyanines, Quartz Crystal Microbalance (QCM) has been used as transducer. A thorough study has been thus performed in the context of this PhD thesis to determine, characterize and validate the most suitable sensing device for BTX monitoring at room temperature.

During this PhD, different aspect of a sensor development including appropriate sensing materials, suitable working conditions and detailed gas/materials interaction mechanism for BTX gases have been investigated. Possible ways to improve further the sensor characteristics mainly magnitude of response and selectivity toward BTX gases will be also discussed. This manuscript is so organized in five chapters.

The first chapter is devoted to the motivation for this PhD with special emphasis on BTX monitoring and the relevance of metallophthalocyanines as sensing materials for the development of microsensors. A thorough description about sources, adverse health effects and guidelines of emissions is detailed. Basic theory of a gas sensor system, metrological requirements and recent bibliography about BTX sensors is then described. The main objectives of this PhD with a focus on choice of phthalocyanines as sensing materials for microsensors development are discussed.

In the second chapter, all experimental details are given about realization and characterization techniques of sensing devices as well as the development of the experimental setup for gas testing.

The third chapter deals with the sensing properties of different types of phthalocyanines associated to QCM devices. The panel includes unsubstituted, substituted and bis-phthalocyanines materials. The main objective is to identify the material exhibiting the best metrological performances for indoor applications. The organizations and morphology of sensing layers have been studied using XRD and SEM characterizations which are correlated to evolution of sensor behavior towards a gas. A molecular scale interpretation of gas/material interactions based on non-covalent forces is given.

The fourth chapter is focused on the assessment of the different metrological characteristics and gas/material interactions mechanisms of QCM device layered with the most sensitive

phthalocyanine identified and justified in the 3rd chapter. Among different sensing characteristics, kinetics, repeatability, reproducibility, resolution, selectivity and limit of detection have been quantified. Gas/material interactions are formalized at first by modelling sensor behavior using a two-step adsorption equation. Further, diffusion of BTX gases is highlighted by sensors development with different thickness of sensing layer. Ageing of sensor and suitable storage condition to prevent such effects are reported.

On-going activities are finally described in the fifth chapter, focused on enhancing sensitivity of BTX gases by using carbon nanotubes/phthalocyanine hybrid based QCM device. In perspective, selectivity among BTX gases is being conceptualized either by using a chemical filter or a preconcentrator based sequential thermal desorption.

Développement, caractérisation et validation expérimentale de microsystèmes capteurs de gaz à base de métallophthalocyanines pour le suivi des hydrocarbures aromatiques dans l'air

Abstract

This thesis deals with metallophthalocyanines and functionalized nanocarbons as sensitive materials for microsensors development dedicated to BTX monitoring at room temperature. Because of the nature of gas/materials interactions involved, QCM has been chosen as transducer. Commercially available phthalocyanines and phthalocyanine/nanocarbons hybrid nanomaterials were layered on transducer electrodes and characterized by SEM, FT-IR and XRD. Such sensing devices were then tested towards BTX gases in different concentration ranges. Different types of phthalocyanines material were investigated and it was found that peripheral groups grafted on macrocycles can affect the sensor response. We have especially established that tert-butyl groups grafted on copper phthalocyanine enhanced the sensitivity towards BTX. Various metrological characteristics were investigated for ttb-CuPc based QCM sensor. It exhibited reversible, reproducible and repeatable response, low detection limit and partial selectivity. Aiming to further improve the sensitivity, ttb-CuPc/CNT hybrid nanomaterials were synthesized. The sensitivity measured for this hybrid nanomaterial was found to be greater as compared to individual sensitivity of ttb-CuPc and CNT.

Résumé :

Cette thèse est dédiée à l'étude des métallophthalocyanines comme matériaux sensibles pour le développement de microsystèmes capteurs dédiés à la surveillance des BTX (Benzène, Toluène et Xylènes) à température ambiante. En raison de la nature des interactions des matériaux et des gaz, le système de microbalance à quartz (Quartz Crystal Microbalance : QCM) a été choisi en tant que transducteur. Les métallophthalocyanines sélectionnées ont été déposées par différents procédés et caractérisées par des techniques d'analyse telles que la microscopie électronique à balayage (MEB), la spectroscopie infrarouge à transformée de Fourier (analyse FTIR) et la diffraction des rayons X, (analyse DRX), Différents types de phthalocyanines ont été étudiés et il a été constaté que les groupes greffés sur la périphérie des macrocycles peuvent affecter la réponse du capteur. Nous avons notamment montré que les groupes tert-butyle (ttb) greffés sur la phthalocyanine de cuivre (CuPc) améliorent la sensibilité vis à vis des BTX. Diverses caractéristiques métrologiques ont été étudiées pour ttb-CuPc, comme la réversibilité, la reproductibilité, les limites de détection,... Dans le but d'améliorer la sensibilité des phthalocyanines, des nanomatériaux hybrides nanotubes de carbone/ttb-CuPc ont été synthétisés. La sensibilité mesurée pour ces nanomatériaux hybrides a été jugée supérieure par rapport à la sensibilité individuelle des ttb-CuPc et nanotubes de carbone.

Mots-clés: phthalocyanines, microbalance à quartz, BTX, capteur de gaz, contrôle de la qualité de l'air, couche mince, caractérisation physico-chimique, interaction gaz/phthalocyanine.

1. Introduction

1.1. Généralité sur les polluants organiques volatiles (COVs)

La pollution atmosphérique est un problème mondial qui touche aujourd'hui toutes les composantes de l'environnement, soit directement, soit indirectement. Avec l'accroissement rapide du trafic urbain et le changement de style de vie, un nouveau type de polluants, les composés organiques volatils (COVs), devient une source réelle de menace pour l'environnement. L'Organisation Mondiale de la Santé (OMS) définit les COVs comme des composés organiques dont le point d'ébullition est dans la plage de 50 ° C à 260 ° C. Parmi tous les composés volatils, on peut citer le benzène, le toluène, l'éthyle-benzène, les xylènes, le chloroforme, le tétrachlorure de carbone, le formaldéhyde, l'acétaldéhyde, l'acide acétique et de nombreux autres composés organiques similaires. Les sources d'émission sont dues aux incendies de forêt et aux éruptions volcaniques, mais la principale source d'émission est d'origine humaine. Cela inclut les émissions des véhicules, des industries, des usines pétrochimiques, stations d'essence, ... On peut également différencier cette pollution en deux grandes classes : la pollution intérieure et la pollution extérieure. Avec le changement de style de vie dans les zones urbaines, la pollution de l'air intérieur est en train de devenir un problème grave. A l'intérieur l'émission des COVs est principalement due aux colorants, à la peinture, aux produits pour le nettoyage de la maison, ... Les effets de ces émissions sont aggravés, en particulier dans les bâtiments modernes, par l'isolation de plus en plus importantes des bâtiment et donc une ventilation limitée. Ces polluants restent donc concentrés dans les espaces clos et nous sommes ainsi constamment exposés à ces polluants. Des études récentes, effectuées dans divers pays européens, révèlent que la concentration moyenne de COVs dans l'environnement intérieur est supérieure à la concentration moyenne de COVs dans l'environnement extérieur [1]. Ceci est mis en évidence dans la figure. 1. Ce graphe résume la concentration en benzène, toluène et xylènes présente dans l'air intérieur

comparée à la concentration de ces gaz présents dans l'air extérieur [2]. On constate en effet que dans beaucoup d'environnements, l'air intérieur peut comporter une plus grande concentration en polluants que l'air extérieur.

Dans ce travail de thèse sur les COVs, nous nous sommes principalement intéressés aux composés du type benzène, toluène et xylènes, généralement appelés en BTX. Les effets néfastes sur la santé de ces polluants ont été établis en fonction de la durée et de la concentration de l'exposition de l'homme. Une exposition à long terme au benzène peut causer hématotoxique, génotoxiques et cancérogènes [3], conduisant à terme à des leucémies [4] et d'autres cancers, l'exposition au toluène peut être neurotoxique et peut provoquer un avortement spontané chez les femmes [5]. Quelques effets secondaires communs à de courtes expositions aux BTX sont les étourdissements, l'euphorie, vertiges, maux de tête, des nausées, faiblesse, somnolence, irritation des voies respiratoires, de la nervosité, œdème pulmonaire, pneumonie, irritation gastro-intestinale, des convulsions et la paralysie [6-8]. Au vu de ces effets néfastes des BTX sur la santé, les agences de protection de la santé (l'OMS : l'organisation mondiale de la santé, l'EPA : Environmental Protection Agency, l'OSHA : Occupational Safety & Health Administration), et les réseaux de mesures de la pollution atmosphérique française AtmoFrance ont réalisé un guide des valeurs d'exposition dans des environnements intérieurs et extérieurs. Ces données sont présentées dans le tableau-1.

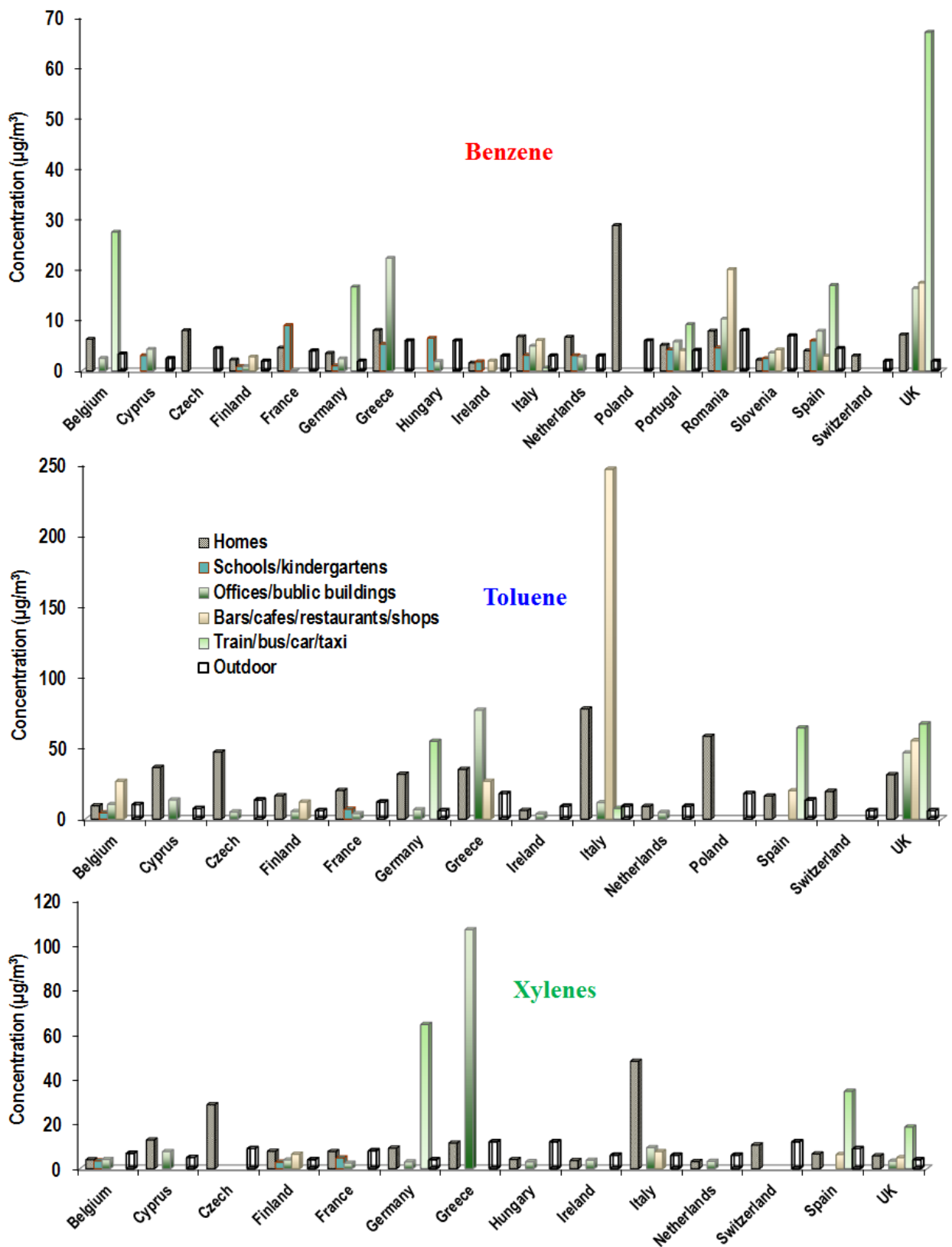


Fig. 1: Étude de l'émission des BTX en Europe dans des environnements différents [9]

Tableau 1: Les directives internationales d'exposition aux BTX dans un lieu professionnel

Organisme de contrôle	Description	Benzène (mg/m ³) (3.18 mg/m ³ = 1 ppm)	Toluène (mg/m ³) (3.76 mg/m ³ = 1 ppm)	Xylène (mg/m ³) (4.33 mg/m ³ = 1 ppm)
ACGIH (USA)	TLV	1.6	750	435
	STEL	8	Non disponible	655
OSHA (USA)	PEL	3.25	750	435
	STEL	16.25	Non disponible	655
NIOSH (USA)	REL	3.25	375	435
	STEL	3.25	560	655
SAOHS (S. Africa)	OEL	1.6	175	435
European Union	OEL	3.25	Non disponible	Non disponible

Threshold limit values (TLV): niveau d'exposition qu'un travailleur typique peut subir sans un risque déraisonnable de maladie ou de blessure.

Short-term exposure limits (STEL): concentration à laquelle les travailleurs peuvent être exposés continuellement pendant une courte période de temps sans souffrir d'irritations, lésions tissulaires chroniques ou irréversibles et réduit l'efficacité du travail.

Permissible exposure limits (PEL): concentration maximale d'une substance chimique à laquelle le travailleur peut être exposé en vertu de la réglementation de l'OSHA (Occupational Health and Safety Administration).

Recommended exposure limit (REL): limite d'exposition professionnelle qui a été recommandé par le National Institute for Occupational Safety and Health (NIOSH).

Occupational exposures limit (OEL): limite de la concentration maximale acceptable d'une substance dangereuse dans l'air en milieu de travail.

Tableau-2: Les directives internationales d'exposition aux BTX dans un lieu non-professionnel

Organisme de contrôle	Description	Benzène (mg/m ³) (3.18 mg/m ³ = 1 ppm)	Toluène (mg/m ³) (3.76 mg/m ³ = 1 ppm)	Xylène (mg/m ³) (4.33 mg/m ³ = 1 ppm)
WHO	1 semaine (toluène)	0	0.26	Non disponible
	24 h (xylène)	0	Non disponible	4.8
AAAQO, Canada	1 h (benzène)	0.003	Non disponible	Non disponible
	24 h (toluène, xylène)	Non disponible	0.4	7
EU directives	Moyenne annuelle	0.005	Non disponible	Non disponible
EPAQS, UK	Moyenne annuelle	0.01625	Non disponible	Non disponible

1.2. Utilité du développement d'un capteur de BTX

Compte tenu des problèmes de santé et environnementaux causés par les émissions de polluants COVs, leur suivi dans l'air ambiant dans tous les type d'environnement est devenu impératif. Un capteur qui pourra être utilisé dans toutes les situations environnementales est la solution idéale. Avec la croissance de la microélectronique et le boom des nanotechnologies, la possibilité de réaliser un microsystème capteur miniaturisé est devenue une réalité. En outre, leur structure compact, à faible coût, avec une faible consommation d'énergie et un fonctionnement autonome font de ces capteurs des dispositifs très pertinents pour la surveillance en continu, à grande échelle et en temps réel de la concentration en BTX.

Un capteur de gaz peut être défini comme un dispositif capable de délivrer un signal de sortie électrique ou optique en réponse à la valeur de concentration en gaz ou d'une classe de gaz (mesurande) présents dans son voisinage. Au-delà de l'identification de gaz, la quantification de l'espèce gazeuse cible dans un mélange complexe d'air doit être atteinte. Le mode de fonctionnement classique des capteurs est expliqué sur la Fig. 2. Ce capteur de gaz consiste en une couche sensible choisie pour sa grande sensibilité au gaz cible associée à un transducteur qui convertit l'information chimique en signal électrique ou optique. Le principe de fonctionnement d'un capteur de gaz est basé sur la variation d'une propriété physique ou chimique de la couche sensible suite à son interaction avec les molécules gazeuses, l'amplitude de variation étant en corrélation avec la concentration de gaz. Ces interactions peuvent se limiter à la surface ou se produire également à l'intérieur de la couche sensible, impliquant une interaction physique ou chimique. Le choix du matériau de détection, ainsi que le mode de transduction est critique. Il dépend fortement de la nature du gaz cible, de l'interaction attendue et de la caractéristique du capteur qui sera modulée, de la présence d'interférents dans l'environnement de mesures et le niveau de performances visé. Conformément à la classification IUPAC (International Union of Pure and Applied

Chemistry), les capteurs chimiques peuvent être distingués sur la base de la nature du transducteur impliqués dans le microsystème capteur [10].

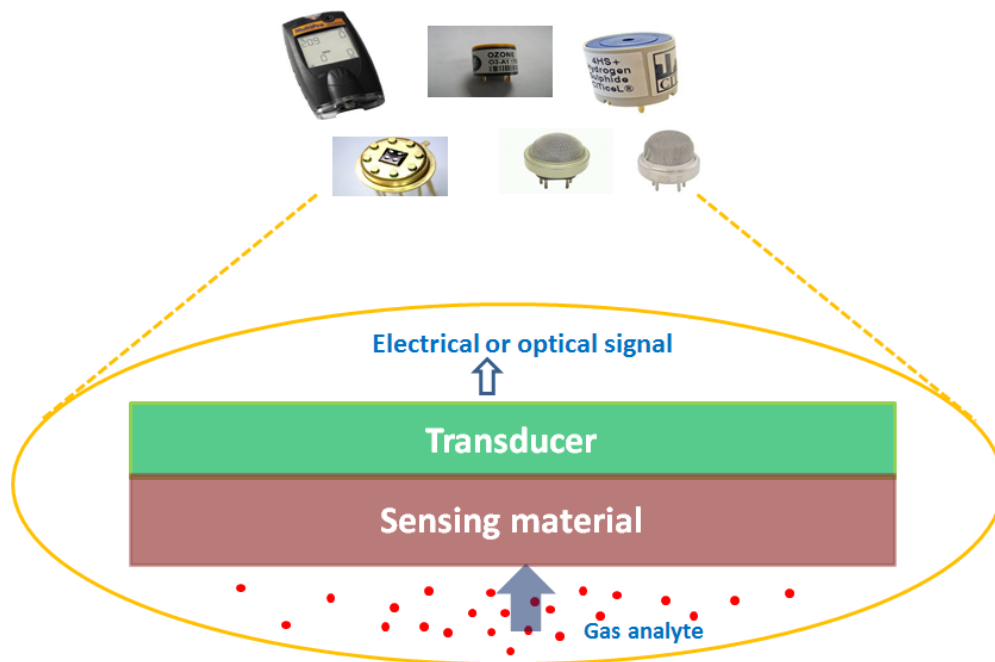


Fig. 2: Représentation de capteurs de gaz

Compte tenu de la nature des BTX, nous avons choisi des matériaux ayant des propriétés semblables pour le développement des couches sensible. Les phtalocyanines sont un bon choix compte tenu de leur structure macrocyclique et des liaisons conjuguées. Leur caractère aromatique couplé avec une délocalisation des électrons π peut conduire à de multiples interactions non covalentes [11] avec les gaz cibles tels que les BTX. La structure moléculaire de base est représentée sur la Fig. 3. La molécule est constituée par un macrocycle plan comportant quatre groupes de l'isoindole. Une autre caractéristique structurale commune à toute les phtalocyanines est la cavité au centre de la molécule, qui permet d'inclure des atomes métalliques. Les rayons ioniques de ces éléments doivent être compris entre 50 pm et 150 pm [12]. De plus, en raison de sites périphériques chimiquement actifs, des atomes d'hydrogène peuvent être substitués par un autre type d'atome ou de

groupements fonctionnels. Pour mesurer les interactions des BTX avec ces matériaux, le système de microbalance à quartz (QCM) semble être le transducteur le plus approprié. Dans ce cas une variation de masse due à l'adsorption/désorption du gaz à la surface du capteur induit une variation de fréquence de résonance d'oscillation du quartz. La masse de l'espèce adsorbées ou désorbées sur l'électrode de détection et la variation de fréquence de l'oscillation en résultant sont reliées par une équation mathématique connue comme étant l'équation de Sauerbrey [13] :

$$\Delta f = - \frac{Cf_0^2 \Delta m}{A} \quad (1)$$

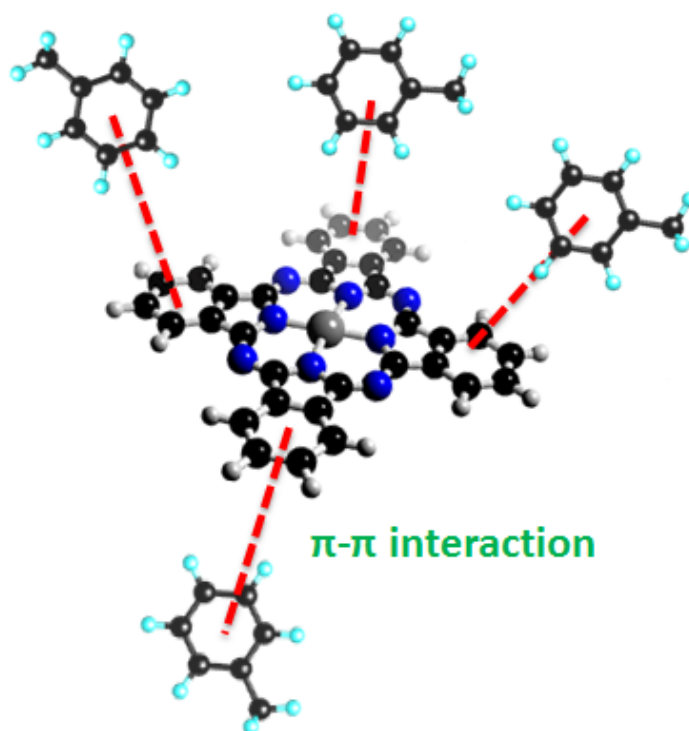


Fig. 3: Représentation des interactions π - π entre une molécule de métallo-phthalocyanine et le toluène.

1.3. Objectifs de la thèse

Ce travail de thèse a été réalisé dans l'équipe Microsystème de l'Institut Pascal de l'Université Blaise Pascal de Clermont-Ferrand, France. Impliqué depuis longtemps dans le

développement de capteurs de gaz pour la mesure de la pollution atmosphérique, ce groupe a entre autre développé des microsystèmes capteur basés sur la détection sélective du dioxyde d'azote (NO_2) et de l'ozone (O_3) dans l'air [14, 15]. Avec les mêmes objectifs de contrôle de la qualité de l'air, ce travail de thèse a été consacré à la mise au point de capteurs de gaz pour la mesure des BTX présents dans les environnements extérieurs et intérieurs. Les résultats attendus sur ce travail de thèse sont en accord avec les objectifs du projet ANR CAPBTX dirigé par le professeur Pauly et le projet exploratoire ASTHME accordée par le CNRS à Jérôme Brunet. Ce travail de thèse comprend l'identification de la couche sensible la plus appropriée, l'élaboration de structures tests, le développement du banc de test, la caractérisation physique et chimique de la couche sensible, des tests capteurs pour la détermination de paramètres caractéristiques du capteurs vis-à-vis des BTX, l'interprétation des interactions gaz/matériau et enfin les pistes d'amélioration possible. Les phtalocyanines ont été déposés en couches minces nanométriques sur les surfaces actives de type quartz avec électrodes en or de chaque côté par des méthodes d'évaporation thermique ou par des techniques de drop casting. Les couches déposées ont été caractérisées par microscopie électronique à balayage (SEM), diffraction à rayons X (XRD), spectroscopie infrarouge à transformée de Fourier (FTIR) et spectroscopie Raman pour corrélérer leurs propriétés structurales et morphologiques aux réponses des capteurs. Ces capteurs ont ensuite été intégrés sur un banc de tests développé au laboratoire et permettant de tester à différentes concentrations ces capteurs QCM. Les tests effectués ont permis l'étude des paramètres métrologiques du capteur en fonction des propriétés des diverses phtalocyanines étudiées. Pour améliorer encore la sensibilité de ces dispositifs, des matériaux hybrides types phtalocyanine/nanotube de carbone (CNT) ont été étudiés comme couches de détection associées à transducteur de type QCM. L'idée étant de profiter de la surface spécifique élevée

des CNT, de leur facilité la fonctionnalisation avec les phtalocyanines et la possibilité de bénéficier d'un rapport surface/volume le plus élevé possible.

2. Caractérisation et optimisation de la couche sensible – résultats expérimentaux

Les métallophthalocyanines et les solvants organiques utilisés dans le développement des capteurs ont été achetés auprès du fournisseur Sigma-Aldrich. Les résonateurs à quartz utilisés pendant cette thèse sont des quartz de la gamme Maxtek présentant des électrodes Au/Cr et sont commercialisés par la société Inficon. Les quartz ont été utilisés tels que reçus, sans autre traitement physique ou chimique de la surface. Des couches minces de matériau sensible ont été déposées sur les quartz par évaporation thermique sous vide secondaire. L'épaisseur typique des couches sensibles est de l'ordre de 400 nm et la vitesse de dépôt a été fixée à 0,2 nm/s afin d'assurer l'homogénéité de la couche. Aucun autre traitement chimique ou physique de l'échantillon n'a été effectué après le dépôt. Les spectres infrarouges des matériaux sous forme de poudre et de film mince déposé sur un substrat de silicium, ont été réalisés par un spectromètre FTIR dans la gamme 400-4000 cm^{-1} avec une résolution de 4 cm^{-1} en mode transmission.

Le dispositif expérimental utilisé pour les mesures de gaz est détaillé dans la figure 4. Il se compose d'un circuit fluide relié à une chambre où se trouve le capteur avec un ordinateur qui commande de façon synchrone les paramètres expérimentaux tels que le taux de dilution des gaz, la commutation de la vanne et l'acquisition des réponses des capteurs. Le gaz vecteur est réalisé à partir de l'air extérieur qui passe à travers des colonnes de silicat gel et de charbon actif pour obtenir un air sec et propre. La ligne fluide est divisée en deux parties: l'une assure le maintien d'un flux d'air propre à un taux fixe et la seconde assure le transport du polluants (toluène ou xylènes) à la concentration demandée.

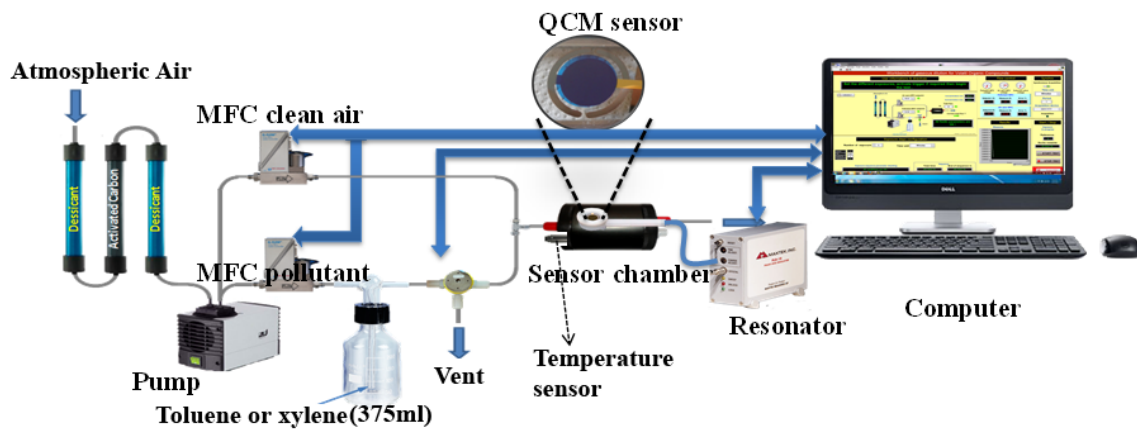


Fig. 4 : synoptique du banc d'exposition aux gaz toluène ou xylènes.

3. Résultats et discussions

3.1. Choix du matériau sensible parmi la grande famille des phtalocyanines

La figure 5 représente la réponse capteur à température ambiante de 3 capteurs réalisés par évaporation thermique à partir de trois metallophtalocyanines différentes soumises à des paliers d'expositions de 500 ppm de toluène. Ces matériaux sont une phtalocyanine de cuivre (CuPc), une phtalocyanine de cuivre tétra-ter-butyl (ttb-CuPc) et une d'hexadéca- fluoro phtalocyanine de cuivre ($F_{16}CuPc$). Le temps d'exposition a été fixé à 2 heures. Comme on le voit, l'exposition au gaz conduit à la diminution de la fréquence de la réponse capteur, ce qui correspond à une augmentation de la masse du matériau sensible consécutivement à adsorption de toluène. Les processus d'interaction entre la couche sensible et le gaz cible sont réversibles comme le confirme le retour rapide à la même ligne de base qui précède l'exposition. Pour chaque cycle, les variations de fréquence correspondant à 500 ppm de toluène sont de l'ordre de 15 Hz, 60 Hz et 5 Hz pour les phtalocyanines de CuPc, ttb-CuPc et $F_{16}CuPc$.

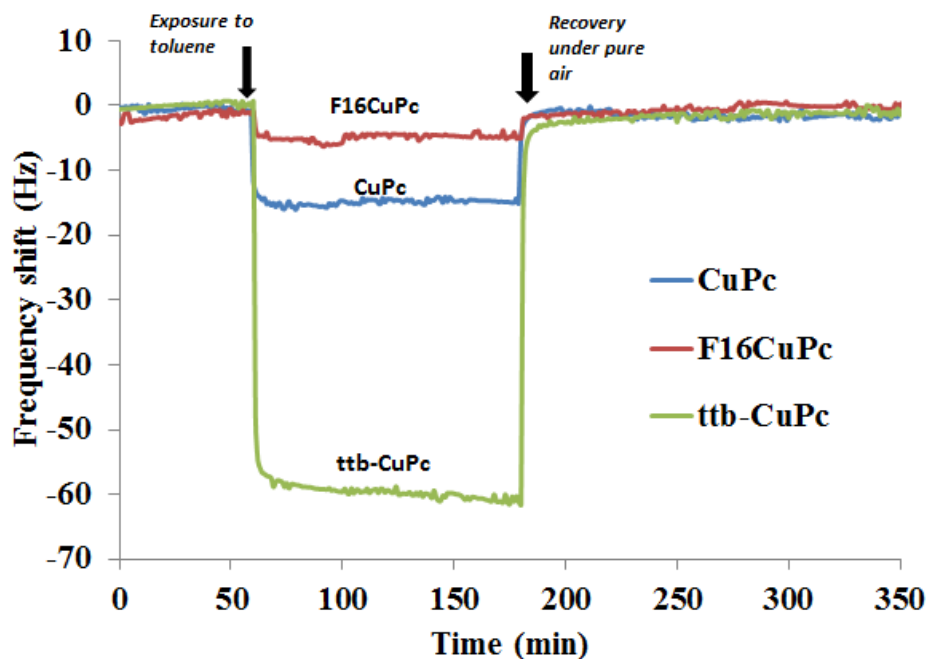


Fig. 5: Comparaison des réponses capteur des phthalocyanines CuPc, ttb-CuPc et F₁₆CuPc à une soumission à 500 ppm de toluène à température ambiante.

La sensibilité la plus importante a été obtenue pour le capteur à base de ttb-CuPc. Grâce à ces résultats expérimentaux, il apparaît clairement que la nature des substituants peut moduler la sensibilité des matériaux vis-à-vis du toluène. Plus particulièrement, les résultats mettent en évidence que le greffage du groupe tert-butyle augmentent les interactions toluène/phthalocyanine tandis que les ligands fluorure les diminue. Par conséquent, afin de bénéficier d'une sensibilité élevée conduisant à une meilleure résolution et un seuil de détection plus faible, la suite de l'étude a été axée sur l'utilisation de la ttb-CuPc comme couche sensible.

3.2. Performances de détection de capteur QCM à base de ttb-CuPc

La figure 6a représente les réponse capteurs des ttb-CuPc exposées à différentes concentrations de benzène, toluène et xylènes à la température ambiante. Cinq cycles d'exposition sous gaz et air propre ont été réalisés à des concentrations connues pour le benzène et le toluène, et 3 cycles ont été mis en œuvre pour les xylènes. La variation de fréquences des QCM en fonction des concentrations de BTX a permis d'établir des courbes

d'étalonnage des capteurs pour une gamme de concentration de 30-200 ppm (Fig. 6b). En regardant les figures 6b et 6a, nous pouvons mettre en évidence la reproductibilité, la répétabilité, la linéarité, la résolution, le retour après chaque exposition à la ligne de base initiale et l'absence de bruit sur la réponse capteur. Les courbes d'étalonnage pour chacun des trois gaz présentent une variation linéaire de la réponse du capteur en fonction de la concentration, ce qui est également une exigence d'un capteur de gaz idéal. Ces courbes montrent également que les réponses des capteurs sont bien distinctes pour une même concentration de benzène, toluène et xylènes.

La limite de détection (LOD en anglais)) d'un système de détection chimique est généralement définie comme étant trois fois l'amplitude du bruit de la réponse capteur sur la sensibilité du signal capteur, ce rapport quantifie également la plus faible concentration de gaz qui peut être détectée [16, 17].

$$LOD = \frac{3Var(f_n)}{S} \quad (\text{équation 1})$$

La sensibilité (S) des capteurs vis-à-vis des gaz BTX est déterminée comme étant la pente de la courbe linéaire représentant la réponse du capteur, le bruit de la réponse des capteurs QCM pour une couche sensible de 400 nm ttb-CuPc a été estimé à 0,06 Hz. L'équation permet d'évaluer la limite de détection à 2,15 ppm, 1,8 ppm et 0,75 ppm pour le benzène, le toluène et les xylènes respectivement. Ces valeurs de LOD des capteurs à base ttb-CuPc sont bien en deçà des seuils de détection établis par les différents organismes de protection de la santé et de l'environnement en particulier pour le toluène et le xylène.

La sélectivité d'un capteur de gaz est également une exigence très importante compte tenu de l'utilisation de ces futurs capteurs dans une atmosphère très complexe fait d'un mélange de différents gaz. La sélectivité de nos capteurs à base de ttb-CuPc a été étudiée par exposition à des polluants atmosphériques classiques comme : NO₂, CO, H₂S et O₃. Les

résultats expérimentaux ne montrent aucune réponse significative à NO₂ dans la plage de 0,1 à 10 ppm comme illustré sur la Fig. 6c. De même, aucune variation de fréquence n'a été mesurée pendant l'exposition au CO dans la gamme de 1-100 ppm, ou lors de l'exposition à H₂S dans la gamme 1-5 ppm. Ainsi ces capteurs apparaissent comme étant insensibles aux gaz potentiellement présents dans notre atmosphère de travail. Par contre leur réponse vis-à-vis de l'O₃ est clairement irréversible comme illustrée sur la figure Fig. 6c. Ceci peut être expliqué par la chimisorption de l'O₃ de manière irréversible sur les doubles liaisons carbone-carbone au niveau des noyaux benzéniques périphériques des molécules de phtalocyanine.

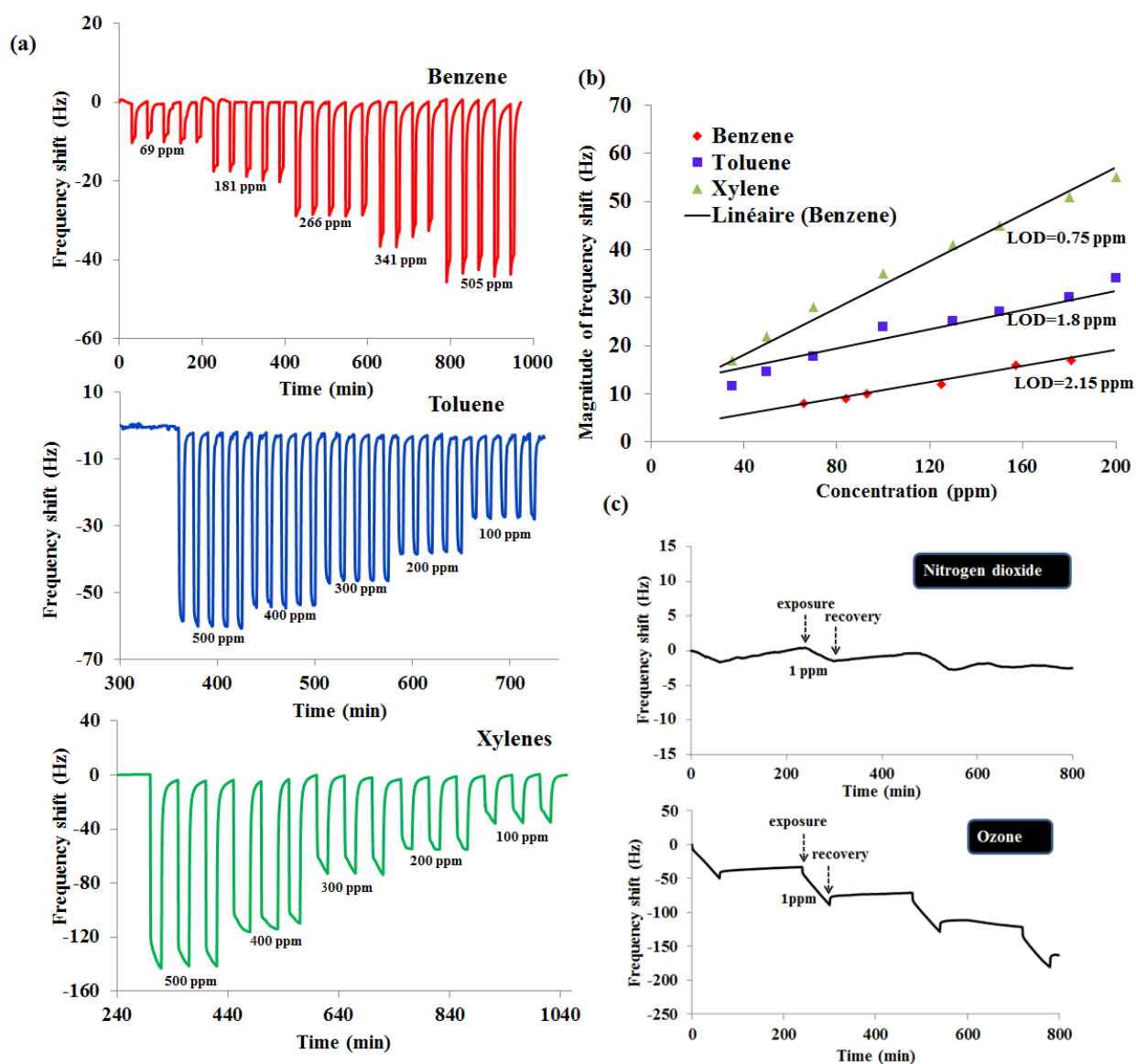


Fig. 6: (a) réponses capteur des ttb-CuPc pour différentes concentrations de BTX, (b) courbe de calibration du capteur en fonction du gaz, (c) influence des interférents tels que l'O3, le NO2 sur la réponse capteur.

4. Travaux en cours_Perspectives

Pour respecter les directives des mesures des BTX, les capteurs que nous développons doivent être capables de détecter des concentrations dans une gamme inférieure au ppm. Pour augmenter le seuil de détection et la résolution de la détection de nos capteurs vis-à-vis des BTX, l'utilisation de couche hybride réalisée à partir de nanotubes de carbone (CNT) et de ttb-CuPc apparaît comme une solution pertinente. En effet la grande surface spécifique des nanotubes de carbone avec la possibilité de les fonctionnaliser avec divers groupes actifs font des nanotubes de carbone une matrice pertinente. De plus la structure des nanotubes de carbone et des phthalocyanines offrent la possibilité de développer des matériaux hybrides sur la base de l'interaction non covalente entre eux à travers des interactions π - π . La structure conjuguée des nanotubes de carbone ayant un groupement benzène étendu peut fournir un grand nombre de sites d'interaction pour l'adsorption des BTX.

Les performances de ce capteur hybride vis-à-vis du toluène sont été représentées sur la Fig. 7. La comparaison de la sensibilité de ttb-CuPc, du matériau hybride ttb-CuPc / CNT et des CNT seul a été étudiée dans une gamme de concentrations de toluène allant de 26 à 1000 ppm. Cette étude révèle clairement que le matériau hybride ttb-CuPc / CNT a une sensibilité plus élevée à toutes les concentrations de toluène étudiées que les ttb-CuPc et CNT testés seuls (Figure 7). On peut par exemple remarquer que la sensibilité de la couche sensible de matériau hybride ttb-CuPc / CNT est trois fois plus élevée à 430 ppm de toluène que la couche sensible de ttb-CuPc seul et quatre fois plus élevée de couche sensible de CNT seul. Si l'on classe par ordre croissant de sensibilité les différentes couche vis-à-vis du toluène on aura CNT, ttb-CuPc et le plus sensible ttb-CuPc / CNT et ceci pour toutes les concentrations étudiées.

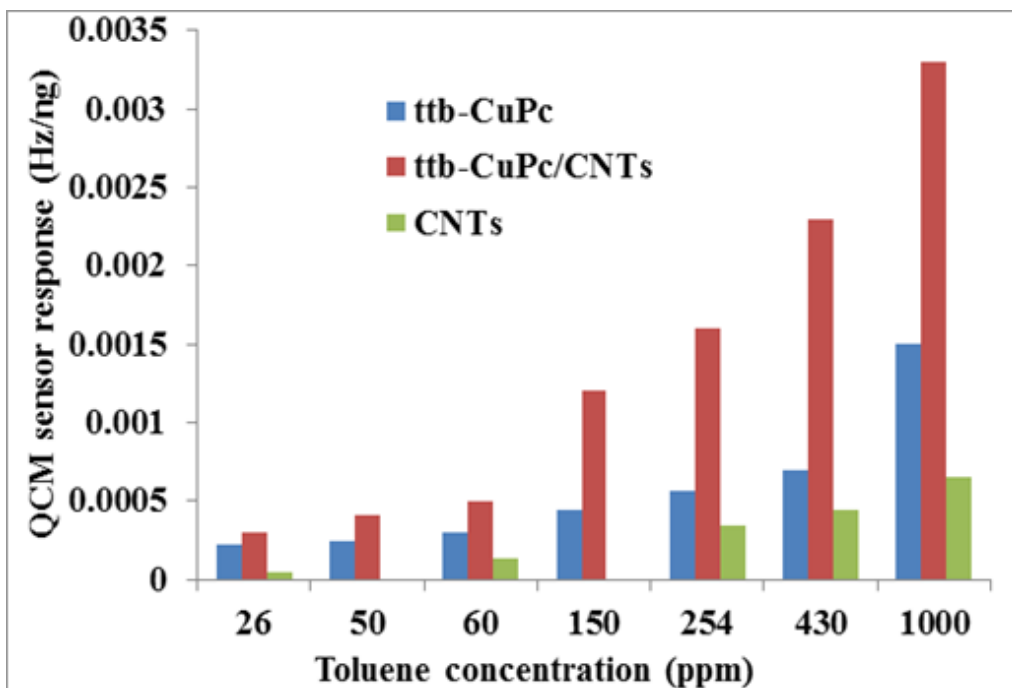


Fig. 7: Comparaisons des réponses capteurs des couches sensibles de ttb-CuPc, ttb-CuPc / CNT et CNT vis-à-vis du toluène dans une gamme de concentration de 26 à 1000 ppm et à température ambiante.

5. Conclusion

Les tests réalisés dans cette thèse sont basés sur différents types de phtalocyanines pour leur application en tant que matériau sensible pour la détection des BTX sur le principe de la microbalance à quartz (QCM). Dans la grande famille que sont les phtalocyanine nous nous sommes intéressés aux metallophthalocyanines. La phtalocyanine de cuivre tétra-ter-butyl utilisée à température ambiante est celle qui présentait les meilleures caractéristiques capteurs. La réponse capteur de cette couche a montré une réponse réversible avec la ligne de base stable. Parmi les diverses caractéristiques métrologiques attendues par un capteur de gaz, nous nous sommes également intéressés à la réversibilité, la répétabilité, la résolution, la limite de détection et la sélectivité. Les tests à différentes concentrations de BTX ont permis de mettre en évidence la répétabilité et la reproductibilité des réponses capteurs pour chacun des trois gaz et une réponse linéaire en fonction de la concentration. La résolution du capteur a été estimée à 10 ppm pour le xylènes et le toluène. La limite de détection pour le benzène, le

toluène et les xylènes a été évaluée à 2,15 ppm, 1,8 ppm et 0,75 ppm respectivement. La sélectivité du capteur a été étudiée en réalisant des études de sensibilité croisées avec les polluants atmosphériques communs. Le capteur ne présente aucune réponse significative au NO₂, CO et H₂S, alors que l'exposition à l'ozone détériore la couche sensible, changeant de façon irrémédiable les caractéristiques métrologiques de celle-ci. Mais ceci n'est pas un réel problème car dans ces études antérieures l'équipe Microsystème capteur a développé un filtre chimique à base d'indigo qui permet de l'éliminer.

Références

1. Maugeri, F.S., *MACBETH –Monitoring of Atmospheric Concentrations of Benzene in European Towns and Homes*. 1999.
2. *Presentation on the INTERA BTEX case study*. INTERA. <http://www.intera-home.eu/NewsEvents/Workshop/Presentations.aspx>.
3. *U.S. Environmental Protection Agency. Integrated Risk Information System (IRIS) on Benzene*. National Center for Environmental Assessment, Office of Research and Development, Washington, DC, 2009.
4. *IARC monographs on the evaluation of carcinogenic risks to humans. Overall evaluations of carcinogenicity: an updating of IARC Monographs*. Lyon, International Agency for Research on Cancer, 1987. Volumes 1 to 42. Suppl. 7: p. 37.
5. Juntunen, J., et al., *Nervous system effects of long-term occupational exposure to toluene*. *Acta Neurol Scand*, 1985. **72**(5): p. 512-7.
6. Kandyala, R., S.P.C. Raghavendra, and S.T. Rajasekharan, *Xylene: An overview of its health hazards and preventive measures*. *Journal of Oral and Maxillofacial Pathology : JOMFP*, 2010. **14**(1): p. 1-5.
7. *Public health statement for benzene*. Agency for Toxic Substances and Disease Registry (ATSDR), 2007. **CAS#: 71-43-2**.
8. *Public Health statement: Toluene*. Agency for Toxic Substances and Disease Registry (ATSDR), 2000(CAS#: 108-88-3).
9. Sarigiannis, D., et al., *INTERA BTEX case study*. 2011.
10. Hulanicki, A., S. Glab, and F. Ingman, *Chemical sensors: definitions and classification*, in *Pure and Applied Chemistry*. 1991. p. 1247.
11. Hunter, C.A., et al., *Aromatic interactions*. *Journal of the Chemical Society, Perkin Transactions 2*, 2001(5): p. 651-669.

12. Dini, D. and M. Hanack, *107 - Physical Properties of -based Materials*, in *The Porphyrin Handbook*, K.M.K.M.S. Guillard, Editor. 2003, Academic Press: Amsterdam. p. 1-36.
13. Sauerbrey, G., *Verwendung von Schwingquarzen zur Wägung dünner Schichten und zur Mikrowägung*. Zeitschrift für Physik, 1959. **155**(2): p. 206-222.
14. Varenne, C., et al., *Comparison of InP Schottky diodes based on Au or Pd sensing electrodes for NO₂ and O₃ sensing*. Solid-State Electronics, 2012. **72**(0): p. 29-37.
15. Brunet, J., et al., *Comparisons between NO₂ and ozone sensing properties of phthalocyanines and n-InP thin films in controlled and noncontrolled atmospheres*. Sensors Journal, IEEE, 2004. **4**(6): p. 735-742.
16. Gautschi, K., et al., *A new look at the limits of detection (LD), quantification (LQ) and power of definition (PD)*. Eur J Clin Chem Clin Biochem, 1993. **31**(7): p. 433-40.
17. Truax, S.B., et al., *Mass-Sensitive Detection of Gas-Phase Volatile Organics Using Disk Microresonators*. Analytical Chemistry, 2011. **83**(9): p. 3305-3311.

Chapter 1: State of art

Air pollution: properties, metrology and sensor-system strategy

1. General Context of Air pollution

The continuous supply of air is indispensable for survival of any life form including human. The quality of air we breathe determines our physical and mental health, and on a broad scale defines the health of population and society. The air we have the right to inhale must be clean and free from any contaminant which can cause short-term or long-term negative impacts on our body. For classical conditions of living, requirement for clean air by human beings is relatively constant at 10–20 m³ per day. The essential nature of this most basic life supporting component is so high that World Health Organization (WHO) in its recent directives has declared the availability of clean air with acceptable quality as a fundamental human right [1]. Rapid increase in industrial, technological and agricultural advancements coupled with massive population growth have led to the deterioration of environment quality all over the world. The expanding urbanization, more traffic on roads, the growing energy consumptions, the waste production and the lack of strict implementation of environmental norms are increasing the release of pollutants into the environment. The natural sink for these pollutants are limited and if exceeded, it is reflected in the form of global warming, unhealthy ambient air in our surroundings and other ecological imbalances. In the 4th assessment report from IPCC (Inter-governmental Panel on Climate Change) published in 2007, it is stated that: "Warming of the climate system is today an indisputable fact and it is very likely that most of the warming has an origin in the anthropogenic interference with the environment" [2]. The extent of contamination has increased so abruptly in the last three decades because of the lack of stringent regulations in most parts of world that the normal human life has been severely affected. The situations are more serious in developing countries where emission norms are often exceeded. More especially, the top ten cities which have the worst air quality are from developing world mainly from Asia. New estimates released by WHO report that in 2012, approximately 7 million people died worldwide because of air

pollution exposure [3, 4]. This corresponds to one in eight global deaths. Such data have confirmed that air pollution is the single largest environmental health risk which the present world is facing today. More than being an environmental trouble, it has become a real public health problem recognized as responsible for the development of chronic diseases and the reduction of human lifetime.

1.1. Classification of Air pollution

Adverse health effects of air pollution are ubiquitous. Whatever the type of environment, humans are continuously exposed to different classes of pollutants. According to the nature of living and working atmospheres, the health risks can be strongly different and consequently, the safety measures to ensure health prevention are specific as well as the air quality guidelines. Thus, a classification of air pollution was necessary to discriminate the conditions, the nature and the context of pollutant exposure in order to set the permissible exposure limit (PEL). Such classification is reported in Fig. 1.

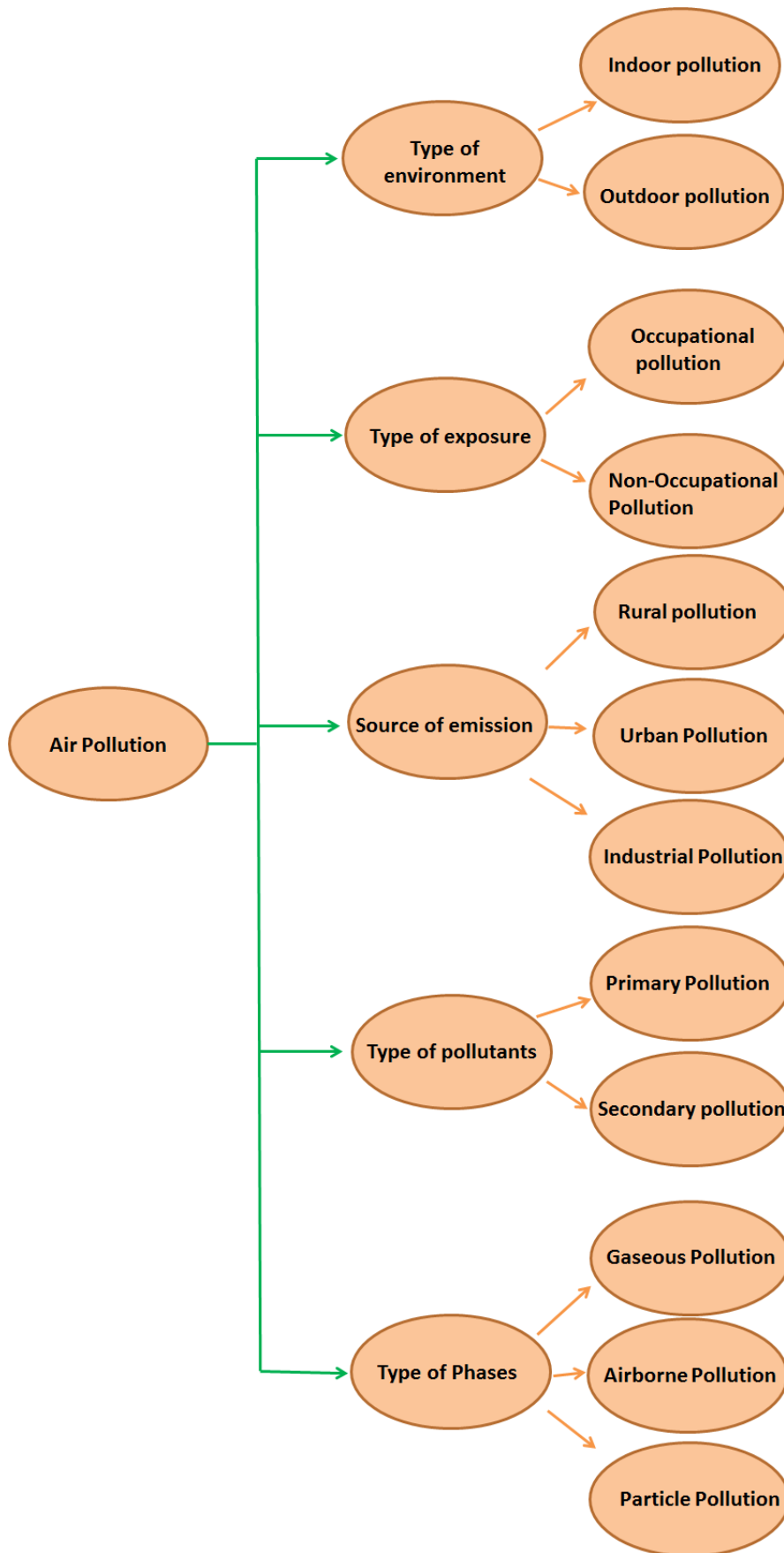


Fig. 1: Classification of air pollutions

A first discrimination occurs depending on the type of exposure: in the context of work or during commuting and living periods. That's why international air quality guidelines are commonly distinguished as occupational and non-occupational levels. Occupational air pollution is defined as the presence of hazardous airborne species within a workplace that may get in contact with people while performing their job. Such workplace pollutants may affect worker's health especially if exposure continues over longer periods of time even at low levels [5]. Non-occupational air pollution is the presence of airborne contaminants injurious to health in general public space except workplace. It can affect any individual living in polluted area. Another partition can be made in relation with confined or open spaces, each environment not exhibiting the same category and concentration levels of pollutant. Thus, indoor pollution is commonly distinguished from outdoor pollution. Indoor atmosphere is defined as air within a building occupied for at least one hour by people of varying states of health. This includes the offices, classrooms, transport facilities, shopping centers, hospitals and homes. Indoor air pollution can be defined as the presence of contaminants in indoor atmosphere because of the activity taking place in the indoor environment, which can cause adverse effects on human health. It is a great cause of worry in urban area nowadays where majority of population spend 90% time indoor. Outdoor air can be defined as air in our surrounding which is outside a confined environment. Outdoor air pollution is the presence of hazardous solids, liquids and gases in outdoor spaces in amounts that are detrimental to human health and/or the environment. Outdoor air can be polluted with emissions from vehicles, electric power plants, incinerators, industrial activities, domestic heating systems and other sources. A slight part can come from natural sources such as forest fires or volcanic activities. Please note that outdoor pollutants can diffuse in confined but not impervious spaces and can alter indoor air quality too.

The harmful effects of air pollution on human and in general entire ecosystem are now well-established. To breathe a clean air and to be informed on the air quality being universal rights for humans, many countries of the world have appointed organizations or national agencies to monitor pollutions, to inform citizens and authorities on air quality, to assess the consequences of pollutants on health and environment, to set guidelines of pollutant exposures and in cooperation, to protect global environment.

1.2.International environmental agencies

To address the public health issues due to air pollution, initiatives have been started through different forum at a local and global level. The first well-known organization which correlates health troubles and pollution exposures is the World Health Organization (WHO). Renowned as the directing and coordinating authority on international health within the United Nations' system, WHO and especially its department of public health and environment, assesses and manages the health risks due to pollution and establishes norms and recommendations to ensure safe working and living conditions. There are six offices of WHO operating in various parts of the world to ensure their missions. These are regional offices of Africa, America, South-east Asia, Europe, Eastern Mediterranean and Western Pacific.

The European Union has created an independent organization under its ambit to collect and disseminate reliable and independent data on environment, the European Environment Agency (EEA). It includes 33 member countries. The EEA provides environmental information to various public and private institutions involved in developing, adopting, implementing and evaluating policies to minimize air pollution problems. Beside this, it provides information to general public about the air quality and related subjects. In France, air quality control and risk management are ensured by the AtMO Federation, a

national network of associations devoted to air pollution monitoring and certified by the French Ministry of Ecology, Sustainable Development and Energy. These associations are distributed into the different administrative regions. Other agencies accredited and focused on environmental problematic assist the associations of the AtMO federation. We can mention ADEME (French agency for the environment and energy management), the LCSQA (French central laboratory for air quality control), the CITEPA (Technical Inter-professional Center of study on Atmospheric Pollution) or the APPA (Association for the Prevention of Atmospheric Pollution).

In the United States of America (USA), the main government organization devoted to air quality monitoring is the Environmental Protection Agency (US EPA). The main objective of this organization is to protect human and ecosystems through a thorough monitoring, analysis and implementation of policies aimed at improving the overall air quality. This agency works in collaboration with other organizations like the Occupational Safety of Health Administration (OSHA), the National Institute for Occupational Safety and Health (NIOSH), the Agency for Toxic Substances and Disease Registry (ATSDR), the American Conference of Governmental Industrial Hygienists (ACGIH). Among its missions, the evaluation of risk in different working environments, the assessment of hazardous effects of different chemicals and the establishment of all the possible routes of exposures to these pollutants are of primary importance. Beside these agencies, a lot of other national air pollution control and monitoring organizations have been created in different countries. We can thus mention Environment Canada, South African Air Quality Information System (SAAQIS), Central Pollution Control Board (CPCB) India or China Air Daily (CAD) China.

Whatever the country, the common aim of all these agencies is to provide guidance to governments and citizens about the level of emissions, harmful effects and abatement practices needed about air pollution. Based on the impact of gaseous pollutants exposures on

human, they define guidelines of emission for the different pollutants in various working environments and living conditions.

1.3. Definition of emission guidelines

In the context of air quality control, a guideline of emission can be defined as the concentration of chemical species considered as harmful to public health and in general ecosystem that should not exceed a standard value above which a recognizable negative impact is observed. These guidelines are broadly divided into two parts. Primary guidelines concerns with health protection of people including "sensitive" populations such as asthmatics, children, and the elderly. Secondary guidelines set standard for public welfare protection, including protection against damage to animals, crops, vegetation, and buildings [6]. Guidelines are intended to provide background information and guidance to governments and local authorities to initiate risk management decisions, particularly in setting standards, but their use is not restricted to this. They also provide information for all who deal with air pollution. Guidelines values are relative to working or living environments. It varies with environment protection agencies which are formulating these guidelines considering their institutional and national objectives. A few terminologies regarding guidelines of emissions should be explained here before going into numerical values and agencies concerned in their formulation in the next section. These terms have been used to provide guidelines values for different specific purposes.

- (a) **Lowest Observed Adverse Effect Level (LOAEL):** it is the lowest exposure level at which there are biologically significant increases in frequency or severity of adverse effects between the exposed population and its appropriate control group [7].
- (b) **No Observed Adverse Effect Level (NOAEL):** it represents the highest exposure level at which there are no biologically significant increases in the frequency or

severity of adverse effect between the exposed population and its appropriate control; some effects may be produced at this level, but they are not considered adverse or precursors of adverse effects [7].

- (c) **8-hours-Time Weighted Averages (TWA):** it is the upper average value of exposure during 8-hours work-shifts in a day.
- (d) **Permissible Exposure Limits (PEL):** these are the maximum amount or concentration of a chemical that a worker may be exposed according to OSHA (Occupational Health and Safety Administration) regulation.
- (e) **Short-Term Exposure Limits (STEL):** it represents the concentration to which workers can be exposed continuously for a short period of time (usually 15 minutes as long as the time weighted average is not exceeded) without suffering from irritations, chronic or irreversible tissues damage and reduced work efficiency.
- (f) **Threshold Limit Values (TLV):** it reflects the level of exposure that a typical worker can undergo without an unreasonable risk of disease or injury.
- (g) **Occupational Exposures Limit (OEL):** it represents the upper limit of the acceptable concentration of a harmful substance in workplace air. It is typically set by competent national authorities and enforced by legislation to protect occupational safety and health.
- (h) **Recommended Exposure Limit (REL):** it is defined as the occupational exposure limit that has been recommended by the National Institute for Occupational Safety and Health (NIOSH), USA. It can be interpreted as the permissible exposure limit for worker safety over his working lifetime if used in combination with engineering and work practice controls, exposure and medical monitoring, posting and labeling of hazards, worker training and individual protective equipment.

1.4. Nature of pollutants

We have previously mentioned that possible classification of gaseous pollutants can be performed either on the basis of nature of sources or chemical and physical properties of pollutants. Depending on the origin of emissions, they can be considered as industrial, domestic and/or traffic pollutants. Vehicular emissions constitute the major contribution to urban air pollution. In contrast, in rural areas of developing countries, domestic emissions resulting from the use of wood and coal for cooking and heating purposes as well as agricultural activities are responsible for the main part of atmospheric pollution. For industrial emissions, they mainly emanate from burning of fossil fuels (coal, petroleum and natural gases). On the basis of chemical and physical nature of pollutants, most of them fall in the categories: redox gaseous species, suspended particulates and hydrocarbon emissions. As their names imply, redox pollutants are produced by oxidation/reduction processes taking place either in industry, vehicle engines or in domestic environments. This class of pollutants includes nitrogen monoxide (NO), nitrogen dioxide (NO₂), sulfur dioxide (SO₂), hydrogen sulfide (H₂S), ozone (O₃), carbon dioxide (CO₂) and carbon monoxide (CO). Suspended Particulates Matters (SPMs) are solid and liquid micro-particles present in atmosphere which are mainly added from coal-fired power plants, woodstoves, diesel engines combustion and reactions of SO₂ and NO₂ in atmosphere. These are broadly of three types PM₁₀, PM_{2.5} and PM₁ depending on the size of the particles in μm. Hydrocarbon pollutants consist of compounds of carbon, which are added to environment mainly through vehicular exhausts, forest fires, volcanic shoots, smoking, consumer goods and the industrial activity involving their production.

From a medical point of view, the impacts of these air pollutants on human health are numerous and strongly dependent of concentration levels and exposure conditions. Human health problems linked to air pollution are lungs, eyes and nose irritations for the lowest

concentrations, respiratory troubles like asthma, bronchitis, decreased resistance to respiratory infections for longer and moderate exposure, pneumonia, stillborn child, cancer and premature death for the worst exposure conditions. If inhalation is the first route of absorption, ingestion and skin contact are other routes of pollutant assimilation in body. Thus, people can also be affected by deposition of air pollutants in environmental media and uptake by plants and animals. It results in chemicals entering the food chain and may present in drinking water and form additional sources of exposure to human.

Atmosphere is a complex mixture of gases, including pollutants and water vapor, submitted to thermal, light and pressure variations. The combined effects of these analytes can be additive, synergistic or antagonistic depending on their chemical nature. The best example concerns the vehicular emission. Petroleum engine from cars generate nitrogen oxides (NO and NO_2), hydrocarbons and Volatiles Organic Compounds (VOCs) at the same time. In the presence of UV radiations, NO_2 in synergy with hydrocarbons and VOCs lead to the formation of a secondary pollutant, ozone (O_3) which is also a toxic gas in lower atmosphere [8]. In the presence of nitrogen monoxide (NO), O_3 reacts with this pollutant to produce NO_2 . That explains why NO_2 and O_3 can coexists with proportions depending from the presence of the others pollutants (NO , hydrocarbons and VOCs). It also explains why the concentration of O_3 is more important in the suburban and at the periphery of high-traffic roads especially during sunny days whereas NO_2 is mainly present close to town centers.

In the recent decades, significant efforts have been made to reduce the conventional air pollution worldwide by the implementation of preventive or curative technologies. It includes introduction of cleaner technologies in coal and petroleum based power plants, discouraging the use of sulfur and lead laden fuels in vehicles and increasing public awareness about pollution effects. As a result of these efforts, emission of some of the major pollutants has declined. The most pronounced effects have been seen for SO_2 which total emission was

reduced by 50% in the period 1980-2000 [9]. Reduction in NO₂ by 15% has been also observed in some European countries. However the PMs and NO₂ remain a great worry especially in developing countries like India and China [10].

1.5. Trends in monitored air pollutants

Because their average concentration levels have not decreased since several years in most of cities of the European Union, nitrogen oxides (NO_x) and ozone (O₃) remains among gaseous pollutants especially monitored by the networks of air quality control. For example, in Paris, the average NO₂ concentration is 2 times greater than the quality objectives set by the legislation while since 15 years, the O₃ level has doubled, the French quality objective being exceeded each summer [11]. Besides these longstanding gaseous pollutants, new classes of air pollutants emanating from the increase in urban traffic, modern furniture and interior furnishings have become a great source of worry in recent years. All these chemical species characterized by their high volatility are designed as Volatile Organic Compounds (VOCs). These compounds are a major concern in urban areas, particularly in indoor environments. Major sources of emission of VOCs in urban areas are vehicular exhausts, petrochemical industries and fuel marketing stations in outdoor environments and consumer goods including paints, coatings, cleaning liquids and disinfectants in indoor environments. Different health risk studies have revealed that VOCs have potential harmful short-term and long-term impact on human [12-16]. Currently a lot of public and private initiatives are underway for the continuous measurement, control and mitigation of these pollutants. This present study is a part of such initiatives and aim to develop a sensor-system able to accurately monitor the concentration of some of these VOCs in different environments.

2. Focus on Volatile Organic Compounds

2.1. Definitions, major components and emissions distribution

WHO defines VOCs as any organic compounds whose boiling point is in the range from 50° C to 260 °C [17]. US EPA defines VOCs as any compound of carbon, excluding carbon monoxide, carbon dioxide, carbonic acid, metallic carbides or carbonates, and ammonium carbonate, which participates in atmospheric photochemical reactions [18]. According to the directive 1999/13/CE of the European Council [19], VOCs can be defined as all organic compounds with a saturation vapor pressure higher than 0.01 kPa at 293.15 K or equivalent volatility in the special using conditions. In respect with these definitions, a broad range of organic compounds having high vapor pressure at room temperature can be considered as VOCs. Such compounds have molecular weight ranging from 50 to 300 g/mol. They exist mainly into the gas phase at the temperature and humidity conditions in indoor atmospheres. Among all volatile compounds, we can mention benzene, toluene, ethylbenzene, xylenes, chloroform, carbon tetrachloride, formaldehyde, acetaldehyde, acetic acid and many other similar organic compounds. VOCs emissions in urban areas are broadly divided into indoor and outdoor emissions. Nevertheless, the measurement of indoor VOCs emission and consequences on human health has become a higher priority as compared to outdoor monitoring. Public awareness and concerns regarding indoor air quality have increased considerably in past 15 years. Moreover, it has been reported through a multiple surveys that VOCs concentrations in indoor environment is approximately 5 times higher as compared to outdoor [20, 21]. These claims are supported by data obtained in the context of the Integrated Exposure for Risk Assessment in indoor environments project (INTERA) [22, 23] as depicted in Fig. 2. Under this project, emissions of Benzene, Toluene, Ethyl Benzene and Xylenes (BTEX) concentrations, which are major and hazardous constituents of VOCs

emissions, were monitored at different places in various European countries. In agreement with previous case studies on VOCs emission, this project also found higher concentrations of BTEX gases in indoor environment than outdoor. The first reason is that most of the modern buildings have higher insulation levels, improved window technologies, making building more airtight in an effort to reduce the energy costs for more efficient heating systems. As these buildings are more airtight, the natural air leakage inside is not sufficient to dilute VOCs pollutants. As a consequence, very high concentrations of VOCs have been measured in indoor air. Among the different VOCs present in indoor air, the presence of BTX is especially alarming because of their detrimental effects even at very low levels. For the effective enforcement of legal norms of emissions of these chemicals, their continuous monitoring is fully required.

In agreement with the as-mentioned noble objective of air quality control, the “Chemical Sensor systems and micro-systems” group at Institut Pascal is working for a long time on the development of chemical gas microsensors. Previously, gas sensor-systems for redox pollutants measurements like NO_2 and O_3 at low concentrations were successfully developed [24, 25]. In agreement with the scientific skills and objectives of this group, this present study is now dedicated to the development of a relevant gas sensor-system for the monitoring of Benzene, Toluene and Xylenes (namely BTX). As a justification, sources of emission of BTX analytes and their toxicity on human health will be described below.

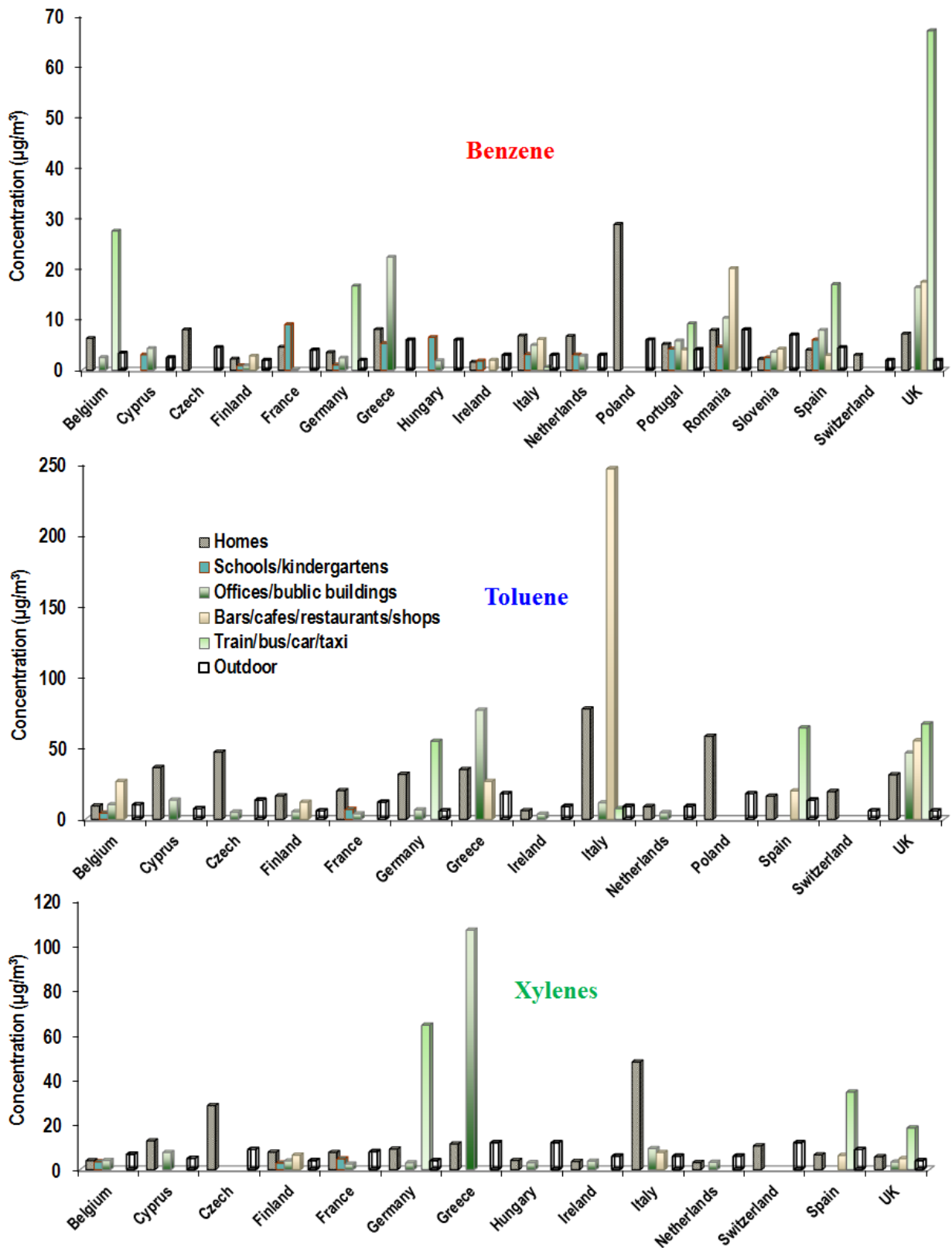


Fig. 2: Case study of BTX emissions in Europe in different environments [22, 23]

2.2.BTX as target gases

2.2.1. Physical and chemical properties of BTX

BTX are aromatic compounds characterized by a six membered cyclic ring of carbon atoms. They are colorless, flammable, odorous and highly volatile. In accordance with their boiling points (T_B), the volatility of these compounds can be classified as:



Heavier than air, they stay into low laying areas. These chemicals have a very low solubility in water (lowest for benzene and highest for xylenes) due to the non-polar nature of benzene ring. Toluene and xylenes are slightly polar because of the peripheral methyl group(s). In liquid phase, these chemicals are generally lighter than water. From structural point of view, these molecules are planar because of the delocalization of π -electrons. Xylenes exist in three isomeric forms namely ortho-, meta- and para-xylene. These compounds are absorbed in the UV-Vis region of electro-magnetic spectrum around 260 nm. These compounds mainly undergo substitution reaction, while addition or ring opening requires drastic condition. The properties of BTX are reported in table 1.

	Benzene	Toluene	o-xylene	m-xylene	p-xylene
<i>Molecular formula</i>	C_6H_6	C_7H_8	C_8H_{10}	C_8H_{10}	C_8H_{10}
<i>Molar mass (g/mol)</i>	78.12	92.15	106.17	106.17	106.17
<i>Melting point ($^\circ C$)</i>	5.5	-95.5	-25.2	-47.9	13.3
<i>Boiling point ($^\circ C$)</i>	80.1	110.6	144.4	139.1	138.4
<i>Density (kg/m^3)</i>	876	867	880	860	861

Table 1: Physical and chemical properties of BTX gases

2.2.2. Sources of emission and exposure

BTX gases enter the environment through natural as well as anthropogenic activities. Natural sources of these gases are crude oil, forest and grassland fires as well as volcanic eruptions whereas in urban areas, anthropogenic activities are the major sources. Emissions from human activities are mainly of exhaust and evaporative nature. In the outdoor environment, major sources are gasoline vehicle exhaust, tobacco smokes, petrochemical industrial emissions and fuel stations. Benzene is predominantly present in vehicular exhaust whereas toluene and xylenes are present in small quantities because nowadays they are blended with gasoline for octane boosting. For example, gasoline contains 4g/L of benzene and very little quantity of toluene and xylenes [26]. Toluene is significantly present in emissions from aircraft exhaust. Unburnt fuel and leakage from storage tank at fuel stations are also a major outdoor emission source of BTX.

The main sources of contamination of the indoor environments include wide ranges of consumer goods (e.g., cleaning agents, polishes, adhesive products, oils, greases, lubricants, fragrances) and building materials (e.g., solvent- and water-based adhesives, sealant, floor coverings, paint, chipboard). The major occupational exposures of BTX gases are to workers who are involved in industrial manufacturing where these compounds are used as solvents and at fuel stations. The major industrial activities comprising occupational exposures of BTX involve manufacturing and processing facilities in pharmaceutical, dye, paints, rubbers, leather and petroleum industries. Spread of unburnt fuel and leakage from storage tank poses a major threat to workers at fuel stations. In dentistry, xylene is used in histological laboratories for tissue processing, staining and cover slipping and also in endodontic treatments. Major non-occupational exposure comes from vehicular exhausts and solvent evaporations. Hazardous waste disposal sites which can spill BTX into the environment are also possible sources of non-occupational exposure.

2.2.3. Health effects of BTX exposure

BTX gases are potential health hazards to human and other animals even at very low concentrations. The possible routes of exposures are ingestion, inhalation, dermal or eyes contacts. The potentiality of these adversities depends on amount of exposure, duration of exposure and age-group of people exposed. The detail about the duration, concentrations and corresponding health effects of BTX gases are reported in table 2.

Exposures to benzene are divided into long-term (more than a year) exposures and short-term exposures (between few minutes to weeks). A few studies related to intermediate-term health impacts have been also reported. Among BTX gases, benzene has the most potent short-term and long-term human health consequences. A few common short-term effects of BTX exposures are dizziness, euphoria, giddiness, headache, nausea, weakness, drowsiness, respiratory irritation, nervousness, pulmonary edema, pneumonia, gastrointestinal irritation, convulsions and paralysis [27-31]. Exposures at very high concentrations (10000-20000 ppm) for a time between 5-10 minutes can result in death. Long term exposures of BTX gases are highly lethal in many cases. More especially, exposures are a serious health risk for workers at their occupational sites. The most significant adverse effects from prolonged exposure to benzene are haematotoxicity, genotoxicity and carcinogenicity [32]. An increased mortality from leukemia has been demonstrated for workers occupationally exposed to benzene for a long time [33, 34]. It is also suspected that benzene exposure affects the fetus development in pregnant women [35] and fertility in men [36, 37].

In long term exposure to toluene vapor, its neurotoxic effects have been reported [38]. Extremely high levels may cause permanent toxicity to the brain. Long-term occupational exposure to women may lead to spontaneous abortion and stillborn baby [39]. Long-term exposure to xylenes may lead to headaches, irritability, depression, insomnia, agitation, extreme tiredness, tremors, impaired concentration and short-term memory [29]. This

condition is sometimes generally referred to as “organic solvent syndrome”. Frequent or prolonged skin contact to BTX liquid can cause irritation and dermatitis, dryness, flaking and cracking of the skin.

Pollutant gas	Concentration	Duration	Health effects
<i>Benzene</i>	50 ppm	10 min	Eye, nose, and respiratory irritation
	300 ppm	30 min	Drowsiness, dizziness and headache
	20000	10 min	Death
	50-300 ppm	4 months to 1 year (occupational)	Heamotoxicity and severe anemia, decrease in WBCs count.
	30 ppm	3.5 months to 19 years (occupational)	Leukemia, anemia and leukopenia
<i>Toluene</i>	100 ppm	6-8 hours (occupational)	Irritation to eyes and nose, headache, dizziness, intoxication, color vision impairment,
	500 ppm	10 min	Irritation of the eyes, mucous membranes, and upper respiratory tract
	167 ppm	2-12 months	No health effects (NOEAL)
	100-150 ppm	10-15 years (occupational)	Impaired color vision, impaired hearing, decreased performance in neurobehavioral analysis, changes in motor and sensory nerve conduction velocity, headache, and dizziness
<i>Xylenes</i>	200-400 ppm	3-5 min	Eye and nose irritation, impaired body balance and reaction times
	50 ppm	2 hours (once)	increased severity scores for headache, dizziness in males; intoxication in males and females
	100 ppm	4 weeks (occupational)	Nose, throat and eye irritations
	14 ppm	7 years (occupational)	Nose, throat and eye irritation, (increased prevalence of nausea, poor appetite and anxiety, forgetfulness, inability to concentrate and other subjective symptoms.

* *Data source: ATSDR, USA*

Table 2: Health consequences of exposure to BTX gases

2.2.4. International guidelines for BTX emissions

Based on the health risk assessment of BTX pollutants, guidelines of emission have been issued by different environment protection agencies for different working environments. Three very important organizations guidelines, which are highly relevant in our context, are WHO guidelines, European Union directives and French government legislation of BTX emissions. The detailed guidelines values for occupational and non-occupational exposures given by the different environment protection agencies mentioned above are reported in tables 3, 4 and 5.

According to WHO, benzene is carcinogenic to human and no safe level of exposures can be recommended. Therefore, no specific guideline has been given for benzene vapor exposure. However for practical use and general guidance, the concentration of airborne benzene associated with an excess lifetime risk of 1/10 000, 1/100 000 and 1/1 000 000 are 17, 1.7 and 0.17 $\mu\text{g}/\text{m}^3$ respectively [40]. For toluene emissions, based on different health risk analysis, the LOAEL value for effects on central nervous system (CNS) is 332 mg/m^3 corresponding to 88 ppm for an occupational exposure [1]. A guideline value of 0.26 mg/m^3 corresponding to 69 ppb has been thus established as an average exposure for a week. For the non-occupational exposure, guideline is based on odor threshold. So, the maximum concentration of toluene in air should be less than 1 mg/m^3 corresponding to 265 ppb (odor threshold of toluene) for a 30 minutes average. The WHO derived a 24-hour guideline value for xylenes of 4.8 mg/m^3 corresponding to 1 ppm for non-occupational exposure [41]. The annual guideline value has been derived to 0.87 mg/m^3 corresponding to 200 ppb.

In Europe, the directive 2000/69/EC of the European Parliament and of the Council of 16 November 2000 states that average annual exposure to benzene must not exceed 5 $\mu\text{g}/\text{m}^3$ corresponding to 1.57 ppb for non-occupational exposure [42]. According to European Directives 2000/39/EC and 97/42/EC (ED), European Union, limit value for occupation

exposure of benzene has been given as 3250 $\mu\text{g}/\text{m}^3$ corresponding to 1 ppm [5, 43]. No specific guidelines for toluene and xylenes emission have been provided by European Commission.

French VOC regulations are based on European Construction Products Directive (CPD), according to which no construction products shall impair human health. For airborne benzene exposure, France accepts the WHO derived guidelines for Benzene. For toluene and xylenes emissions, the average occupational exposure for 28 days period should not exceed 600 mg/m^3 and 400 mg/m^3 corresponding to 160 ppm and 100 ppm respectively [44]. More precisely, there are four levels of mean exposures for toluene and xylenes respectively in an occupational condition as shown in the table 3. In this classification A⁺ is the purest air quality and C is the worst quality.

Classes	C	B	A	A ⁺
Toluene	>600	<600	<450	<300
Xylenes	>400	<400	<300	<200

**Concentrations in mg/m^3*

Table 3: French government guidelines for toluene and xylene emissions

Regulatory agency	Description	Benzene (mg/m³) (3.18 mg/m ³ = 1 ppm)	Toluene (mg/m³) (3.76 mg/m ³ = 1 ppm)	Xylene (mg/m³) (4.33 mg/m ³ = 1 ppm)
ACGIH (USA)	TLV	1.6	750	435
	STEL	8	Not available	655
OSHA (USA)	PEL	3.25	750	435
	STEL	16.25	Not available	655
NIOSH (USA)	REL	3.25	375	435
	STEL	3.25	560	655
SAOHS (S. Africa)	OEL	1.6	175	435
European Union	OEL	3.25	Not available	Not available

Table 4: International BTX guidelines of occupational exposure

Regulatory agency	Description	Benzene (mg/m³) (3.18 mg/m ³ = 1 ppm)	Toluene (mg/m³) (3.76 mg/m ³ = 1 ppm)	Xylene (mg/m³) (4.33 mg/m ³ = 1 ppm)
WHO	1 week (toluene)	0	0.26	Not available
	24 h (xylene)	0	Not available	4.8
AAAQO, Canada	1 h (benzene)	0.003	Not available	Not available
	24 h (toluene, xylene)	Not available	0.4	7
EU directives	Annual mean	0.005	Not available	Not available
EPAQS, UK	Annual mean	0.01625	Not available	Not available

Table 5: International BTX guidelines of non-occupational exposure

3. BTX monitoring: normalized protocol and limitations

3.1. Protocols of monitoring

In view of health and environmental troubles caused by BTX emissions, their monitoring in all types of environments has become imperative. As normative methods, governmental and autonomous environment protection agencies responsible of air quality monitoring have adopted two protocols for the quantification of BTX gases in ambient air. These are (i) continuous monitoring of BTX by means of automatic chromatographs implemented in air quality stations and (ii) chronic sampling of polluted air at different locations followed by subsequent analysis in laboratory.

These two different ways of measurements are distinct mainly by the nature of information they deliver. The first method involves continuous measurements of BTX in polluted air by automatic gas analyzers integrated with chromatography techniques. This strategy of measurement is followed considering the European Union directives established by the European Committee of Normalization (CEN) [45-47]. These apparatus are highly selective and sensitive towards target pollutants and give real-time information. The second method is based on passive or diffusive sampling of air sample through a specific adsorbent exposed during a determined period then collecting to a stainless steel canister [48]. After the period of sampling, target chemical species are extracted from the adsorbent and quantified in laboratory by chromatography to determine the average concentration of BTX gases into the collected air. Low cost involved in the sampling (5 to 10 €) is very attractive as compared to automatic analyzers (several ten thousand of euros).

3.2.Limitations of normative monitoring methods

Despite their metrological performances, intrinsic limitations make these methods of measurement restrictive. Continuous measurements of BTX using a gas chromatograph are done in air-conditioned micro-environment in a fixed air quality control station or a station with a reduced mobility. Because of this, the number of measurement points is limited and it remains impossible to achieve a high-resolution mapping of an area. Moreover, these analytical set-up are expensive (20000 to 40000 €) and instrumentations used in gas analyser setup are complex and bulky. Because of these restrictions, the monitoring of BTX into large public spaces is non-realistic as well as permanent assessment of personal exposure. Sampling gives cumulative measurements of pollutants for the period they were exposed. Quantification of pollutants gives only an average value during the sampling time and remains not adapted to pollution peak detection. Moreover, during transportation of sampled pollutants from field to laboratory, the actual concentrations of gases may change because of leakage or other factors.

3.3.Interest of sensor development

It has been highlighted in various scientific studies [49-51] that fixed air quality control stations can give an accurate quantification of pollutants in the background location of these stations, but systematically underestimate the real exposure of workers at their occupational sites, driver and commuters in passenger compartments, pedestrian in general public spaces. Therefore, to enhance the spatial resolution of pollution cartography as well as to perform a better assessment of individual exposures, the development of sensing devices with high mobility, high metrological performances and suitable to any kind of environments is full of interest. Such device must satisfy all the important specifications required in such

kind of applications. It includes accuracy, spatial and temporal discrimination, selectivity, high resolution, fast response time and low-power consumption. Moreover devices well-adapted to different working environment, indoor and outdoor, able to work on a large concentration range are also a very important requirement. Taking into account the as-mentioned needs, gas sensor-systems could be a suitable and attractive solution. With the growth of microelectronic and progresses in nanotechnology, miniaturized sensing devices and sensor-systems have become a reality. So, their compact size, low cost, low power consumption and autonomous operation make these devices highly relevant for the continuous, wide scale and real-time monitoring of BTX gases in atmospheres.

4. Gas sensors

4.1. Technical definitions and working principles

Gas sensors are technological devices that deliver an electric or optical output signal as a response to the concentration (measurand) of one analyte or a class of analytes present in its vicinity. Beyond gas identification, the quantification of the target gaseous species into a complex air mixture must be achieved. According to the level of discrimination performed, it can be designed to target only one gas or to ensure multi-gases detection. If specific applications require a high level of discrimination, many metrological approaches have been led on the development of multi-sensors and sensor arrays. The schematic of gas sensors developed in this study is shown in Fig. 3. A gas sensor consists in a sensitive element selected for its high sensitivity toward the target analyte (recognition part) associated to a transducer that converts chemical information into electrical or optical signal (transducing part).

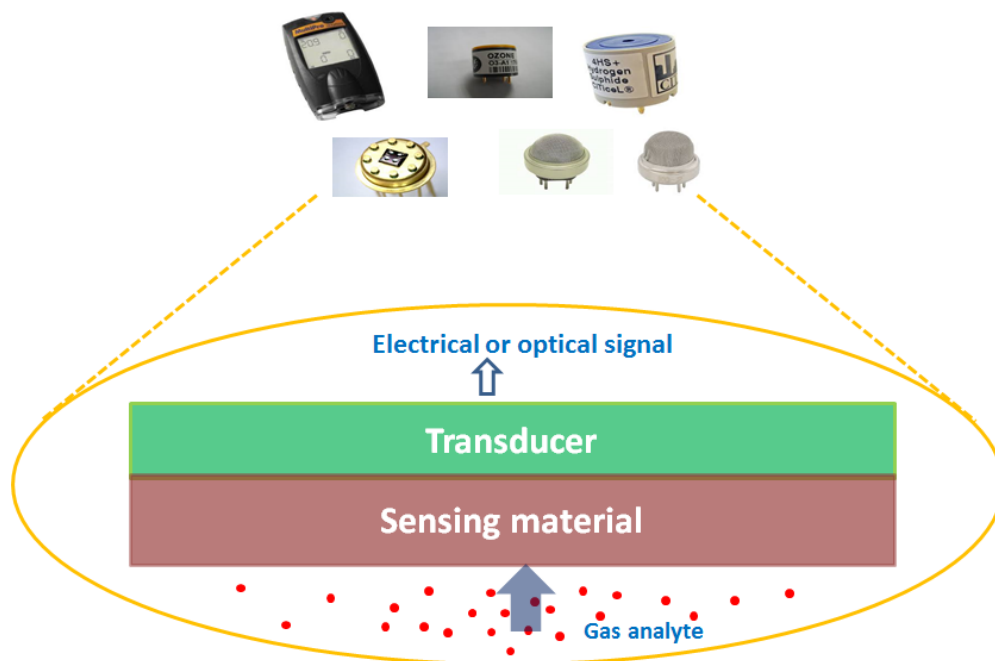


Fig. 3: Representation of gas sensors

Sensing material coated on the transducer surface must exhibit a strong affinity with the targeted gas. It can be a metal, metal oxide, polymer or hybrid material [52]. Transducer is a device which converts one physical variable to another. In the context of gas sensor including sensitive layer, it transforms into electrical or optical signal a property of the sensing material modulated by physical or chemical stimulus as a result of interaction with gas analyte.

The working principle of a gas sensor including sensitive layer is firstly based on the modulation of a physical or chemical property of the sensing material consequently to its interaction with gaseous molecules, the variation magnitude being correlated to gas concentration. Such interactions can remain limited to the surface or can occur deeply into the bulk, involving physical or chemical sorption. For sensors based on optical detection, gaseous molecules modulate a property of a light radiation (wavelength, optical absorption...), this variations being correlated to gas concentration. The variations of the material or radiation property are then converted by means of the transducer into functional signal to be operated by signal treatment and/or data storage units. The choice of the sensing material as well as the transducing mode is strategic. It strongly depends of the nature of the target gas, the interaction expected and so the modulated property of sensing material, the co-existing interfering gaseous species into the environment in which measurements will be perform and the level of performances referred.

4.2.Metrological requirements

With so many gas sensors described in literature and proposed by manufacturers, one general question arises: which one is the best? The answer is not simple and cannot be disconnected from the application to satisfy. The relevance of sensing devices can be considered from a metrological, technical and economic point of view. A general perception

which serves the purpose is the best sensor is the one that will do the job, at a cost which justifies its use. The cost must be viewed in terms of money, time, and ease of use [53].

The performances of sensing devices can be assessed from metrological characteristics determined during gas exposures. If they are fully observed, all these criteria define the ideal sensor. Below are listed the main required metrological specifications adapted from the 3rd International vocabulary of metrology [54]:

- (a) **Sensitivity:** Sensitivity of a sensor is defined as the change in output signal of the sensor per unit change in the concentration of gas being measured.
- (b) **Selectivity:** It can be defined as the ability of a sensor to respond primarily to only one specie (analyte) in the presence of other species.
- (c) **Measuring interval:** it represents the set of gas concentration that can be measured by the sensing device with specified instrumental measurement uncertainty, under defined conditions.
- (d) **Detection threshold:** it is defined as the largest gas concentration being measured that causes no detectable change in the corresponding output signal
- (e) **Baseline drift:** it is the variations in baseline signals of sensors usually during a long duration of sensor operation. It may result from changes of temperature, electronics stabilizing, or aging of the transducer or electronic components.
- (f) **Resolution:** it represents the smallest change in gas concentration that causes a perceptible change in the corresponding output of sensor.
- (g) **Limit of detection (LOD):** it is defined as the minimum value of gas concentration that can produce a sufficiently different signal from the highest measurable signal observed for a blank sample.
- (h) **Response time:** The response time can be defined as the time required for a sensor output to change from its initial state to a final steady state value within a tolerance

band of the correct new value. In the present experimental context Response Time (90%) or $t_{90\%}$ has been used. It means that time required for the sensor output to change from its baseline value to 90% of the value of steady state when sensor is under pollutant exposure. The time characteristic corresponding to return to the initial state (stimulus removed) is called recovery time.

- (i) **Hysteresis:** Hysteresis refers to the characteristic that a device is unable to repeat, in the opposite direction of operation, the data that have been recorded in one direction.
- (j) **Reversibility:** Reversibility in the context of gas sensing means that the sensor signal returns to its previous value as soon as the measurand variation is removed.
- (k) **Reproducibility:** Reproducibility of a sensor is the degree to which all sensing characteristics can be accurately reproduced or replicated by other sensors of same type (sensing materials, transducer), under the same conditions of gas exposure and device parameters.
- (l) **Repeatability:** Repeatability of the sensor is the degree to which all sensing characteristics can be accurately repeated for the same sensor for similar given condition of gas exposures.
- (m) **Stability:** stability is defined as the property of sensing device to maintain constant in time all the metrological properties.

In the context of this work, all these metrological specifications will be evaluated and discussed.

4.3. Gas sensor technologies for BTX detection

No universal principle can be used to classify all the available chemical gas sensors. It can be based on types of transducers, materials, target gases and area of applications. Nevertheless, in accordance with IUPAC classification, we have decided to distinguish

chemical sensors on the basis of nature of transducer involved into sensor-systems [55]. For each class, the most promising developments on sensors especially aimed to BTX measurements are reported.

4.3.1. Optical sensors

An optical sensor is a device that measures gas concentration from the variations of a property of light radiations, these variations being caused by the presence of the gaseous molecules on the optical path. The detection can be localized into UV or IR regions of light spectrum and the modulated optical properties include absorbance, reflectance, luminescence, fluorescence, refractive index or light scattering. An optical sensor is generally a part of a larger system that integrates the optical sensors and all electronic circuits for signal treatment, data collection, digital/analog converter and chronic recalibration.

BTX sensors based on such technology were deeply studied during the past two decades. Especially sensors implementing UV-Visible radiation were investigated in detail by different research groups. Y. Uno et al. [56-60] made a detailed investigation of air borne BTX using a microfluidic device integrated with an optical detector. This strategy of detection exhibited very high sensitivity (10 ppb limit of detection for toluene) and selectivity of BTX gases (for a gas mixture of 10 ppm) for a sampling time of 30 minutes. S. Camou et al. proposed a sensor-system for benzene detection based on bubbling extraction followed by UV-Visible detection [61, 62], which shows detection limit of 200 ppb for a measurement time of 10 minutes. In recent years, J. Hue et al. [63] have proposed a sensor-system consisting in nano-porous concentrator and a spectrophotometer detector for benzene and xylene detection. The sensor exhibited detection limit of 20 ppm and 10 ppm for benzene and xylene respectively for a measurement time of 2 hours. Although optical BTX sensors are

sensitive and selective towards BTX gases, bulky instrumentation limits their wide scale application. Moreover, they require long measurement times and remain very expensive.

4.3.2. Electrochemical gas sensors

Electrochemical sensors are based on ionic conductivity of a solid or liquid electrolyte. In electrochemical sensing devices, gas molecules are oxidized or reduced at the porous working electrode and then can diffuse into the electrolyte through this electrode. On the other side, an electrode non-exposed to the sampling gas is used as reference. The non-homogeneous distribution of mobile ions into electrolyte near the electrodes results in an electromotive force depending on gas concentration present at the working electrode. According to the electrical properties measured, difference of potential or resulting current, potentiometric and amperometric electrochemical sensors can be distinguished.

In the last decade, some interesting works have been reported about electrochemical detection of BTX gases [64, 65]. They used sensor configuration with Strontium doped Lanthanum Chromite (abbreviated as LSCO) and Pt electrodes with Ytria-Stabilized Zirconia electrolyte. Sensor exhibited high BTX sensitivity with limit of detection close to 0.5 ppm. Cross-sensitivity of BTX gases is the main limiting point with such technology. Furthermore, these sensors have a very narrow range of operating temperature and exhibit short life-time.

4.3.3. Conductimetric gas sensors

Their working principle is based on the change of electrical properties of materials as a result of the interaction with the target analyte. These sensors can be further sub-divided based on the nature of electrical properties (resistance, capacitance, work function and conductivity variations) and type of materials (metal oxides, molecular materials, organic

polymers, and carbon nanotubes) used as sensitive layer. Among the different conductimetric sensors, resistive devices are the most widely investigated and at present dominate the commercial gas sensor market. It works on the principle of change in resistance of the material consecutively to the injection or the trapping of electronic charges by chemisorbed molecules. As a consequence, they are often called chemoresistors.

Among conductimetric gas sensors, metal oxide based chemoresistors are the most investigated one. Sensors based on metal oxide semiconductors are mainly applied to detect target gases through redox reactions between the target gases and the metal oxide surface. This process includes redox reactions, during which O^- distributed on the surface of the materials react with molecules of target gases, leading to an electronic variation of the oxide surface and so to a variation of oxide layer resistivity. Chemoresistors based on SnO_2 [66-69], WO_3 [70, 71], TiO_2 [72, 73] and Cr_2O_3 [74] have been investigated in past for their potential application as a BTX sensors. The advances made in SnO_2 based chemoresistors are noticeable. High sensitivity for benzene (detection limit of 500 ppb) [66] was observed with a response time to few seconds. For toluene, the linear relationship between the response and the gas concentration was found in the range of 10–300 ppm with a response and recovery time assessed to 1 and 5 seconds respectively [68]. WO_3 based chemoresistors exhibited very high sensitivity for toluene (10 ppb limit of detection) and a fast response (70 seconds). TiO_2 chemoresistors also showed high sensitivity (0.1 ppm) for BTX and fast response (20-40 seconds). Recent development of a ZnO based BTX sensors by Bhattacharyya et al. [75] reported a detection limit of 0.5 ppm for benzene and response time in a few seconds. Although metal oxide semiconductor sensors are most studied and commercialized sensors, some remaining drawbacks limit their wide scale application. It includes requirements of high working temperature (greater than $200^\circ C$) which raises the power consumption for sensor

operation. Moreover, reproducibility, selectivity and drift of baseline often remain a concern in such sensors.

With the development of nanomaterials and nanotechnologies, carbon nanotubes or nanotube-composites based chemoresistors have emerged in the field of gas sensors even for BTX detection. Carbon nanotube is known to possess high resistance and act as a good adsorbent for aromatic compounds like benzene, toluene and xylenes [76]. A miniaturized integrated sensing array employing hybrid nanomaterials consisting in metal decorated multi walled nanotube demonstrated a sensitive (50 ppb limit of detection) and selective detection of benzene with a response time less than one minute [77, 78]. Carbon nanotube/polymer composite based electronic nose were reported by Castro et al. for the discrimination of VOCs [79]. Chemoresistors using single walled nanotube (SWNT) as a sensing layer for VOCs detection were also reported by K. parikh et al. [80]. It was a preliminary study to use SWNT as a sensing layer and test was conducted at 10000 ppm of toluene. Nevertheless, despite their attractive sensing properties, high cost involved in sensor fabrication, poor stability of sensor, reproducibility in response and selectivity are the main challenges to overcome.

4.3.4. Acoustic gas sensors

Based on piezoelectric substrates, acoustic sensors exploit the variations of acoustic waves propagation which can be modulated by different parameters like temperature, pressure, mass or strain. In the case of acoustic sensors dedicated to gas measurement, piezoelectric substrates are coated with a sensitive material able to induce selective and reversible sorption of some gaseous species. Among the properties of the coated materials able to disturb the wave propagation, we can mention the elasticity, viscosity or layer thickness. Nevertheless, for acoustic sensors devoted to chemical species detection, it has been established that mass effect due to gas sorption is predominant as compared to the

effects induced by the other influence parameters [81]. The mass change results in a shift in resonance frequency of piezoelectric crystals. Quartz Crystal Microbalance (QCM) and Surface Acoustic Wave (SAW) devices are two widely investigated transducers of this kind. QCM and SAW sensors are based on the measurement of resonance frequency changes of coated quartz crystals caused by the adsorption of a mass of analyte. If wave propagation occurs into the bulk of quartz crystals for QCM transducer, it remains confined to the surface of quartz for SAW transducers.

QCM is a well-known and widely used device which was at first used in a sensing mode by G. Sauerbrey [82]. Developments have been reported in the past about the use of polymer and composites as sensitive coatings on QCM for BTX detection. B. Pejčić et al. have reported a high sensitivity towards BTX for different combination and proportions of polymers and nanotubes coated on QCM transducer with detection limits in a range of 0.6–3 ppm [83]. Si et al. reported a sensitive detection of toluene (detection limit close to 20 ppm) and xylenes (detection limit to 4 ppm) using a coating of conducting polymers [84]. A partial selectivity was achieved for benzene and toluene using principle component analysis (PCA) method. QCM coated with cross linked molecularly imprinted polymers (MIPs) were used for the selective detection of toluene and xylenes [85, 86]. Such sensors exhibited good selectivity for toluene and xylenes and detection limit for these gases were assessed at 540 ppm and 170 ppm respectively. A few other researches based on QCM coated with a Langmuir Blodgett film of metal complex of organic polymer were reported in the past [87-89]. Detection limits for toluene and xylenes were found in a range of 40-200 ppm for different polymers. QCM transducers coated with polymers and composites are promising sensors for BTX detection as demonstrated from the discussion. However, detection limit and selectivity are too high characteristics which need to be improved.

SAW based sensors have aroused attention for BTX detection because of low cost, miniaturized size, possible integration in portable device and ease of use [90]. M. Penza et al. made a detailed investigation of SAW sensors using carbon nanotube or related hybrid materials for toluene detection [91-93]. They used a molecular imprinting strategy to enhance selectivity of individual BTX gases. Sensors exhibited high sensitivity with detection limit of 1.2 ppm for toluene and good selectivity. I. Sayago et al. reported studies about SAW device using composites based on carbon nanotubes and organic polymer [94, 95] for toluene detection. High sensitivity, good repeatability, good stability and low detection limit to toluene (1.7 ppm) were performed. The selectivity was achieved for toluene by varying proportions of nanotube in the composites materials. Although SAW devices are portable and also not very expensive, enhanced sensitivity and selectivity toward BTX gases remain challenges at the current stage of development.

Besides QCM and SAW sensors a few other acoustic sensors have been developed for aromatic hydrocarbon detection. It includes CMOS based silicon microresonators [96] and amorphous polymer-metglass based magnetoelastic sensors [97]. Sensors exhibited high sensitivity for BTX gases with detection limit of 5.2, 1.2, 0.6 ppm for benzene, toluene and xylenes respectively.

Despite all the advances achieved on sensing material and sensor-systems, we can notice that sensitivity and selectivity towards BTX are often high as compared to the guidelines given for non-occupational exposures. Moreover, the resolution is not systematically quantified and remains weak. As a consequence, our scientific contribution in this field of applications will aim to develop microsensors with optimized sensing characteristics and more especially high sensitivity, high resolution and selectivity at room temperature (low power consumption).

5. Strategy of research

5.1. Global approach

This PhD work was carried out in the “Chemical Sensor-System and Microsystem” group at Institut Pascal, Blaise Pascal University in Clermont Ferrand, France. Involved since a long time in the development of environmental gas sensors, this group has previously developed gas sensor-systems focused on the sensitive and selective measurements of NO₂ and O₃ in complex gaseous phases [24, 25, 98] with the financial support from French National Research Agency (ANR) on scientific collaborative projects entitled POLL-CAP. These sensor-systems include phthalocyanine-based chemoresistor and III-V semiconductor based schottky diodes. The relevance of such technological solutions to selectively monitor these pollutants at ppb level was established.

With the same objectives of air quality control, this PhD work is devoted to the development of gas sensors tailored for the measurement of BTX gases in outdoor and indoor environments. The expected results of this PhD work are in agreement with the objectives of CAPBTX collaborative ANR project led by Prof. Pauly and the ASTHMAA exploratory project granted by the CNRS in 2015. The PhD work encompasses the identification of a suitable material, elaboration of samples, development of testing setup, characterization of sensing layers, testing of sensors towards BTX and interpretation of metrological output of sensors. Taking into account the aromatic nature of the target gases, aromatic molecules were investigated as sensing materials. The sensitivity of different substituted and unsubstituted metallophthalocyanines was studied towards BTX. The choice of the transducing mode was based on the nature of gas/material interactions which occurs. QCM was chosen as transducer for this task and will be discussed in the following. Phthalocyanines materials were deposited in thin layers on transducers active surface through thermal evaporation process or solution

casting methods. The deposited layers were characterized by Scanning electron microscope (SEM), X-Ray Diffraction (XRD), Fourier Transform Infrared Spectroscopy (FTIR) and Raman spectroscopy to correlate their structural and morphological properties to sensor responses. These sensors were then integrated into a laboratory setup equipped with continuous target gas generation at desired concentrations and electronic components for data acquisitions. Tests were performed to investigate the effect of material's properties on metrological performances on devices. Cross-sensitivity studies were also performed to assess the level of selectivity of phthalocyanines-based QCM devices towards BTX gases and interfering species like CO, NO₂, H₂S or O₃. For a better understanding of gas/material interactions and their extent, influence of layer thickness of phthalocyanines on BTX responses was studied. Based on the structural and morphological characteristics of sensing layers and observed metrological properties of sensors, an adsorption model was proposed. At last, lifetime of the sensing layers was studied according to storage and working conditions. As a conclusion, few outlooks on-going activities to reach optimum performances will be discussed.

5.2. Phthalocyanines as investigated materials

5.2.1. Generalities

Phthalocyanines are a group of organic molecular materials [99, 100] which have drawn a lot of interest in multiple research domains because of their outstanding electrical and optical properties. In terms of intermolecular forces molecular materials can be defined as the materials having intermolecular forces between two adjacent molecules less than 10 kcal/mol. These are different from polymers in which individual monomers are linked to each other via covalent bond (intermolecular forces 50-100 kcal/mol). Out of various research fields

explored so far, organic electronics is a leading area where these materials have found a lot of applications dominated by gas sensors and photovoltaics. Commercially, these materials are widely used as a dye and pigments in textile industry. Although phthalocyanines were discovered many years ago, their applications in research areas remain numerous. As justification, in the last ten years period over 1000 articles were published annually based on phthalocyanines research. In the year 2000 “The Society of Porphyrins and Phthalocyanines” was established by leading researchers in these areas to foster active research collaborations.

With improvements in synthesis procedures, different approaches have been adopted for synthesizing these materials [101, 102]. Metal-free and metallophthalocyanines without any peripheral ligands and/or large axial coordinated ligands were synthesized by cyclotetramerization reaction of phthalyl derivatives such as phthalonitrile, phthalic anhydride, 1,3-diiminoindoline, phthalimide and phthalic acid [103, 104]. But these unsubstituted phthalocyanines are highly insoluble in common organic solvents, which prevents them from being applied broadly in materials chemistry research areas. To address this issue many synthesis strategies were developed by synthesizing peripherally and axially substituted metallophthalocyanines [101].

5.2.2. Molecular structure and thin film arrangements

With the advancements in modern analytical techniques, correlations between the structure and properties of phthalocyanines became possible. The basic molecular structure of a phthalocyanine molecule is shown in Fig. 4a. The molecular unit is constituted by a large planar macrocycle including four isoindole groups circularly linked by azamethine bridges. From an electronic point of view, such arrangement leads to a π -conjugated structure having delocalization of 18 π -electrons over the cyclic core. One common structural feature is the

cavity in the center of the molecule, which can coordinate a lot of metallic atoms of the periodic table. The ionic radii of element coordinating inside the phthalocyanine cavity are in a range of 50 pm to 150 pm [105]. The distortion degree and molecular shape of phthalocyanines skeletons depend mainly on the size of the atoms coordinated in the center of macrocycles. Furthermore, the coordination geometries of the central metal ions, the number and steric effect of axial ligands bound to the central metal atoms and the peripheral ligands present on the macrocycle boundary also play an important role in determining shape of macrocycle.

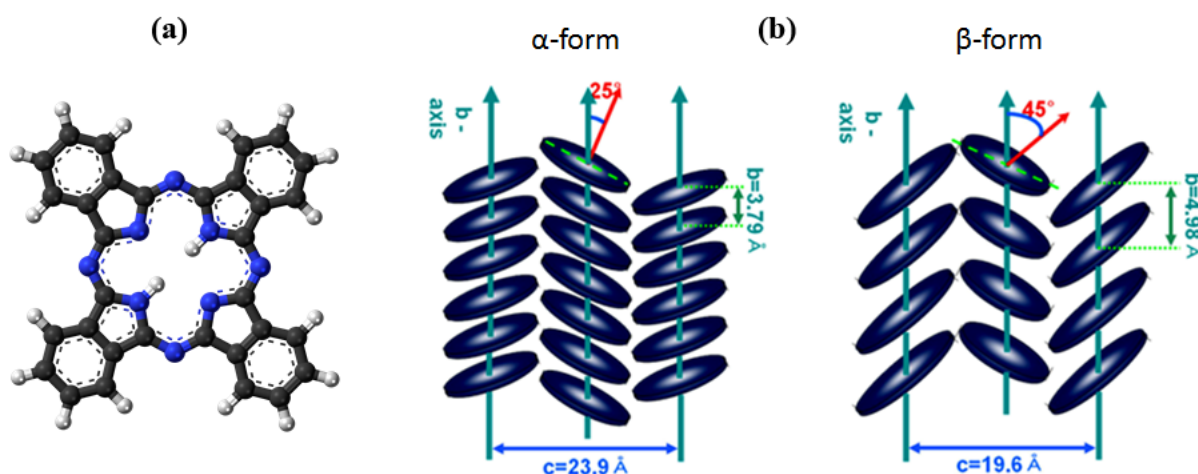


Fig. 4: Structure of (a) phthalocyanine molecule and (b) arrangements of phthalocyanines in thin films

The arrangement of phthalocyanine molecules in thin film is determined primarily by the π -electrons interaction of one macrocycle with the other. XRD and TEM analysis confirmed stacking of macrocycle on each other because of interactions of delocalized π -electrons of neighboring molecules [106]. The nature of the substrate surface and peripheral ligands affect the thin film organization too. Many unsubstituted metallophthalocyanines are semicrystalline in their solid state and exhibit polymorphisms [107]. Although copper phthalocyanine lattices are arranged in monoclinic form in herringbone geometry in crystalline phase, X-ray diffraction analysis of copper phthalocyanine [108] has highlighted

10 polymorphs. Among these, α and β -polymorphic forms are most common. The α and β crystalline polymorphs differ in particular in the inclination of the planar phthalocyanines molecules relative to the stacking axis as shown in Fig. 4b. Regardless of the orientation of molecules in different polymorphs, the geometries, intramolecular bond distances and angles of the molecules in the two crystalline polymorphs are very similar.

5.2.3. Chemical properties

Many applications of metallophthalocyanines strongly depend on their redox properties. In its most common oxidation state, phthalocyanine unit carries two negative charges and often designated as Pc(-2). This unit is capable of oxidation or reduction, thus oxidation by one or two electrons yields Pc(-1) and Pc(0), while reduction by one to four electrons forms Pc(-3), Pc(-4), Pc(-5) and Pc(-6) respectively [109]. Divalent metal atom forms a metallophthalocyanine having planar geometry. Monovalent, divalent, trivalent and tetravalent metal atom can coordinate with the phthalocyanine central cavity resulting in the formation of planar, double decker or triple-decker phthalocyanines. Many metallophthalocyanines system binds one or two axial ligands. Schematic representation of unsubstituted, substituted (peripherally as well as axially), polymeric and double-decker metallophthalocyanines have been shown in Fig. 5.

Most of unsubstituted metallophthalocyanines have limited solubility in common organic solvent [110] and water. Phthalocyanines dissolve in highly acidic media such as concentrated sulfuric acid, chlorosulphuric acid and anhydrous hydrofluoric acid due to protonation of bridging nitrogen atom. The solubility in sulfuric acid also depends on concentration and temperature. Generally phthalocyanines are stable in non-oxidizing inorganic acids. Solubility in bases like liquid ammonia is also weak at room temperature. Because of low solubility of phthalocyanines, substitution of hydrogen atoms by relevant

groups at their peripheral sites is an attractive alternative to make them soluble in common organic solvents. Lee et al. highlighted the solubility enhancement after peripherally substitution of metal free phthalocyanines with a bulky organic ligand [111].

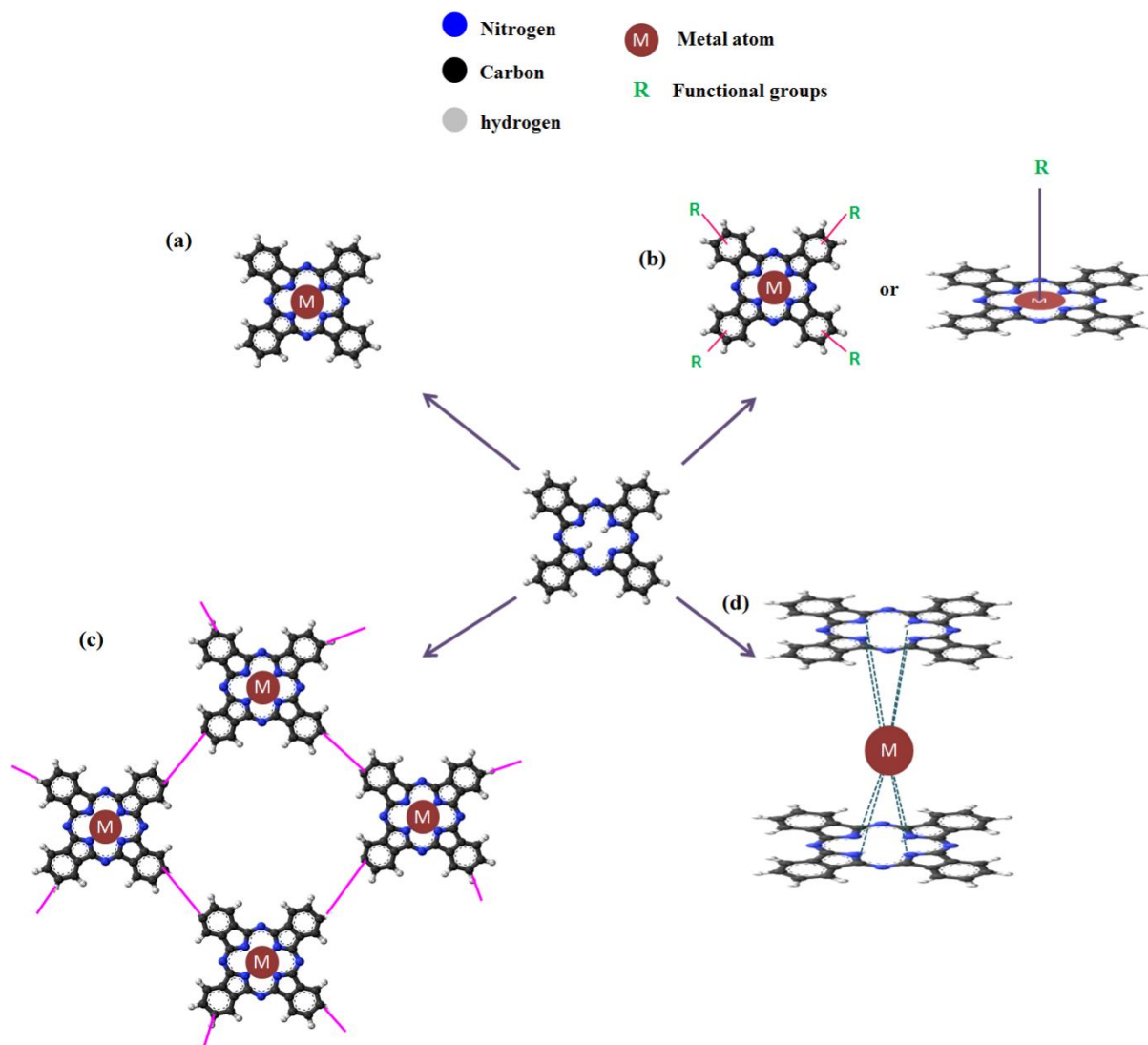


Fig. 5: Representation of (a) unsubstituted monomeric metallophthalocyanines, (b) substituted monomeric metallophthalocyanines (peripheral or axial), (c) polymeric metallophthalocyanines and (d) double-decker metallophthalocyanines.

Because of their stable electronic configuration, these molecules are chemically inert. Their chemical reactivity remains restricted to substitution or redox reactions in which electrons or hydrogen atoms are switched by suitable oxidizing/reducing agents, acid/base

reactions or central metal atoms substitution without altering the aromatic character of the macrocycle. Additions or ring opening are not commonly observed reactions in phthalocyanines and require drastic conditions. Phthalocyanines are thermally very stable with sublimation temperatures higher than 400°C. Their robustness to chemical agents and intense electromagnetic radiations are also noticeable.

5.2.4. Electronic properties and gas sensing applications

Besides different properties of metallophthalocyanines highlighted above, electronic properties and particularly π -electron delocalization on macrocycles are of prime importance in context of their applications in organic electronics including gas sensors. Two dimensional delocalization of π -electrons in disk shaped divalent metallophthalocyanines gives rise to interesting optical and electrical properties. These electrons are distributed on a molecular surface area of $55 \times 10^{-20} \text{ m}^2$, which forms molecular surface density of 7.5×10^{19} loosely bound and mobile π -electrons per square meter in phthalocyanine ring. Because of the delocalization of these π -electrons on macrocycle, these materials manifest intense absorption in the visible region of electromagnetic spectrum. That is why these materials are stable blue and green dyes and pigments. The flexibilities of these materials to manipulate their structure impart tremendous variations in their optoelectronic properties [112-116].

Multiple chemical calculations for the determination of the electronic structure of phthalocyanines were reported in the past [117, 118]. All these calculations were mainly focused on the determination of Highest Occupied Molecular Orbital (HOMO) and Lowest Unoccupied Molecular Orbital (LUMO) levels without considering the low lying molecular energy levels. The molecular orbitals of metallophthalocyanines are formed by the linear combination of metal orbitals and phthalocyanine electronic orbitals, provided metal orbitals have similar symmetry as of phthalocyanine orbitals [119]. The molecular energy levels of

metallophthalocyanines have been represented in a simple scheme in Fig. 6. The names of the orbitals are based on the D_{4h} symmetry of metallophthalocyanines in space. The presence of central metal atom introduces a new energy level having a close resemblance to the parent electronic states of the central metal atom. Different electronic transitions as shown in the scheme give rise to various bands in optical absorption spectra of phthalocyanines. In thin film arrangements, the molecular energy states of metallophthalocyanines modifies because of intermolecular interactions. The forces which keep the molecules in condensed phase are of an electrical nature, being mostly dipole-dipole or induced dipole-induced dipole attractions. Molecules in the condensed phase are stacked on each other through π - π interactions.

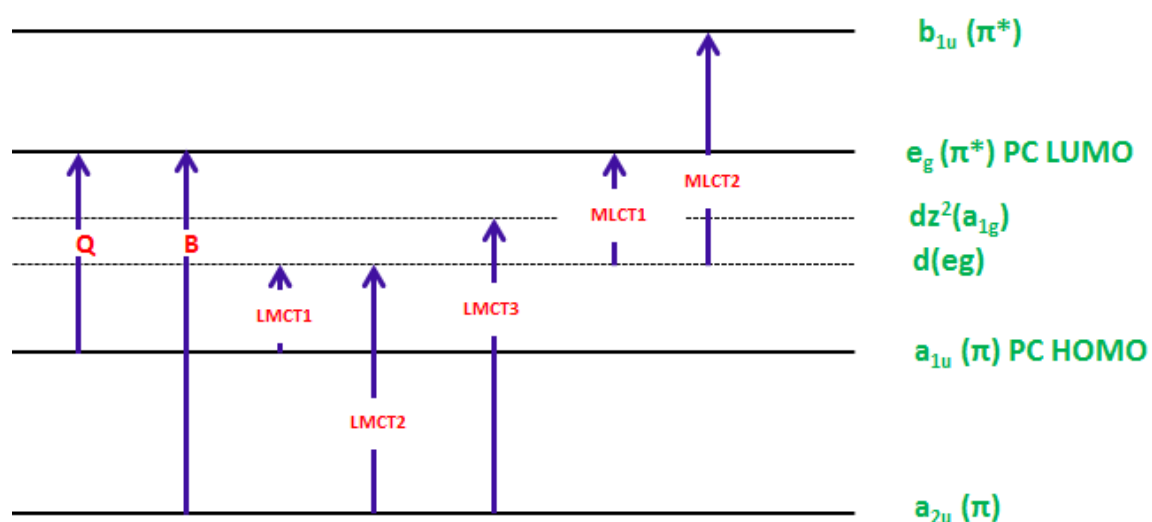


Fig. 6: Electronic energy levels of a metallophthalocyanine molecule.

Because of continuous delocalization of π -electrons on the phthalocyanine macrocycle they exhibit attractive semiconducting behavior [120]. The conductivity phenomenon in metallophthalocyanine systems can be due to either the intrinsic properties of a particular phthalocyanine or generally to the organization of the molecules at supramolecular level with an extended orbital overlap along the conducting pathway. Many phthalocyanines in solid state exhibit n-type or p-type semiconducting behavior. The type of the semiconducting nature

is decided by the nature of central metal atom and substituents present at the peripheral sites [121, 122]. For example, copper phthalocyanine (CuPc) is a p-type semiconductor with a band gap (HOMO-LUMO energy gap) of 2.04 eV whereas hexadecafluoro copper phthalocyanine (F₁₆CuPc) is n-type semiconductor of band gap 1.93 eV. The variation in electrical properties coming because of change in central metal atom is manifested in lutetium bis-phthalocyanine, which is an intrinsic radical semiconductor (p-type) of band gap 0.5 eV. Such diverse semiconducting properties of these materials are utilized in their applications in photovoltaics [123-127] and gas sensors [128-132]. The versatility of these materials because of their semiconducting properties, optical absorption and aromatic structure make them relevant for gas detection as sensitive layer on different types of transducers. Scientific works were reported in past about the use of phthalocyanines in resistive [24], optical [133] and acoustic transducers [134] for gas detection. A large number of chemical species which are known as potential pollutants in atmosphere were targeted using phthalocyanines based gas sensors. It includes VOCs [134], NO₂ [98], Ozone [135] and H₂S [136].

More especially, the relevance of phthalocyanines for their potential use as a sensitive coating for BTX detection is associated to the presence of π -electron density, their aromatic character and the presence of benzene ring in the macrocycle. Because of the presence of delocalized π -electrons in both phthalocyanines and BTX, they can interact to each other through π - π stacking [137-141] as depicted in Fig. 7. This is a non-covalent interaction between two delocalized π -systems because of mutual polarization of π -system of interacting species. Considering the non-covalent nature of interactions, these are weak forces in terms of magnitude as explained in the previous section for stacking of phthalocyanines macrocycles. Such interaction can lead to reversible adsorption of BTX molecules on phthalocyanines thin films. The strength and extent of these interactions can be modulated by changing the

electronic environment around the macrocycle through peripheral substitution or via change of metal atom.

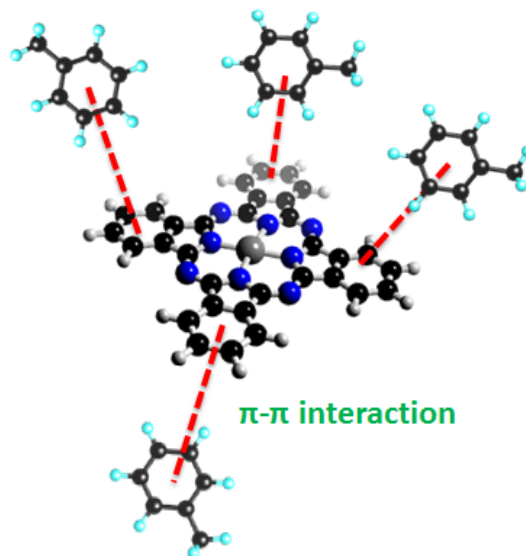


Fig. 7: Representation of π - π interactions between metallophthalocyanines and toluene.

5.3. Choice of transducing mode

If the nature of the sensitive material is the first key-parameter in gas sensor development, the transducing mode must be chosen for its ability to convert one property of the sensing material modulated by the target gas into suitable signal. Because of the nature of interactions involved between phthalocyanines and BTX gases, Quartz Crystal Microbalance (QCM) was selected. The working principle of QCM will be detailed in next chapter. Phthalocyanine materials because of their rich solution chemistry and high thermal stability can be coated on the active electrode area of QCM using multiple deposition techniques. The exposure to BTX gases can lead to their adsorption on the sensor surface because of π - π stacking leading to an overall increase in mass of the QCM and thereby decrease in oscillating frequency of QCM in accordance with Sauerbrey equation. With the availability

of synthesis methodologies for substituted phthalocyanines, a variety of structural modifications can be performed to enhance sensitivity and selectivity. Thus, several types of phthalocyanine (free, metallic, dimer, and substituted) will be investigated and their sensing potentialities will be assessed.

5.4. Phthalocyanines based QCM sensors for BTX detection: previous studies

This scientific approach is motivated by the previous studies on phthalocyanines-based QCM sensors focused on BTX measurements in gaseous phases. Most of the developments were done for a panel of VOCs including among others BTX gases. The use of phthalocyanine materials as active coating on QCM device for VOCs detection was explored in detail at first by W. Gopel [142]. Although it was a generalized study of VOCs detection using thin film coating of phthalocyanines and similar materials (inducing π - π interaction with aromatic analytes) on QCM, it established the affinity of benzenoid chemical species towards these materials. In the same year, a few other studies were reported about phthalocyanines based QCM sensors for VOCs detection by Ozturk et al. [143]. They used peripherally substituted and multi-nuclear metallophthalocyanines coated on QCM. They used long alkyl chain peripheral ligand to facilitate dissolution of metallophthalocyanines in organic solvents and improved adherence at the QCM surface. The sensors showed high sensitivity to VOCs especially to species with high boiling points such as tetra-chloroethylene, toluene and chloroform. Detection limit for toluene was measured as 5 ppm. K-D Schierbaum et al. [144] reported VOCs sensing properties of QCM coated with different soluble transition metallophthalocyanines. Sensor was sensitive (detection limit for toluene 50 ppm) and had fast response time (7 min). In 1996, A. Battenberg et al. proposed an interesting studies of

different phthalocyanines materials based QCM sensors for organic solvents vapor detection [145]. He studied VOCs sensing properties of different unsubstituted and substituted metallophthalocyanines on QCM. Later works by Fietzek et al. [134, 146] were exemplary which highlighted the sensitivity of different substituted metallophthalocyanines towards BTX gases. The interactions of gas molecules on sensor surface were highlighted in particular and an adsorption model for gas binding on the sensing layer was proposed. In recent years, M. Harbeck et al. [147, 148] highlighted enhanced sensitivity of soluble metallophthalocyanines substituted with fluoroalkyl oxy coated on QCM towards VOCs in gas as well as in liquid media. Sensor exhibited very high sensitivity for toluene and xylene with detection limit of 13 and 2 ppm respectively.

References

1. *Air quality guidelines for Europe. Copenhagen, WHO Regional Office for Europe.* WHO Regional Publications, European Series, No. 91, 2012. **second edition.**
2. Pachauri, R.K. *IPCC, 2007: Climate Change 2007: Synthesis Report. Contribution of Working Groups I, II and III to the Fourth Assessment Report of the Intergovernmental Panel on Climate Change.* IPCC Geneva, 2007
3. *7 million premature deaths annually linked to air pollution.* WHO media center, Geneva, 25 March 2014.
4. Lelieveld, J., et al., *The contribution of outdoor air pollution sources to premature mortality on a global scale.* Nature, 2015. **525**(7569): p. 367-371.
5. Edokpolo, B., et al., Connell, *Health Risk Assessment of Ambient Air Concentrations of Benzene, Toluene and Xylene (BTX) in Service Station Environments.* International Journal of Environmental Research and Public Health, 2014. **11**(6): p. 6354-6374.
6. *National Ambient Air Quality Standards (NAAQS).* Air and Radiation, US EPA 2015; Available from: <http://www3.epa.gov/ttn/naaqs/>.
7. *Health Effects Glossary.* Air and Radiations, US EPA 2015; Available from: <http://www3.epa.gov/airtoxics/hlthef/hapglossaryrev.html>.
8. Rani, B., et al., *Photochemical Smog Pollution and Its Mitigation Measures.* Journal of Advanced Scientific Research, 2011. **2**(4): p. 28-33.
9. *Europe's Environment: The Second Assessment — an overview.*, European Environment Agency., Copenhagen 25 June 1998.
10. Sateesh. N., et al., *Urban air pollution trend in India- present scenario.* International Journal of Innovative Research in Science, Engineering and Technology, 2013. **2**(8): p. 3738-3747.
11. *Air quality in Paris region 2014.* AirParif, Paris May 2015.

12. Kim, H.H., et al., *Risk assessment of volatile organic compounds (VOCs) and formaldehyde in Korean public facilities : Derivation of health protection criteria levels*. Asian Journal of Atmospheric Environment. **5**(2): p. 121-135.
13. He, Z., et al., *Pollution characteristics and health risk assessment of volatile organic compounds emitted from different plastic solid waste recycling workshops*. Environment International, 2015. **77**(0): p. 85-94.
14. Akdeniz, N., et al., *Health risk assessment of occupational exposure to hazardous volatile organic compounds in swine gestation, farrowing and nursery barns*. Environmental Science: Processes & Impacts, 2013. **15**(3): p. 563-572.
15. Chang, E.-E., et al., *Health risk assessment of exposure to selected volatile organic compounds emitted from an integrated iron and steel plant*. Inhalation Toxicology, 2010. **22**(S2): p. 117-125.
16. Chang, T.Y., et al., *Exposure and Health Risk Assessment of Volatile Organic Compounds on Residents Adjunctive With the Central Industrial Park*. Epidemiology, 2006. **17**(6): p. S159.
17. *Indoor air - Part 6: Determination of volatile organic compounds in indoor and test chamber air by active sampling on Tenax TA sorbent, thermal desorption and gas chromatography using MS or MS-FID*. ISO 16000-6, 2011. **3**: p. 29.
18. *Volatile Organic Compounds (VOCs); Technical Overview*. US EPA 2015; Available from: <http://www.epa.gov/iaq/voc2.html>.
19. *On the limitation of emissions of volatile organic compounds due to the use of organic solvents in certain activities and installations. Council Directive no. 1999/13/CE of 11 March 1999* European council.
20. Maugeri, F.S., *MACBETH –Monitoring of Atmospheric Concentrations of Benzene in European Towns and Homes*. 1999.

21. Wallace, L., *The Total Exposure Assessment Methodology (TEAM) Study: Summary and Analysis*. Office of Research and Development, U.S. EPA, Washington, D.C, 1987. **1**.
22. Sarigiannis, D., et al., *INTERA BTEX case study*. Appendix-5, March 2012; Available from: <http://www.intera-home.eu/TheProject/FinalReports.aspx>.
23. *Presentation on the INTERA BTEX case study 2012*; Available from: <http://www.intera-home.eu/NewsEvents/Workshop/Presentations.aspx>.
24. Brunet, J., et al., *An optimised gas sensor microsystem for accurate and real-time measurement of nitrogen dioxide at ppb level*. Sensors and Actuators B: Chemical, 2008. **134**(2): p. 632-639.
25. Varenne, C., et al., *Comparison of InP Schottky diodes based on Au or Pd sensing electrodes for NO₂ and O₃ sensing*. Solid-State Electronics, 2012. **72**(0): p. 29-37.
26. Verma, D.K., et al., *Benzene in gasoline and crude oil: occupational and environmental implications*. AIHA J (Fairfax, Va), 2002. **63**(2): p. 225-30.
27. *Occupational safety and health guidelines for benzene: a potential human carcinogen*. NIOSH, USA, 1988.
28. *Public health statement for benzene*. Agency for Toxic Substances and Disease Registry (ATSDR), 2007. **CAS#: 71-43-2**.
29. Kandyala, R., et al., *Xylene: An overview of its health hazards and preventive measures*. Journal of Oral and Maxillofacial Pathology : JOMFP, 2010. **14**(1): p. 1-5.
30. *Public Health statement: Toluene*. Agency for Toxic Substances and Disease Registry (ATSDR), 2000(CAS#: 108-88-3).
31. *Occupational health guidelines for Toluene*. NIOSH, USA, 1978.

32. *Integrated Risk Information System (IRIS) on Benzene*. National Center for Environmental Assessment, Office of Research and Development, US EPA, Washington, DC, 2009.
33. *IARC monographs on the evaluation of carcinogenic risks to humans. Overall evaluations of carcinogenicity: an updating of IARC Monographs*. International Agency for Research on Cancer, Lyon 1987. **1-42. Suppl. 7**: p. 37-38.
34. Hayes, R.B., et al., *Benzene and the dose-related incidence of hematologic neoplasms in China*. Chinese Academy of Preventive Medicine--National Cancer Institute Benzene Study Group. J Natl Cancer Inst, 1997. **89**(14): p. 1065-1071.
35. Protano, C., et al., *A systematic review of benzene exposure during pregnancy and adverse outcomes on intrauterine development and birth: still far from scientific evidence*. Ann Ig, 2012. **24**(6): p. 451-463.
36. Katukam, V., et al., *Effect of benzene exposure on fertility of male workers employed in bulk drug industries*. Genet Test Mol Biomarkers, 2012. **16**(6): p. 592-597.
37. Mandani, P., et al., *Cytotoxic Effects of Benzene Metabolites on Human Sperm Function: An In Vitro Study*. ISRN Toxicology. Article ID 397524, 2013. **2013**: p. 1-6.
38. Juntunen, J., et al., *Nervous system effects of long-term occupational exposure to toluene*. Acta Neurol Scand, 1985. **72**(5): p. 512-517.
39. Donald, J.M., et al., *Reproductive and developmental toxicity of toluene: a review*. Environmental Health Perspectives, 1991. **94**: p. 237-244.
40. David Penney, V.B., Stylianos Kephelopoulos, Dimitrios, *WHO Guidelines for indoor air quality: selected pollutants*. World Health Organization, Geneva, 2010.
41. *International Program on chemical safety, Environmental Health Criteria 190: Xylene*. World Health Organization Geneva, 1997.
42. *Air Quality Standard: Benzene*. European Commission, 2010.

43. *Relating to limit values for benzene and carbon monoxide in ambient air.* European Union Directive 2000/69/EC of the European parliament and of the council of 16 November 2000. Off. J., 2000. **313**: p. 10.
44. *French Regulations on VOC emissions from construction products: Compulsory VOC emissions labelling.* 2011.
45. Serrano, G., et al., *Assessing the reliability of wall-coated microfabricated gas chromatographic separation columns.* Sensors and Actuators B: Chemical, 2009. **141**(1): p. 217-226.
46. Zampolli, S., et al., *Real-time monitoring of sub-ppb concentrations of aromatic volatiles with a MEMS-enabled miniaturized gas-chromatograph.* Sensors and Actuators B: Chemical, 2009. **141**(1): p. 322-328.
47. Lahlou, H., et al., *Gas phase micro-preconcentrators for benzene monitoring: A review.* Sensors and Actuators B: Chemical, 2013. **176**(0): p. 198-210.
48. Thammakhet, C., et al., *Monitoring of BTX by passive sampling in Hat Yai.* Songklanakarin J. Sci. Technol. Environmental & Hazardous Management, 2004. **26**: p. 10.
49. Chan, L., et al., *A study of bus commuter and pedestrian exposure to traffic air pollution in Hong Kong.* Environment International, 1993. **19**(2): p. 121-132.
50. Son, B., et al., *Estimation of occupational and nonoccupational nitrogen dioxide exposure for Korean taxi drivers using a microenvironmental model.* Environ Res, 2004. **94**(3): p. 291-296.
51. Chan, L.Y., et al., *Commuter exposure to particulate matter in public transportation modes in Hong Kong.* Atmospheric Environment, 2002. **36**(21): p. 3363-3373.
52. Moseley, P.T. and J. Crocker, *Sensor Materials.* CRC Press 1996: Taylor & Francis.
53. Janata, J., *Principles of Chemical Sensors.* 2 ed. 2009: Springer US.

54. International Vocabulary of Metrology– *Basic and General Concepts and Associated Terms (VIM)*, 3rd ed. 2008.
55. Hulanicki, A., et al., *Chemical sensors: definitions and classification*, in *Pure and Applied Chemistry*. 1991. **63(9)**: p. 1247-1250.
56. Ueno, Y., et al., *Microfluidic Device for Airborne BTEX Detection*. *Analytical Chemistry*, 2001. **73(19)**: p. 4688-4693.
57. Ueno, Y., et al., *Air-Cooled Cold Trap Channel Integrated in a Microfluidic Device for Monitoring Airborne BTEX with an Improved Detection Limit*. *Analytical Chemistry*, 2002. **74(7)**: p. 1712-1717.
58. Ueno, Y., et al., *Portable automatic BTX measurement system with microfluidic device using mesoporous silicate adsorbent with nano-sized pores*. *Sensors and Actuators B: Chemical*, 2003. **95(1–3)**: p. 282-286.
59. Ueno, Y., et al., *Separate Detection of BTX Mixture Gas by a Microfluidic Device Using a Function of Nanosized Pores of Mesoporous Silica Adsorbent*. *Analytical Chemistry*, 2002. **74(20)**: p. 5257-5262.
60. Ueno, Y., et al., *High benzene selectivity of uniform sub-nanometre pores of self-ordered mesoporous silicate*. *Chemical Communications*, 2004(6): p. 746-747.
61. Camou, S., et al., *Selective aqueous benzene detection at ppb level with portable sensor based on pervaporation extraction and UV-spectroscopy*. *Procedia Chemistry*, 2009. **1(1)**: p. 1495-1498.
62. Camou, S., et al. *Ppt-level aqueous benzene detection with an UV-spectroscopy based portable sensor*. *Sensors, 2009 IEEE*: p 2021-2024.
63. Hue, J., et al., *Benzene and xylene detection by absorbance in the range of 10–100 ppb application: Quality of indoor air*. *Sensors and Actuators B: Chemical*, 2013. **189**: p. 194-198.

64. Sekhar, P.K., et al., *Detection of Harmful Benzene, Toluene, Ethylbenzene, Xylenes (BTEX) Vapors Using Electrochemical Gas Sensors*. ECS Electrochemistry Letters, 2014. **3**(2): p. B1-B4.
65. Xu, Z., et al., *Detection of Benzene, Toluene, Ethyl Benzene, and Xylenes (BTEX) Using Toluene Dioxygenase-Peroxidase Coupling Reactions*. Biotechnology Progress, 2003. **19**(6): p. 1812-1815.
66. Ghaddab, B., et al., *Benzene monitoring by micro-machined sensors with SnO₂ layer obtained by using micro-droplet deposition technique*. Sensors and Actuators B: Chemical, 2011. **152**(1): p. 68-72.
67. Zhang, W.-M., et al., *Detection of VOCs and their concentrations by a single SnO₂ sensor using kinetic information*. Sensors and Actuators B: Chemical, 2007. **123**(1): p. 454-460.
68. Qi, Q., et al., *Synthesis and toluene sensing properties of SnO₂ nanofibers*. Sensors and Actuators B: Chemical, 2009. **137**(2): p. 471-475.
69. Lee, D.-S., et al., *Fabrication and characteristics of SnO₂ gas sensor array for volatile organic compounds recognition*. Thin Solid Films, 2002. **416**(1–2): p. 271-278.
70. Kanda, K., et al., *Development of a WO₃ thick-film-based sensor for the detection of VOC*. Sensors and Actuators B: Chemical, 2005. **108**(1–2): p. 97-101.
71. Ke, M.-T., et al., *A MEMS-based Benzene Gas Sensor with a Self-heating WO₃ Sensing Layer*. Sensors, 2009. **9**(4): p. 2895-2906.
72. Dutta, K., et al., *An efficient BTX sensor based on p-type nanoporous titania thin films*. Microelectronics Reliability, 2015. **55**(3–4): p. 558-564.
73. Zhu, B.L., et al., *Improvement in gas sensitivity of ZnO thick film to volatile organic compounds (VOCs) by adding TiO₂*. Materials Letters, 2004. **58**(5): p. 624-629.

74. Ma, H., et al., *Highly toluene sensing performance based on monodispersed Cr₂O₃ porous microspheres*. Sensors and Actuators B: Chemical, 2012. **174**: p. 325-331.
75. Acharyya, D., et al., *An efficient BTX sensor based on ZnO nanoflowers grown by CBD method*. Solid-State Electronics, 2015. **106**: p. 18-26.
76. Li, Z., et al., *Carbon Nanotube Film Sensors*. Advanced Materials, 2004. **16**(7): p. 640-643.
77. Leghrib, R., et al., *Room-temperature, selective detection of benzene at trace levels using plasma-treated metal-decorated multiwalled carbon nanotubes*. Carbon, 2010. **48**(12): p. 3477-3484.
78. Leghrib, R., et al., *Quantitative trace analysis of benzene using an array of plasma-treated metal-decorated carbon nanotubes and fuzzy adaptive resonant theory techniques*. Analytica Chimica Acta, 2011. **708**(1-2): p. 19-27.
79. Castro, M., et al., *Novel e-nose for the discrimination of volatile organic biomarkers with an array of carbon nanotubes (CNT) conductive polymer nanocomposites (CPC) sensors*. Sensors and Actuators B: Chemical, 2011. **159**(1): p. 213-219.
80. Parikh, K., et al., *Flexible vapour sensors using single walled carbon nanotubes*. Sensors and Actuators B: Chemical, 2006. **113**(1): p. 55-63.
81. Zimmerman, C., *Conception, réalisation et étude de micro-capteurs à ondes de Love pour applications en milieu gazeux : Cas de la détection de composés organophosphorés*. thesis, 2002.
82. Sauerbrey, G., *Use of quartz oscillators for weighing thin layers and for microbalance*. Zeitschrift für Physik, 1959. **155**(2): p. 206-222.
83. Pejcic, B., et al., *Modifying the response of a polymer-based quartz crystal microbalance hydrocarbon sensor with functionalized carbon nanotubes*. Talanta, 2011. **85**(3): p. 1648-1657.

84. Si, P., et al., *Polymer coated quartz crystal microbalance sensors for detection of volatile organic compounds in gas mixtures*. *Analytica Chimica Acta*, 2007. **597**(2): p. 223-230.
85. Matsuguchi, M., et al., *Molecular imprinting strategy for solvent molecules and its application for QCM-based VOC vapor sensing*. *Sensors and Actuators B: Chemical*, 2006. **113**(1): p. 94-99.
86. Matsuguchi, M., et al., *Chemically modified copolymer coatings for mass-sensitive toluene vapor sensors*. *Sensors and Actuators B: Chemical*, 2008. **131**(2): p. 652-659.
87. Filippov, A.P., et al., *Quartz crystal microbalance modified with Cu(II) stearate and octadecylamine co-ordination chemical compounds for detection of volatile organic compounds*. *Sensors and Actuators B: Chemical*, 2007. **126**(2): p. 375-381.
88. Şen, Z., et al., *Metal complexes of vic-dioximes for chemical gas sensing*. *Sensors and Actuators B: Chemical*, 2011. **160**(1): p. 1203-1209.
89. Zhou, R., et al., *Silicon-containing monomers, oligomers and polymers as sensitive coatings for the detection of organic solvent vapors*. *Sensors and Actuators B: Chemical*, 1995. **26**(1-3): p. 121-125.
90. Grate, J.W., *Acoustic Wave Microsensor Arrays for Vapor Sensing*. *Chemical Reviews*, 2000. **100**(7): p. 2627-2648.
91. Penza, M., et al., *Carbon nanotubes as SAW chemical sensors materials*. *Sensors and Actuators B: Chemical*, 2004. **100**(1-2): p. 47-59.
92. Penza, M., et al., *Carbon nanotubes-based surface acoustic waves oscillating sensor for vapour detection*. *Thin Solid Films*, 2005. **472**(1-2): p. 246-252.
93. Penza, M., et al., *Carbon nanotubes-coated multi-transducing sensors for VOCs detection*. *Sensors and Actuators B: Chemical*, 2005. **111-112**(0): p. 171-180.

94. Sayago, I., et al., *Surface acoustic wave gas sensors based on polyisobutylene and carbon nanotube composites*. *Sensors and Actuators B: Chemical*, 2011. **156**(1): p. 1-5.
95. Sayago, I., et al., *New sensitive layers for surface acoustic wave gas sensors based on polymer and carbon nanotube composites*. *Sensors and Actuators B: Chemical*, 2012. **175**(0): p. 67-72.
96. Truax, S.B., et al., *Mass-Sensitive Detection of Gas-Phase Volatile Organics Using Disk Microresonators*. *Analytical Chemistry*, 2011. **83**(9): p. 3305-3311.
97. Baimpos, T., et al., *A polymer-Metglas sensor used to detect volatile organic compounds*. *Sensors and Actuators A: Physical*, 2010. **158**(2): p. 249-253.
98. Brunet, J., et al., *Improved selectivity towards NO₂ of phthalocyanine-based chemosensors by means of original indigo/nanocarbons hybrid material*. *Talanta*, 2014. **127**(0): p. 100-107.
99. Leznoff, C.C. and A.B.P. Lever, *Phthalocyanines: Properties and applications*. Vol. 1-4. 1989, 1993, 1996: Wiley.
100. Kadish, K.M., K.M. Smith, and R. Guilard, *The Porphyrin Handbook: Phthalocyanines : properties and materials*. 2003: Academic Press.
101. Nemykina, V.N., et al., *Synthesis of substituted phthalocyanines*. *ARKIVOC*, 2010(i): p. 136-208.
102. BEKAROĞLU, Ö., *Synthesis of phthalocyanines and related compounds*. *Journal of Porphyrins and Phthalocyanines*, 2000. **04**(05): p. 465-473.
103. Dini, D., et al., *Synthesis of axially substituted gallium, indium and thallium phthalocyanines with nonlinear optical properties*. *ARKIVOC*, 2006(3): p. 77-96.
104. Çoşut, B., et al., *Synthesis and properties of axially-phenoxy-cyclotriphosphazenylyl substituted silicon phthalocyanine*. *Polyhedron*, 2010. **29**(2): p. 675-682.

105. Dini, D. and M. Hanack, *107 - Physical Properties of Phthalocyanine-based Materials*, in *The Porphyrin Handbook*, K.M.K.M.S. Guillard, Editor. 2003, Academic Press: Amsterdam. p. 1-36.
106. Kobayashi, T., et al., *High-resolution TEM images of zinc phthalocyanine polymorphs in thin films*. Acta Crystallographica Section A, 1981. **37**(5): p. 692-697.
107. Denisyuk, I.Y., et al., *Polymorphism of phthalocyanine nanocrystals: $\beta \rightarrow X \rightarrow \beta$ polymorphous transformations*. Optics and Spectroscopy, 2004. **96**(2): p. 235-239.
108. Hassan, A.K., et al., *Structural Studies of Thermally Evaporated Thin Films of Copper Phthalocyanine*. physica status solidi (a), 1992. **132**(1): p. 91-101.
109. Milaeva, E.R., et al. *The Redox Chemistry of Metallophthalocyanines in Solution*. 1992; Available from: <http://handle.dtic.mil/100.2/ADA251744>.
110. Ghani, F., et al., *Solubility Properties of Unsubstituted Metal Phthalocyanines in Different Types of Solvents*. Journal of Chemical & Engineering Data, 2012. **57**(2): p. 439-449.
111. Lee, W., et al., *Synthesis and characterization of solubility enhanced metal-free phthalocyanines for liquid crystal display black matrix of low dielectric constant*. Dyes and Pigments, 2012. **92**(3): p. 942-948.
112. Neghabi, M., et al., *Investigation of structural and optoelectronic properties of annealed nickel phthalocyanine thin films*. Materials Science in Semiconductor Processing, 2014. **17**(0): p. 13-20.
113. Pirriera, M.D., et al., *Optoelectronic properties of CuPc thin films deposited at different substrate temperatures*. Journal of Physics D: Applied Physics, 2009. **42**(14): p. 145102.

114. Soliman, H.S., et al., *Structural and transport properties of evaporated iron phthalocyanine (FePc) thin films*. The European Physical Journal - Applied Physics, 2003. **21**(03): p. 187-193.
115. Soliman, H.S., et al., *Structural and electrical properties of thermally evaporated cobalt phthalocyanine (CoPc) thin films*. The European Physical Journal - Applied Physics, 2007. **37**(01): p. 1-9.
116. Riad, S., *Dark and photoelectric conversion properties of p-MgPc/n-Si (Organic/Inorganic) heterojunction cells*. Thin Solid Films, 2000. **370**(1–2): p. 253-257.
117. Lee, L.K., et al., *Theoretical characterization of phthalocyanine, tetraazaporphyrin, tetrabenzoporphyrin, and porphyrin electronic spectra*. The Journal of Physical Chemistry, 1982. **86**(20): p. 3926-3931.
118. Gouterman, M., et al., *Spectra of porphyrins: Part II. Four orbital model*. Journal of Molecular Spectroscopy, 1963. **11**(1–6): p. 108-127.
119. Liao, M.-S., et al., *Electronic structure and bonding in metal phthalocyanines, Metal=Fe, Co, Ni, Cu, Zn, Mg*. The Journal of Chemical Physics, 2001. **114**(22): p. 9780-9791.
120. de la Torre, G., et al., *Functional Phthalocyanines: Synthesis, Nanostructuration, and Electro-Optical Applications*, in *Functional Phthalocyanine Molecular Materials*, J. Jiang, Editor. 2010, Springer Berlin Heidelberg. p. 1-44.
121. Bouvet, M., et al., *Electrical transduction in phthalocyanine-based gas sensors: from classical chemiresistors to new functional structures*. Journal of Porphyrins and Phthalocyanines, 2009. **13**(01): p. 84-91.

122. Murdey, R., et al., *Frontier Electronic Structures in Fluorinated Copper Phthalocyanine Thin Films Studied Using Ultraviolet and Inverse Photoemission Spectroscopies*. *Molecular Crystals and Liquid Crystals*, 2006. **455**(1): p. 211-218.
123. Varotto, A., et al., *Phthalocyanine Blends Improve Bulk Heterojunction Solar Cells*. *Journal of the American Chemical Society*, 2010. **132**(8): p. 2552-2554.
124. Walter, M.G., et al., *Porphyrins and phthalocyanines in solar photovoltaic cells*. *Journal of Porphyrins and Phthalocyanines*, 2010. **14**(09): p. 759-792.
125. Yoon, S.M., et al., *Fluorinated Copper Phthalocyanine Nanowires for Enhancing Interfacial Electron Transport in Organic Solar Cells*. *Nano Letters*, 2012. **12**(12): p. 6315-6321.
126. Yuen, A.P., et al., *Photovoltaic properties of M-phthalocyanine/fullerene organic solar cells*. *Solar Energy*, 2012. **86**(6): p. 1683-1688.
127. Ragoussi, M.-E., et al., *Recent Advances in Phthalocyanine-Based Sensitizers for Dye-Sensitized Solar Cells*. *European Journal of Organic Chemistry*, 2013. **2013**(29): p. 6475-6489.
128. Zhou, R., et al., *Phthalocyanines as Sensitive Materials for Chemical Sensors*. *Applied Organometallic Chemistry*, 1996. **10**(8): p. 557-577.
129. Muzikante, I., et al., *A Novel Gas Sensor Transducer Based on Phthalocyanine Heterojunction Devices*. *Sensors*, 2007. **7**(11): p. 2984-2996.
130. Öztürk, Z.Z., et al., *Recent studies chemical sensors based on phthalocyanines*. *Journal of Porphyrins and Phthalocyanines*, 2009. **13**(11): p. 1179-1187.
131. María, L.R.-M., et al., *Sensor Arrays Based on Phthalocyanines*, in *Multisensor Systems for Chemical Analysis*. 2014, Pan Stanford Publishing. p. 139-179.
132. Basova, T.V., et al., *Mesomorphic phthalocyanine as chemically sensitive coatings for chemical sensors*. *Sensors and Actuators B: Chemical*, 2003. **96**(1-2): p. 70-75.

133. Granito, C., et al., *Toluene vapour sensing using copper and nickel phthalocyanine Langmuir-Blodgett films*. Thin Solid Films, 1996. **284–285**: p. 98-101.
134. Fietzek, C., et al., *Soluble phthalocyanines as suitable coatings for highly sensitive gas phase VOC-detection*. Sensors and Actuators B: Chemical, 2000. **65**(1–3): p. 85-87.
135. Schütze, A., et al., *Quantitative ozone measurement using a phthalocyanine thin-film sensor and dynamic signal evaluation*. Sensors and Actuators B: Chemical, 1995. **23**(2–3): p. 215-217.
136. Kumar, A., et al., *Room temperature detection of H₂S by flexible gold–cobalt phthalocyanine heterojunction thin films*. Sensors and Actuators B: Chemical, 2015. **206**: p. 653-662.
137. Hunter, C.A., et al., *The nature of .pi.-.pi. interactions*. Journal of the American Chemical Society, 1990. **112**(14): p. 5525-5534.
138. Hunter, C.A., et al., *Aromatic interactions*. Journal of the Chemical Society, Perkin Transactions 2, 2001(5): p. 651-669.
139. Martinez, C.R., et al., *Rethinking the term "pi-stacking"*. Chemical Science, 2012. **3**(7): p. 2191-2201.
140. Sinnokrot, M.O., et al., *High-Accuracy Quantum Mechanical Studies of π - π Interactions in Benzene Dimers*. The Journal of Physical Chemistry A, 2006. **110**(37): p. 10656-10668.
141. Grimme, S., *Do Special Noncovalent π - π Stacking Interactions Really Exist?* Angewandte Chemie International Edition, 2008. **47**(18): p. 3430-3434.
142. Göpel, W., *Supramolecular and polymeric structures for gas sensors*. Sensors and Actuators B: Chemical, 1995. **24**(1–3): p. 17-32.

143. Öztürk, Z.Z., et al., *Soluble phthalocyanines for the detection of organic solvents: thin film structures with quartz microbalance and capacitance transducers*. Sensors and Actuators B: Chemical, 1995. **26**(1–3): p. 208-212.
144. Schiebaum, K.D., et al., *The interaction of transition metal phthalocyanines with organic molecules: a quartz-microbalance study*. Sensors and Actuators B: Chemical, 1995. **24**(1–3): p. 69-71.
145. Battenberg, A., et al., *Synthesis and test of organometallic materials as sensitive layers on quartz microbalance devices*. Sensors and Actuators B: Chemical, 1996. **30**(1): p. 29-34.
146. Fietzek, C., et al., *Soluble phthalocyanines as coatings for quartz-microbalances: specific and unspecific sorption of volatile organic compounds*. Sensors and Actuators B: Chemical, 1999. **57**(1–3): p. 88-98.
147. Harbeck, M., et al., *Phthalocyanines as sensitive coatings for QCM sensors: Comparison of gas and liquid sensing properties*. Sensors and Actuators B: Chemical, 2011. **155**(1): p. 298-303.
148. Harbeck, M., et al., *Preferential sorption of polar compounds by fluoroalkoxy substituted phthalocyanines for the use in sorption based gas sensors*. Sensors and Actuators B: Chemical, 2010. **150**(2): p. 616-624.

Chapter 2:

Experimental and characterization techniques

Chapter 2

Technical Overview of sensor developments

This chapter details all the techniques of realization, characterization, tests and validation implemented in the context of this work. At first, realization of sensing layers on crystal active surface is detailed. Processing of these materials and their layering on crystal surface were carried out at Institut Pascal, Clermont-Ferrand. Powdered and layered materials were then characterized through UV-Vis, FT-IR, SEM and XRD to confirm chemical purity of powdered materials, the structural stability of materials after deposition and organizations of molecules into the layers. Investigation of sensing characteristics of phthalocyanines based QCM sensors towards BTX were achieved on a lab-developed testing facility at room temperature. Development of sensor-testing setup was a multistage process which will be detailed. Calibration of this testing setup highlights a strong impact of surrounding temperature on sensor output signal. Such influences of thermal change were investigated in detail and temperature compensation was applied on sensor data to remove sensor response drifts due to temperature fluctuation.

1. Sample elaboration

1.1. Materials

We used commercially available phthalocyanines purchased from Sigma-Aldrich. These materials were used without any further purification for different scientific investigations. Following phthalocyanines materials were used for depositions on QCM surface:

- Copper (II) 2,9,16,23-tetra-tert-butyl-29H,31H-phthalocyanine (dye content >97%),
- Zinc (II) 2,9,16,23-tetra-tert-butyl-29H,31H-phthalocyanine (dye content >97%),
- 29H,31H-phthalocyanine (dye content >98%),
- Copper (II) phthalocyanine (dye content >90%),
- Zinc (II) phthalocyanine (dye content >97%),
- Cobalt (II) phthalocyanine (dye content >97%),
- Iron (II) phthalocyanine (dye content >90%),
- Copper (II) 1,2,3,4,8,9,10,11,15,16,17,18,22,23,24,25-hexadecafluoro-29H,31H-phthalocyanine (dye content > 80%),
- Zinc (II) 1,2,3,4,8,9,10,11,15,16,17,18,22,23,24,25-hexadecafluoro-29H,31H-phthalocyanine (dye content > 80%).

For BTX vapor generation, anhydrous benzene (99.8%), toluene (99.8%) and xylenes (99.8%) were purchased from Sigma-Aldrich. Lutetium bis phthalocyanine was used as received from our research collaborator at ICMUB, Dijon, where it was synthesized through solid phase reaction using Lutetium (III) acetate hydrate (99.9%), 1,2-dicyanobenzene (98%) in 1:8 molar ratio followed by treatment with DMF and ethanol for pure product extraction [1-3].

1.2. Transducing mode

As previously justified by the nature of predicted gas/material interactions, QCM were chosen as transducer in this work. Quartz is a natural oxide of silicon as SiO_2 in crystalline form. The high quality crystalline quartz is prepared by artificial route in vertical autoclave at high temperature and pressure. It exists in two different crystalline phase namely α -quartz and β -quartz. At low temperature α -quartz is stable which transforms into β -form at 573°C .

In the quartz crystal, cut-angle of the crystal determines the mode of oscillation of crystals. For QCM studies, AT-cut quartz is most commonly used. It is fabricated by slicing through a quartz rod with a cut angle of $35^\circ 10'$ with respect to the optical axis, as shown in Fig. 1. The main advantage of using AT cut quartz crystal in the context of our study is its nearly zero frequency drift with temperature around room temperature, i.e. for our working temperature. It is sometime also called as ST-cut or temperature stable cut QCM.

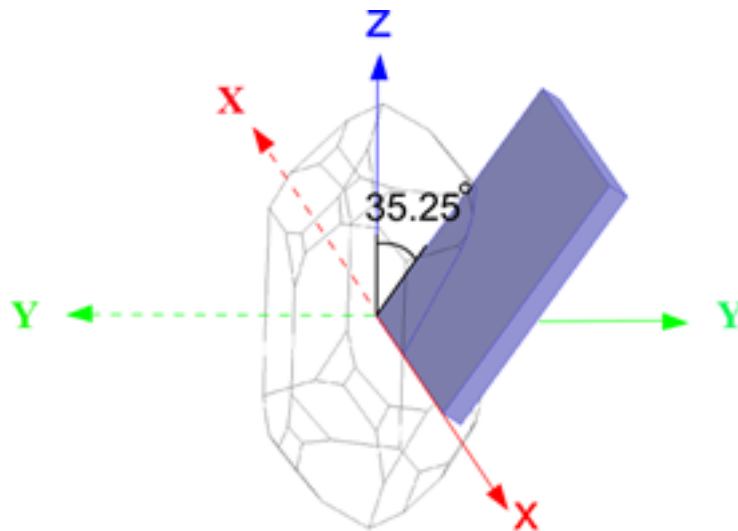


Fig. 1: AT-geometrical cut of a quartz crystal.

In QCM transducers, a thin disk sliced from single crystal of the α -quartz is used. The disk is sandwiched between two metal electrodes that are deposited on either side of the crystal. Gold electrodes have been the most commonly used in QCM studies, because of the

ease with which Au is evaporated and its superior electrical contact in electronic circuits. However, Cu, Ni, Pt and other metals have also been employed. A sub-layer of Cr can also be deposited to strengthen the adhesion of gold electrode onto the quartz. A typical quartz crystal is depicted in Fig. 2.

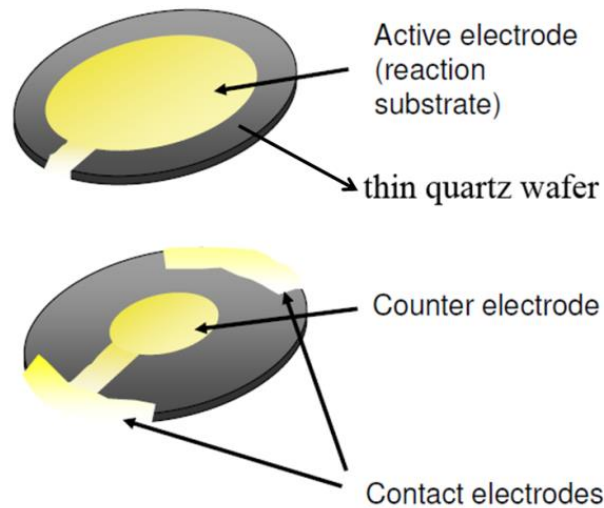


Fig. 2: Front and rear side of quartz crystal microbalance sensor.

When an electric field is applied between the electrodes the piezoelectric effect excites the wafer into mechanical vibration. The vibration motion of the quartz crystal leads to establishment of a transverse acoustic wave that propagates across the crystal, reflecting back into the crystal at the surface. A standing wave condition or resonance can be established when the acoustic wavelength is equal to twice the combined thickness of the crystal and electrodes. Thus, the resonance frequency is related to the thickness of the crystal by the following equation:

$$f_0 = v/2t \quad \text{Eq. 1}$$

where v is the velocity of the acoustic wave in AT cut quartz (3.34×10^4 m/sec), f_0 is the resonance frequency of the quartz crystal prior to the mass change and t is the thickness of the

quartz resonator. Typical operating frequencies of the QCM lie within the range of 5 to 10 MHz.

Application of QCM as a mass sensor is based on the fact that even a slight change in mass on the crystal surface induces a change in its resonance frequency. The quantitative estimation of this property was first given by G. Sauerbrey, according to that the change of mass per unit area, Δm , caused by adsorption or deposition of a substance on one side of the QCM is related directly to the change of frequency, Δf_m , by the equation (2) popularly known as Sauerbrey equation [4, 5]

$$\Delta f_m = -C_m \Delta m \quad \text{Eq 2}$$

where C_m is proportional to square of fundamental frequency of QCM f_0 according to equation shown below:

$$C_m = C_m^0 f_0^2 \quad \text{Eq 3}$$

The constant C_m^0 is determined by the properties of quartz only. For AT-cut quartz resonators, $C_m^0 = 2.257 \times 10^{-6} \text{ cm}^2 \text{ mg}^{-1} \text{ Hz}^{-1}$.

Thus, QCM-based sensor were developed on 5 MHz AT-cut quartz crystals of diameter 1 inch with Au/Cr electrodes purchased from MAXTEK, Inficon [6]. Crystals were used as received from the supplier without any further chemical and physical treatment before coatings.

1.3.Processing

As previously mentioned in chapter 1, the thermal stability of phthalocyanine macrocycle makes thermal evaporation suitable for thin layer achievement. It is a PVD deposition technique in which vapors can be produced from materials located in a source which is heated by direct resistance, radiations, electron-beam, laser-beam, eddy current or an

arc discharge. In our experimental procedures, resistive evaporator was used. It is most widely used technique for the organic compounds especially for those which are insoluble in common organic solvents. It has following advantages [7]:

- a) Impurity concentrations in the films will be very low.
- b) Materials sublime at lower temperature under vacuum.
- c) Mean free path of the vapor atoms are considerably large at lower pressure and hence homogeneous films are observed.
- d) A wide range of substrate can be used.

Phthalocyanines materials were layered on quartz crystals substrates using Veeco 770 thermal evaporator. Complete evaporation setup combined with vacuum system are depicted in Fig. 3. It consists of deposition chamber, vacuum pumps, evaporation source, substrate holder, rate monitor and process control. Vacuum in a range of 10^{-5} to 10^{-6} mbar was created inside the deposition chamber through a pumping system (combination of primary and secondary pump) linked to the bottom of the chamber. The material to be evaporated was heated in a tantalum crucible fixed between two electrodes in an evacuated chamber. The pressure measurements inside the vacuum chamber was achieved by a thermocouple gauge (for higher than 10 mbar) and penning gauge (lower than 10^{-3} mbar). For homogeneous and pure deposition of layers on substrate, minimum vacuum required in the evaporation chamber was 10^{-5} mbar. The rate of evaporation was controlled by an electronic rate controller integrated with the evaporation system. It consists of a feedback loop to control the power of the source and hence its temperature and evaporation rate. In all the evaporations performed, 0.2 nm/s rate was maintained. The thickness of evaporated mass on sensor substrate was monitored by a quartz crystal placed in close vicinity of substrate. From the frequency shifts of QCM because of material deposition, thickness of thin film was calculated (using density of material and acoustic impedance of device). It was assumed that thickness on substrate

surface is same as on QCM surface with negligible error. The substrates were maintained at room temperature during evaporation. No further heat treatment on deposited samples was performed post evaporation.

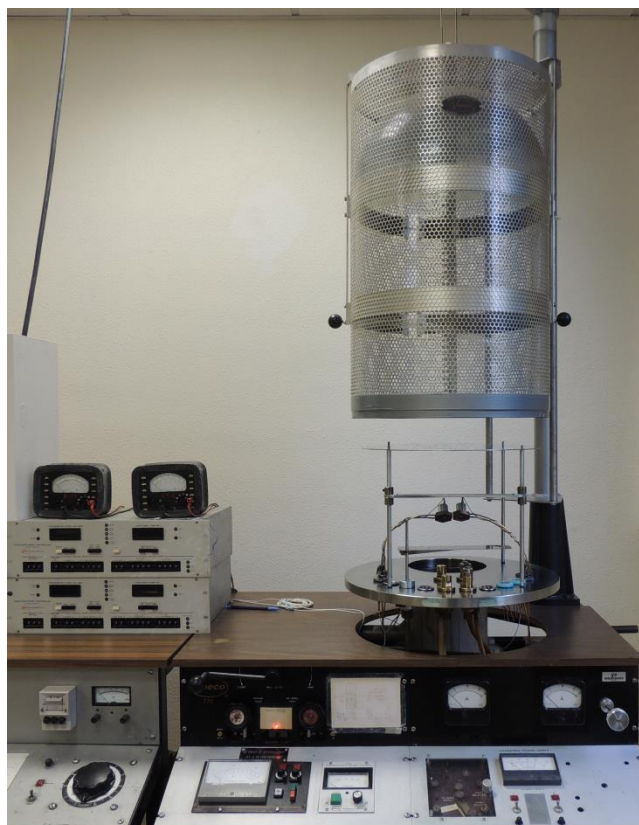


Fig. 3: Thermal evaporation system used to layer phthalocyanines materials on QCM at Institut Pascal, Clermont-Ferrand

2. Physical and chemical characterizations of materials

2.1. UV-Vis absorption

When an electromagnetic radiation passes through material (either in solution or in thin film) electrons in ground state can be promoted to excited state. Such electronic transition is accompanied by absorption of a part of the electromagnetic wave. If wavelength or frequency of absorbed photon lies in the ultraviolet or visible region of spectrum, it gives UV-Vis spectra of material. Quantification of such absorption phenomenon is explained by Beer-Lambert's law of optical absorption [8, 9].

Such absorption phenomena are studied by absorption spectrophotometer. In conventional spectrometers, hydrogen or deuterium lamps are commonly used as a source of UV-radiations while tungsten lamp is used for visible-radiation source. These electromagnetic radiations are passed through the sample which is held in a small square-section cell (usually 1 cm wide internally). Samples can be liquid (materials dissolved in solvents) or solid (usually in thin film coating). Radiation across the whole of the ultraviolet/visible range is scanned over a period of approximately 30 second, and radiation of the same frequency and intensity is simultaneously passed through a reference cell containing only the solvent or coating substrate. Photocells then detect the radiation transmitted and the spectrometer records the absorption by comparing the difference between the intensity of the radiation passing through the sample and the reference cells.

UV-Vis spectra of powdered material dissolved into appropriate organic solvents were recorded using Lambda 2S Perkin-Elmer spectrometer and using a 1 cm path length. The spectra were recorded in the 250–850 nm regions. In most of cases, materials were at first dissolved in chloroform solution followed by sonication for 20 min. Comparison of UV-Vis

absorption spectra of studied phthalocyanines materials from already established values can confirm the information provided by manufacturer about the purity of materials.

2.2. Fourier Transform Infrared spectroscopy

Infrared absorption spectroscopy is a part of electronic spectroscopy that concerns with the infrared region of electromagnetic spectrum. It can be used to identify and study the nature of chemical bonding between atoms in a molecule. It exploits the fact that molecules absorb infrared frequencies specific to their structure. The origin of such spectra relies on presence of vibrational energy component within a molecule. The vibrational energy component is a higher energy term and corresponds to the absorption of energy by a molecule as the component atoms vibrate about the mean center of their chemical bonds. When exposed to infrared radiation source, sample molecules selectively absorb radiation of specific wavelengths which causes vibration of specific sets of chemical bonds within molecule leading to a subsequent change in dipole moment (fundamental requirement of infrared activity). Consequently, the vibrational energy levels of sample molecules transfer from ground state to excited state. The frequency of the absorption peak determines the vibrational energy gap.

A basic IR spectrum is essentially a graph of infrared light absorbance (or transmittance) on the vertical axis vs. frequency or wavelength on the horizontal axis. Typical units used in IR spectra are reciprocal centimeters or wavenumbers. The common used region for infrared absorption spectroscopy is $4000 \sim 400 \text{ cm}^{-1}$ because the absorption radiations of most organic compounds are within this region. Fourier Transform Infrared (FT-IR) spectrometry was developed in order to overcome the limitations encountered with conventional IR measurement instruments. The main difficulty was the slow scanning

process. A method for measuring all of the infrared frequencies simultaneously, rather than individually, was needed. A common FT-IR spectrometer consists of a source, interferometer, sample compartment, detector, amplifier, A/D convertor, and a computer. The source generates infrared radiation which passes the sample through the interferometer and reaches the detector. Then the signal is amplified and converted to digital signal by the amplifier and analog-to-digital converter, respectively. Eventually, the signal is transferred to a computer in which Fourier transform is carried out.

Infrared spectra of studied phthalocyanine materials were recorded in powdered and layered forms using a Thermo Nicolet 5700 FT-IR spectrometer in transmission and ATR mode in a range of 400–4000 cm^{-1} with resolution 4 cm^{-1} . Since we used thermal evaporation method to achieve thin sensitive layers, thermal stability of phthalocyanines in evaporated films remains a concern. High temperature of evaporations can be critical to soft organic molecules like phthalocyanines. This is especially true for phthalocyanines substituted with bulky peripheral organic groups. An intercomparison of FT-IR spectra can technically highlight potential changes in chemical bonds into the molecular unit and so is an appropriate characterization technique to determine the effect of thermal evaporation on material.

2.3. X-Ray Diffraction

X-ray diffraction (XRD) is an analytical technique primarily used for phase identification of a crystalline material. It also gives information about organization of molecules/atoms in thin films and can provide information about their orientation, unit cells size and shape. X-ray diffraction is based on constructive interference of monochromatic X-rays and a crystalline sample. The interaction of the incident X-rays with the sample produces

constructive interferences (and a diffracted ray) when conditions satisfy Bragg's Law described by eq. 4:

$$n\lambda = 2d\sin\theta \quad \text{Eq. 4}$$

This law relates the wavelength λ of electromagnetic radiation to the diffraction angle θ and the lattice spacing d in a crystalline sample. These diffracted X-rays are then detected, processed and counted. This technique is non-destructive, so no special sample preparation is required.

A coating of 250 nm of studied phthalocyanine materials were made on glass substrate for X-ray diffraction analysis. These coatings were made keeping substrate at room temperature and no further heat treatment of samples was made after deposition. Crystallinity of the films coated on glass and powder phthalocyanines materials was determined by Siemens D501 diffractometer with Cu (K_{α}) radiation (the wavelength λ is 1.5418 Å) at room temperature. The scanning range was between from 4 to 80° at a scanning speed of 0.2° min⁻¹. The crystallites size L of materials was computed using the Scherrer expression [10] according to eq. 5:

$$L = \frac{k\lambda}{\beta\cos\theta} \quad \text{Eq. 5}$$

Where, $k=0.9$ is a shape constant;

β is full width at half maxima of XRD peak.

θ is Bragg's angle.

The phase of the phthalocyanines molecules in thin film arrangements, inter-plan distance, grain size, number of molecules in a unit cells and density of materials were determined by analyzing XRD patterns of these materials. Evolutions of XRD pattern also give an idea of extent of crystallinity in the materials.

2.4. Scanning Electron Microscopy (SEM)

The SEM is a microscope that uses electrons instead of light to form an image. It has many advantages over traditional optical microscope. Since it uses electrons instead of visible light to scan the surface, it has very high resolution because of low wavelength of electrons. Moreover, the SEM has a large depth of field, which allows higher surface of a specimen to be in focus at one time. Use of electromagnetic lenses enables better control and enhanced magnification. Since, measurement condition requires vacuum and scanning with a beam of electron, a special preparation of sample is followed.

In our study, we deposited a 250 nm thin film of metallophthalocyanines on a copper substrate in high vacuum. Substrate surface was maintained at room temperature and no further heat treatment was performed post evaporation. SEM micrographs were recorded using Cambridge Scan 360 SEM operating at 3 kV using a LaB₆ emitter. Scans were performed on a scale of 1 μ m, 2 μ m, 200 nm, 100 nm and 10 nm. The observed SEM pictures of layered metallophthalocyanines can give information about surface organization. Arrangements of molecular units on surface determine in turn their behavior towards targeted gas analytes. Thus SEM pictures can give an important clue about the mechanism of gas interactions on sensor surface.

3. Generation of BTX vapor

Vapor mixtures from a volatile liquid can be generated by a variety of methods [11-15]. These are divided into two categories: static methods and dynamic methods. All the static methods of vapor generation work on the following principle. A measured volume of liquid is injected into a defined volume container filled with carrier gas. The injected liquid evaporates and mixes well with the carrier gas, and gives a known concentration of evaporated liquid. If this method is suitable for vapor generation at high concentration, the main drawback is the adsorption and condensation of vapor on the wall of container. Another disadvantage is that only a limited amount of test gas is generated at once. Compared to static methods, dynamic methods are based on continuous diluting gas flow (carrier gas) through the generation system and mixing with the vapor at a known generation rate. They are although complex and expensive but addresses well the drawbacks of static methods. These methods are broadly divided into four categories: (a) injection, (b) permeation, (c) diffusion and (d) evaporation methods. In our experimental investigations, we used evaporation method for generating toluene and xylenes vapor while benzene vapor was generated using permeation method for safety reasons.

3.1. Evaporation method for toluene and xylenes vapor generation

It operates on working principle in which a diluting carrier gas is used to bubble through a liquid or pass over a liquid surface at a known flow rate leading to generation of vapor of liquid of known concentrations [16]. The flow rate is maintained at sufficiently low value in order to ensure that the vapor concentration reaches the state of saturation. The saturated vapor stream emerging from output channel can be diluted with a fixed flow of carrier gas for further analysis.

In order to produce gaseous toluene and xylene, a generation system based on continuous bubbling of carrier gas was realized and characterized. The experimental setup is depicted in Fig. 4. Atmospheric air was pumped through two columns of silica gel and one column of active carbon to obtain clean and dried carrier gas. Zero air is then injected into a sealed bottle containing a known volume of liquid toluene or xylenes. It resulted in bubbling in the liquid which increases the rate of vaporization. After few minutes an equilibrium is established into the bottle and gas concentration is stabilized at a constant value depending on flow rate. A mass flow controller implemented upstream the bottle and driven by a flow regulator (Alpha Gaz, Air Liquid) set the pollutant source flow.

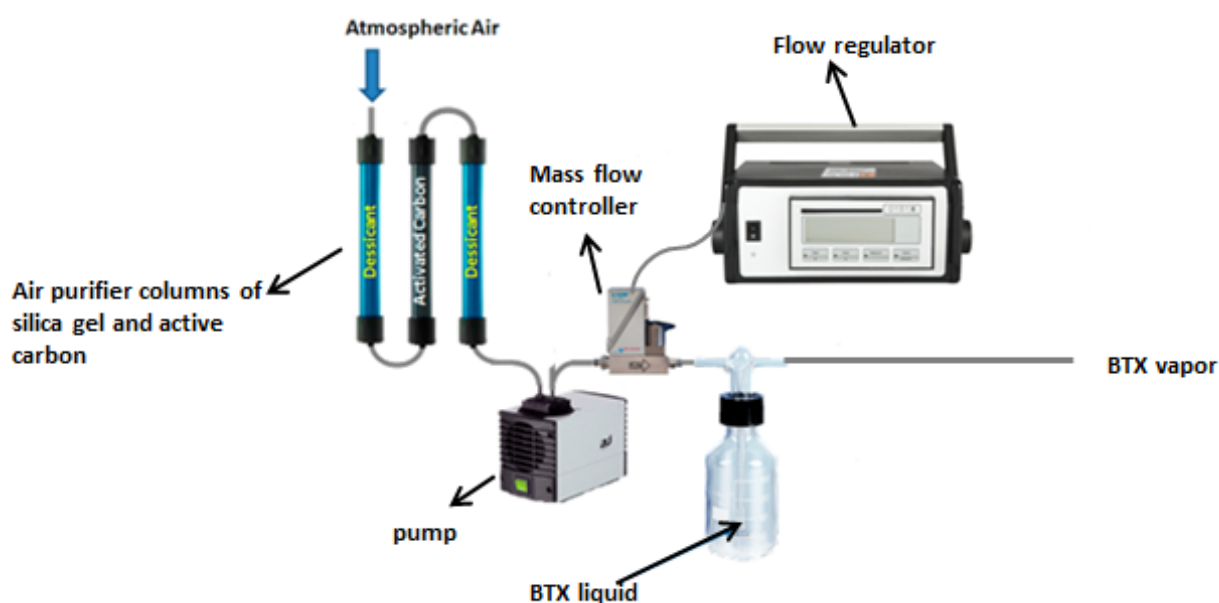


Fig. 4: Experimental setup developed as toluene and xylenes vapor source.

As calibration protocol, BTX concentrations delivered by our system versus gas flow were determined from the measurements of BTX volume lost by evaporation during few hours of generation. A fixed flow of carrier gas was maintained in the bottle containing 350 ml of toluene or xylene in liquid phase during several hours. The loss of liquid (ΔV) was

measured and then was converted into moles of liquid evaporated according to the following equation 6:

$$\Delta n = \frac{\Delta V \rho}{M} \quad \text{Eq. 6}$$

where ρ is the density of the liquid and M is the molar mass.

Assuming that toluene or xylenes vapor produced at low gas flow behaves like an ideal gas, change in volume of toluene vapor was calculated using the equation 7 given below:

$$(\Delta V)_{\text{vapor}} = \Delta n \times 22.4 \times \frac{298.15}{273.15} = \Delta n \times 24.43 \quad \text{Eq. 7}$$

Finally concentration of volatile vapor in ppm was given by the equation 8:

$$(\text{ppm})_{\text{vapor}} = (\Delta V)_{\text{vapor}} \times \frac{10^6}{\text{gas flow rate in the bottle}} \quad \text{Eq. 8}$$

For different gas flow rate in the bottle, concentrations of toluene and xylene vapors in ppm were thus calculated. Bubbling was performed only at lower flow rate because at higher flow instability was observed. The calibration experiments were performed at room temperature without any temperature control of the liquid in bottle. The bottle was kept in a thermally insulated chamber. Calibration curves relative to toluene and xylene sources are given in Fig. 5.

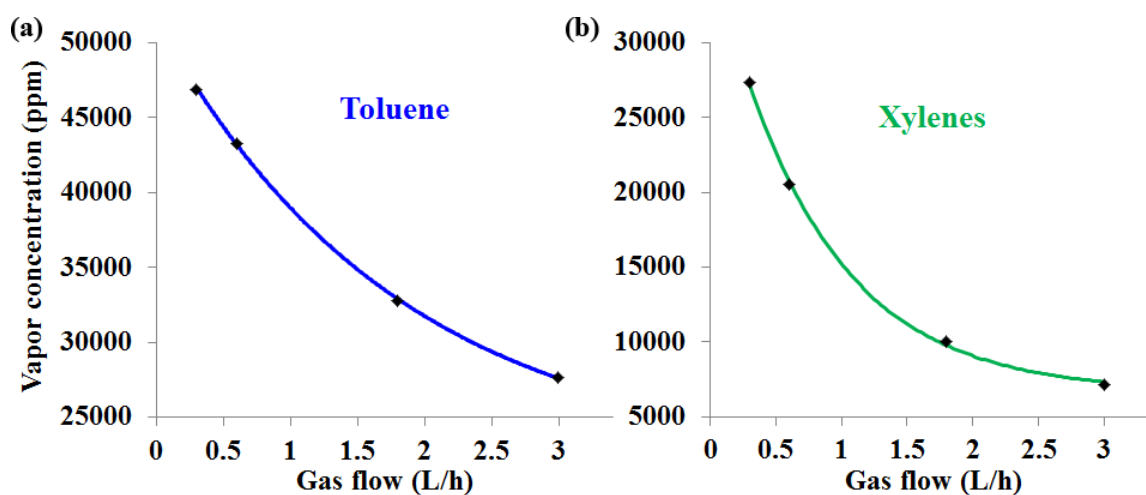


Fig. 5: Calibration curves of vapor generation by bubbling in the liquid: (a) toluene and (b) xylene.

3.2. Permeation method for benzene vapor generation

Permeation methods are based on Fick's law which express the permeation rate (R) of any gas through a membrane (polyethylene, PTFE, silicone rubber, cotton) of thickness L and surface area A by the following equation 9 [11].

$$R = \frac{DS(p_1 - p_2)A}{L} \quad \text{Eq. 9}$$

where D is the diffusion coefficient, S is the solubility constant and p_1 and p_2 are the partial pressures on the two sides of the membrane.

Permeation tubes are prepared by sealing a liquid into a tube with a membrane which porosity can be modulated by temperature control. Vapor generated from a liquid diffuses through the membrane with a constant permeation rate if the temperature remains constant. The sealed tube acts as a stable source generating the vapor, which then permeates into the diluting gas flow on the other side of tube. Parameters as the operating temperature, the tube length and its material, and the wall thickness influence the permeation rate, which will further affect the concentration of the vapor in the carrier gas.

In our investigation, we used a homemade permeation system by sealing a fixed mass of benzene into a glass tube of known volume using cotton as a permeation membrane. The vapor of the liquid was allowed to permeate into a chamber in which a continuous flow of carrier gas (clean and dried atmospheric air) at a fixed rate was maintained. For generating different concentrations of benzene vapor different sized glass tubes and dilution rate were used. Each tube was calibrated at room temperature without using any temperature stabilization of permeation tube.

4. Experimental setup for sensor calibration

4.1. General overview

A schematic of the complete experimental setup for test under gas is shown in Fig. 6. This setup is organized in 4 parts: a) Vapor generation; b) Exposure chamber; c) Gas dilution unit; d) Automation.

The vapor generation setup being previously explained, followings subsections detail the remaining parts of our bench.

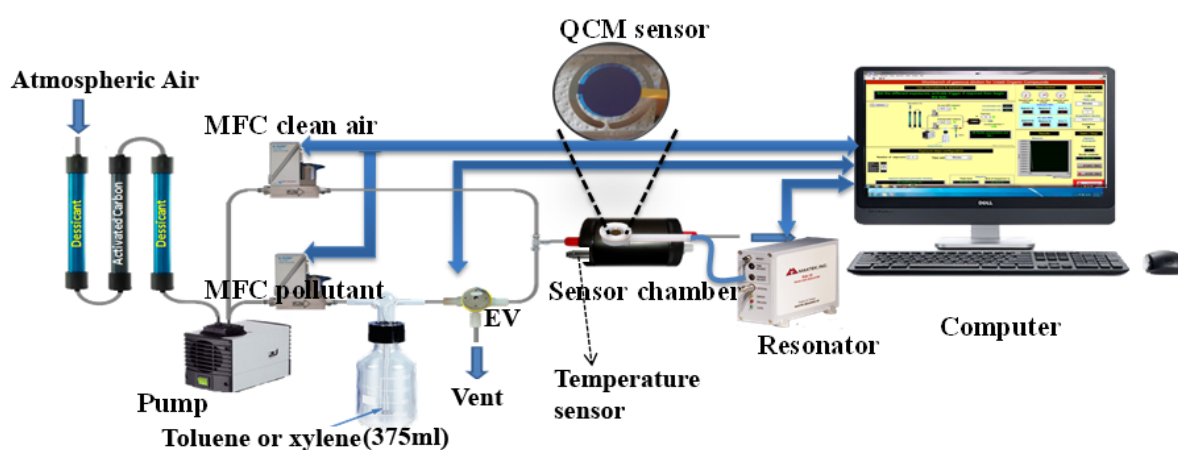


Fig. 6: Schematic representation of gas sensing setup for toluene and xylenes.

4.2. Exposure chamber

AT-cut quartz crystals previously described and justified were used in all sensor testing experiments. These crystals were purchased from Inficon and were used as-received. The front and rear electrodes were of gold with an adhesion layer of chromium. The surface of the Quartz crystals used in our studies was optically polished to 50 Å° average surface roughness. The thickness of the crystal was 0.333 μm. Although AT-cut crystals are designed

to minimize the change in frequency due to temperature, the effect of temperature can be significant when attempting to resolve small mass (frequency) changes over long period of time. Considering this aspect in mind, AT-cut quartz crystals stabilized at 25°C (almost negligible temperature dependence around this temperature) were used.

A phase lock oscillator from Inficon named PLO-10i was used to excite quartz crystal to achieve state of resonance. Further details of working principle can be found in reference [17].

Sensor cell consists of the sensor chamber, the quartz crystal sensor inserted in crystal holder, the PLO-10i oscillator and an agilent frequency counter. Sensor chamber was made up of highly inert Poly Tetra Fluoro Ethylene (PTFE) and was of cylindrical shape. Quartz crystal was excited at 5 MHz by Maxtec PLO-10i oscillator and frequency variations were measured by frequency counter Agilent 5313A. A temperature sensor was also introduced inside the sensor chamber to decorrelate frequency shifts due to temperature variations from those due to gas adsorption.

Different components of sensor cells are highlighted in the experimental test bench developed at Institut Pascal, Clermont Ferrand in Fig. 7.

4.3. Gas dilution unit

It includes a fluidic circuit which allows the gas flow in different parts of experimental setup. As schematically represented in Fig. 6 and also shown in the real test bench in Fig. 7, the fluidic line culminating as an input for bubbling in the bottle was bifurcated into two fluidic sub-lines. One intended for bubbling in the bottle while other was for maintaining clean air flow for dilution of source vapor mixture coming from the bottle. The flow in these two fluidic lines was controlled by mass flow controllers. Gas flow with different rates were maintained by varying extent of valve opening of mass flow controllers which were in turn

controlled by automated software. Just before being introduced into the sensor chamber, test vapor at source concentration was diluted by mixing with clean air. This was achieved by opening the electronic valve (EV) and letting the vapor at source concentration (from bottle) into the mixing chamber. In the open mode electronic valve allows vapor at source concentration to pass into the mixing chamber while in close mode vapor is vented out. Thus use of electronic valve prevents overconcentration of test gas at the beginning of exposure cycle. The total flow in the sensor chamber at any given point during sensor testing was constant at 45 L/h.

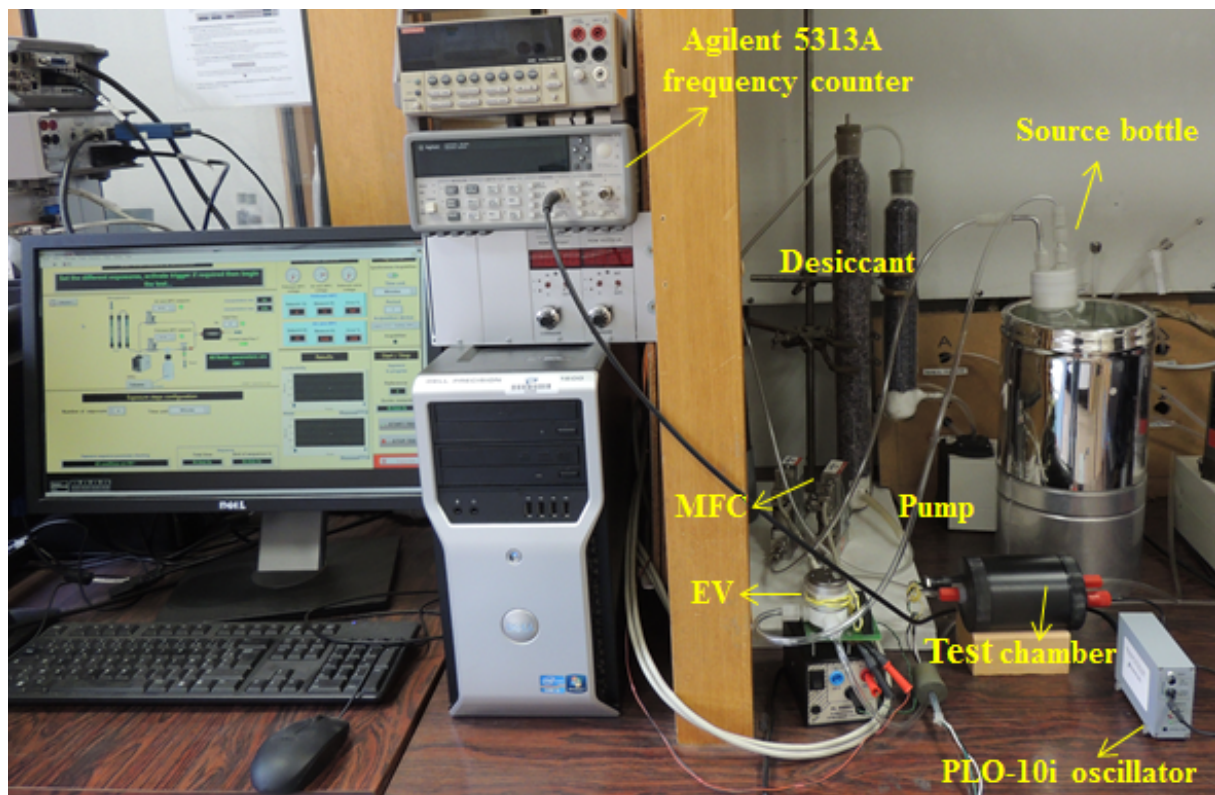


Fig. 7: Experimental gas testing bench at Institut Pascal, Clermont Ferrand.

4.4. Automation

Different electronic and fluidic parameters during a gas testing experiments were controlled by home-made LabVIEW™ Virtual Instrument (VI). The purpose of the automation

was to accurately control the BTX sources, to regulate the opening of mass flow controllers for gas dilution, to clock the sequences of test, to synchronous acquired sensors signals and save experimental results for post-treatments.

The gas source concentrations as well as the dilution rates depending from the ratio of flows through mass flow controllers were controlled as a function of the calibration curve of gas generators fed into LabVIEW™ automation. All fluidic switches, gas exposure runs and data acquisitions were controlled by LabVIEW™ VI via a computer including NI PCI-6229 data acquisition board. The validity of this automated control was certified by the chronic measurements of volume loss of solvent made to calculate the real concentration of BTX during experiments, these experimental values being compared to setpoint values.

5. Experimental sensor response

5.1. Raw sensor data

A phthalocyanine based QCM sensor was tested towards consecutive cycles of exposures with recovery under pure air at room temperature. Sensor was tested toward two different concentrations of toluene. A typical sensor response in terms of frequency shifts of QCM has been depicted in blue in Fig. 8. The order of change of test gas concentrations has been shown in red in the same figure. Decrease in QCM frequency during exposure and increase during recovery points towards normal operation of a QCM sensor assuming the phthalocyanines material on QCM is sensitive to test gas. Moreover different magnitude of QCM signal at varying test gas concentrations are in agreement with the previously explained Sauerbrey's equation.

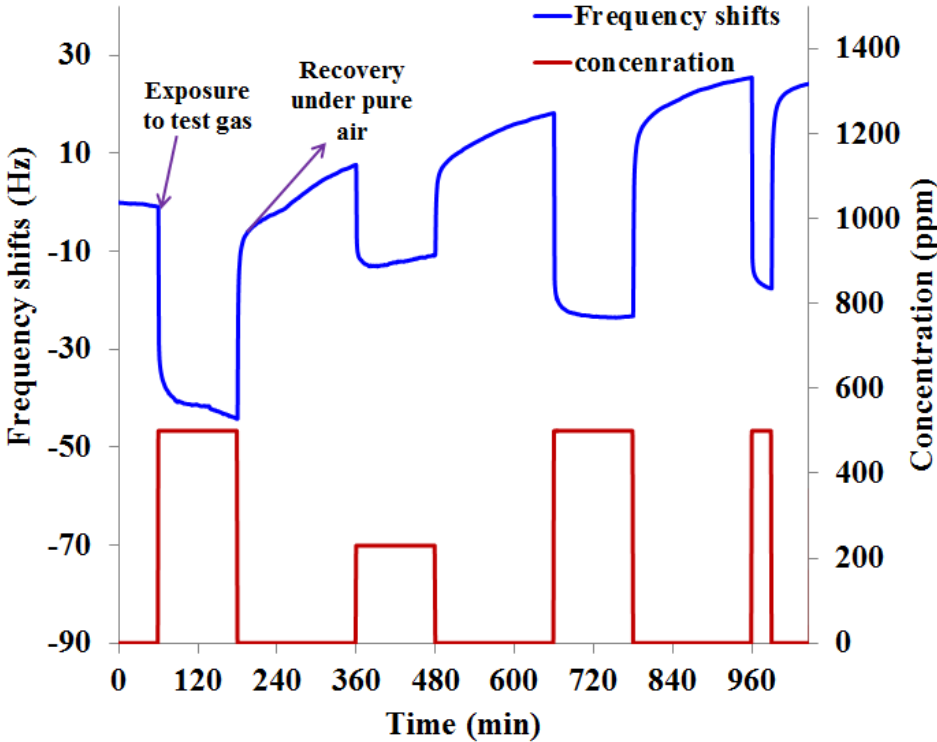


Fig. 8: phthalocyanine-based QCM sensor signal for consecutive exposures of a test gas at room temperature with recovery under clean air.

Although, similar frequency shifts were observed for all cycle of test gas exposures of the same concentration, baseline of sensor signals was drifting with increasing cycles. Multiple reasons can be attributed for such drifts of baseline signal. It may include temperature fluctuation in the surrounding environment of sensor, irreversible adsorption of a fraction of gas molecules, irreversible diffusion of gas molecules and operational uncertainty in fluidic and electronic components. Temperature dependence of QCM frequency evolution was reported in the past [18, 19]. In order to establish a correlation between temperature variation and signal instability, synchronous measurements of temperature close to sensor environment were achieved.

5.2. Temperature corrections

The temperature dependence of QCM frequency variation is an important factor when QCM measurements are carried out continuously for long time without any temperature regulation. To validate the effect of temperature on sensor signal baseline, a temperature sensor was inserted in the test chamber and simultaneous evolution of sensor response under different test gas concentration and surrounding temperature was measured. The sensor response in terms of frequency shifts of QCM at tested concentration and temperature variations in the sensor surrounding during the progress of sensing experiments has been shown in Fig. 9. Frequency variations of sensing device exposed to a fixed concentration of test gas was simultaneously compared to temperature change. Although, magnitude of frequency caused by test gas exposure are similar for different cycles and not significantly affected by temperature, a noticeable drift in baseline sensor signal in the reverse direction of temperature drift was observed as seen in Fig. 9.

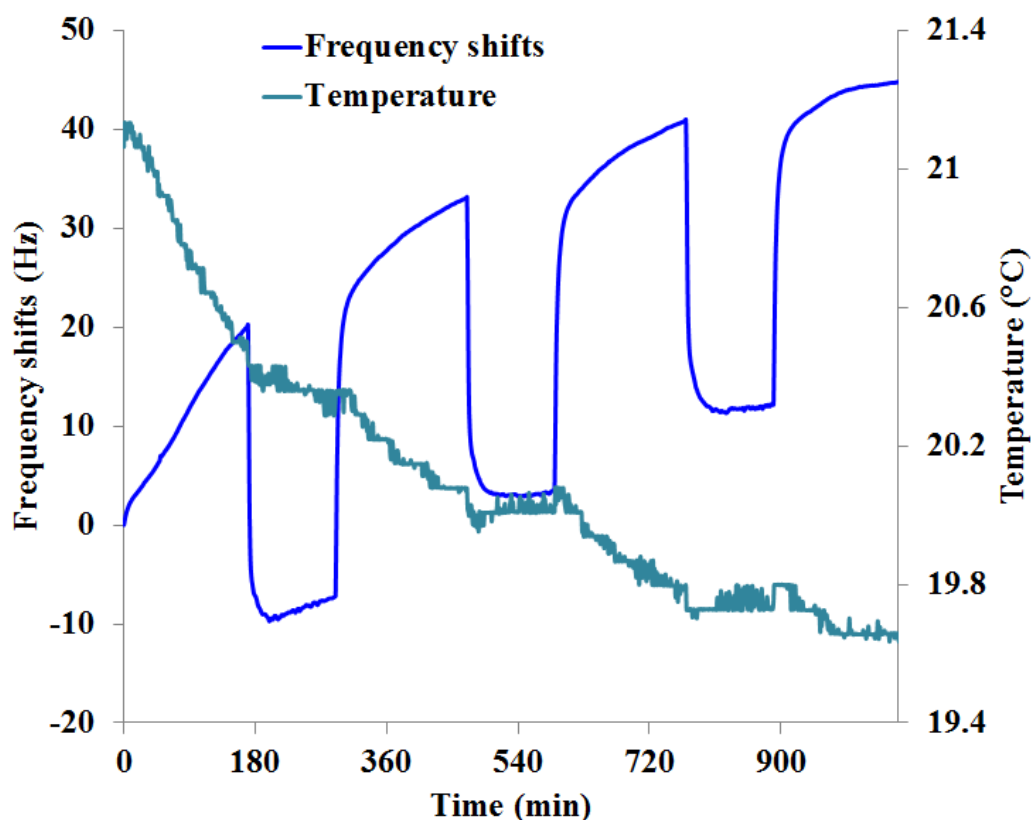


Fig. 9: phthalocyanine-based QCM sensor response to a test gas and simultaneous variations of room temperature in sensor surrounding.

To quantify this temperature dependence, the influence of thermal environment inside the sensor chamber on quartz was investigated. For this purpose, the temperature variations inside the sensor chamber was recorded synchronously with frequency of QCM-based sensor maintain under clean and dried air. Thus, resonance frequency of AT-cut quartz crystals coated with phthalocyanine material versus temperature is reported in Fig. 10. In theory, AT-cut Quartz crystal is known to have very low temperature coefficient (weak dependence of frequency with temperature fluctuation). Nevertheless, our experimental investigation shown noticeable frequency drifts due to small fluctuation in room temperature. The temperature coefficient of QCM sensor, which is represented by the slope of the linear fit on experimental calibration curve in Fig. 10, was calculated to $19.6 \text{ Hz}/^\circ\text{C}$. This value is much higher than the value given by the manufacturer.

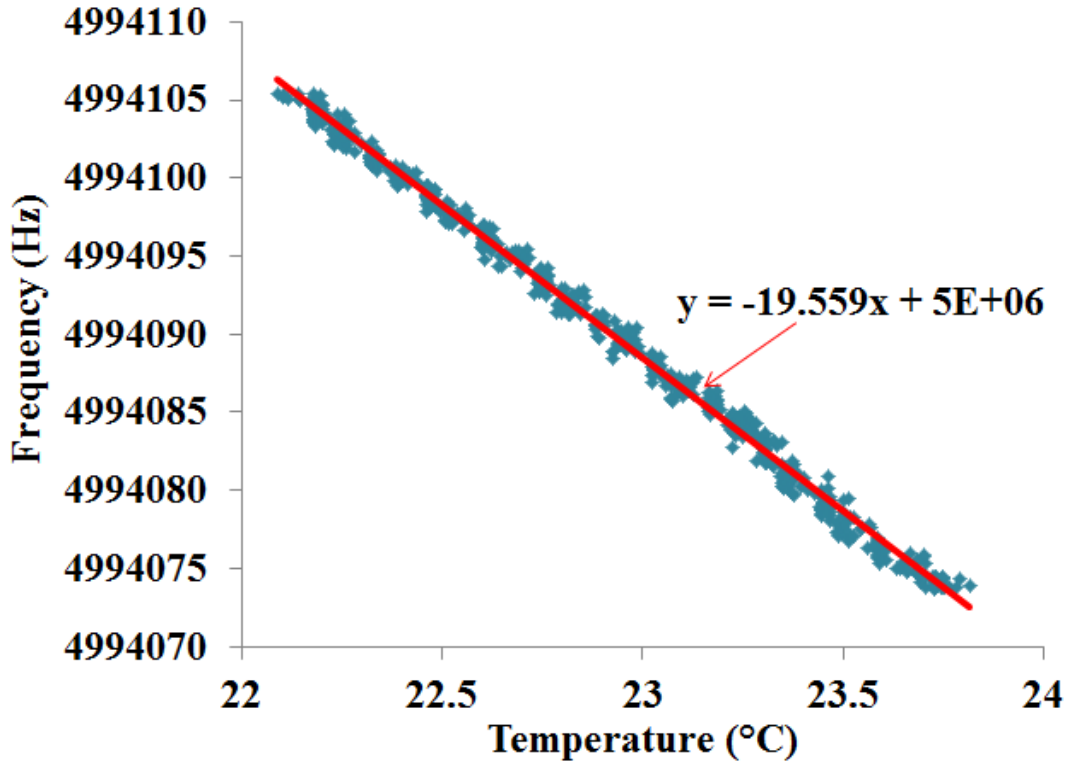


Fig. 10: Resonance frequency evolution of AT-Cut Quartz crystal with temperature.

Such temperature dependence of QCM signal is problematic and put in obviousness the need of temperature regulation of QCM devices. Such strategy also has a few inherent limitations associated including higher power consumption, low mobility and uneasy miniaturization. In contrast, temperature correction of QCM sensor signals appears as the best solution to enhance the sensor stability and reproducibility. Taking into consideration manufacturer data ($\Delta f = 0$ zero @ 30°C , > 0 below 30°C and < 0 above [20]) and the temperature coefficient previously determined, a correction factor was applied to the measurements. Thus, the corrected frequency of QCM sensor f_{corr} , is calculated from the following first-order linear equation 10:

$$f_{\text{corr}} = f_{\text{meas}} - K \cdot (T_0 - T) \quad \text{Eq. 10}$$

In the above equation, $K = 19.6 \text{ Hz}/^{\circ}\text{C}$ is the thermal sensitivity of quartz crystal, $T_0 = 30^{\circ}\text{C}$ is the temperature corresponding to zero frequency drift, T is working temperature in $^{\circ}\text{C}$ and f_{meas} the measured frequency delivered by QCM sensor. The previous determination of the

correction factor and the simultaneous measurement of temperature in gas test chamber allow us to make real-time correction on each recorded frequency. The result of temperature correction on sensor signal is illustrated in Fig. 11. Figure 11a depicts the response of a phthalocyanine based QCM sensor to five cycles of a test gas exposure/recovery and the simultaneous temperature variations whereas Fig. 11b depicts sensor signal after thermal correction. By comparison, we can see that more than 70 % of baseline instability is overcome. At the same time, we confirm that sensor sensitivity and repeatability to tested vapors are almost unaffected. However, the slow drifts in frequency during gas exposure and recovery steps were not completely removed by thermal compensation. Such behavior can be attributed to diffusion of analyte gas within the bulk of the sensing layer. Since diffusion coefficient increases exponentially with increasing temperature [21], baseline of sensor responses changes accordingly. It can be noticed in Fig. 11a that during the 4th and 5th exposure to test gas, the thermal gradient is comparatively higher. Even after applying the temperature correction term, drifts in sensor response are higher as compared to previous exposures. Nevertheless, diffusion remaining easily versatile event at room temperature, no significant impact on the reversibility in sensor response for successive cycles was observed.

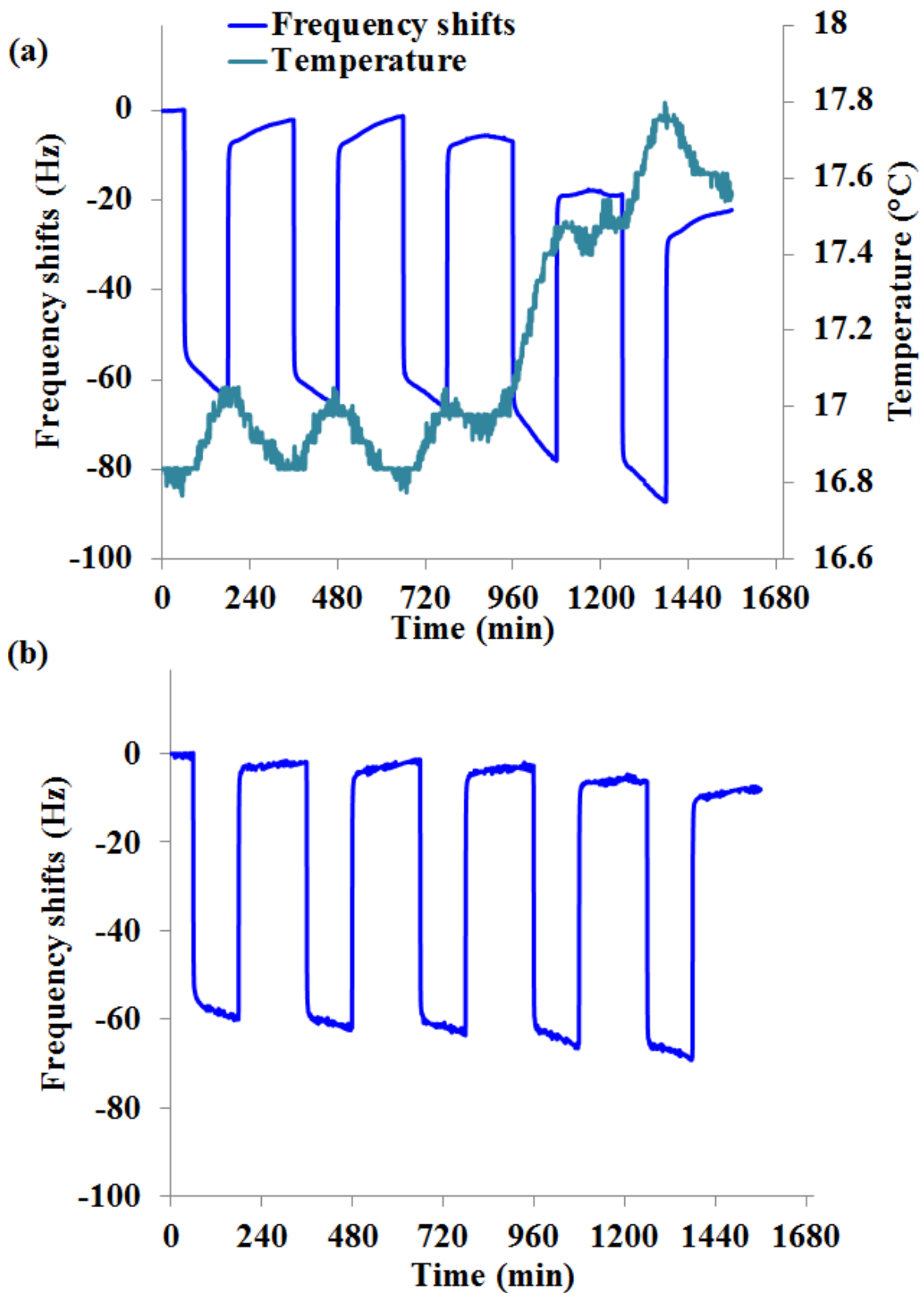


Fig. 11: *tb*-CuPc coated QCM sensor responses to 500 ppm of toluene at room temperature (a) as-measured signal, (b) corrected signal.

References

1. Clarisse, G., et al., *Synthesis and characterization of some lanthanide phthalocyanines*. Inorganica Chimica Acta, 1987. **130**(1): p. 139-144.
2. Linaje, M., et al., *Improvement of the synthesis of lutetium bisphthalocyanine using the Taguchi method*. Analyst, 2000. **125**(2): p. 341-346.
3. MacKay, A., et al., *Preparation and properties of some rare-earth phthalocyanines*. Australian Journal of Chemistry, 1974. **27**(5): p. 955-964.
4. Sauerbrey, G., *Use of quartz oscillators for weighing thin layers and for microbalance*. Zeitschrift für Physik, 1959. **155**(2): p. 206-222.
5. Sauerbrey, G., Phys. Verh., 1957. **8**: p. 2.
6. *PLO-10i Phase Lock Oscillator*. Inficon, Available from:
(<http://products.inficon.com/en-us/Product/Detail/PLO-10i?path=Products%2FResearch-QCM>).
7. S. Ismat Shah, G.H.J., Emre Yassitepe and Bakhtyar Ali, *Evaporation: Processes, Bulk Microstructures, and Mechanical Properties*, in *Handbook of Deposition Technologies for Films and Coatings*, P.M. Martin, Editor. 2010, Elsevier.
8. Swinehart, D.F., *The Beer-Lambert Law*. Journal of Chemical Education, 1962. **39**(7): p. 333.
9. Ricci, R.W., et al., *Discovering the Beer-Lambert Law*. Journal of Chemical Education, 1994. **71**(11): p. 983.
10. Patterson, A.L., *The Scherrer Formula for X-Ray Particle Size Determination*. Physical Review, 1939. **56**(10): p. 978-982.
11. Namies'nik, J., *Generation of standard gaseous mixtures*. Journal of Chromatography A, 1984. **300**: p. 79-108.

12. Kim, Y.-H., et al., *Generation of Sub-Part-per-Billion Gaseous Volatile Organic Compounds at Ambient Temperature by Headspace Diffusion of Aqueous Standards through Decoupling between Ideal and Nonideal Henry's Law Behavior*. *Analytical Chemistry*, 2013. **85**(10): p. 5087-5094.
13. Kim, Y.S., et al., *Gas sensor measurement system capable of sampling volatile organic compounds (VOCs) in wide concentration range*. *Sensors and Actuators B: Chemical*, 2007. **122**(1): p. 211-218.
14. Li, Y., et al., *Test Gas Generation from Pure Liquids: An Application-Oriented Overview of Methods in a Nutshell*. *International Journal of Chemical Engineering*, 2012. Article ID 417029, **2012**: p. 6.
15. Barratt, R.S., *The preparation of standard gas mixtures. A review*. *Analyst*, 1981. **106**(1265): p. 817-849.
16. Koziel, J.A., et al., *System for the generation of standard gas mixtures of volatile and semi-volatile organic compounds for calibrations of solid-phase microextraction and other sampling devices*. *Journal of Chromatography A*, 2004. **1025**(1): p. 3-9.
17. Hojong, C., et al. *New modified Butterworth Van-Dyke model for high frequency ultrasonic imaging*. in *Ultrasonics Symposium (IUS), IEEE International 2012*. p. 576-579.
18. Rocklein, M.N., et al., *Temperature-Induced Apparent Mass Changes Observed during Quartz Crystal Microbalance Measurements of Atomic Layer Deposition*. *Analytical Chemistry*, 2003. **75**(19): p. 4975-4982.
19. Kumar, A., et al., *Tetra-tert-butyl copper phthalocyanine-based QCM sensor for toluene detection in air at room temperature*. *Sensors and Actuators B: Chemical*, 2015. **210**: p. 398-407.

20. QCM research crystals Inficon, Available from:
<http://products.inficon.com/GetAttachment.axd?attaName=9e8fae67-ba67-4743-b516-aafc332166e1>.
21. Seager, S.L., et al., *Temperature Dependence of Gas and Vapor Diffusion Coefficients*. Journal of Chemical & Engineering Data, 1963. **8**(2): p. 168-169.

Chapter 3:
**Relevance of phthalocyanines as
sensitive materials for BTX detection**

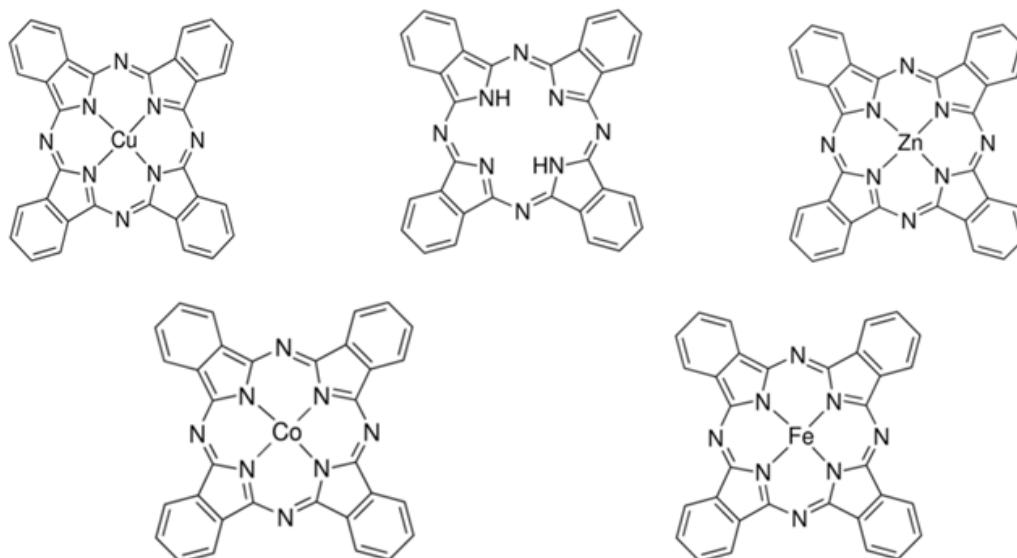
1. Choice of phthalocyanines and sensing strategy

The choice of phthalocyanines as sensing materials layered on QCM transducers for the detection of BTX is motivated by their structural similarities with benzenoid organic analytes, their extended conjugated π -electrons distribution and the possibility to modulate their chemical properties by functionalization processes. If the presence of benzene rings into the macrocycle can provide a first level of selectivity towards aromatic hydrocarbons, continuous π -electron delocalization also leads to a molecular organization of the thin layers which can induce favorable adsorption sites to BTX gaseous molecules. Moreover, the property of the molecule to generate π -stacking interactions with similar conjugated carbonaceous macromolecular organization opens a way to develop new hybrid sensing materials aiming to the enhancement of sensor sensitivity. With their high specific surface areas and aromaticity, nano-carbonaceous materials can be especially attractive as functionalizable matrix.

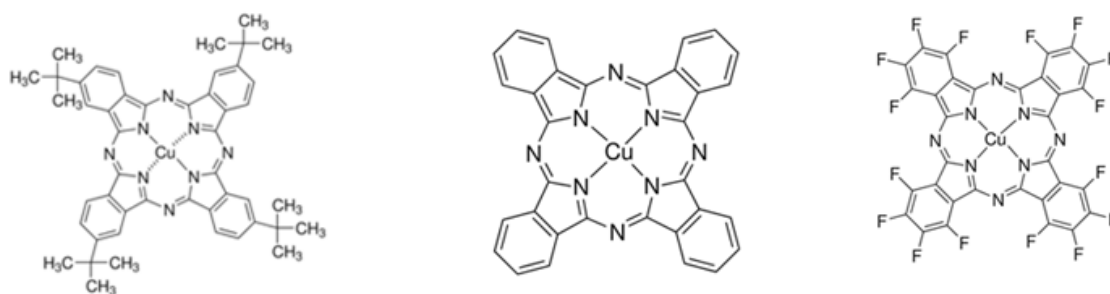
The possibility of flexible tailoring of molecular/atomic parts in phthalocyanine macrocycles has made these organic materials suitable for several applications. More especially in chemical gas sensors field, the great diversity of phthalocyanines (central hydrogen atoms replaceable by more than 70 metal atoms, substituted or unsubstituted, monomeric, dimeric or polymeric) is a real opportunity to select the sensing material which physical and chemical properties are the most relevant to satisfy the targeted performances: sensitivity, stability, selectivity, reversibility, etc... The selection of the most appropriate phthalocyanines for the development of BTX sensors from such a vast group required a systematic study we have performed. Taking into account their commercial availability, their purity level as well as their easy and cheap shaping in thin layers by thermal evaporation process, three different classes of phthalocyanines were investigated as sensitive layer. All are

depicted in Fig. 1. Monomeric unsubstituted metallophthalocyanines were firstly studied. Considered as the most common phthalocyanines, the objective was to assess the role of different complexed metal atoms in the center of macrocycles on sensor response. Further phthalocyanines including electroactive groups in substitution of the peripheral hydrogen atoms were also selected. It involved peripherally substituted mono-macrocyclic phthalocyanines. Tert-butyl groups and fluorine atoms were chosen as electron-donor or electron-acceptor groups respectively. The role of these grafted groups at the periphery of phthalocyanine macrocycles on sensor response to BTX as well as on layer morphology was particularly emphasized. In order to benefit from a higher aromaticity, a double-decker phthalocyanine containing two macrocycles and consequently 8 benzene rings per molecule was finally studied. Potential improvement in sensitivity due to the presence of two macrocycles was investigated through LuPc₂ based QCM sensors. The responses of QCM-based sensors implementing these three classes of phthalocyanines were compared. The results of intercomparison of these characteristics were aimed to define the best suited sensing material for the development of sensitive and efficient BTX micro sensors.

(a) Change of central metal atoms



(b) Change of peripheral substituents



(c) Change in number of macrocycles

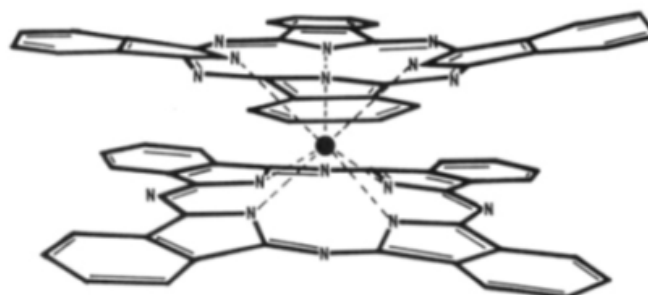


Fig. 1: Investigated phthalocyanines for BTX sensor development: (a) unsubstituted metallophthalocyanine, (b) substituted metallophthalocyanines and (c) double decker metallophthalocyanines

2. Optical spectroscopic characterizations of materials

2.1. UV-Vis spectra of phthalocyanines

To completely characterize the commercial powdered phthalocyanines, UV-Vis spectroscopy was the first technique used. Indeed, the wavelengths corresponding to the prominent experimental UV-Vis peaks are modulated according to the nature of the studied phthalocyanine. Particularly in a highly conjugated molecule like phthalocyanine, it can give information about the nature of metal atoms complexing within its central cavity and the electronic nature of groups ligating at its periphery. UV-Vis spectroscopy can be considered as the first step to confirm the chemical information provided by manufacturers. The studied phthalocyanines and its derivatives show electronic spectra with two strong absorption regions: one of them in the UV region at around 240–345 nm (B or Soret-band) and the other in the visible part of the spectrum at around 650–700 nm (Q band), which are in agreement with typical UV-Vis absorption spectra of phthalocyanines [1]. The origin of Q and B bands follows electronic transitions $a_{1u} \rightarrow e_g$ (HOMO \rightarrow LUMO) and $a_{2u} \rightarrow e_g$ (Lower $\pi \rightarrow$ LUMO) respectively in a phthalocyanine molecule. Both transitions are from $\pi \rightarrow \pi^*$ orbitals. The absorption maxima (λ_{\max}) of the two prominent bands were experimentally determined and compared to data from literature, which are given in Table-1.

Presence of a central metal atom and peripheral ligands affect the absorption spectra of phthalocyanines. To highlight this effect, electronic absorption spectra of H₂Pc, ZnPc and ttb-ZnPc have been compared in Fig. 2. The Q band of the metal-free phthalocyanine was observed as two split bands at $\lambda_{\max} = 656$ and 693 nm which is attributed to D_{2h} symmetry of this molecule that breaks its degeneracy [2]. The Q-band is associated with a blue-shifted weak satellite at 598 nm. A less intense and broad peak at 341 nm with a shoulder at around 391 nm represents the B band of H₂Pc. The metalation of phthalocyanine has an obvious

impact on its electronic absorption spectra, leading to the substitution of doublet of Q-band by a single intense Q-band centered at 672 nm in the spectra of ZnPc in Fig. 2. The single Q band in ZnPc and other metallophthalocyanines given in Table-1 are characteristic of metalation, which maintains the planarity of the molecule and increases the symmetry to D_{4h} [3]. B-band of ZnPc is indicated by a broad and less intense peak centered at 341 nm. The presence of peripheral ligands mainly affects the relative position of Q and B-bands of parent unsubstituted phthalocyanines [4]. Electron-donating substituents generally give rise to the red-shift of the Q-band while electron-withdrawing substituents have little effect on the position of the Q-band unless their π -electrons or lone-pair electrons take part in the expansion of the π -conjugation system of the macrocycle. Change in UV-Vis spectra of phthalocyanine due to the presence of a peripheral ligand is highlighted in the spectra of ttb-ZnPc as illustrated in Fig. 2. Because of the presence of four tert-butyl groups in ttb-ZnPc, Q band shifts from to 672 nm to 679 nm.

Solubility of studied unsubstituted metallophthalocyanines and their fluoro-derivatives in chloroform was very low. Therefore, scattering and baseline instabilities were observed in the spectral measurements of a few compounds. For example, CuPc dissolved in chloroform has a lot of suspended particles in solution which caused multiple scattering during measurements. For similar reason, a downward spike in the middle of H_2Pc spectra is also attributed to scattering because of its poor solubility in chloroform. All UV-Vis spectra being in agreement with data extracted from references, all commercial phthalocyanines correspond to the expected materials.

Materials	B-Band		Q-Band		Reference
	$(\lambda_{\max})_{\text{measured}}$	$(\lambda_{\max})_{\text{reference}}$	$(\lambda_{\max})_{\text{measured}}$	$(\lambda_{\max})_{\text{reference}}$	
H ₂ Pc	341	343	656 and 693	664 and 699	[1, 5]
CuPc	NA	343	NA	666	[6, 7]
CoPc	340	339	663	657	[1, 8]
ZnPc	341	335	672	667	[9]
FePc	340	340	664	659	[1, 8], 8]
LuPc ₂	318	320	660	662	[10]
ttb-CuPc	348	349	677	677	[11]
ttb-ZnPc	352	351	679	678	[12, 13]
F ₁₆ ZnPc	352	357	669	674	[14]
F ₁₆ CuPc	NA	356	NA	675	[15]

*NA: materials were not enough soluble to record their UV-Vis spectra without any dispersion.

Table 1: UV-Vis spectral bands of phthalocyanines materials

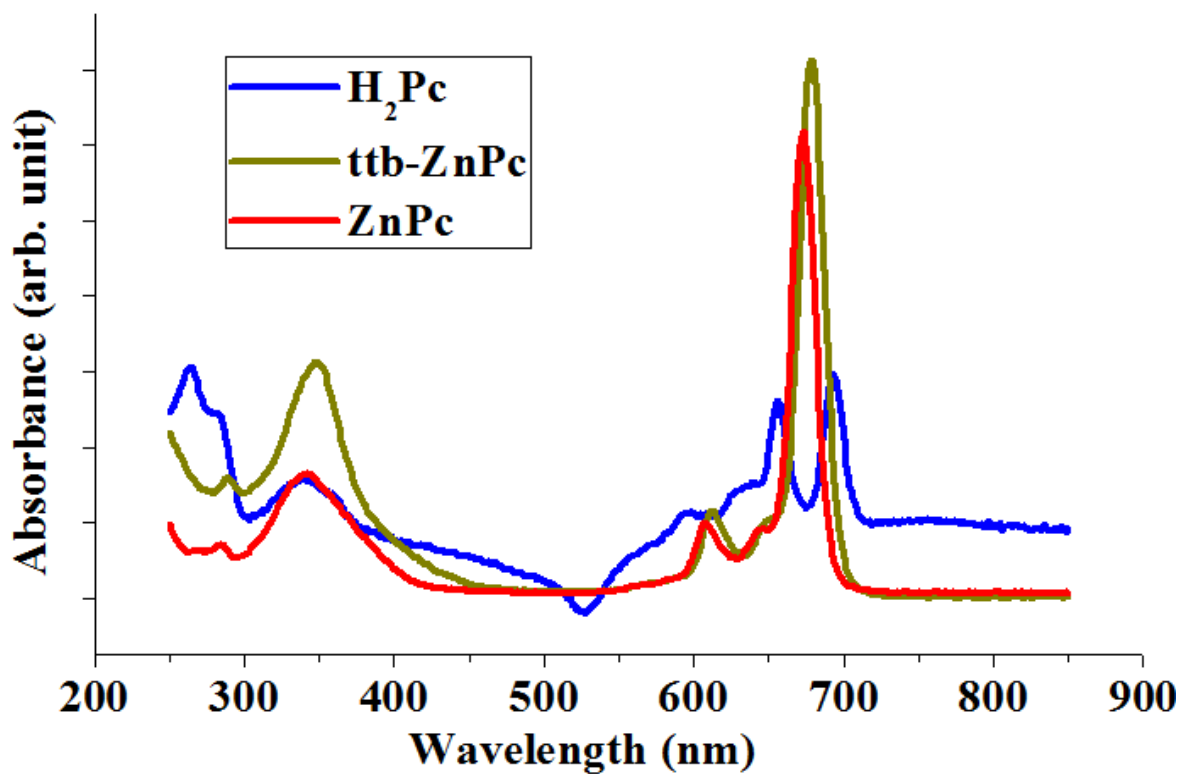


Fig. 2: UV-Visible spectra of powdered H₂Pc, ZnPc and ttb-ZnPc dissolved into chloroform.

2.2. FT-IR spectra of phthalocyanines

FT-IR spectra basically give information about the nature of the chemical bonds involved into probed molecules. Intercomparison of FT-IR spectra of powdered and layered materials is a method to evaluate the structural stability of the molecular units while undergoing layering process. In our case, thermal evaporation was used to achieve phthalocyanine thin layers with well-controlled thicknesses and deposition rates. Although it is an easy and versatile method for the realization of homogeneous films, at the same time high temperatures of evaporation can be destructive to soft materials like phthalocyanines [16]. This is especially true when sterically big alkyl groups or long chain ligands are grafted at the peripheral sites. High evaporation temperature can be prejudicial to the bonding of such groups and may cause their removal during evaporation. As a consequence, the intercomparison of FT-IR spectra of powder and evaporated films of substituted metallophthalocyanines like ttb-MPCs is necessary to monitor if any thermo-oxidative degradation of materials occurred during evaporation process.

FT-IR spectra of powder and thin films of the studied phthalocyanines were compared. As expected, no additional or removed vibrational peak is noticeable between powder and layer neither for monomeric metallophthalocyanines, nor for fluorinated ones. These results are in agreement with previous reported studies [17-19]. Thermal evaporation is so a soft deposition process for monomeric metallophthalocyanines. As mentioned above, degradation of materials by thermal sublimation is more probable for substituted phthalocyanine with huge substituents. Figure 3a depicts FT-IR spectra of tetra-tert-butyl copper phthalocyanine in powder and layer forms determined in transmission mode. The peaks positions in the 400–3600 cm^{-1} range were shown. The regions of spectra within 1700–2500 cm^{-1} and 3600–4000 cm^{-1} were masked because of absence of any prominent peaks within these regions. The

vibrational peaks characteristic of phthalocyanine can be observed in each spectrum. Approximately the same position of different vibrational bands can be noticed in both spectra. The absence of any peak close to 1000 cm^{-1} confirms the presence of metal atom in phthalocyanine, which otherwise originates from N–H bending vibration, these N-H existing in free phthalocyanine (H_2Pc). The binding of metal atom with pyrrolic nitrogen gives the typical IR band at 893 cm^{-1} because of metal–ligand vibration. The band corresponding to –C=C– macrocycle ring deformation appears at 1616 cm^{-1} . The peripheral tert-butyl ligands are responsible of the peak localized at 2955 cm^{-1} corresponding to C–H stretching frequency of methyl group. In general, FT-IR pattern of films are slightly blue-shifted as compared to powder because of additional intermolecular interactions in films. Conclusions from FT-IR characterizations established for ttb-CuPc are similar to those which can be formalized for powdered and layered ttb-ZnPc as shown in Fig. 3b.

Despite the substitution of peripheral hydrogen atoms on macrocycle by fluorine atoms or tert-butyl groups, thermal stability of all investigated phthalocyanines make them enough robust to perform thin sensitive layers by thermal evaporation without any molecular destructuring as confirmed by FT-IR analysis. Thermal evaporation is thus an easy and soft deposition process appropriate for the development of phthalocyanine-based chemical sensors achieving sensitive layer with well-controlled characteristics.

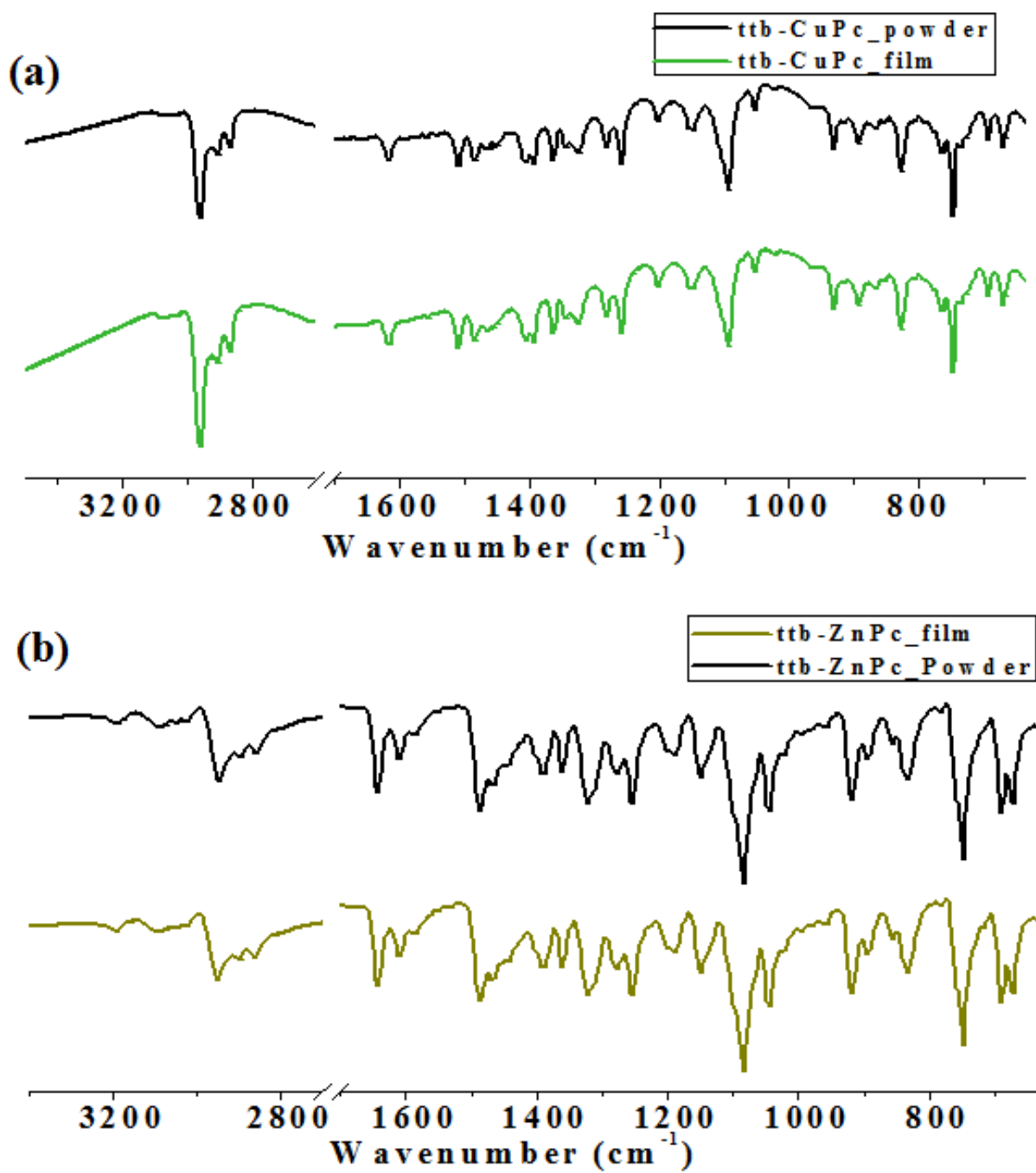


Fig. 3: Comparison of FT-IR spectra of powdered and layered (a) ttb-CuPc and (b) ttb-ZnPc.

3. General sensor responses to BTX

3.1. Unsubstituted phthalocyanines

The sensing properties of four unsubstituted metallophthalocyanines towards benzene, toluene and xylenes were firstly studied. This first panel of organic materials included H₂Pc, CuPc, ZnPc, and CoPc. The sensing performances of these mono-macrocylic phthalocyanines were determined by the magnitude of sensor responses and the kinetics of responses. Beyond sensing potentialities, the likely influence of the central metal atom on sensor responses was studied. The objective of the first measurements under gas is to define the more appropriate material enable to satisfy a good metrology of the target gases. The involved interaction mechanisms and the correlation between sensor response and thin film properties will be detailed in section 4 devoted to layer characterizations and in section 5 about interacting forces involved at molecular scale.

QCM sensor responses corresponding to one cycle of exposure and recovery of unsubstituted metal-free phthalocyanine (H₂Pc) and three metallophthalocyanines (CoPc, CuPc, ZnPc) are reported in Fig. 4. All results were obtained at room temperature on 400 nm thick layers. Since the generation system of benzene vapors is less flexible as compared to toluene and xylenes, so it could not be generated at the same concentration as toluene and xylenes. Sensor was exposed to 835 ppm of benzene and 500 ppm of the toluene and xylenes. The exposure times were 20 minutes for benzene and 2 hours for toluene and xylenes, while recovery times were set as 40 min for benzene and 3 hours for toluene and xylenes. First of all, results exhibit adsorption of all BTX gases on the sensitive layer with increasing magnitude from benzene to xylenes. Moreover, a complete reversibility of response corresponding to an easy desorption process at room temperature and involvement of weak interactions between material and analytes can be underlined. This is confirmed by the

decrease in resonance frequency of coated QCMs during exposures, corresponding to mass increase on the sensitive layer and increase in frequency under pure air to approximately the same frequency measured before exposure. Fig. 4 also emphasizes that all the studied unsubstituted metallophthalocyanines and metal-free-phthalocyanine have low and similar responses. Frequency shifts of QCMs during sorption events for benzene, toluene and xylenes were in a range of 4–10 Hz, 9–15 Hz and 30–40 Hz respectively for the different phthalocyanines. We can notice that sensor response increases with the boiling temperature of these volatiles organic compounds: 80°C for benzene, 110°C for toluene and from 138 to 144°C for xylenes. On one hand, a weak effect on sensor responses towards each gas due to the presence of central metal atoms in phthalocyanine can be highlighted. Indeed, the frequency shifts measured for H₂Pc based QCM sensor exposed to 500 ppm of toluene and xylenes are equal to 9 Hz and 30 Hz respectively while increasing to 15 Hz and 40 Hz respectively for metallophthalocyanines. On the other hand, the intercomparison of sensor sensitivities between CuPc, CoPc and ZnPc reveals negligible differences. In contrast, a noticeable variations in kinetics of adsorption/desorption of these gases are observed. The kinetics of sorption of toluene and xylenes on phthalocyanines surfaces were studied from the response and recovery times of different QCM samples. These parameters were determined for each material and are summarized in Table 2. In the case of benzene, the low sensitivity coupled with non-repeatability in responses made difficult response and recovery times determination with sufficient accuracy. From the Table 2, we can note that CuPc and CoPc lead to similar kinetics of response and faster as compared to H₂Pc or ZnPc. The response time for QCM coated by CuPc was 12 min and 4 min for toluene and xylenes respectively, while recovery times were assessed to 23 min and 26 min. On the other hand, H₂Pc and ZnPc based sensors exhibited lower rate of gas sorption. ZnPc based QCM showed 24 min and 22

min as response time and long recovery time of 80 min and 65 min for toluene and xylenes respectively.

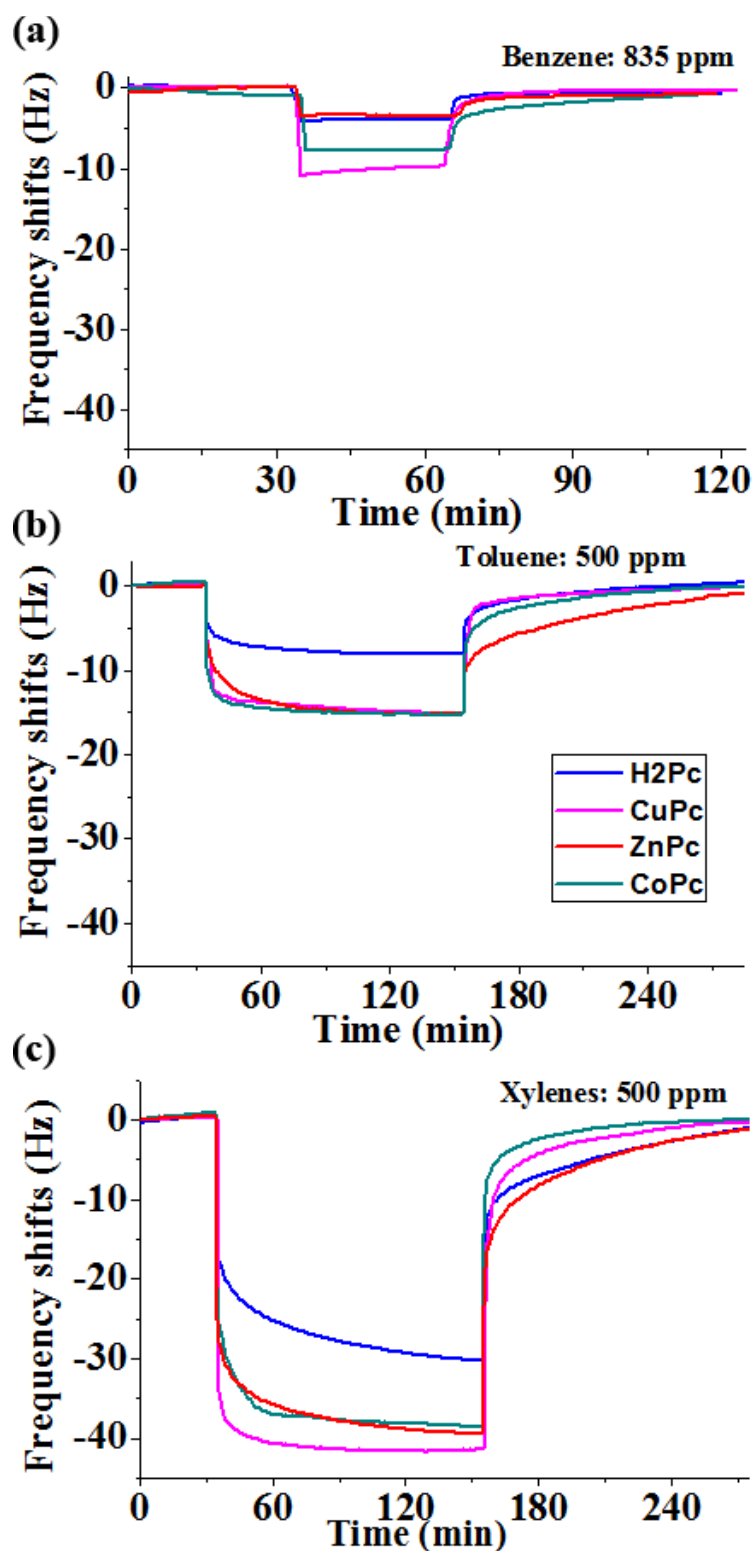


Fig.4: unsubstituted phthalocyanines-based QCM sensors responses for one cycle of exposure to BTX and recovery under pure air.

Material	Response Time (min)		Recovery time (min)	
	Toluene	Xylenes	Toluene	Xylenes
H₂Pc	22	44	55	80
CuPc	12	4	23	26
ZnPc	24	22	80	65
CoPc	9	14	42	13

Table 2: Response and recovery times of QCM coated with different metallophthalocyanines.

Although the magnitude of sensor response of metallophthalocyanines based QCM sensors is slightly higher than metal-free-phthalocyanine, such small increase remains insignificant at low sensor sensitivity. Moreover, response and recovery times are higher than 10 minutes. Despite their aromaticity, these organic materials are not able to induce high and fast sorption rates. Different sensing characteristics including limit of detection, resolution and discrimination of sensor signals for different concentrations were unable to satisfy the required objectives of an ideal BTX sensor taking into account the environmental guidelines and legislations.

To benefit from better sensing performances, the optimization of sensing material is required. We have clearly established that the change of the central metal atom in mono-macrocyclic unsubstituted phthalocyanines not appears as a relevant way to enhance BTX sensitivity. A second approach with phthalocyanines to modulate their sensing properties concerns the substitution of hydrogen atoms at the periphery of macrocycles by functional groups. By means of molecular engineering, a partial or complete substitution of hydrogen

atoms can be achieved and many groups with specific electronic and steric properties can be grafted. It constitutes a great opportunity to tailor sensitive material as function of the gas we want to detect. Beside this, phthalocyanine molecules consisting of two macrocycles can be also a promising candidate for improving BTX sensitivity.

3.2. Substituted phthalocyanines

Taking advantage of the rich and flexible synthesis chemistry developed for substituted phthalocyanines and their commercial availability, these materials were deposited on QCM as a sensing layer. Metallophthalocyanines substituted with two opposite electro-active ligands were investigated. These ligands were tert-butyl classified as electron-donor groups and fluorine atoms classified as electron-acceptor. To highlight the effect of these groups on sensor sensitivity, the sensor responses on quartz crystal coated with these substituted phthalocyanines were compared to those observed for the unsubstituted analogs. Although comparison of sensor responses will be restricted to measurements under toluene, similar behavior was obtained towards xylenes as discussed in the next chapter about detailed sensing characteristics investigation of most sensitive material.

The response at room temperature of ttb-CuPc, F₁₆CuPc and CuPc layers of 400 nm thickness coated on QCM towards 500 ppm of toluene with consecutive recovery step under pure air are shown in Fig. 5. At first, the dissimilar frequency shifts assigned to the different sensing devices during toluene exposure point out the strong impact on toluene adsorption rate and consequently on sensor sensitivity due to peripheral substitution of hydrogen atom on CuPc macrocycle. Compared to unsubstituted CuPc-based sensor, ttb-CuPc-based sensor exhibits 4-times higher response with frequency shift close to 60 Hz while F₁₆CuPc showed 3-times less response with 5 Hz of magnitude. Secondly, results from Fig. 5 show a complete

reversibility for *ttb*-CuPc as illustrated by the stable baseline after each toluene exposure step and a high level of repeatability. In contrast, F_{16} CuPc-based QCM sensor has low and unstable responses. Fluorine atoms seem inhibit the adsorption of BTX on phthalocyanines molecular units whereas tert-butyl groups strengthen it.

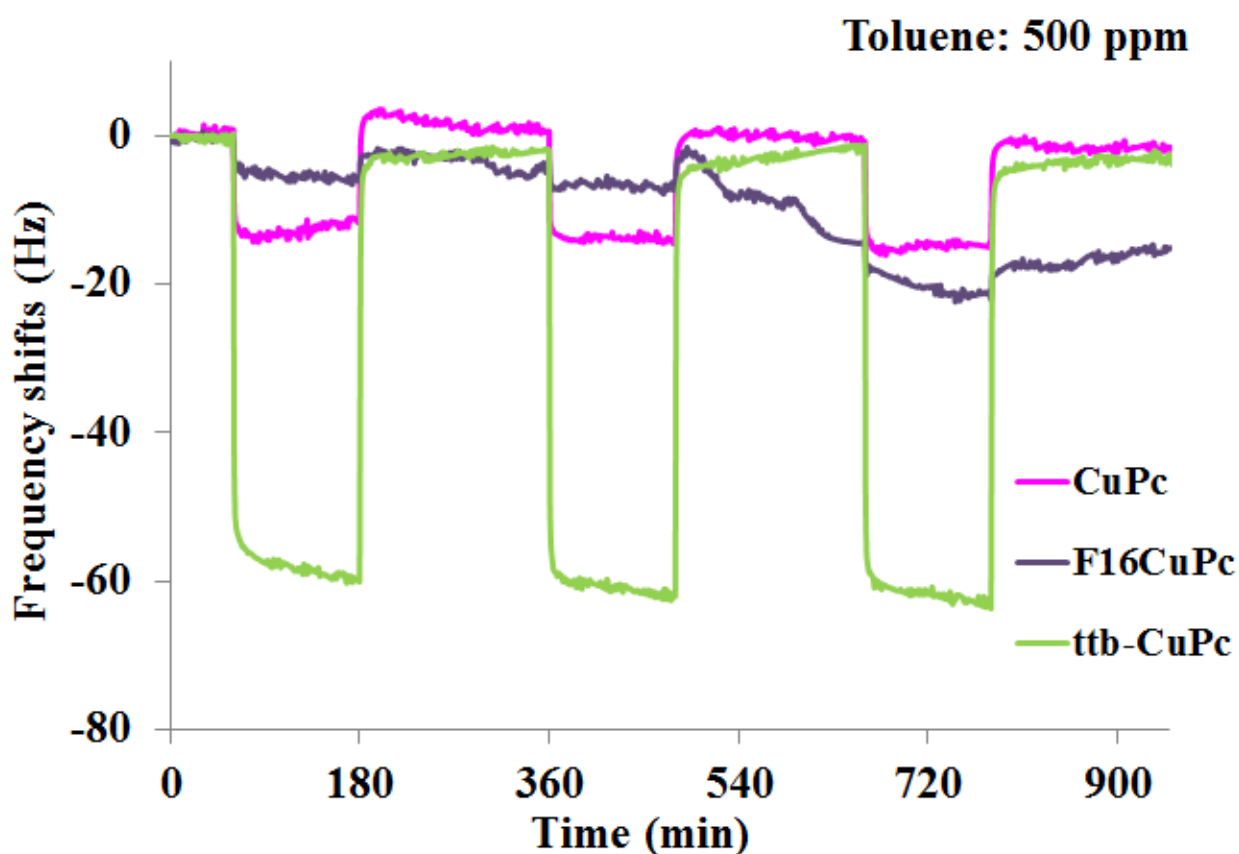


*Fig. 5: Comparison of *ttb*-CuPc, CuPc and F_{16} CuPc based QCM sensors responses exposed to 500 ppm of toluene at room temperature.*

Conclusions extracted from results obtained with copper phthalocyanines are confirmed by a similar behavior observed with zinc phthalocyanines. Figure 6 depicts *ttb*-ZnPc, ZnPc and F_{16} ZnPc coated QCM sensors responses to toluene exposure at 500 ppm at room temperature. While frequency shift for ZnPc is 13 Hz, those measured for *ttb*-ZnPc and F_{16} ZnPc were 60 Hz and 5 Hz respectively. All these results clearly establish that peripheral grafted electron-

acceptor groups like fluorine on phthalocyanines macrocycles induce a decrease in the sensitivity towards toluene while electron-donor groups like tert-butyl strongly increase it. At the same time, intercomparison of the results of the Fig. 5 and Fig. 6 confirms that there is insignificant impact of the nature of the central metal atom in metallophthalocyanines on toluene sensitivity for the same substituents. This is in agreement with the conclusions of studies made on unsubstituted metallophthalocyanines reported in section 3. Similar effects of these peripheral ligands are expected towards benzene and xylenes considering their chemical similarities with toluene. This study will be deeply discussed in next chapter.

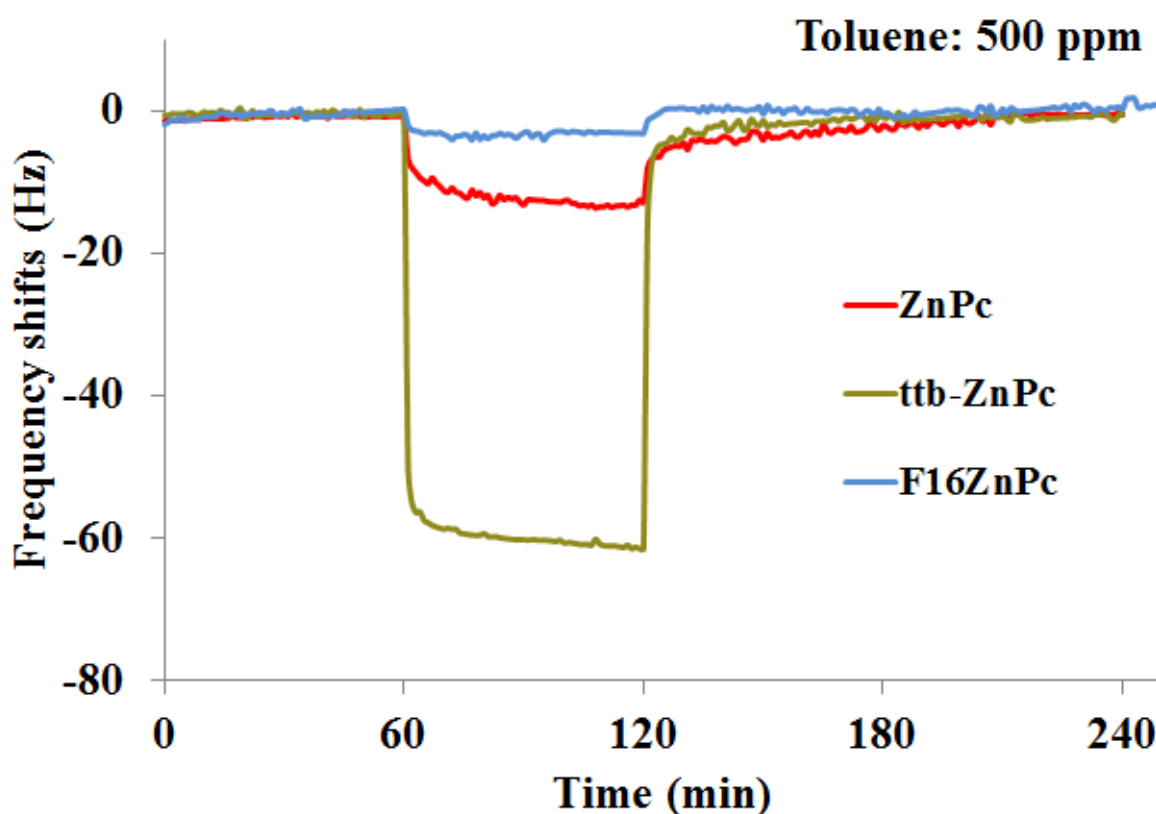


Fig.6: Comparison of ttb-ZnPc, ZnPc and F₁₆ZnPc based QCM sensor responses exposed to 500 ppm of toluene at room temperature.

If the sensitivity is a crucial specification for gas sensors, the response and recovery times are also of prime importance to ensure fast detection, reversibility and to be able to monitor fast variations of gas concentrations. Beyond sensitivity, response and recovery times attributed to substituted and unsubstituted metallophthalocyanines have been determined and summarized in table 3. Besides higher sensor responses, tert-butyl substituents on phthalocyanine macrocycles fasten the kinetics of toluene adsorption and desorption on materials. Such improvements is confirmed by the more than 4-times less response time and more than 8-times less recovery time of ttb-CuPc and ttb-ZnPc as compared to their unsubstituted counterparts. Thus, they were measured to less than 3 minutes at room temperature. For hexadecafluoro-substituted metallophthalocyanines, the lack of signal stability during periods both under toluene and pure air makes impossible the accurate determination of these characteristics. Taking into account the very low magnitude of frequency shifts as compared to other materials, F₁₆CuPc and F₁₆ZnPc can be considered as insensitive to toluene.

Materials	<i>Frequency shifts (Hz)</i>	<i>Response time (min)</i>	<i>Recovery time (min)</i>
CuPc	15	12	23
ttb-CuPc	60	<3	<3
F₁₆CuPc	5	NA*	NA*
ZnPc	13	24	80
ttb-ZnPc	60	<3	<3
F₁₆ZnPc	5	NA*	NA*

NA: Response and recovery time are not possible to calculate.*

Table 3: Variations in sensing characteristics of substituted and unsubstituted metallophthalocyanines at room temperature

3.3. Bis-phthalocyanine

Bisphthalocyanines are molecular organic semiconductors in which a metal atom is complexed by two phthalocyanine macrocycles. Besides their semiconductor character, they are characterized by a high number of benzene rings per molecular unit which can be considered as adsorption sites for BTX molecules. As a consequence, a higher sensitivity towards these gases can be expected as compared to monomeric one. For this purpose, we initiated sensing device development on a well-known bis-phthalocyanine: lutetium bis-phthalocyanines, LuPc₂. Considered as an intrinsic radical semiconductor with relatively higher conductivity than mono-macrocyclic phthalocyanines [20], this material was previously investigated for the development of chemoresistors [21]. In the context of our works, the high electron density in two phthalocyanine macrocycles can make this material more sensitive than previously studied metallophthalocyanines.

Frequency variations of quartz crystals coated with 400 nm of LuPc₂ exposed to 500 ppm of toluene at room temperature were measured. Sensor responses for successive cycles of 2 hours of exposure followed by 3 hours of recovery are reported in Fig.7. As shown, exposures to toluene lead to fast and strong decreases in frequency of LuPc₂ coated QCM followed by a complete recovery under pure air at room temperature. In contrast to the low sensitivity of unsubstituted mono-macrocyclic phthalocyanines, average frequency shifts for successive cycles of exposures were close to 70 Hz. Responses are completely reversible and repeatable for consecutive measurements. The study of the kinetics of sensor response reveals that LuPc₂-based QCM sensor shows fast adsorption as characterized by the low response time but slow desorption under pure air as justified by long recovery time. Indeed, response and recovery times were assessed to 6 minutes and 42 minutes respectively. Although a slight improvement in sensitivity is noticeable on LuPc₂ coated QCM devices, the main drawbacks is linked to the slower toluene desorption processes which confer to sensing devices slower

kinetic of response as compared to previous studied monomeric tert-butyl substituted metallophthalocyanines.

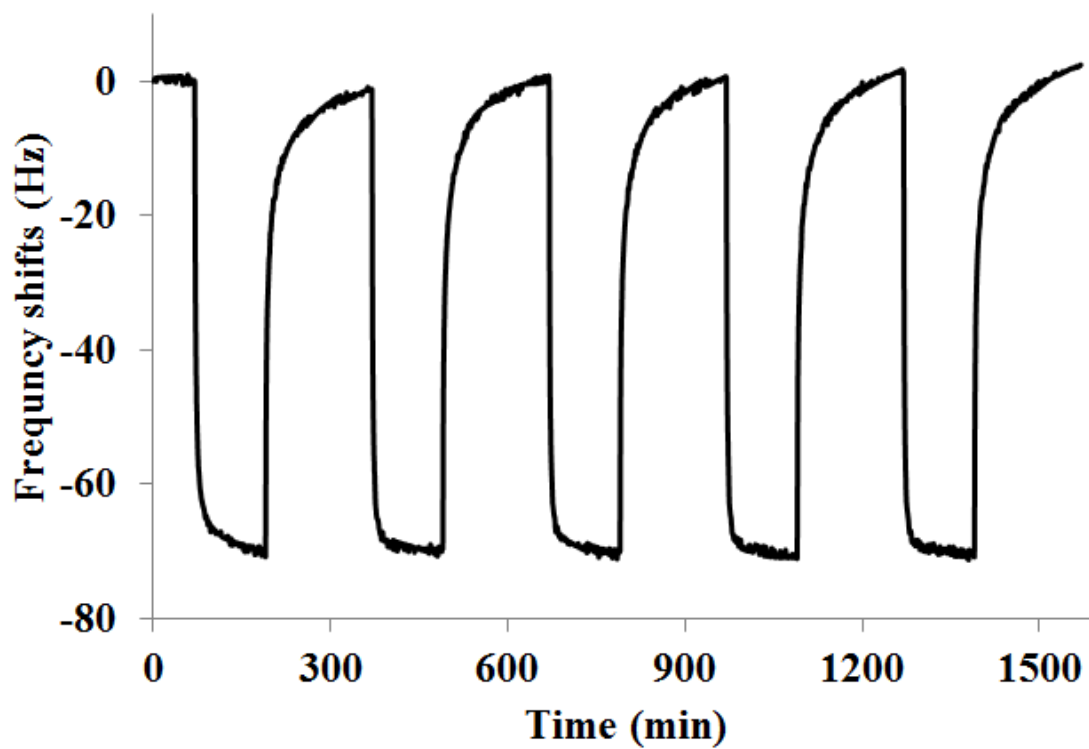


Fig.7: LuPc₂ based QCM sensor response to 500 ppm of toluene at room temperature.

4. Effect of thin layer organizations on BTX sensing behavior

From the results on the response of phthalocyanines based QCM sensors towards toluene previously described, a great variation in sensitivity for different types of phthalocyanines is established. More especially, we have highlighted that the grafting of electron-donor groups and the use of bisphthalocyanines are in favor of sensitivity with however a slower desorption for LuPc₂. Besides the nature of investigated materials, previous studies on gas sensing have established that the structure and the morphology of sensing layers play a decisive role in determining sensitivity to target gases [22-24]. In the present case, the strong effects of peripheral ligands on sensitivity can be linked to the modulation of gas/material interactions but also to the dissimilar organization of phthalocyanine macrocycles in thin films which can in turn affect the gas sorption within the sensing layer. Thus, structural and morphological characterizations of thin layers have been performed by X-Ray diffraction and Scanning Electron Microscopy. These results were then correlated to sensing results.

4.1. Structural characterization of layers by X-Ray Diffraction

In order to determine the potential effect of peripheral tert-butyl groups on the layer structure, i.e. the molecular organization, CuPc, ZnPc, ttb-CuPc and ttb-ZnPc layers coated on glass substrates maintained at room temperature were characterized by XRD. The thickness of all the films was chosen to 250 nm and no post-deposition annealing or chemical treatment was performed on the sample. XRD patterns are shown in Fig. 8. One prominent sharp peak at $2\theta = 6.92^\circ$ is observed for CuPc and ZnPc, while a broad peak develops at $2\theta = 5.23^\circ$ and 5.39° for ttb-CuPc and ttb-ZnPc respectively. Interplanar distances corresponding to these different diffraction peaks are summarized in table 4.

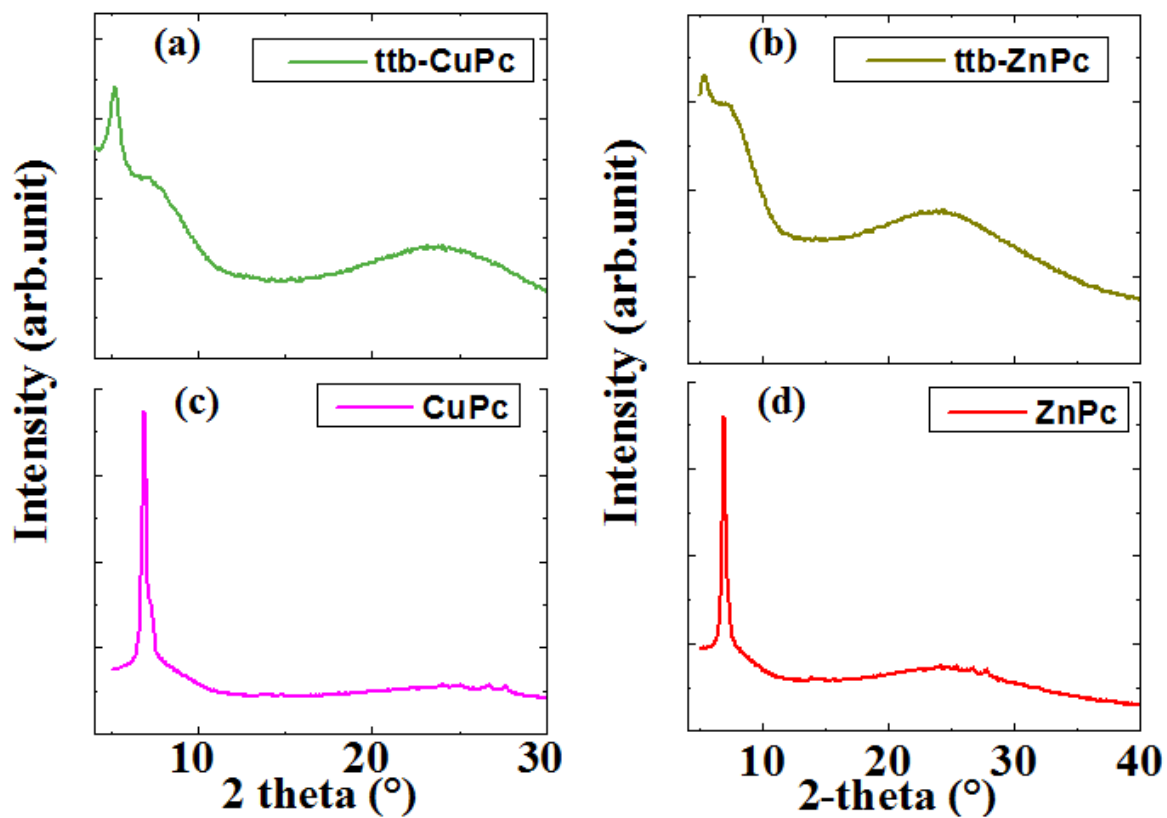


Fig.8: XRD patterns of *ttb-CuPc*, *CuPc*, *ttb-ZnPc* and *ZnPc*.

Material	2θ ($^{\circ}$)	d (\AA)
<i>CuPc</i>	6.92	12.75
	26.04	3.33
<i>ZnPc</i>	6.92	12.75
	26.64	3.34
<i>ttb-CuPc</i>	5.23	16.75
	24.45	3.64
<i>ttb-ZnPc</i>	5.39	16.41
	24.44	3.64

Table 4: Inter-planar distances in phthalocyanines

From the number and nature of peaks of XRD pattern of the different materials, we can remark that all films have low level of crystallinity. Nevertheless, the intercomparison of XRD patterns between unsubstituted and substituted metallophthalocyanines reveals a locally organized structure in unsubstituted metallophthalocyanines thin layers. The main characteristic diffraction peak of CuPc and ZnPc are at $2\theta = 6.92^\circ$ which corresponds to interplanar distance of 12.75 \AA . This value is in agreement with the distance between stacking axis of two phthalocyanine columns also determined earlier from high resolution TEM studies [25-27]. The presence of weak peaks in XRD patterns indicates the molecular orientation on the substrate of CuPc and ZnPc. Peaks at $2\theta = 26.04^\circ$ for CuPc and 26.64° for ZnPc correspond to a d-spacing of 3.33 \AA and 3.34 \AA respectively. These distances represent the distance between two macrocycles in a given column [28-30], as illustrated in Fig. 9. For ttb-CuPc and ttb-ZnPc, no prominent diffraction peaks appears: thin layers of ttb-MPCs are highly amorphous. Only small peaks at $2\theta = 5.23^\circ$ and 5.39° for ttb-CuPc and ttb-ZnPc corresponding to a d-spacing of 16.75 \AA and 16.41 \AA respectively could correspond to the distance between staking axis of two localized molecular columns. Higher column spacing as well as the intermolecular spacing within a column for ttb-CuPc and ttb-ZnPc as compared to unsubstituted macrocycles can be attributed to steric factor associated with bulky tert-butyl ligands.

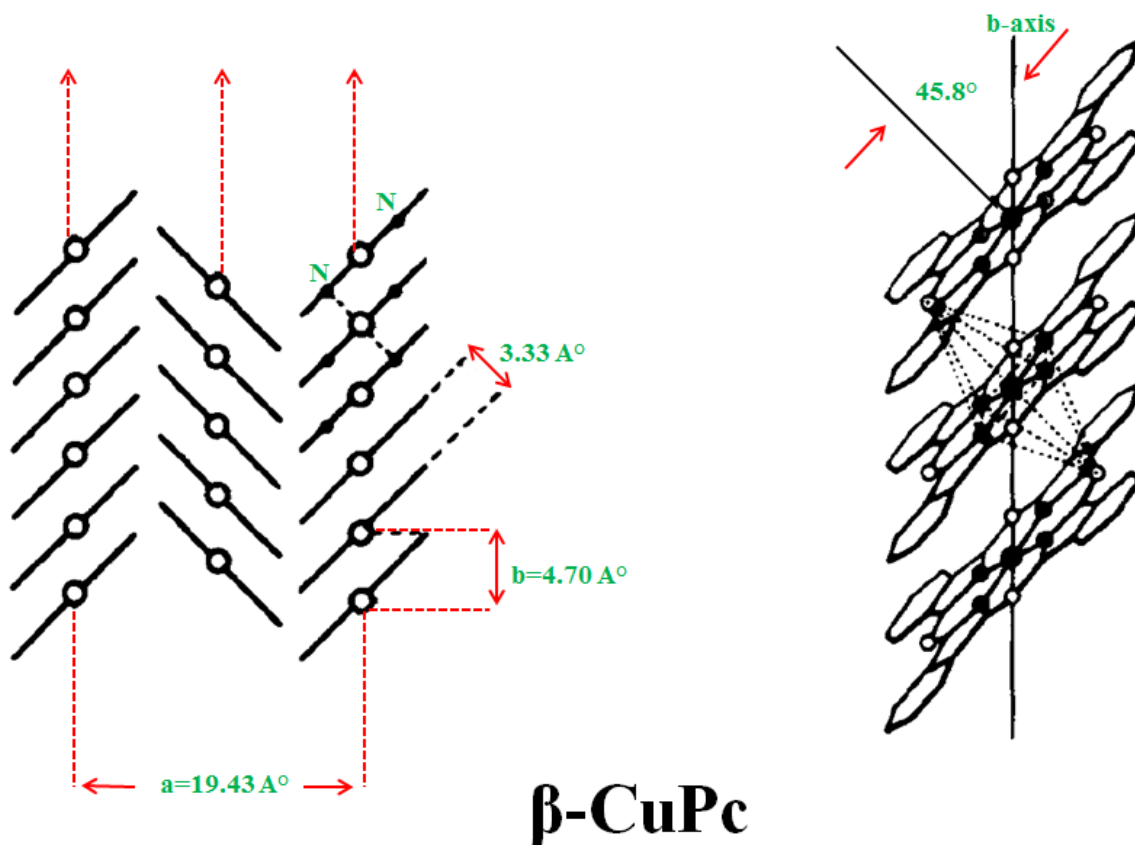


Fig. 9: Schematic representation of arrangements of CuPc macrocycle in β -phase.

The phase identification of CuPc and ZnPc films were carried out using JCPDS-ICDD database. Further the full pattern profile matching was performed by FULLPROF software in order to find the lattice parameters. These parameters are reported in table 5.

Material	a (Å)	b (Å)	c (Å)	β (°)	Density (g/cm ³)
CuPc	19.43	4.70	14.79	120.37	1.625
ZnPc	19.22	4.87	14.52	120.03	1.61

Table 5: lattice parameters of CuPc and ZnPc semi-crystalline layer

Comparing the lattice parameters a , b , c and β from the earlier published papers [26, 27], organization of CuPc and ZnPc were established as predominantly in β -phase. In β -phase, phthalocyanines macrocycles are organized in a staggered arrangement in which metal atom of one macrocycle remains perpendicular to pyrrolic nitrogen atom of the opposite stacked units as shown in Fig. 9. Such arrangement is stable because of interaction of nitrogen of one phthalocyanine to the central metal atom of the other. The crystals are monoclinic having two molecules per unit cell with the column axis corresponding to the b -axis. From these parameters, crystal density of CuPc and ZnPc were assessed to 1.625 and 1.61 g/cm³. The crystalline phases are localized but overall layers have low crystallinity as confirmed by the low intensity of peaks in XRD pattern. For thicker films, molecular orientation remains more uncertain because of defects and dislocations arising with increasing thicknesses.

4.2. Morphological characterization of layers by Scanning Electron Microscopy

Complementary to structural characterization by XRD spectroscopy, Scanning Electron Microscope (SEM) was used to scan the surface of the sensitive layer. SEM pictures of CuPc, ZnPc, ttb-CuPc and ttb-ZnPc layers with 250 nm of thickness deposited on copper substrate maintained at room temperature are reported in Fig. 10.

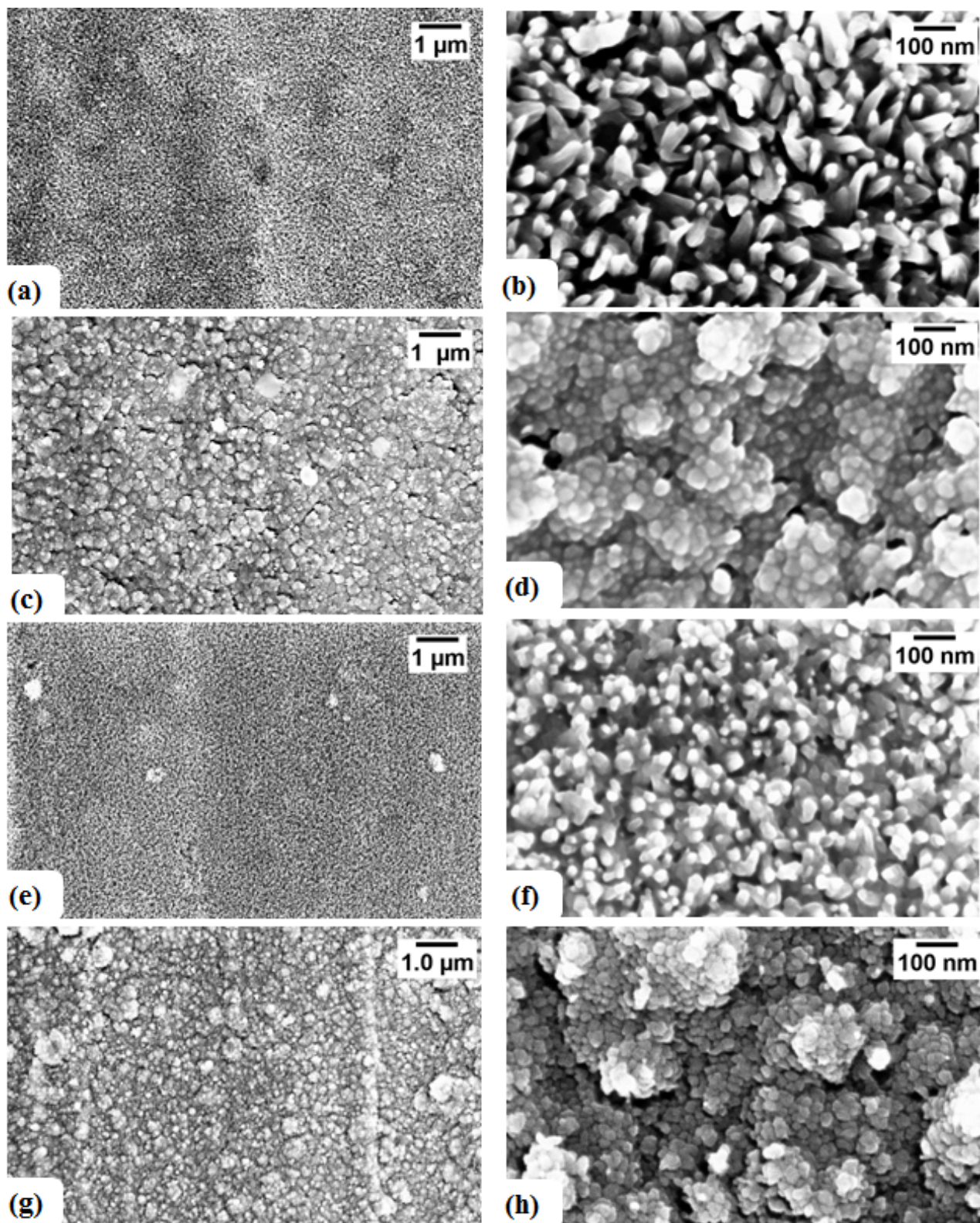


Fig. 10: SEM micrographs of CuPc (a,b), ttb-CuPc (c,d), ZnPc (e,f), and ttb-ZnPc (g,h) with enlargement for 1μm and 100 nm are X10000 and X100000 respectively.

Figs. 10a and 10e clearly indicate that at microscopic scale with an enlargement equal to X10000, CuPc and ZnPc layers are smooth and constituted by fine grains. In contrast, Figs. 10c and 10g reveal that tert-butyl substituted metallophthalocyanines show a rougher surface and larger grains size. Such a wide distinction in films growth between substituted and unsubstituted metallophthalocyanines manifests the effects of nature of ligands grafted at the periphery of macrocycle on thin film morphology. These effects are more obvious at the nanometric scale. Thus, Figs. 10b, 10d, 10f and 10h represents the SEM images of CuPc, ttb-CuPc, ZnPc and ttb-ZnPc with an enlargement equal to X100000. The local semi-crystalline organization and columnar arrangements of unsubstituted phthalocyanine layers deduced from XRD characterizations and the previous reported TEM studies [25, 27] are confirmed by SEM micrographs. Indeed, Figs. 10b and 10f highlight the columnar arrangement of phthalocyanine molecules. Although such needle arrangement is observable at local place, a lack of homogeneity can be observed on all the scanned surface. More especially for ZnPc, smaller grain size as well as few localized aggregations is observed. On the contrary, a highly amorphous organization is manifested on tetra-tert-butyl metallophthalocyanines that is in agreement with conclusions from XRD analysis. SEM pictures let appear ttb-MPc layers as aggregates constituted by an assembly of nanoflakes. Similar morphologies of these materials were reported in the past [29, 30]. The effect of peripheral ligands on layer morphology is so noticeable.

The formation of large needle like crystallites in CuPc is because of strong inter-macrocycle staking interactions in β -phase which is facilitated by the ability of copper to coordinate up to six ligands. On the contrary, maximum coordination number of Zinc is four, which is already occupied by the pyrrolic nitrogen of the phthalocyanine macrocycle, making zinc atom unavailable to participate in interaction with neighboring phthalocyanines. It results in relatively weak staking in staggered β -phase column manifested by smaller needles of

ZnPc. Small crystallites size and aggregation in substituted metallophthalocyanines can be attributed to tert-butyl ligands grafted at the periphery of macrocycle. The presence of bulky tert-butyl groups destabilizes π - π stacking between macrocycles by enhancing distance between them because of steric repulsion leading to tiny sized crystallites. At the same time, high spatial volume of tert-butyl provides a large surface for dispersion interaction between two tert-butyl substituted metallophthalocyanines. The simultaneous attractive and repulsive behavior induced by tert-butyl groups are because of distance dependence of dispersion forces. At inter-macrocylic distance of 3.6 Å in ttb-MPc, dispersion forces are repulsive in nature which become attractive at longer distances. This is manifested in the formation of aggregates of small-sized crystallites of ttb-CuPc and ttb-ZnPc. Thus, morphologies of tert-butyl substituted metallophthalocyanines films predict weaker staking of macrocycles within a crystallites and stronger interactions between crystallites and vice-versa in the case of unsubstituted metallophthalocyanines. These differences in organization of substituted and unsubstituted macrocycles in thin films can strongly affect the gas interaction on surfaces.

4.3. Discussion

Low sensitivities of unsubstituted phthalocyanines-based QCM sensors towards BTX can be justified by the structural and morphological properties of the sensing layers. As previously described, SEM and XRD analyses of CuPc and ZnPc coatings confirm that such layers consist in closely packed columns with a very short distance between macrocycles involved into the columns (3.33 Å for CuPc). Consequently, BTX molecules can mainly involve interactions with macrocycles localized at the top of crystallites and interactions with macrocycles localized inside the columns is weakly probable. Even if BTX gaseous molecules can diffuse into the volume of the layer, interactions with the columnar walls are negligible considering the nature of possible interacting forces involved. This can be understood by

considering the arrangements of CuPc macrocycle within a column in Fig. 9. Adsorption sites for BTX gases can be available only on the plane of a macrocycle and not along the columnar wall. Dissimilarity in kinetics of sensors response can be also correlated to the structure and morphology of the sensing layers. SEM pictures of CuPc and ZnPc show that ZnPc crystallites are smaller and more tightly packed as compared to CuPc. Such close packing of ZnPc crystallites can lead to smaller pores in the layers as compared to CuPc. This can result in slow diffusion processes of gaseous molecules, which can justify the longer response and recovery times measured for ZnPc-based QCM sensors. In CuPc layers, larger pores ensure relatively fast gas diffusion resulting in shorter response and recovery times.

Strong impacts of peripheral substituents in metallophthalocyanines on BTX sensitivity can be primarily attributed to their electronic and steric nature. These properties determine the morphology of the films near the surface, the arrangement of macrocycles into the layers but also the extent and the strength of probable adsorption sites on the surface as well as into the volume. Change in morphology and structure of layers because of peripheral substitution were clearly established through SEM and XRD studies of tetra-*tert*-butyl substituted metallophthalocyanines. Aggregations of molecular clusters into an island like geometry provide larger surface area for gas adsorption in *t*tb-CuPc and *t*tb-ZnPc layers, that results in higher QCM sensor responses. Moreover, in contrast to the compact columnar packing of crystallites observed for CuPc and ZnPc layers, *t*tb-MPc layers consist in loose (distance between crystallites is 16.75 Å° at local level organization) and highly disordered arrangements of crystallites, leading to easier diffusion of BTX gases within the layers. Because of the amorphous nature of *t*tb-MPc layers, the number of gas adsorption sites in its volume increases, which further adds to sensor responses. Furthermore, the amorphous nature of *t*tb-CuPc and *t*tb-ZnPc layers develops nano-channels within it, which help in fast diffusion through enhanced mobility of adsorbed BTX gases. It also explains the short response and

recovery times of QCM sensors coated by these materials. Short response and recovery times are further supported by the higher inter-crystallites separation in ttb-CuPc and ttb-ZnPc compared to CuPc and ZnPc. To summarize, if BTX molecules adsorption is limited on available sites localized close to the surface for unsubstituted metallophthalocyanine layers, this adsorption is extended to all available sites present into the volume of the layer for ttb-CuPc and ttb-ZnPc samples.

4.4. Effects of layer thickness on sensitivity

To validate the surface and volume interactions in unsubstituted and tert-butyl substituted metallophthalocyanines respectively, effects of sensing layer thickness on toluene sensitivity was investigated. CuPc and ttb-CuPc based-QCM sensors having coatings of 200 nm, 300 nm and 400 nm were exposed to 500 ppm of toluene at room temperature. The magnitude of frequency shifts of these sensing devices are depicted in Figure 11. It is obvious from the QCM response that toluene interaction with CuPc layers remains almost independent of layer thickness while a strong effect appears with ttb-CuPc. The frequency shifts of CuPc based QCM sensors were found to be approximately constant at three different film thicknesses. In contrast, a linear increase in response of ttb-CuPc based QCM was measured with increasing thickness of the sensing layer. Such results confirm the porous nature of ttb-CuPc layer which ensures fast diffusion of toluene into the volume. The sensor response of 400 nm thick layer was more than double in magnitude relative to 200 nm layer. It implies that active sites where toluene molecules can interact during exposure cycles are present on the surface as well as in the sub-layers. As a conclusion, such variations in QCM response with sensing layer thickness confirm the predominant surface interaction of toluene on CuPc layer while an extended interaction occurs within the layer volume of ttb-CuPc.

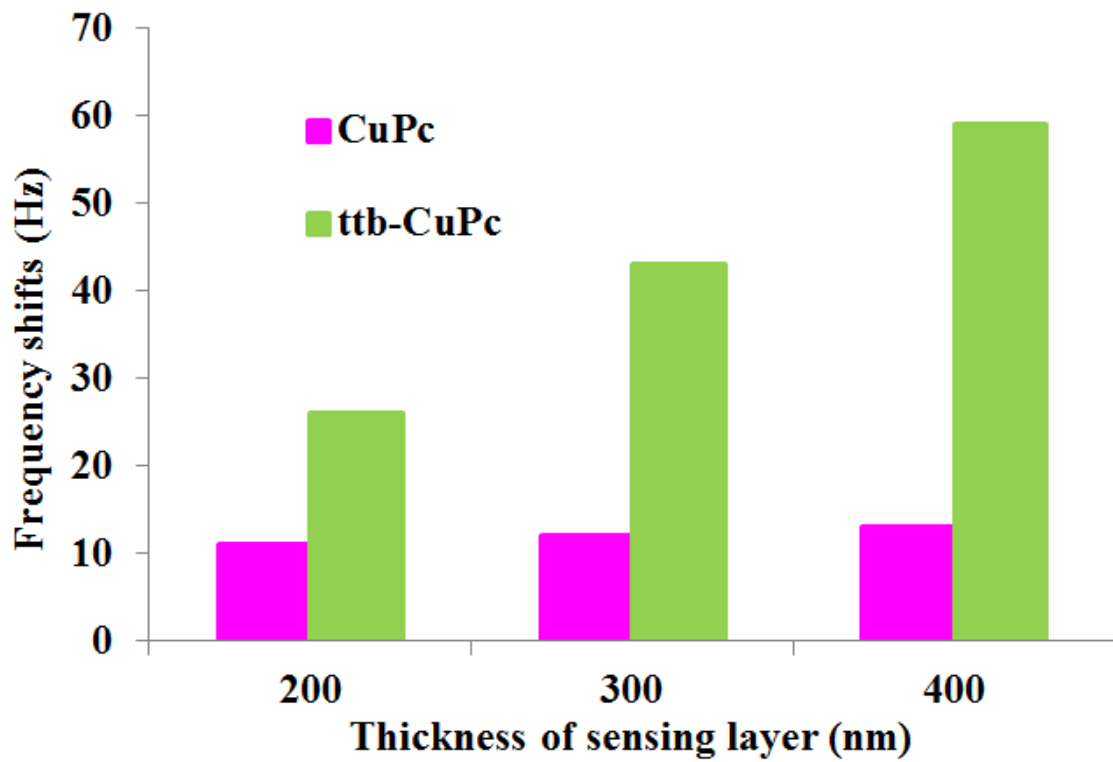


Fig.11: Intercomparison of CuPc and ttb-CuPc based QCM sensors responses at different layer thickness exposed to 500 ppm of toluene at room temperature.

5. Gas/material interactions at molecular scale

The organization of phthalocyanine macrocycles into thin films previously characterized derives from their molecular properties and more especially are strongly dependent from the electronic and steric nature of ligands. The intermolecular interactions existing between phthalocyanine macrocycles but also between phthalocyanines and BTX molecules involve non-covalent forces responsible for layer organization as well as gas adsorption. Taking into consideration the different sensitivity variations as a function of materials, interactions taking place between phthalocyanines and BTX gases at molecular level must be considered.

5.1. Non-covalent forces acting between phthalocyanines and BTX

Depending on the structure and the electronic properties of phthalocyanines and BTX, interaction during gas exposure is primarily because of non-covalent forces. As the name implies, these forces don't involve a covalent bond between the interacting systems. If these forces act between aromatic rings, they are commonly known as aromatic interactions [31]. Non-covalent interactions take place mainly because of two types of forces: (a) electrostatic and (b) dispersion forces. Considering the variations in electronic density and shape of the associated ligands in metallophthalocyanines, different types of aromatic interactions can take place with BTX. These interactions can have either only electrostatic component, only dispersion component or mix of these two.

5.1.1. Electrostatic forces based interactions

As explained above, aromatic interactions between phthalocyanines and BTX can be of electrostatic nature. Among them, we can mention π - π and M- π interactions. π - π

interactions remain the main interest considering the global distribution of π -electrons in both interacting molecules. A lot of approaches have been adopted to explain this phenomenon and a generalized description is not yet available. A π - π interaction model proposed by Hunter and Sanders [32] is relevant in our case because they considered porphyrin as a template molecule. According to them, electronic distribution within an aromatic molecule can be considered as a quadrupole consisting of positively charged σ -framework sandwiched between two negatively charged π -electron clouds as shown in Fig. 12a for benzene molecule. A π - π interaction can be considered as interaction between two such quadrupole systems as illustrated in Fig. 12b. The electrostatic attraction takes place between π -electron clouds of one molecule to sigma framework of other. On the other hand, electrostatic repulsion occurs between π -electron clouds of interacting molecules. Different configurations are possible as shown in Fig. 12b [33]. This interaction can be attractive only when σ - π attraction outweighs π - π repulsion.

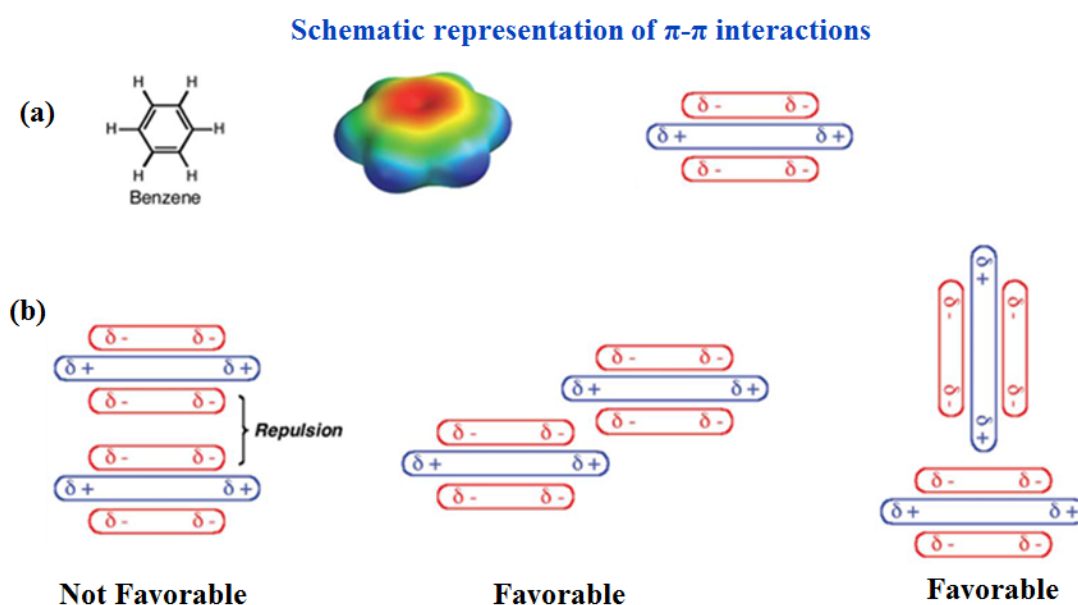


Fig. 12: (a) Representation of electronic distribution in a benzene molecule through a simplified quadrupole; (b) Various geometrical configuration of π - π interaction.

In a metallomacrocyclic, metal atom acts like a positive charge center. $M-\pi$ interaction is an attractive electrostatic force between metal atom and π -electron cloud of another aromatic molecule. The strength and geometry of this interaction depends on the coordination number, size and electron present in valence shell of metal atom.

5.1.2. Dispersion forces based interactions

London dispersion force is the weakest attractive intermolecular force (0.1–1 Kcal/mol) that exists between all molecules without regard to their polarity. Even though a molecule may have no permanent dipole, it does have a cloud of rapidly moving electrons. If this cloud is distorted, no matter how briefly, the molecule will then have a temporary negative charge at one end and a temporary positive charge at the other end. In other words, the molecule has a temporary dipole. This temporary dipole can distort the electron clouds of nearby molecules so that they have temporarily induced dipoles too. The forces of attraction between the temporary partial positive charges on some molecules and the temporary partial negative charges on neighboring molecules are the dispersion forces. The only factor which modulates the extent of this force is the surface area of the neighboring molecules in contact (at Van der Waals radii) of each other. A molecule with a large spatial volume is expected to provide extended surface area for dispersion interaction. Interactions between methyl group(s) of BTX and tert-butyl groups in tetra-tert-butyl-metallophthalocyanines can be considered of this type.

5.1.3. Electrostatic and dispersion forces based interactions

C–H bond in a hydrocarbon has certain ionic character because of electronegativity difference of carbon and hydrogen. An aromatic molecule has sp^2 hybridized carbon atoms,

which electronegativity is higher than alkane carbon having sp^3 hybridization. So, hydrogen atoms in an aromatic molecule are slightly polarized with positive charge. CH- π interaction is an attractive force between positively polarized hydrogen of one aromatic with π -electron cloud of other [34, 35]. The forces involved in such interactions are combination of electrostatic and dispersion in which dispersion remains dominant. The strength and extent of this interaction depends on the shape and number of hydrogen atom present in the aromatic molecule. A typical range of this interaction is 2.1–2.4 Kcal/mol.

5.2. Interactions on unsubstituted metallophthalocyanines

Considering the structure and π -electrons distribution in unsubstituted phthalocyanine and BTX gases, main interacting forces responsible for adsorption on sensor surface are aromatic interactions [31-33, 36]. Among them we can mention the main constituents as: π - π , M- π and CH- π . Although all these forces are weak, their relative strengths are in the order of CH- π < M- π < π - π . From a sensing point of view, the weak interaction forces involved are a great advantage to ensure reversible responses even at room temperature as justified by reversible desorption process under pure air and fast recovery. Low sensitivities experimentally measured on unsubstituted metallo and metal-free phthalocyanines can be attributed to the limited number of available sites for gas adsorption into the sensitive layer. Because of the columnar structure of these MPCs layers, π - π interactions are mainly involved between macrocycles into the staking. Nevertheless, the slight higher sensitivity in metallophthalocyanines as compared to free-phthalocyanine can result from two factors:

- the presence of metal atom can act as an extra adsorption sites for BTX gases on sensor surface through M- π interactions [37-39];

- the electronic conjugation in phthalocyanines is extended because of donation of electron from the d-orbital of metal atom leading to enhanced π - π interactions with BTX molecules [40-43].

As experimentally established, the increasing sensitivity from benzene to xylenes of the different unsubstituted metallophthalocyanines can be justified by the substituents effects in BTX analytes on aromatic interactions as reported earlier [44-51]. The interaction of benzene and unsubstituted phthalocyanines occurs mainly through π - π and M- π non-covalent forces. Toluene and xylenes are mono-substituted and di-substituted aromatic π -system respectively. In addition to π - π and M- π interactions, methyl group(s) in toluene and xylenes also interacts with the π -electronic cloud of the material. Moreover, dispersion forces, which strongly depend on the surface area of interacting systems, increase in the case of toluene and xylenes. Effects of substituents in aromatic interactions being additive in nature as reported earlier [46], it could explain the increase in sensor sensitivity with the number of the methyl groups on the target gaseous molecules and the highest response of QCM-based sensors towards xylenes.

5.3. Interactions on substituted metallophthalocyanines

The grafting of functional groups at the periphery of phthalocyanine macrocycles can affect their interaction with BTX gases in two ways: i) the electronic nature of substituents can modulate the intrinsic π -electron density within the macrocycle and ii) direct interactions can take place between substituents and the opposite interacting system. The modulation of the strength and the extent of these interactions are linked to the electron-donating or electron-withdrawing character of ligands as well as their steric effects. Tert-butyl group is an electron-donor ligand because of its inductive properties and possesses a high spatial volume. As a

consequence, they increase the π -electron density of the delocalized electronic system of the material and can provide larger surface area for the dispersion interactions with BTX molecules. Adsorption of BTX gaseous molecules on ttb-CuPc or ttb-ZnPc molecular units involves:

- π - π interactions between π -electron clouds;
- CH- π interactions between methyl group(s) of BTX and π - electron cloud of phthalocyanines as well as between peripheral tert-butyl groups of macrocycles and π -electron clouds of BTX molecules;
- Dispersion interactions between tert-butyl groups and BTX molecules.
- M- π interactions

A simplified scheme of these involved gas/material molecular interactions is given in Fig. 13.

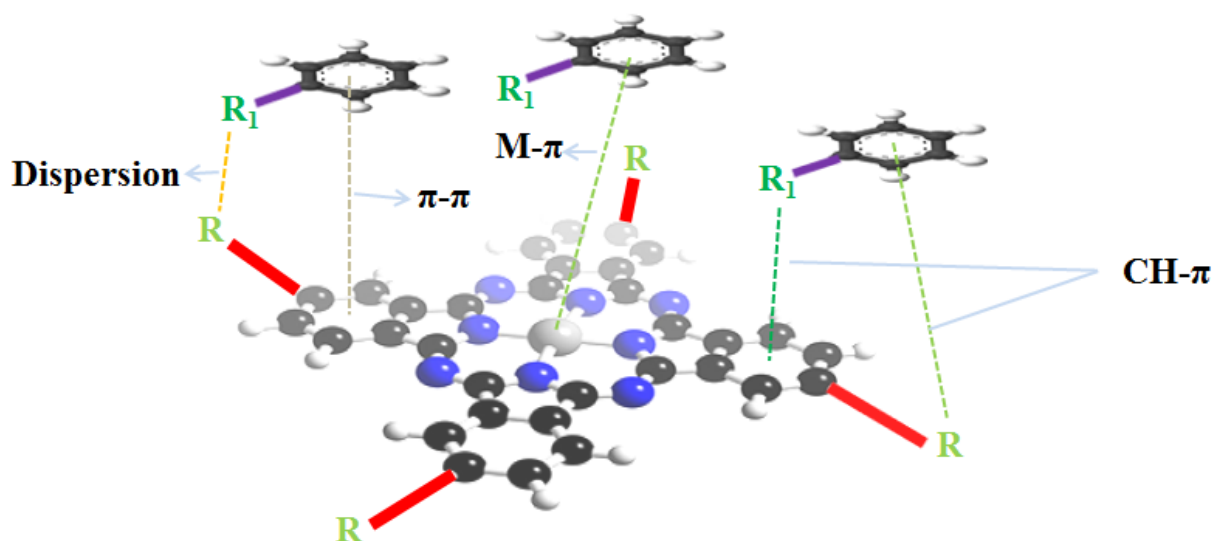


Fig.13: Schematic representation of molecular gas/material interactions between gaseous monocyclic hydrocarbons molecules and substituted phthalocyanines.

The possible larger extent of non-covalent interactions can explain the high sensitivity of ttb-CuPc and ttb-ZnPc based QCM sensors. Strong decrease in response and recovery times of tert-butyl substituted metallophthalocyanines based QCM sensors gives an insight

into the main contributing forces leading to improved sensitivity of these sensors. More than 8-times decrease in response time and more than 25-times decrease in recovery times were established for ttb-ZnPc as compared to ZnPc toward toluene. Grafting of tert-butyl groups on ZnPc macrocycle increases electron density as well as molecular volume. If high increase in magnitude of response is attributed to rise in π - π interaction, then sorption times should be also comparable to un-substituted metallophthalocyanines based QCM. On the contrary, response and recovery times decrease sharply. That is why, increase in molecular volume because of tert-butyl substitution play the lead role in improving sensitivity of ttb-CuPc and ttb-ZnPc through dispersion interactions. Because of the presence of tert-butyl ligands, sensing layers can be visualized as one consisting of large number of possible adsorption sites which can involve relatively weaker interactions to BTX as compared to π - π . Thus, it can be emphasized that, π - π interaction lead the gas/material interaction in unsubstituted phthalocyanines while dispersion plays a predominant role in tert-butyl substituted metallophthalocyanines. This is also in agreement with previous studies, highlighting the predominant role of direct interaction of substituents with opposite interacting system in aromatic interactions [44, 46, 52].

The insensitivity of hexadecafluoro-substituted metallophthalocyanines is mainly attributed to the distortion of the electronic cloud of phthalocyanine molecular units due to the presence of 16 fluorine atoms in substitution of hydrogen atoms on the macrocycles. Because of its highest electronegativity, fluorine acts as an electron-acceptor group. The substitution at all the peripheral sites by fluorine leads to a distortion of the electronic cloud in which π -electrons being attracted towards the periphery. Thus, such modulation in distribution of the π -electrons cloud in F₁₆CuPc significantly decreases the π - π interaction forces with BTX gases. Moreover, because of the small spatial volume of fluoride groups, F₁₆CuPc or F₁₆ZnPc macrocycle volume remains similar to CuPc or ZnPc respectively and no significant increase

in dispersion interactions can be expected. Consequently, fluoro-substitutions at all the peripheral sites of metallophthalocyanines result in the decrease in π - π interactions with BTX gases, which justifies the 3-times lower sensitivity of $F_{16}CuPc$ and $F_{16}ZnPc$ as compared to $CuPc$ and $ZnPc$ as previously highlighted.

5.4. Case of $LuPc_2$

The presence of two macrocycles in conjugation to each other via an electron donor metal atom can strongly influence the π -electron environment within the $LuPc_2$ molecules [53-55]. On the other hand, because of very small gap between SOMO (semi-occupied molecular orbital) and LUMO (Lowest unoccupied molecular orbital) orbitals, electronic delocalization within the two macrocycles can be very high. This is particularly supported by the very high electrical conductivity of $LuPc_2$ as compared to other phthalocyanines [20, 53, 56-59]. Since no peripheral ligands are grafted on the macrocycles, the predominant non-covalent forces leading to toluene adsorption is π - π interactions. The presence of two macrocycles combined with strong π -electron delocalization increases the extent of interactions highlighted by higher sensor response as well as strength of interactions confirmed by longer recovery time as compared to *ttb*-MPcs. Thus gas/material interactions are predominantly driven by π - π interactions similar to other studied unsubstituted phthalocyanines.

Conclusion

In this chapter, sensitivities of coated QCM by phthalocyanine thin layers toward BTX were measured. A systematic study on different types of phthalocyanines was performed starting from simple mono-macrocyclic unsubstituted phthalocyanines to peripherally substituted and double decker phthalocyanines. Because the main technical objective was to select the most appropriate phthalocyanine associated to QCM transducers to perform fast, sensitive and reversible detection of BTX gases, effects of the central metal atom, peripheral substituents and number of macrocycles on sensing performances were especially investigated. Firstly characterized by UV-Vis absorption spectroscopy, commercial products were confirmed to expected materials. The comparison between powdered and layered materials by Fourier-Transform Infrared Spectroscopy confirmed the thermal stability of metallophthalocyanines, their possible sublimation without molecular destructuring and the processability as thin films by thermal evaporations even if bulky ligands like tert-butyl substitute peripheral hydrogen atoms. XRD and SEM pictures have established amorphous or localized semi-crystalline organizations in the layers depending upon the substituents grafted or metal atom present in the center of molecules. SEM images in particular clearly reveal a needle-form and an island-form organization of molecular units for unsubstituted and tert-butyl substituted metallophthalocyanines respectively. Intercomparison of sensor responses highlighted non-significant effect of central metal atom of studied phthalocyanines (CuPc, H₂Pc, ZnPc, FePc and CoPc) on BTX sensitivities which remain low for all sensing devices.

To benefit from higher sensitivities, two approaches were followed: (a) peripheral substitution on phthalocyanine macrocycles and (b) increase in number of macrocycles by using a double decker LuPc₂. In contrast to non-significant effects of central metal atom, strong effect of tert-butyl group in phthalocyanines on BTX sensitivity has been established.

The high sensor responses obtained on tert-butyl substituted metallophthalocyanines were attributed to electron-donating and high spatial volume ligands, which also influences the structure and morphologies of sensing layer making it favorable for gas adsorption. Substitution by fluorine of all the peripheral hydrogen atoms of metallophthalocyanines induces a decrease in BTX sensitivity. Study of kinetics of gas sorption reveals that adsorption of BTX gases on unsubstituted metallophthalocyanines is predominantly explained by π - π interactions while dispersion forces play a crucial role in sharp increase in tert-butyl substituted metallophthalocyanines-based sensors response. On the other hand, high electronegativity of fluorine leads to the distortion of π -electronic cloud within the macrocycle, leading to negligible sensor responses toward toluene. The high increase in toluene sensitivity in LuPc₂-based QCM as compared to monomeric metallophthalocyanines was attributed to the presence of two macrocycles and strong π -electron enrichment of both macrocycles through electron donation from lutetium. Nevertheless, such increase in response can be attractive, the slow kinetics of gas sorption is the main drawback.

Because of the better sensing performances exhibited by ttb-MPc-based QCM sensors and the commercial availability with high purity of these materials, tetra-tert-butyl substituted metallophthalocyanines are appropriate materials for the development of efficient sensors for BTX monitoring in atmosphere. Their high sensitivities and low response and recovery times at room temperature being well established by experimental measurements, others metrological characteristics must be assessed to validate the potentialities of these sensors for environmental application.

References

1. Isago, H., *Optical Spectra of Phthalocyanines and Related Compounds: A Guide for Beginners*. 2015: Springer Japan.
2. Yilmaz, I., et al., *Synthesis and Characterization of Novel Phthalocyanines with Four 16-Membered Diazadithia Macrocycles*. *Chemische Berichte*, 1996. **129**(8): p. 967-971.
3. Mack, J., et al., *Assignment of the optical spectra of metal phthalocyanines through spectral band deconvolution analysis and zindo calculations*. *Coordination Chemistry Reviews*, 2001. **219–221**: p. 993-1032.
4. Kobayashi, N., et al., *Effect of Peripheral Substitution on the Electronic Absorption and Fluorescence Spectra of Metal-Free and Zinc Phthalocyanines*. *Chemistry – A European Journal*, 2003. **9**(20): p. 5123-5134.
5. Stillman, M.J., et al., *Orbital reduction factors in the lowest excited state of the phthalocyanine ring and their measurement by magnetic circular dichroism spectroscopy*. *Journal of the Chemical Society, Faraday Transactions 2: Molecular and Chemical Physics*, 1974. **70**: p. 805-814.
6. Kadish, K.M., K.M. Smith, and R. Guillard, *The Porphyrin Handbook: Phthalocyanines : spectroscopic and electrochemical characterization*. 2003: Academic Press.
7. Whalley, M., *Conjugated macrocycles. Part XXXII. Absorption spectra of tetrazaporphins and phthalocyanines. Formation of pyridine salts*. *Journal of the Chemical Society (Resumed)*, 1961. **182**: p. 866-869.
8. Stillman, M.J., et al., *Assignment of the charge-transfer bands in some metal phthalocyanines. Evidence for the $S=1$ state of iron (II) phthalocyanine in solution*.

- Journal of the Chemical Society, Faraday Transactions 2: Molecular and Chemical Physics, 1974. **70**: p. 790-804.
9. Mack, J., et al., *Transition Assignments in the Ultraviolet–Visible Absorption and Magnetic Circular Dichroism Spectra of Phthalocyanines*. Inorganic Chemistry, 2001. **40**(4): p. 812-814.
 10. Vivas, M.G., et al., *Study of singlet excited state absorption spectrum of lutetium bisphthalocyanine using the femtosecond Z-scan technique*. Chemical Physics Letters, 2012. **531**: p. 173-176.
 11. Freyer, W., et al., *Synthese von Metallkomplexen des Tetra-(2,3-anthra)-tetraazaporphins und Vergleich ihrer Elektronenabsorptionsspektren mit denen anderer anellierter Tetraazaporphinsysteme*. Monatshefte für Chemie / Chemical Monthly, 1986. **117**(4): p. 475-489.
 12. Kagaya, Y., et al., *Rapid reactions of phthalocyanines with tellurium tetrachloride in non-aqueous solutions*. Journal of Porphyrins and Phthalocyanines, 1999. **3**(6-7): p. 537-543.
 13. Konami, H., et al., *Synthesis and Spectroscopic Properties of Zn(II) tetra-ter-butyl phthalocyanine*. Chemistry Letters, 1988. **17**(8): p. 1359-1362.
 14. Brendel, M., et al., *The Effect of Gradual Fluorination on the Properties of F_nZnPc Thin Films and F_nZnPc/C60 Bilayer Photovoltaic Cells*. Advanced Functional Materials, 2015. **25**(10): p. 1565-1573.
 15. Tang, Q., et al., *Photoswitches and Phototransistors from Organic Single-Crystalline Sub-micro/nanometer Ribbons*. Advanced Materials, 2007. **19**(18): p. 2624-2628.
 16. Lawton, E.A., *The Thermal Stability of Copper Phthalocyanine*. The Journal of Physical Chemistry, 1958. **62**(3): p. 384-384.

17. Verma, D., et al., *Role of coordinated metal ions on the orientation of phthalocyanine based coatings*. Spectrochimica Acta Part A: Molecular and Biomolecular Spectroscopy, 2008. **70**(5): p. 1180-1186.
18. Zhang, X.-X., et al., *IR and Raman Vibrational Assignments for Metal-free Phthalocyanine from Density Functional B3LYP/6-31G(d) Method*. Chinese Journal of Chemistry, 2004. **22**(4): p. 325-332.
19. Ziminov, A.V., et al., *Correlation dependences in infrared spectra of metal phthalocyanines*. Semiconductors, 2006. **40**(10): p. 1131-1136.
20. Bouvet, M., et al., *Electrical properties of rare earth bisphthalocyanine and bisnaphthalocyanine complexes*. Chemical Physics Letters, 1990. **172**(3-4): p. 299-302.
21. Muzikante, I., et al., *A Novel Gas Sensor Transducer Based on Phthalocyanine Heterojunction Devices*. Sensors, 2007. **7**(11): p. 2984-2996.
22. Wan, X., et al., *Gas sensing properties of Cu₂O and its particle size and morphology-dependent gas-detection sensitivity*. Journal of Materials Chemistry A, 2014. **2**(33): p. 13641-13647.
23. Jafari, M.J., et al., *Effect of post-deposition annealing on surface morphology and gas sensing properties of palladium phthalocyanine thin films*. Surface and Interface Analysis, 2012. **44**(5): p. 601-608.
24. De Angelis, R., et al., *Surface InP Quantum Dots: Effect of Morphology on the Photoluminescence Sensitivity*. Procedia Engineering, 2012. **47**: p. 1251-1254.
25. Kobayashi, T., et al., *High-resolution TEM images of zinc phthalocyanine polymorphs in thin films*. Acta Crystallographica Section A, 1981. **37**(5): p. 692-697.
26. WILLIS, M., *Structural and Polymorphic Considerations on the Effects of Copper Phthalocyanine Pigment on Polypropylene Nucleation*. Electronic Thesis or

- Dissertation. University of Cincinnati, Ohio Link Electronic Theses and Dissertations Center, 2007.
27. Fryer, J.R., *Transmission electron microscopy of organic pigments*. Journal of Microscopy, 1980. **120**(1): p. 1-14.
 28. Senthilarasu, S., et al., *Structural analysis of zinc phthalocyanine (ZnPc) thin films: X-ray diffraction study*. Journal of Applied Physics, 2007. **102**(4): p. 043512 (1-6).
 29. Lee, Y.-L., et al., *Effects of heat annealing on the film characteristics and gas sensing properties of substituted and un-substituted copper phthalocyanine films*. Applied Surface Science, 2001. **172**(3-4): p. 191-199.
 30. Lee, Y.-L., et al., *Substrates effects on the growth behavior of Copper tetra-tert-butyl phthalocyanine films studied by atomic force microscopy*. Thin Solid Films, 2003. **423**(2): p. 169-177.
 31. Hunter, C.A., et al., *Aromatic interactions*. Journal of the Chemical Society, Perkin Transactions 2, 2001(5): p. 651-669.
 32. Hunter, C.A., et al., *The nature of .pi.-.pi. interactions*. Journal of the American Chemical Society, 1990. **112**(14): p. 5525-5534.
 33. Martinez, C.R., et al., *Rethinking the term "pi-stacking"*. Chemical Science, 2012. **3**(7): p. 2191-2201.
 34. Nishio, M., *The CH/[small pi] hydrogen bond in chemistry. Conformation, supramolecules, optical resolution and interactions involving carbohydrates*. Physical Chemistry Chemical Physics, 2011. **13**(31): p. 13873-13900.
 35. Plevin, M.J., et al., *Direct detection of CH/ π interactions in proteins*. Nat Chem, 2010. **2**(6): p. 466-471.

36. Hunter, C.A., *Quantifying Intermolecular Interactions: Guidelines for the Molecular Recognition Toolbox*. Angewandte Chemie International Edition, 2004. **43**(40): p. 5310-5324.
37. Yang, Y., *Effects Induced by Axial Ligands Binding to Tetrapyrrole-Based Aromatic Metallomacrocycles*. The Journal of Physical Chemistry A, 2011. **115**(32): p. 9043-9054.
38. Yorita, H., et al., *Evidence for the Cation- π Interaction between Cu_2^+ and Tryptophan*. Journal of the American Chemical Society, 2008. **130**(46): p. 15266-15267.
39. Dougherty, D.A., *Cation- π Interactions in Chemistry and Biology: A New View of Benzene, Phe, Tyr, and Trp*. Science, 1996. **271**(5246): p. 163-168.
40. Liao, M.-S., et al., *Electronic structure and bonding in metal phthalocyanines, Metal=Fe, Co, Ni, Cu, Zn, Mg*. The Journal of Chemical Physics, 2001. **114**(22): p. 9780-9791.
41. Zawadzka, A., et al., *Structural and nonlinear optical properties of as-grown and annealed metallophthalocyanine thin films*. Thin Solid Films, 2013. **545**: p. 429-437.
42. Topkaya, D., et al., *Axial binding and host-guest interactions of a phthalocyanine resorcinarene cavitand hybrid*. Dalton Transactions, 2014. **43**(5): p. 2032-2037.
43. Xu, H., et al., *Construction of Subphthalocyanine-Porphyrin and Subphthalocyanine-Phthalocyanine Heterodyads through Axial Coordination*. Inorganic Chemistry, 2008. **47**(17): p. 7921-7927.
44. Wheeler, S.E., *Understanding Substituent Effects in Noncovalent Interactions Involving Aromatic Rings*. Accounts of Chemical Research, 2012. **46**(4): p. 1029-1038.
45. Cockroft, S.L., et al., *Substituent effects on aromatic stacking interactions*. Organic & Biomolecular Chemistry, 2007. **5**(7): p. 1062-1080.

46. Wheeler, S.E., *Local Nature of Substituent Effects in Stacking Interactions*. Journal of the American Chemical Society, 2011. **133**(26): p. 10262-10274.
47. Wheeler, S.E., et al., *Probing Substituent Effects in Aryl–Aryl Interactions Using Stereoselective Diels–Alder Cycloadditions*. Journal of the American Chemical Society, 2010. **132**(10): p. 3304-3311.
48. Wheeler, S.E., et al., *Origin of substituent effects in edge-to-face aryl–aryl interactions*. Molecular Physics, 2009. **107**(8-12): p. 749-760.
49. Ringer, A.L., et al., *Substituent Effects in Sandwich Configurations of Multiply Substituted Benzene Dimers Are Not Solely Governed By Electrostatic Control*. Journal of the American Chemical Society, 2009. **131**(13): p. 4574-4575.
50. Ringer, A.L., et al., *The Effect of Multiple Substituents on Sandwich and T-Shaped π – π Interactions*. Chemistry – A European Journal, 2006. **12**(14): p. 3821-3828.
51. Sinnokrot, M.O., et al., *Unexpected Substituent Effects in Face-to-Face π -Stacking Interactions*. The Journal of Physical Chemistry A, 2003. **107**(41): p. 8377-8379.
52. Wheeler, S.E., et al., *Substituent Effects in the Benzene Dimer are Due to Direct Interactions of the Substituents with the Unsubstituted Benzene*. Journal of the American Chemical Society, 2008. **130**(33): p. 10854-10855.
53. Bidermane, I., et al., *Experimental and theoretical study of electronic structure of lutetium bi-phthalocyanine*. The Journal of Chemical Physics, 2013. **138**(23): p. 234701-234708.
54. L'Her, M., et al., *Electrochemical behaviour of lutetium diphthalocyanine in methylene chloride*. Journal of Electroanalytical Chemistry and Interfacial Electrochemistry, 1983. **157**(1): p. 183-187.
55. Rousseau, R., et al., *Extended Hückel molecular orbital model for lanthanide bisphthalocyanine complexes*. Journal of Molecular Structure, 1995. **356**(1): p. 49-62.

56. Bouvet, M., *Radical phthalocyanines and intrinsic semiconductions*. The Porphyrin Handbook: Application of phthalocyanine, ed. K.M. Kadish. Vol. 118. 2003: Academic Press.
57. Jones, R., et al., *Structure, electrical conductivity and electrochromism in thin films of substituted and unsubstituted lanthanide bisphthalocyanines*. Thin Solid Films, 1997. **298**(1–2): p. 228-236.
58. Altindal, A., et al., *Charge transport mechanism in bis(double-decker lutetium(III) phthalocyanine) (Lu_2Pc_4) thin film*. Synthetic Metals, 2005. **150**(2): p. 181-187.
59. Andre, J.-J., et al., *Electrical and magnetic properties of thin films and single crystals of bis(phthalocyaninato)lutetium*. Chemical Physics Letters, 1985. **115**(4–5): p. 463-466.

Chapter 4:
Sensing properties of ttb-CuPc coated
QCMs toward BTX gases

1. Investigation of sensor characteristics: general approach

In the previous chapter, we have clearly established that among all the investigated sensors developed with different types of metallophthalocyanines, ttb-CuPc coated on QCM transducer was the most sensitive device toward BTX gases. If typical responses were given to highlight and interpret the interaction mechanisms, a complete experimental study for the determination of the metrological performances of such sensors must be accomplished. Therefore, all the sensing properties able to assess the potentialities of ttb-CuPc-based QCM sensors to satisfy the requirements of the target application must be quantified.

The most important metrological characteristics that chemical sensors dedicated to pollutant monitoring must satisfy include:

- high magnitude of response to benefit from measurements with high resolution,
- fast kinetics of response for real time measurements,
- high level of repeatability for accurate measurements,
- complete reversibility to avoid poisonous effect on the sensing material and to enhance sensor stability,
- low hysteresis to be not influenced by previous gas exposure conditions,
- low limit of detection to enable low concentration measurements,
- high level of selectivity for a good discrimination between all the target gases and avoid the influence of interfering species in a complex gaseous phase like atmosphere.

Thus, all these characteristics were determined for ttb-CuPc based QCM sensors exposed to BTX at concentrations in the ppm range. Since the generation systems of benzene and xylenes vapors are less flexible as compared to toluene, a few sensing characteristics including hysteresis and resolution of sensor cannot be accurately determined for these

aromatic hydrocarbons. As a consequence, metrological characteristics were determined for toluene and when it was possible, for benzene and xylenes. From experimental results, a model based on isotherms of adsorption and describing the sensor response versus gas concentration was formalized. This model was established taking into account gas adsorption and gas diffusion into the sensitive layers with different thicknesses. As a conclusion, ageing studies were performed to evaluate the lifetime of device as well as the storage conditions required to ensure sensor stability in time.

2. Sensing performances of ttb-CuPc coated QCM sensors

2.1. General sensing behavior towards benzene, toluene and xylenes

Figure 1 depicts the ttb-CuPc based QCM sensor responses at room temperature towards three successive cycles of exposure to a constant concentration of BTX. Consecutively to each pollutant exposure, recovery of sensor was ensured under pure air. The concentration of benzene was 341 ppm while toluene and xylene concentrations were 500 ppm. The exposure and desorption times for benzene was 1 and 3 hours respectively, while in the case of toluene and xylenes, these parameters were set to 2 and 3 hours respectively. Firstly, as described in the previous chapter, gas exposures lead to a decrease in resonance frequency of coated QCMs corresponding to a mass increase of the sensing material due to BTX adsorption. The high reversibility under pure air of the gas interactions even at room temperature must be underlined. Indeed, a fast return of sensor signal to the initial frequency measured before pollutant exposure is observed. About repeatability, the magnitude of frequency shifts for 3 successive exposure/recovery cycles are closely similar. For each cycle, frequency shifts for benzene, toluene and xylenes were 32, 60 and 136 Hz respectively. For benzene results, the peak of frequency decrease just at the beginning of exposure period is attributed to an over concentration of gas when system commute from air zero to benzene source. This effect is attributed to the experimental setup and not intrinsic to sensor. The increasing order of magnitude of response from benzene to xylenes is in agreement with (a) direct interactions of methyl group(s) of BTX gases to ttb-CuPc layers and (b) additive nature of these interactions [1-3]. Furthermore, methyl group also acts as an electron donor which can add to π -electron density of benzene ring, which in turn strengthen the aromatic interactions with the sensing layer. Combined effects of all these forces are manifested in order of sensor response as benzene < toluene < xylenes.

Beyond sensitivity, our attention was also focused on the study of kinetics of sensor response, repeatability, limit of detection, resolution, effects of gas exposure history and selectivity of *ttb*-CuPc based QCM sensors. Inter-comparative studies of these sensing performances among BTX gases are detailed below.

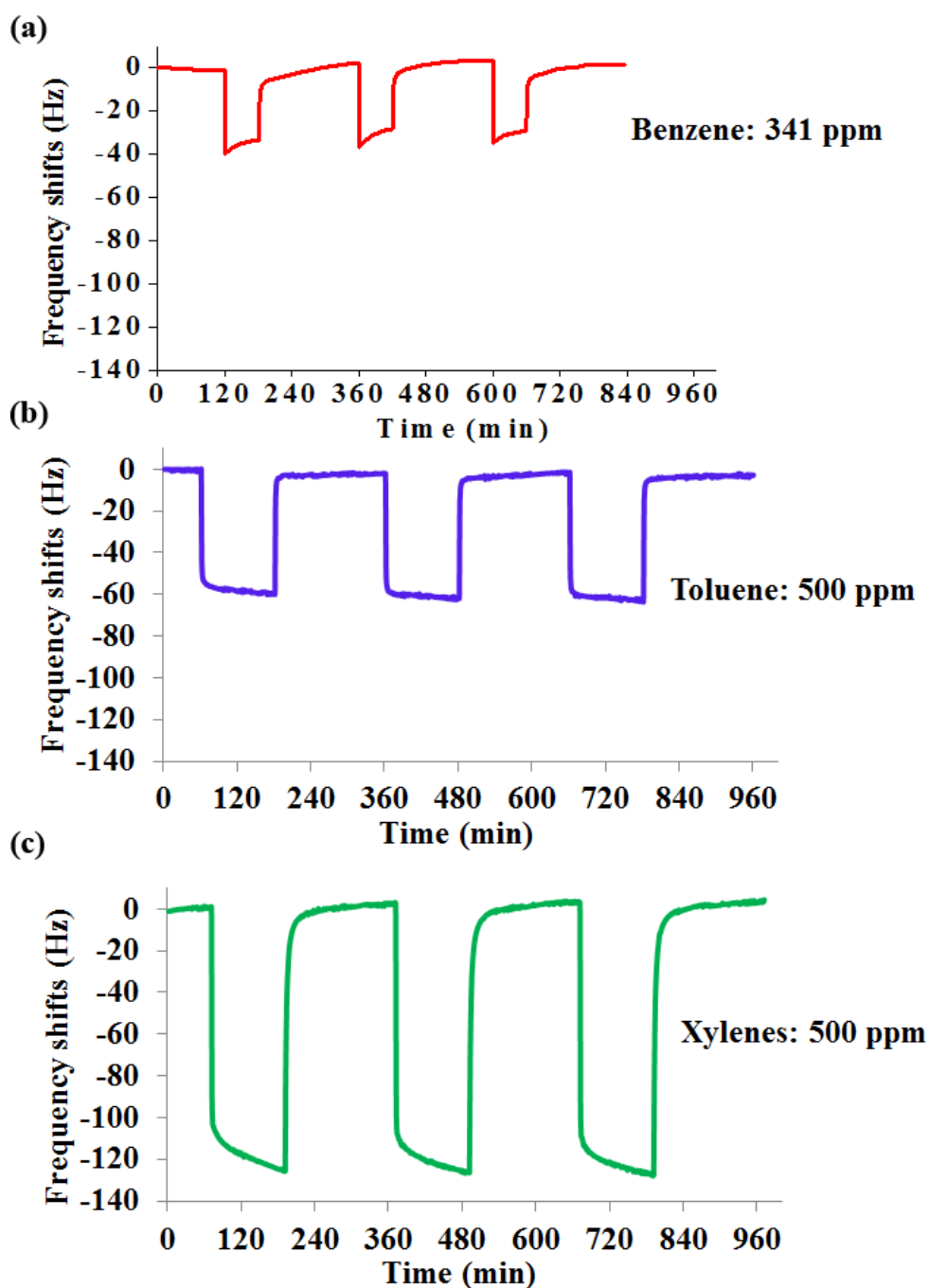


Fig.1: ttb-CuPc based QCM sensor responses to (a) benzene, (b) toluene and (c) xylenes at room temperature

2.2. Response and recovery times

The kinetics of responses was determined from the response and recovery times of the sensing device. As defined in chapter 1, response and recovery times of sensor are defined as the time at which the device has produced a signal variation equal to 90% of the complete magnitude of sensor signal due to a variation of the measurand, i.e. gas concentration in our case. If response and recovery times can be accurately determined for toluene and xylenes, a systematic initial over concentration attributed to experimental setup made impossible the accurate determination of response time toward benzene. As a consequence, only the recovery time will be determined for this gaseous pollutant.

To estimate the response and recovery times, one exposure/recovery cycle was extracted from Fig. 1 as depicted in the Fig. 2. Sensor responses being highly repeatable from one cycle to another, similar results were obtained for all cycles of exposure. For each studied gas, it can be pointed out that kinetics of adsorption and desorption are closely similar. Indeed, for toluene as well as xylenes, response time is equal to recovery time. Thus, desorption is complete and not required more time as compared to gas adsorption. Involved interaction forces remain weak, making desorption process easy even at room temperature. Nevertheless, if sensor responses to toluene or xylenes correspond to fast variations in QCM frequency, experiments also point out the slower desorption of benzene from the sensitive layer as compared to other monocyclic hydrocarbons. Quantitatively, response and recovery times were measured to 3 minutes for toluene exposures and 11 minutes for the same concentration of xylenes. In contrast, recovery time corresponding to benzene desorption was found close to 35 minutes.

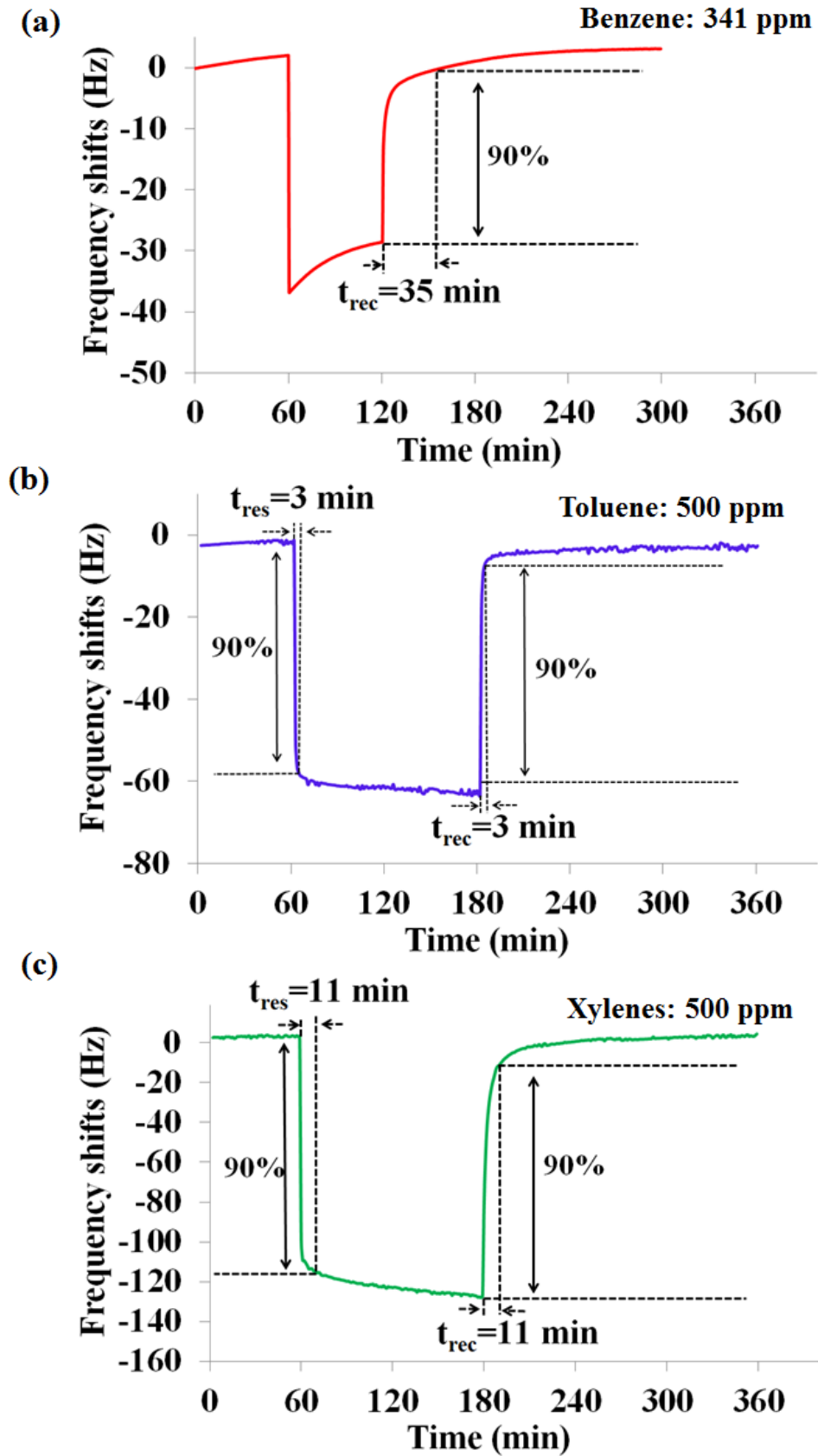


Fig. 2: Determination of response and recovery times of *tb*-CuPc based QCM sensors at room temperature consecutively to (a) benzene, (b) toluene and (c) xylenes exposures.

These differences in kinetics of responses of ttb-CuPc based QCM sensors toward benzene, toluene and xylenes can be attributed to the interactions forces involved and the steric nature of the target molecules. The presence of methyl group(s) in toluene and xylene at the periphery of the aromatic ring further reinforces already predominant dispersion component in interactions with ttb-CuPc. This leads to fast adsorption and desorption of these gases on sensor surface. On the other hand, benzene interactions at the sensor surface/layers are driven mainly by CH- π interactions (tert-butyl group of ttb-CuPc with π -plane of benzene and C-H of benzene with π -plane of phthalocyanine). Comparing the strength of these non-covalent forces, CH- π interactions are relatively stronger [4-6] than dispersion [7, 8] that is responsible of the slower kinetics of benzene desorption on macrocycles. At the same time, SEM pictures and XRD studies have already established the amorphous and porous organizations of layered ttb-CuPc macrocycles. During exposure, BTX gases can immediately diffuse into the bulk of the layer through available pores. However, the presence of two methyl groups on xylene molecules which provides a favorable condition for dispersion interactions results to a slower diffusion along the pores due to steric hindrance. With only one methyl group, toluene can progress more easily into the volume and can quickly reach the available active sites localized into the bulk of the layer. This justifies the shorter response and recovery times observed for toluene as compared to xylenes.

2.3.Sensitivity and repeatability

Figure 3 represents frequency shifts of ttb-CuPc based QCM sensor exposed to different concentrations of BTX gases at room temperature. Exposures to toluene and xylenes were in a decreasing mode from 500 to 100 ppm with 100 ppm as a variation step while benzene exposures were in 69-505 ppm range with increasing mode. Since experimental methods of benzene vapor generation didn't allow a precise control of concentration, a

constant variations step could not be achieved. Nevertheless, this doesn't constitute a critical point for the realization of calibration curve. Based on the response and recovery times previously determined, exposure times for benzene, toluene and xylenes were set to 20 minutes, 5 minutes and 20 minutes respectively, while recovery times were set to 30 minutes, 10 minutes and 30 minutes respectively. Five consecutive cycles of exposure/recovery were realized for each concentration of benzene and toluene, while 3 consecutive cycles were recorded for each concentration of xylenes. In addition to time-evolution of sensor response during each experiment, the variations of QCM frequency versus gas concentrations were established as a calibration curve. These two depictions are given in Fig. 3.

Firstly, all experiments emphasize the high level of repeatability of the sensing device. Indeed, the frequency shifts measured for the five consecutive exposures to the same concentration of gas are exactly the same. It is more clearly highlighted on the calibration curves: all the experimental points obtained in the same experimental conditions are perfectly superimposed. Moreover, the magnitude of frequency shifts measured at 500 ppm of toluene and xylenes or at 341 ppm of benzene is similar to the values obtained for previous sample (see Fig.1 for intercomparison). Secondly, for all investigated hydrocarbons, calibration curves exhibit linearity between sensor response and the measurand, which is also a requirement of an ideal sensor. At last, experimental results also highlight that sensor is well resolved in our experimental conditions, as illustrated by the widely discriminated responses in the studied concentration range. For an easier intercomparison of responses toward the different analytes, calibration curves have been plotted on the same graph as reported in Fig. 4. We can notice that in the 100–500 concentration range, responses to benzene are the lowest, those to xylenes are the highest while responses to toluene are intermediate. However, the sensitivity, previously defined as the ratio between the variation of sensor signal generated by a variation of the measurand and the magnitude of this ratio is highest for xylene but

similar for benzene and toluene. Indeed, although the offset is different between the calibration curves for benzene and toluene, the slopes have the same value.

As compared to other metallophthalocyanines, the high sensitivity and the good reversibility which is a key factor to benefit from repeatable responses are the consequences of the contribution of tert-butyl groups which provide large extent of surface and volume active sites as well as low strength of interaction because of predominant dispersion contribution. Let us focus now on the highest sensitivity of the sensing device toward xylenes illustrated in Fig.4. Such singularity for xylenes emerges from two diffusion modes responsible for adsorption within sensing layers. At low concentrations, adsorption is dominated by subsurface diffusion while at higher concentrations, bulk diffusion can take place providing an extra adsorption sites [9]. On the other hand, benzene and toluene follow a monotonous diffusion mode leading to their adsorption. Such variations in adsorption of these gases can be understood taking into consideration their molecular size and shape. Molecular size and shape can strongly affect adsorption of a molecule at subsurface. Kinetic diameter of a molecule is an indicative factor for the ease of diffusion of the molecule within pores available on surface [10-12]. Kinetic diameter of benzene, toluene and p-xylene are similar and are equal to 0.585 nm. o-xylene and m-xylene have higher value equal to 0.680 nm [13, 14]. Based on these kinetic diameter and position of methyl group(s) in BTX, a scheme for gas diffusion within the pores of the layers is proposed in Fig 5. At lower concentrations, the steric hindrance of o-xylene and m-xylene making unfavorable their penetration into the pores while benzene, toluene and p-xylene can easily penetrate [15]. It results in relatively less diffusion of xylenes. At higher concentrations, o-xylene and m-xylene compete to occupy the limited surface adsorption sites and can enter the constricted pores leading to bulk diffusion in addition to surface adsorption. This can justify the higher response observed for xylenes at high concentration as compared to benzene and toluene.

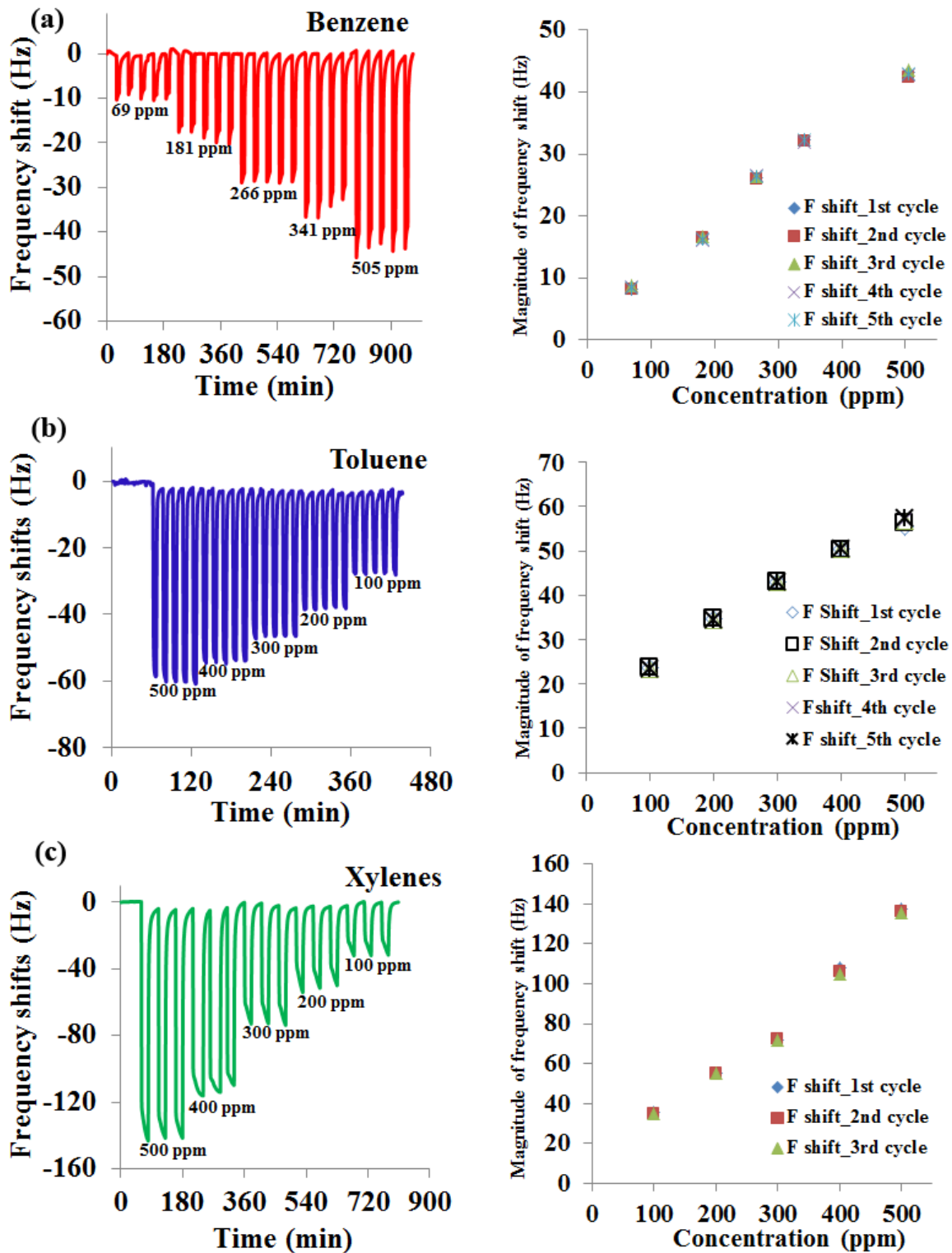


*Fig. 3: Time-variations of sensor responses and corresponding calibration curves of *ttb*-CuPc based QCM sensors successively exposed to (a) benzene, (b) toluene and (c) xylenes and recovered under pure air.*

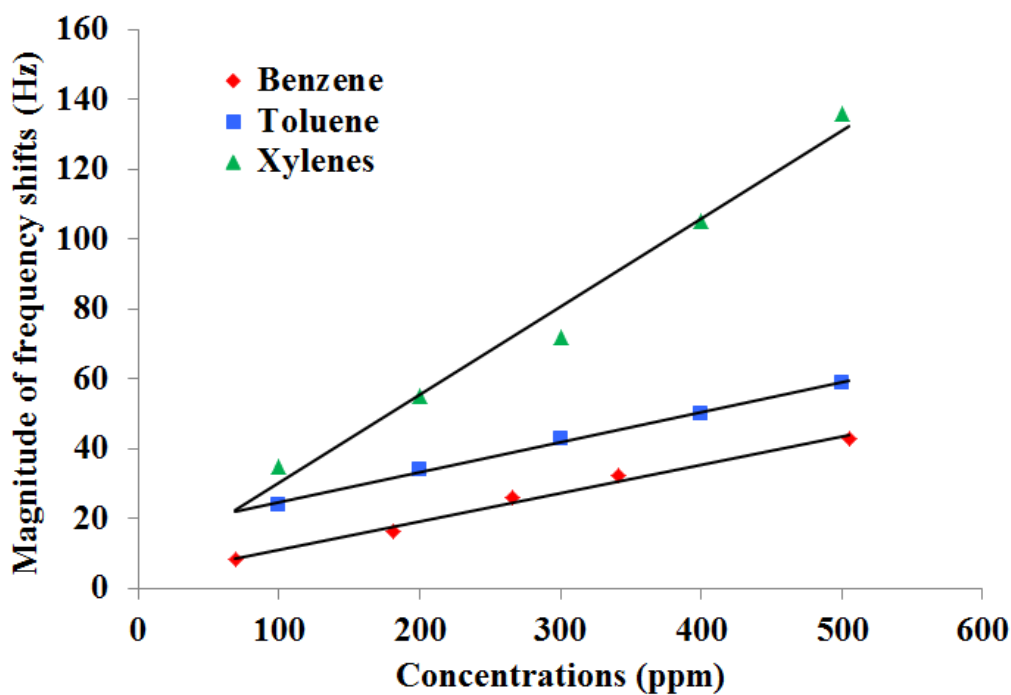


*Fig. 4: Inter-comparison of experimental calibration curves of *ttb*-CuPc based QCM sensors exposed to BTX.*

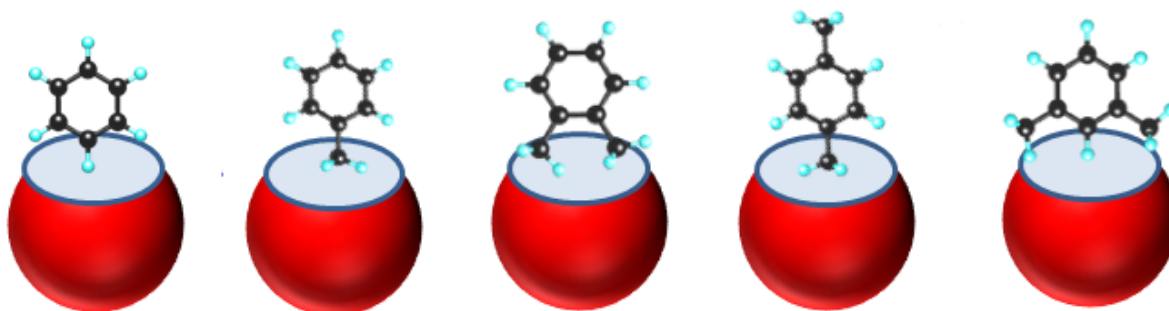


Fig. 5: Scheme of benzene, toluene, xylenes entering the nano-pores of sensor surface.

2.4. Effects of gas exposure history

Repeatability of the sensor was determined in the previous section by the monotonic variations in gas concentrations. However, it can be strongly affected by the history of gas exposure, i.e. the higher or lower gas concentrations during the previous exposures. Therefore, comparison of sensor responses obtained for increasing and decreasing

concentration steps were performed. The response of a 400 nm ttb-CuPc based QCM sensor exposed to toluene in the 100–500 ppm concentration range with 100 ppm as variation step was measured. Two approaches were carried to investigate the potential effect of exposure conditions on repeatability. As a first mode, gas exposure was performed in an increasing mode (from 100 ppm to 500 ppm) and consecutively in a decreasing mode (from 500 ppm to initial concentration). As a second mode, exposure was initiated in the decreasing mode and followed in the increasing mode. For each concentration, 5 consecutive exposure/recovery cycles were realized.

Results are shown in Fig. 6 for two different starting gas concentrations following a non-monotonic variation as explained above. Figure 6a and 6b represent frequency shifts of sensor estimated after 3 minutes of gas exposure for each exposure/recovery cycles. The real-time variations in gas concentrations have been also depicted on the same graph for each cycle. The corresponding response curves for each experiment have been compared for increasing and decreasing concentration variations on the right of each figure. Results depicted in Fig. 6 show that frequency variations due to toluene adsorption on ttb-CuPc are almost of same magnitude for a constant gas concentration. This is true for the increasing as well as for the decreasing mode for both experiments as illustrated by the overlapping of measurement points. Consequently a very low level of hysteresis is noticeable and for each concentration, sensor responses are systematically lower for increasing mode than those for decreasing mode. This is true irrespective of the starting gas concentration and variations of the concentration steps.

Such behavior can be justified by two factors:(1) incomplete desorption of diffused gas molecules within the given recovery time and (2) adsorption of toluene molecules on sensor surface depends on the number of active sites at the surface of the sensitive material already occupied by toluene molecules. Such behavior has been previously observed and discussed

for NO₂ adsorption on CuPc thin films [16, 17]. Although experiments were realized at room temperature, these effects remain small and leave no significant influence on sensor performances. The discrimination of sensor signals at different concentrations of toluene can be clearly established from Fig. 6.

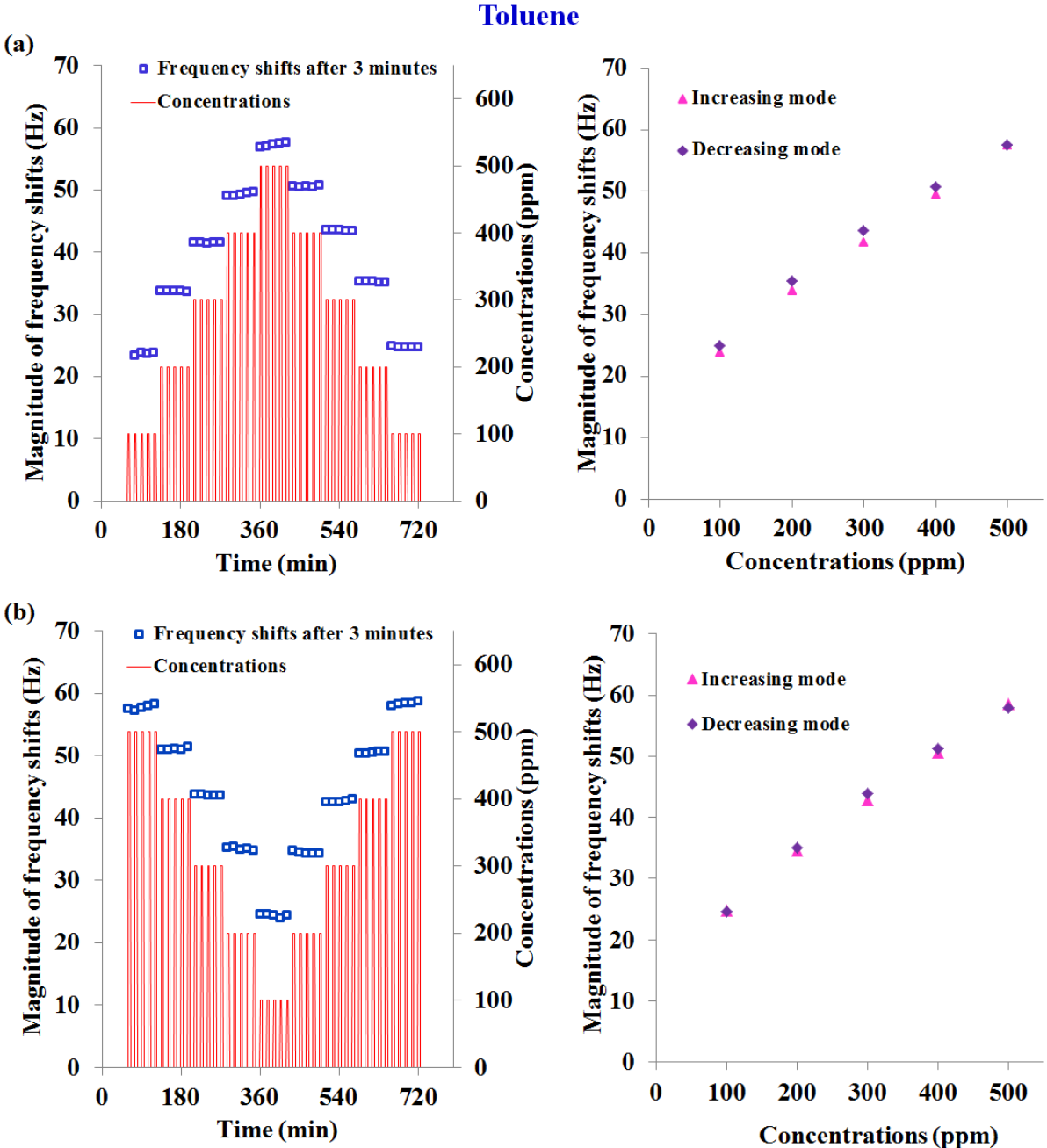


Fig. 6: 400 nm ttb-CuPc based QCM sensor response to toluene in a range of 100-500 ppm concentrations with a step of 100 ppm, (a) Increasing mode followed by a decreasing mode and (b) decreasing mode followed by increasing mode.

2.5.Resolution

High resolution of a gas sensor is a very important specification especially for industrial, medical and environmental applications for which a distinction among pollutants concentrations fluctuating even by a very small interval must be satisfied. The resolution of our chemical sensors was experimentally determined for toluene by means of successive gas exposures with small concentration step. The response of a 400 nm ttb-CuPc based QCM sensor exposed to toluene in the 30–200 ppm concentration range with 10 ppm as variation step was measured. The two measurement protocols previously implemented were renewed. Thus , gas exposure was firstly performed in an increasing mode (from 30 ppm to 200 ppm) then consecutively in a decreasing mode (from 200 ppm to initial concentration). Secondly, exposure was initiated in the decreasing mode and followed in the increasing mode. For each concentration, 5 consecutive exposure/recovery cycles were realized. These experiments exhibit the additional advantage to estimate the repeatability and the effect of gas exposure history for lower concentration range too.

The experimental data corresponding to the frequency shifts of ttb-CuPc based QCM sensor exposed to the different concentrations of toluene are reported in Fig. 7. Graphs at the left side represent sensor responses versus time measured during experiments whereas graphs at the right side represent sensor response versus gas concentration. On each figure are reported measurements obtained for increasing then decreasing mode (a) as well as for decreasing then increasing mode (b). As shown in Fig. 7, responses for toluene are always discriminated for 20 ppm of gap and often for 10 ppm of gap whatever the mode of concentration variations. This value can be considered as the resolution of the ttb-CuPc based QCM sensors for toluene.

Toluene

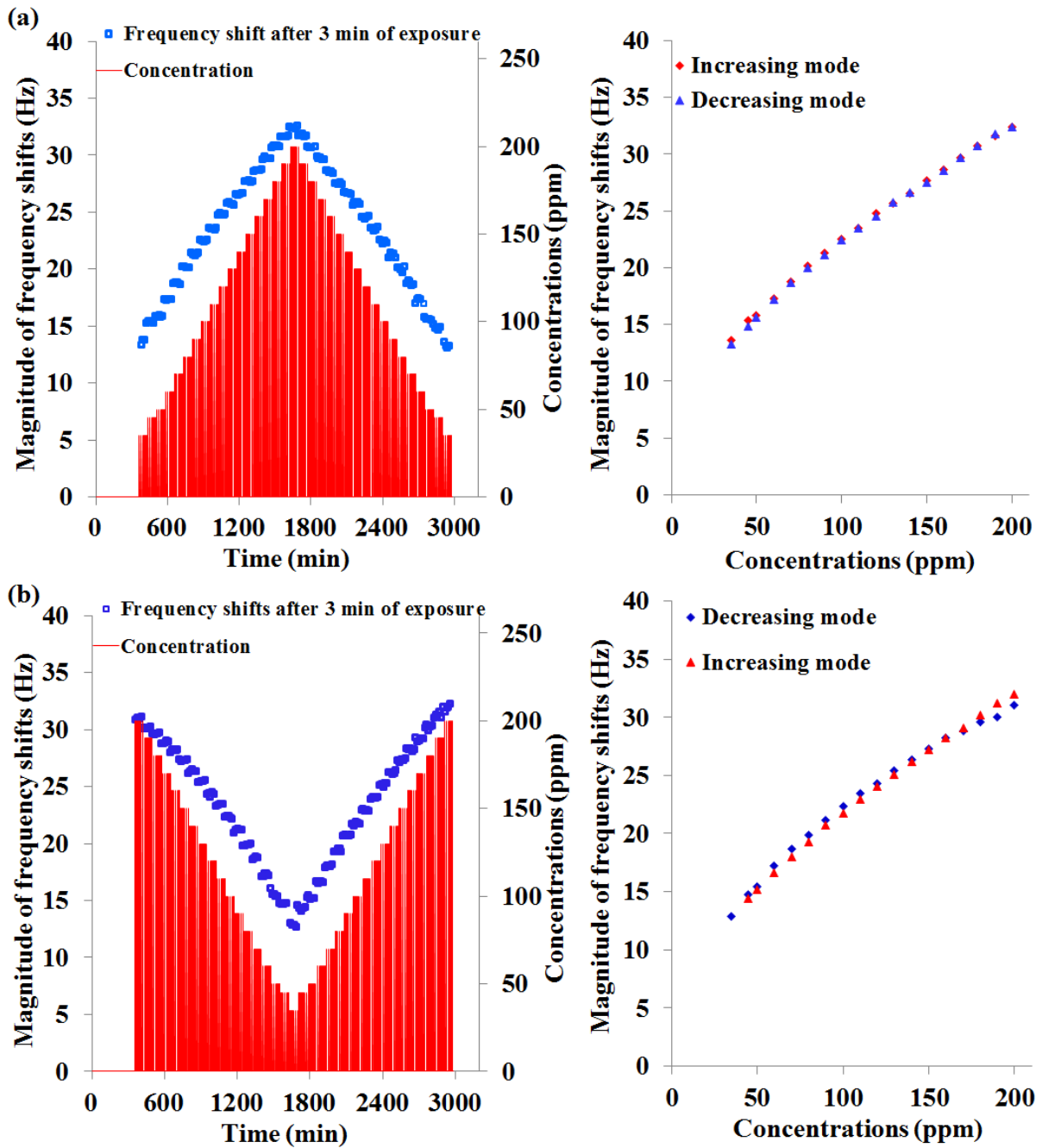


Fig.7: 400 nm ttb-CuPc based QCM sensor response to toluene in a range of 35-200 ppm concentrations with a step of 10 ppm, (a) Increasing mode followed by a decreasing mode and (b) decreasing mode followed by increasing mode.

Nevertheless, we must keep in mind that sensor resolution depends from:

- the repeatability of responses which can be assessed by the dispersion of measurements obtained in the same experimental conditions;

- the level of uncertainty intrinsic to gas dilution system and concentration of gas source, these being more important for low concentrations. A continuous monitoring of gas concentration upstream the exposure chamber by specific commercial analyzers could improve the quality of the calibration curve;

- the influence of gas exposure history which can lead to a hysteresis phenomenon and so to dissimilar values for previous gas exposure conditions.

As a consequence, sensor resolution is better than 20 ppm.

2.6.Selectivity

Among all the characteristics, the selectivity still remains the most difficult challenge to overcome in the field of chemical sensors to make them relevant especially for air quality monitoring. Previous investigations on organic chemoresistors as gas sensors have highlighted the strong interactions occurring between other gaseous pollutants like nitrogen dioxide (NO₂) or ozone (O₃) and metallophthalocyanines [18, 19]. In such sensing devices, the electronic charge transfer between the oxidizing gaseous molecules and the phthalocyanines molecular units consecutively to reversible gas adsorption mechanisms is responsible for the electronic conductivity variations of the sensitive material and so the response of chemoresistors. Thus, all gases which could interact with the sensitive material through adsorption sites and able to modulate one material property that is converted by the selected transducer in useful output signal can be considered as interfering analytes leading to unselective detection.

The selectivity of ttb-CuPc based QCM sensors has been investigated according to two complementary configurations:

- ttb-CuPc thin films deposited by thermal evaporation on 5 MHz AT-cut quartz crystals and exposed to nitrogen dioxide and ozone on the experimental test benches developed at our

laboratory; frequency variations versus time of coated quartz crystal exposed to pollutants and then maintained under clean air are depicted in Fig. 8;

- ttb-CuPc thin films achieved by drop-casting deposition process from dispersion in ethanol on 10 MHz AT-cut quartz crystals and exposed to nitrogen dioxide, carbon monoxide and hydrogen sulfide on the experimental test bench developed at ENEA - Technical Unit of Technologies for Material of Brindisi, Italy. Such measurement campaign in collaboration with ENEA has been the topic of one short term scientific mission in the framework of the COST ACTION TD1105 –EuNetAir [20] in which our team is involved.

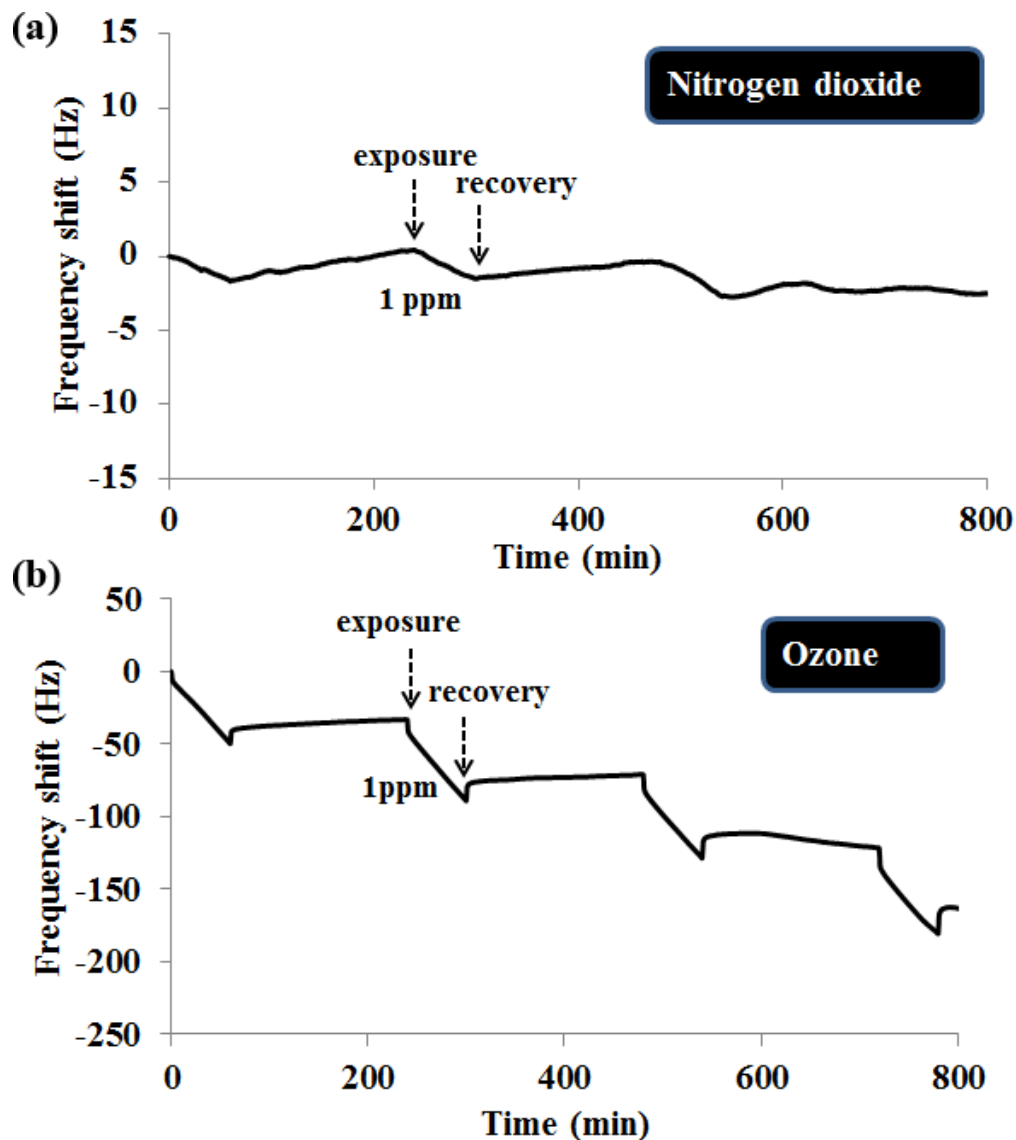


Fig. 8: 400nm ttb-CuPc based QCM sensor response to (a) NO₂ and (b) O₃ at room temperature.

Experimental results reveal no significant response towards NO_2 in the 0.1–10 ppm range neither on thermally evaporated layers as illustrated in Fig. 8a, nor on coatings by drop-casting (frequency variations not measurable because of too low signal-noise ratio). Similarly, no frequency variation on 10 MHz quartz crystals coated with ttb-CuPc was measured neither during exposures to CO in the 1-100 ppm concentration range, nor during exposures to H_2S in the 1–5 ppm concentration range. Thus, ttb-CuPc-based QCM sensors are insensitive to these analytes in our working conditions. A first level of selectivity is so performed.

In contrast with the previous investigated analytes, ozone interacts with phthalocyanine macrocycles leading to irreversible reaction with ttb-CuPc as illustrated by the irreversible and cumulative decrease in frequency after each exposure (see Fig. 8b). This result is a proof of the irreversible chemisorption of O_3 on phthalocyanine macrocycles. Indeed, O_3 strongly reacts with carbon–carbon double bonds, resulting in the breaking of these bonds and to the formation of isatin and isatoic anhydride. The reaction process called ozonolysis is described in Fig. 9. In our case, ozonolysis occurs on the carbon-carbon double bonds of the phthalocyanine macrocycles. The formation of the oxygenated reaction products, isatin and isatoic anhydride, induces a progressive increase in mass of the coatings and so, the irreversible decrease in frequency with successive cycle of exposure. Such irreversible reaction has been already observed on CuPc-based chemoresistors [21] leading to the irreversible decrease in electronic conductivity of the semiconducting material. We can also notice a fast but low increase in frequency during the first minutes of recovery. This is attributed to the desorption of the small part of O_3 molecules physisorbed on the sensitive layer but not yet chemisorbed. As a consequence, ozone can be considered as a strong interfering gas which can damage the sensing material. If it is simultaneously present with the target gases, its removal is necessary to perform BTX detection with ttb-CuPc-based gas

sensors. The implementation of selective in-line ozone filter like indigo [22] upstream the sensor appears as an attractive approach to satisfy selectivity and stability requirements.

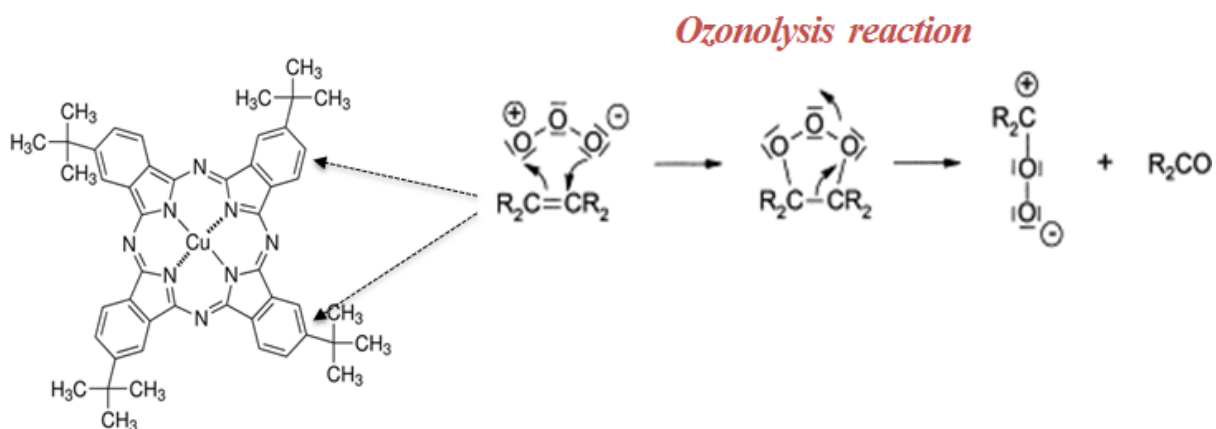


Fig. 9: schematic representation of ozonolysis reaction taking place at sensor surface.

Although previous results highlight a first level of selectivity, another challenge is to achieve highly discriminated measurements of each aromatic hydrocarbon investigated in the context of this work. If experimental results reveal differentiated calibration curves as established above, we can see in Fig. 4 that the absolute value of the sensor response doesn't allow determining both the nature and the concentration of gas which cause this sensor signal. For example, a frequency shift corresponding to 30 Hz can be attributed approximately to an exposure to 100 ppm of xylenes, 150 ppm of toluene or 320 ppm of benzene. Strategies and work in progress on original sensor-systems which could be developed to improve the selectivity and especially discriminate benzene from toluene and xylene will be discussed in the next chapter.

2.7.Limit of detection

To estimate the concentration range of all sensing devices, the determination of the threshold of detection is fundamental. Thus, the limit of detection (LOD) quantifies the lowest

concentration of analyte that can be reliably detected. More precisely, the LOD of a device is defined as the ratio between 3 times the standard deviation of the blank signal and the slope of the calibration curve [23]. More basic definition of limit of detection has been discussed elsewhere [24-29]. The mathematical definition of the limit of detection is given by:

$$LOD = \frac{3\sigma_0}{S} \quad \text{Eq. 1}$$

with σ_0 , the standard deviation of the blank signal and S the sensor sensitivity.

By definition, the standard deviation of a QCM sensor can be expressed by:

$$\sigma_0 = \sqrt{\frac{\sum_{i=1}^n (f_{0i} - \bar{f}_0)^2}{n-1}} \quad \text{Eq.2}$$

with f_0 is the initial frequency of QCM without any gas exposure and \bar{f}_0 is the average value of initial frequencies during the measurement period.

We can notice that in literature noise magnitude is often considered as a good estimation of the standard deviation of the blank signal. As a consequence, because noise magnitude of the QCM sensors coating by 400 nm of ttb-CuPc was measured approximately to 0.06 Hz, we have attributed this value as the standard deviation. The limits of detection have been calculated for each target gas from the calibration curves determined in the 30-200 ppm concentration range and given in Fig. 10. They were estimated to 2.15 ppm for benzene, 1.8 ppm for toluene and 0.75 ppm xylenes. These values for BTX gases are lower than the guidelines set by different health and environment protection agencies especially for toluene and xylenes. The measurement ranges of such sensing devices are in agreement with the specifications of the target application.

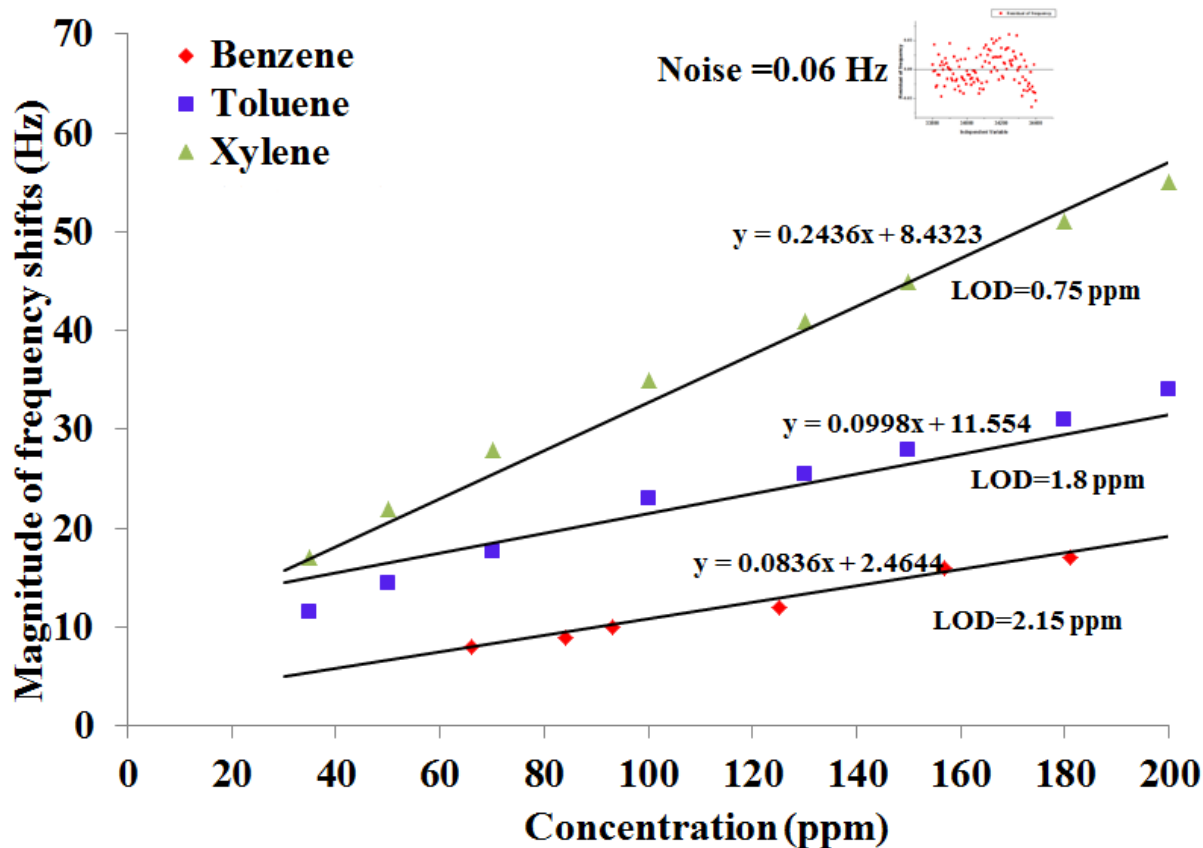
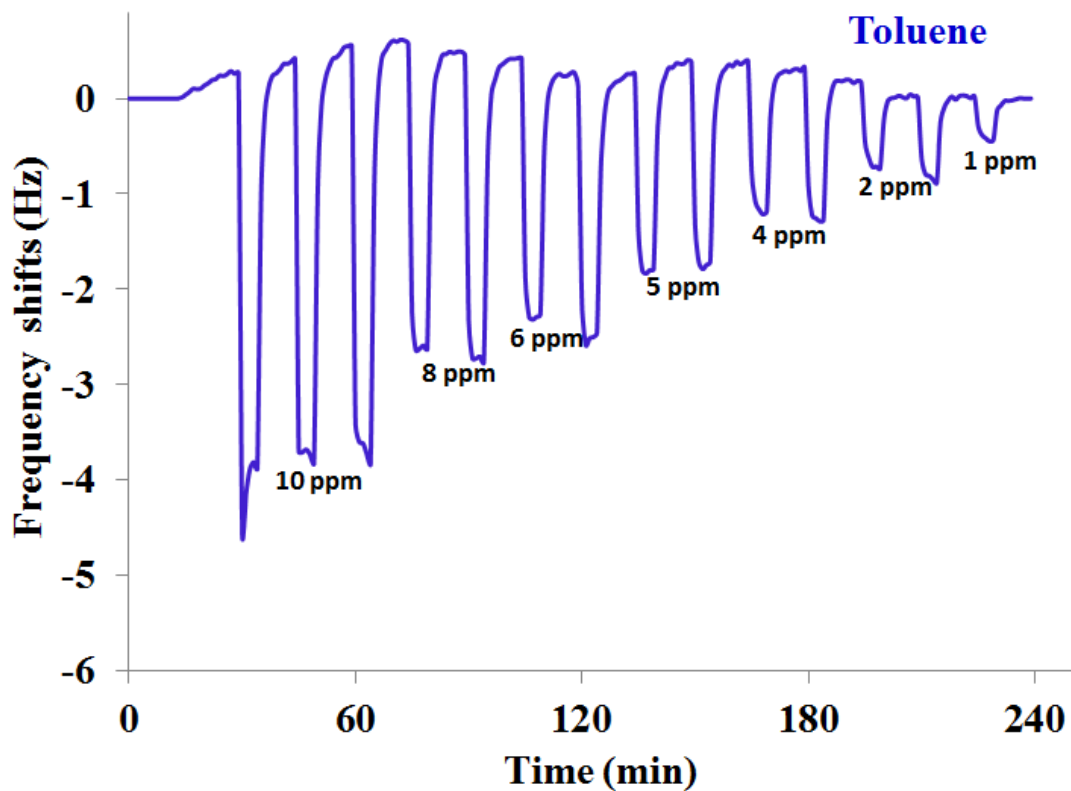


Fig. 10: Calibration curves and determination of limits of detection of 400 nm ttb-CuPc based QCM sensors toward BTX gases in the 30-200 ppm concentration range.

In order to validate the estimated LOD values of the sensor, complementary measurement have been performed to concentrations from 1 to 10 ppm. Fig.11 represents the time-evolution of sensor response at room temperature for 14 cycles of exposure to different concentrations of toluene. To benefit from higher accuracy, toluene was delivered by a commercial cylinder and then diluted by mass flow controller in pure air. It is manifested from experimental results that sensor gave a significant and low noisy response even at 1 ppm. Moreover, because of easy gas desorption, reversible and repeatable responses are obtained. As a consequence, ttb-CuPc based QCM sensors exhibit potentialities for the detection of aromatic hydrocarbons even at sub-ppm concentration with low-power consumption.



*Fig 11: *ttb*-CuPc based QCM sensor response in the 1–10 ppm concentration range at room temperature.*

3. Interpretation and modeling of sensor behavior

3.1. Sorption mechanisms on metallophthalocyanine thin layers

The interaction of a gas on a solid surface primarily involved adsorption processes [30]. In terms of solid-gas interface, adsorption is defined as the adhesion of gaseous molecules at the surface of a solid material. If the energetic conditions enable the reversibility of this phenomenon, we can speak about desorption. The adsorbed gaseous molecules constitute the adsorbate and the solid surface on which adsorption takes place is the adsorbent. According to the nature of forces operating between adsorbate and adsorbent, we can distinguish two kinds of adsorption: physical adsorption denoted by the term physisorption and chemical adsorption denoted by the term chemisorption. According to IUPAC, the physisorption is adsorption in which the forces involved are intermolecular forces (Van der Waals forces) and which do not involve a significant change in the electronic orbital patterns of the species involved. Chemisorption is adsorption in which the forces involved are stronger and of the same nature as those operating in the formation of covalent compounds [31]. Because of the weak interaction forces involved in physical adsorption, this is easily reversible [32]. Taking into consideration the good reversibility of sensor response at room temperature under pure air, sorption mechanism between ttb-CuPc and BTX molecules is typical from physisorption.

The rate of adsorbed molecules onto an adsorbent as a function of the partial pressure or gas concentration at constant temperature and at equilibrium between the gaseous and the solid phase have been described by different isotherms of adsorption. These include Langmuir [33], Freundlich [34], Henry [35] and others models. To interpret the adsorption of redox gases on phthalocyanines and porphyrin surfaces, Richardson et al. [36-39] have used Elovich equation with the required assumption that all specific sites are identical and no displacement

of the adsorbed molecules from one active site to another. They established the relevance of this model to describe the interactions occurring between porphyrin thin films and NO₂ molecules. Macagnano et al. have established that adsorption of VOCs including BTX gases on metalloporphyrins as sensitive material layered on QCM transducer can be interpreted using Brunauer Emmett Teller (BET) method with multilayer adsorption of gas analytes considered [40].

Complementary studies focused on the kinetics of BTX adsorption on different types of solid surfaces were also reported. F. Su et al. have studied the adsorption of BTEX on NaOCl-oxidized CNT and proposed a kinetic model based on Langmuir and Freundlich isotherms [41]. I. Capan et al. have made a detailed studies on the adsorption of benzene and toluene on metalloporphyrins coated by Langmuir Blodgett method on QCM [42]. They especially highlighted the key role of π - π interactions between aromatic rings and dipole moment of the molecules on kinetics of adsorption. Other studies about the kinetics of adsorption of BTX gases were also recently reported [43-46].

3.2. Adsorption model of BTX on ttb-CuPc thin layers

From the different calibration curves previously included above (see Fig. 4 and Fig. 10), a linear behavior of sensor response versus gas concentration can be considered in first approximation in the 30-100 ppm and 200-500 ppm ranges. Nevertheless, at lower concentrations, we observe sensor responses higher than those predicted according to the linear model. This is confirmed by the calibration curve of 400 nm ttb-CuPc based QCM sensor to toluene exposure in the 1-500 ppm concentration range depicted in Fig. 12. It is obvious from the figure that if the calibration curve can be locally described by a linear variation, this cannot be generalized across the probed range. The sensitivity is higher at low concentration (< 30 ppm) than for high concentrations. Such non-linear behavior of the sensor

can be interpreted taking into account the specific or preferential aromatic interactions and non-specific interactions of BTX with phthalocyanines. At low concentrations, toluene interacts with ttb-CuPc preferentially by relatively stronger π - π , M- π and CH- π interactions. A low variation of gas concentration ΔC induces a high variation of the adsorption rate and consequently, a higher sensitivity relative to low concentrations. At higher toluene concentrations, these specific interaction sites on ttb-CuPc layer are saturated with toluene. Any further interactions of toluene will take place mainly with tert-butyl groups of ttb-CuPc through relatively weaker and non-specific dispersion forces. Because of these weak and non-specific additional dispersion interactions, the same low variation of gas concentration ΔC gives a lower variation of the adsorption rate and so a lower sensitivity at high toluene concentrations. A similar evolution of adsorption pattern was pointed out by Fietzek et al. and others authors [47-49]. We have adopted a similar approach to model the calibration curve in Fig. 12.

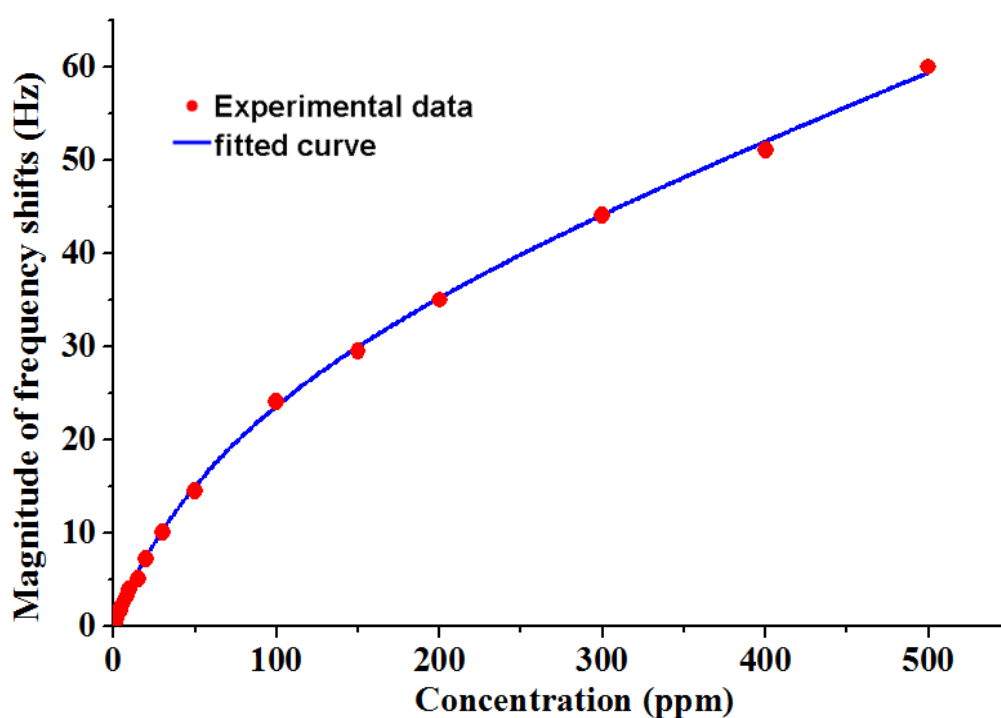


Fig. 12: Calibration curve of 400 nm ttb-CuPc based QCM sensor exposed to toluene in the 1-500 ppm range at room temperature as a fitting of experimental sensor response by Langmuir-Henry dual adsorption equation.

For the quantitative analysis of such non-linear calibration curve, a two-step sorption model was considered. The increase in sensor response at low gas concentration originates from adsorption of toluene molecules on limited number of free specific adsorption sites, which can be described by a Langmuir adsorption model according to the relation:

$$\Delta f_{\text{Langmuir}}(c) = A \cdot K_{\text{Langmuir}} \cdot \frac{c}{1 + K_{\text{Langmuir}} \cdot c} \quad \text{Eq. 3}$$

In the above Langmuir isotherm, C is the gas concentration, A is a constant which is proportional to the specific adsorption sites on the sensor surface and can be interpreted as the maximum QCM sensor signal achievable only by Langmuir sorption mode, K_{Langmuir} is the ratio of $K_{\text{adsorption}}$ and $K_{\text{desorption}}$ of the reversible sorption process.

The Langmuir isotherm reaching a constant value of sensor response at high concentrations (saturation corresponding to full coverage of all specific active sites by gaseous molecule and no multilayer adsorption), this one is not sufficient to model the increase in sensor response in all the investigated concentration range. To take into consideration the linear variations of response at higher concentrations, a linear adsorption isotherm described by Henry's law could complete the first model. The Henry isotherm is defined by the relation:

$$\Delta f_{\text{Henry}}(c) = K_{\text{Henry}} \cdot c \quad \text{Eq. 4}$$

where K_{Henry} is a constant describing the sensitivity of the sensor with predominant dispersion interaction with the gas analytes. Thus, the adsorption model relative to our sensing device can be described by the additive contributions of Langmuir and Henry isotherms according to the relation:

$$\Delta f_{\text{total}}(c) = A \cdot K_{\text{Langmuir}} \cdot \frac{c}{1 + K_{\text{Langmuir}} \cdot c} + K_{\text{Henry}} \cdot c \quad \text{Eq. 5}$$

The calibration curve of sensor depicted in Fig. 12 was fitted using the above mention model using MatLab software. The different adsorption coefficients extracted from the best correlation between experimental data and model are given in Table 1. Using these parameters, sensor response at any given concentration of toluene in a range of 1–500 ppm can be predicted from our model and compared to experimental data. Figure 13 describes individual and synergic contribution of Langmuir and Henry adsorption in the total adsorption of gas at any given concentration.

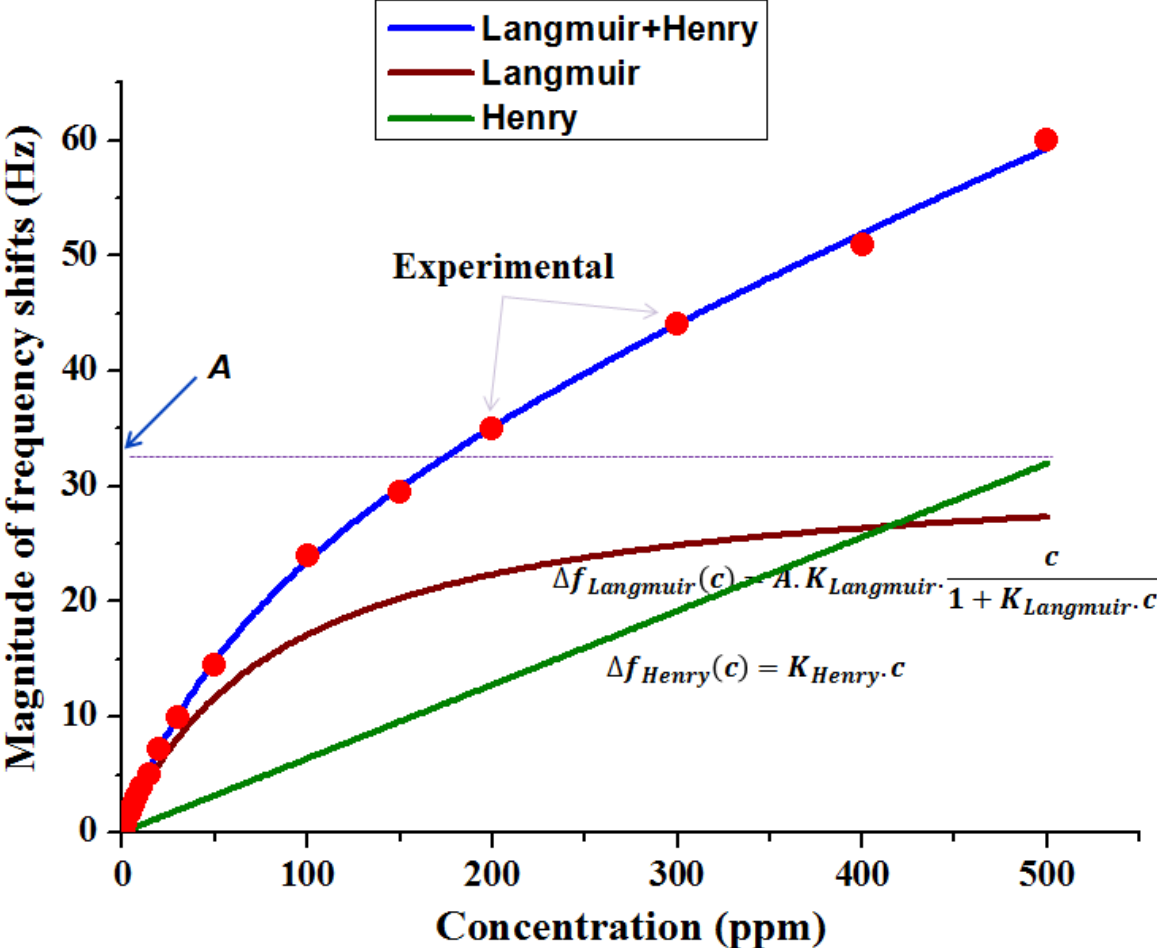


Fig. 13: Model of sensor response versus gas concentration based on Langmuir and Henry isotherms of adsorption.

A	$K_{Langmuir}$	K_{Henry}
32.12	0.01141	0.06396

Table 1: Constant determination of the adsorption model

At concentrations lower than 50 ppm, Langmuir adsorption is the major contribution as highlighted by the strong similarity between experimental curve and Langmuir isotherm. According to parameter calculation, if adsorption is restricted to one monolayer of gas molecule as assumed for Langmuir model, the complete saturation of all specific active sites would lead to a maximum frequency shift close to 32 Hz (denoted A and represented by the dark red line in Fig. 13). This is confirmed by the asymptotic value of Langmuir isotherm corresponding to our experimental conditions. At concentrations higher than 200 ppm, we can notice that the curve tends toward a linear asymptote which slope is close to the K_{Henry} factor. At high toluene concentrations, a multilayer adsorption seems occurring. As a conclusion, model and experimental measurements comparison illustrated in fig. 13 shows that Langmuir adsorption is predominant at lower concentrations whereas Henry adsorption is in agreement with sensor behavior at higher concentrations.

This modelling of gas/material interactions by a combination of two isotherms of adsorption validates our previous conclusions about the predominant role of dispersion forces in ttb-CuPc interactions with BTX gases. The role of tert-butyl group in enhancing sensitivity to BTX gases is also re-confirmed. The tert-butyl group in ttb-CuPc enhances number of specific recognition sites (thus increases possibility of π - π , M- π and CH- π interactions) as well as provides extended surface for non-specific dispersion interactions. By the use of this model, individual contribution of aromatic and dispersion interactions on sensor response at a given concentration can be determined.

3.3.Role of diffusion

We have previously discussed about adsorption of gaseous molecules on solid surface considering that all active sites can be easily reached by the adsorbate. Nevertheless, we must keep in mind the layered nature of the sensitive element. The mutual interactions of phthalocyanine macrocycles can be at the origin of the structure and the morphology of these thin films. More especially, the roughness and the porosity depend of this molecular organization. In the cases of porous sensing layers, diffusion processes of the target molecules into the volume strongly influence the sensing behavior. Previous researches highlighting the porous nature of phthalocyanines layers [50, 51], diffusion of BTX gases were thus studied to further elucidate gas/material interaction phenomenon. This was achieved on substituted and unsubstituted metallophthalocyanines thin layers with different thicknesses.

3.3.1. Effect of thickness: case of ttb-CuPc

ttb-CuPc based QCM sensors with layer thicknesses of 50, 100, 200, 300 and 400 nm were exposed at room temperature to toluene and xylenes in the 100-500 ppm concentration range with 100 ppm as a variation step. The sensor responses for toluene and xylene exposure at 100 ppm, 300 ppm and 500 ppm versus thickness are depicted in Fig. 14. As shown, a linear increase in responses is manifested for each concentration with increasing thickness of the sensing layer. The high linearity is also highlighted in the graphs by fitting parameter R^2 which is close to 1. Such trend reveals the favorable diffusion of gases into the volume of ttb-CuPc layers and so confirms the porous nature of the layers. The number of adsorption sites (specific as well as non-specific) increases linearly with increasing thickness of the layer. Particularly, Langmuir constant A and Henry parameter K_{Henry} have a linear dependence with the thickness of the sensing layer, while $K_{Langmuir}$ remains independent [47]. Increasing slopes

of linear plots in Fig. 14 with rise in gas concentrations also results from higher dispersion interaction.

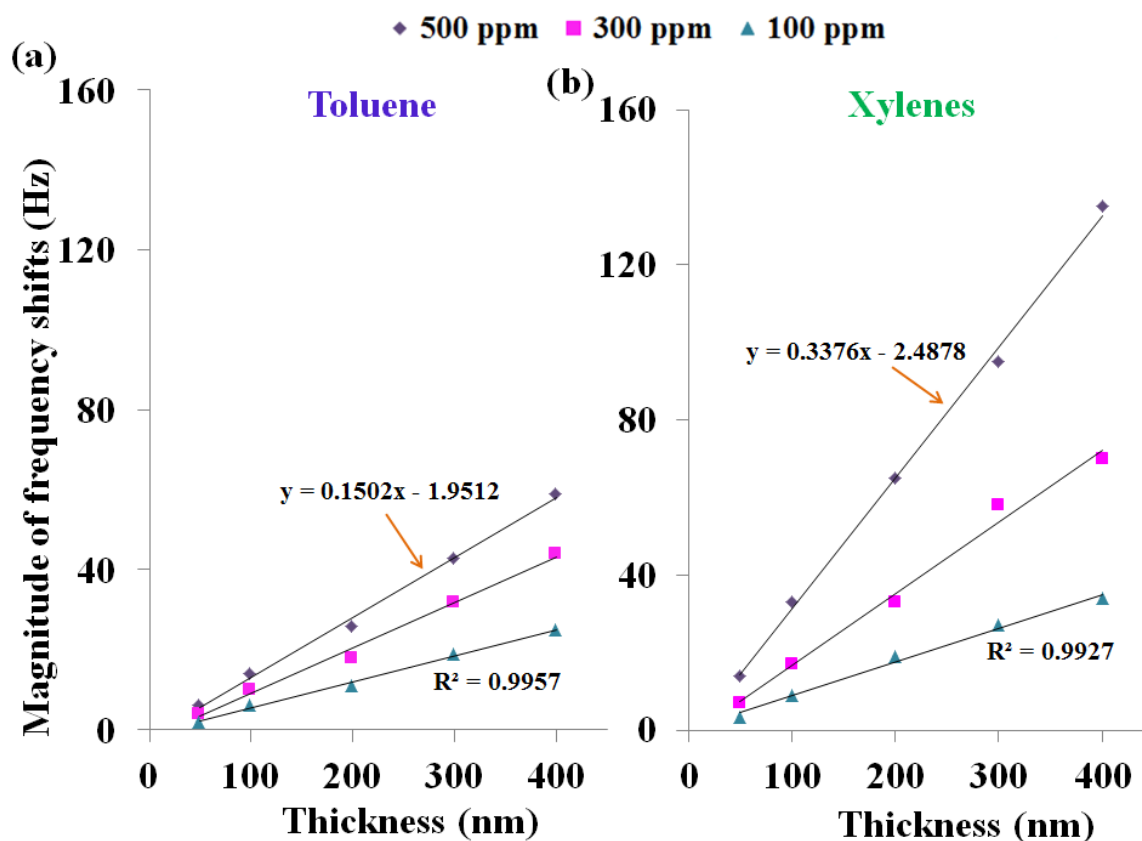


Fig. 14: *ttb*-CuPc based QCM sensor response to 500 ppm, 300 ppm and 100 ppm of (a) toluene and (b) xylenes versus layer thickness.

The kinetics of gas diffusion into the sensing layer was studied by the determination of the response and recovery times for different thicknesses of *ttb*-CuPc. The response and recovery times measured for toluene and xylenes exposure at 500 ppm on layers with 50 nm, 100 nm, 200 nm and 400 nm of thickness are represented in Fig. 15. Sensors exhibited little increase in response and recovery times with increasing layer thickness for toluene (from 1 to 3 minutes) while a fast increase especially for thicker films can be underlined in the case of xylenes (from 1 to 10 minutes). The variations of response and recovery times as a function of layer thickness clearly justifies diffusion process occurring into the volume of the sensitive

layers. Moreover, the highest effects observed for xylenes can be justified by the higher steric hindrance of xylene molecules as compared to toluene that slows down their progress along the diffusion channels. That's in accordance with previous discussion illustrated by Fig. 5. More especially, because of the position of their two methyl groups, o- and m-xylenes will progress slowly as compared to toluene or p-xylene. A delay is noticeable on response time as well as on recovery time (extraction from deep sites is slower). In contrast, toluene molecules because of relatively lower molecular volume will pass through swiftly within the sub-layers and will come out with ease during the recovery steps.

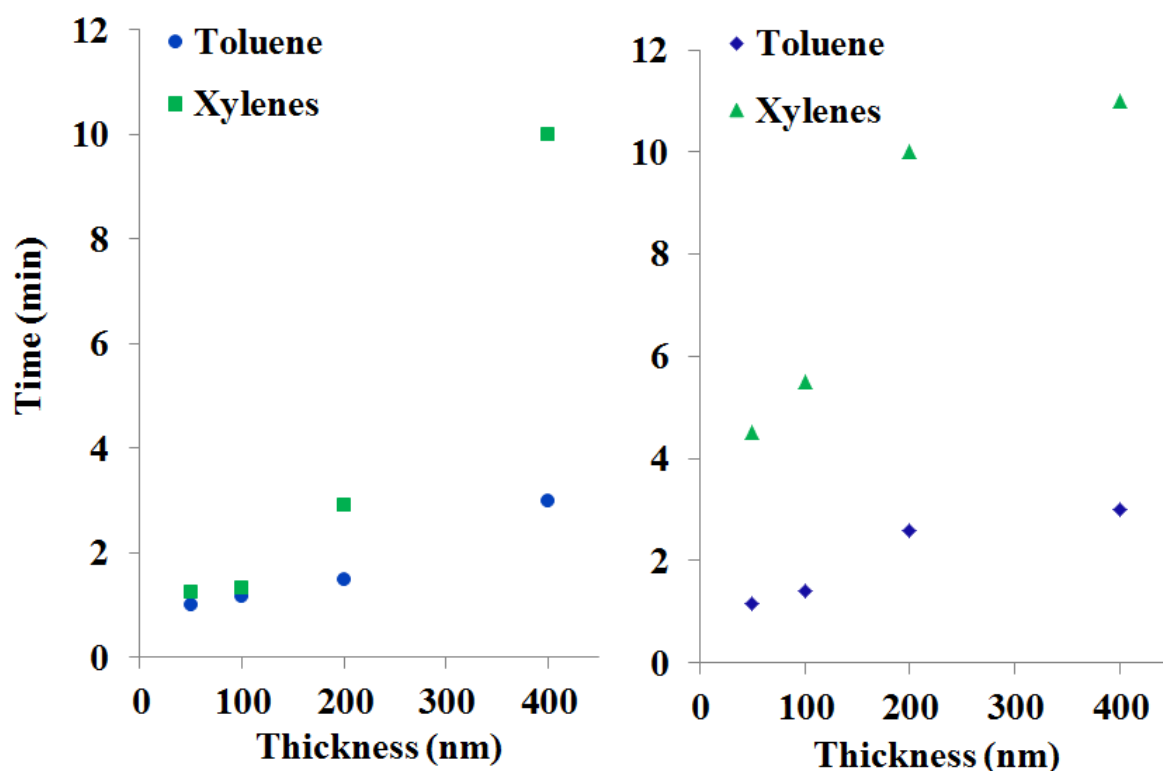


Fig. 15: Inter-comparative study of (a) response and (b) recovery times of toluene and xylenes at varying sensing layer thicknesses.

3.3.2. Influence of tert-butyl group on adsorption: intercomparison with CuPc

In order to emphasize the contribution of tert-butyl groups on sorption mechanism, previous results have been compared to CuPc as sensitive material. Thus CuPc-based QCM devices with 100, 200, 300 and 400 nm as layer thickness were realized and their responses toward toluene and xylenes were measured in range of 100-500 ppm concentrations with a step of 100 ppm. The variations in sensor response to 100 ppm, 300 ppm and 500 ppm of toluene and xylenes versus layer thickness are shown in Fig. 16. Approximately, similar sensor responses were measured except for the lowest thickness (100 nm) which exhibits a lower response both for toluene and xylenes. The low dispersion of measurements with CuPc layer thickness is typical from a sorption restricted to the surface of the sensitive material. The number of surface adsorption sites seems largely unaffected by the increase in layer thickness especially from 200 nm. Actually, CuPc macrocycles strongly interact together into the column as previously debated into the third chapter. As a consequence, even if the diffusion of BTX molecules cannot be excluded in CuPc thin layers, gas adsorption on deep macrocycles is weakly probable and mainly localized to the top of the columnar stacking. Above 200 nm [45], the number of adsorption sites for aromatic hydrocarbons remains approximately constant, whatever the layer thickness. The lower responses to toluene and xylenes at 100 nm of layer thickness can be attributed to low surface roughness. Indeed, a previous AFM studies on CuPc layers established that surface roughness increases with increasing layer thickness up to 160 nm and then reach a saturation [52].

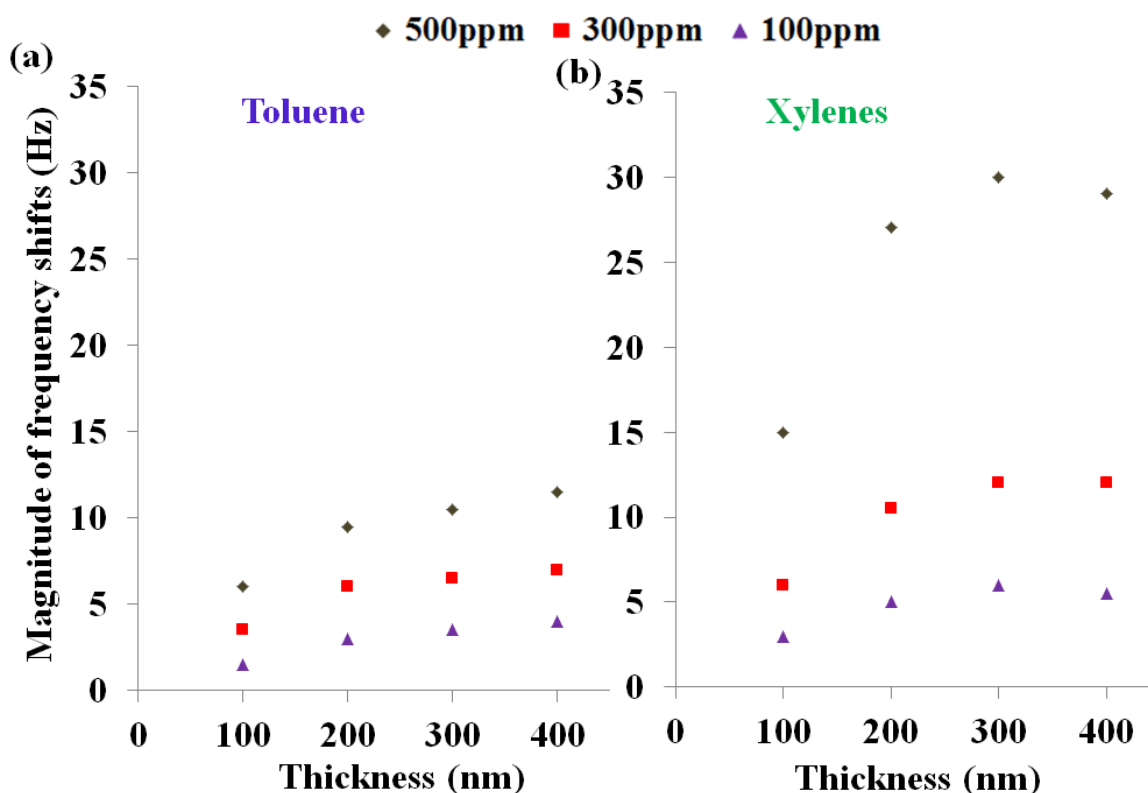


Fig. 16: CuPc based QCM sensor response to 500 ppm, 300 ppm and 100 ppm of (a) toluene and (b) xylenes at varying layer thicknesses.

As a partial conclusion, the organization of the molecular units within the layers makes possible the diffusion of mono-aromatic hydrocarbons into the volume. Nevertheless, for un-substituted copper phthalocyanines, adsorption of BTX molecules is mainly limited to macrocycles localized at the surface and more exactly at the top of the nano-columns. Thus, the increase in layer thickness is not a judicious approach to benefit from higher responses. In contrast, the tert-butyl groups are responsible for an amorphous structure of the ttb-CuPc sensitive layer providing a lot of available adsorption sites. BTX diffusion can occur within the whole volume leading to a linear increase in sensor response with layer thickness. At the same time, the kinetics of response and recovery are affected by this parameter. Therefore, the optimal ttb-CuPc layer thickness for sensor development strongly depends on the required sensitivity, response and recovery times in the context of the target application.

4. Ageing of the ttb-CuPc sensor layer

Phthalocyanines materials are molecular materials known for their robustness toward atmospheric, thermal and photo-chemical treatments [53-55]. Nevertheless, the constant exposure of phthalocyanine thin films in different environmental conditions can be prejudicial to its long-term stability, thus affecting its electrical and optical properties. Researches have been reported in the past about the degradation of these materials with time. These long-term degradations can be due to different extreme conditions: extended irradiation under UV and visible light [56], high and extended thermal environments [57] as well as slow oxidation in atmospheric conditions [58-61]. In the latter case, this is especially prejudicial to semiconductor gas sensors limiting their lifetime.

To investigate the ageing of ttb-CuPc sensing layers, a 400 nm thin layer was exposed to successive cycles of exposure and recovery during a period of 33 days. Toluene concentration was set to 500 ppm whereas exposure and recovery times were set to 2 and 3 hours respectively. Fig. 17 represents the time variation of frequency shift of QCM sensor at room temperature for all cycles of measurement. From this ageing study, we can distinguish two phases: an increase in sensor response with exposure number during the first days followed by a slow but continuous decrease.

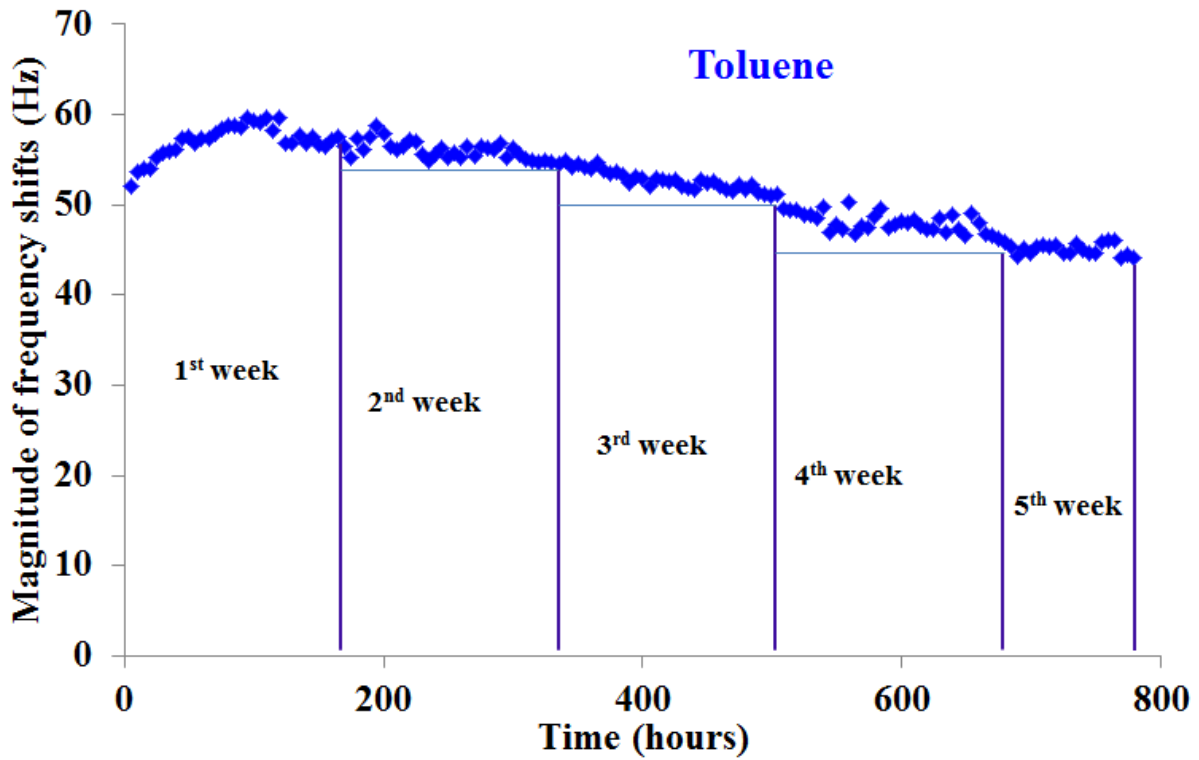
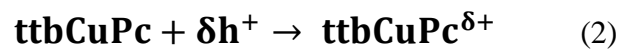
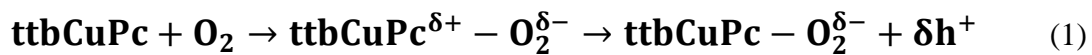


Fig. 17: Time variations of QCM sensor response exposed to successive exposures to 500 ppm of toluene. After each exposure, sensor returns under pure air.

The ageing of the layer could be attributed to its slow irreversible oxidation. The gradual irreversible chemisorption of molecular oxygen can be described by the following reactions [59]:



The above sequence of chain reaction leads to gradual depletion of adsorption sites available for binding with gas molecules.

If the ageing of the sensitive layer is noticeable for continuous working mode, the storage conditions of devices can also lead to sensor response drifts in time. In order to prevent layer alteration throughout the storage period, we evaluated the long-term stability of the sensing devices for storage in two different environments: atmospheric air and nitrogen.

Thus, two similar *ttb*-CuPc based QCM sensors (layer thickness = 400 nm) were stored for 2 months in atmosphere and in a confined nitrogen atmosphere at room temperature. Responses of each device were measured just after their realization and compared to those measured on the same device after 2 months of storage. The variations in sensor response after 2 months of storage in different environments are reported in Fig. 18 for 500 ppm of xylenes and toluene. From experimental measurements, storage under nitrogen appears as the best conditions to prevent decrease in sensor sensitivity. The frequency shifts measured on stored samples exposed to toluene and xylenes are equal to 60 Hz and 126 Hz respectively and are unchanged as compared to value obtained on as-deposited layers. In contrast, samples kept in atmosphere exhibit decline in frequency shifts to 38 Hz for toluene and 98 Hz for xylenes. The irreversible chemisorption of molecular oxygen on the binding sites within the *ttb*-CuPc layers as explained in the reaction scheme can be given as the main cause for the weakening in sensors response of QCM samples stored in atmosphere.

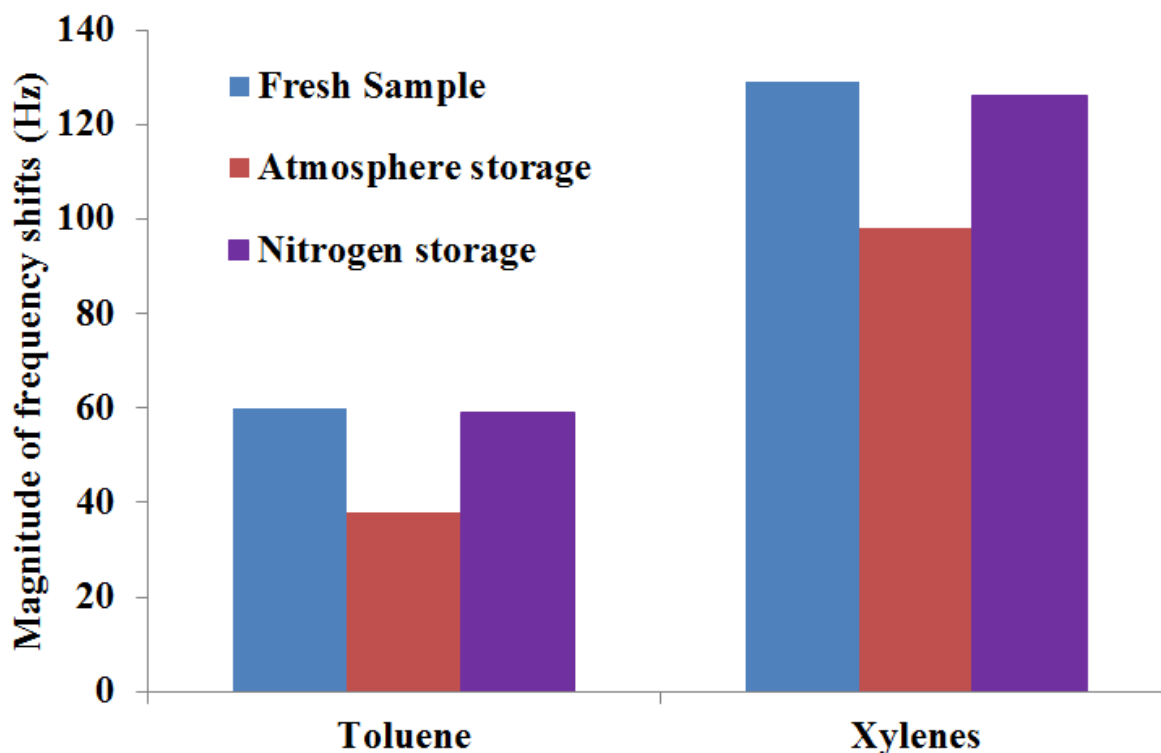


*Fig. 18: Comparison of *ttb*-CuPc based QCM sensor responses exposed to 500 ppm of toluene or xylenes before and after 2 months of storage period under air and constant flow of nitrogen.*

We must also underline that responses toward toluene and xylene of these devices are closely similar to those measured for another batch of sensors in the same experimental conditions whose results are reported on Fig. 3. The good reproducibility is so established

Conclusion

Based on the previous investigations of different types of metallophthalocyanines for their application as potential sensing materials coated on QCM transducer for BTX sensor development, tert-butyl substituted metallophthalocyanines were established as a preferred choice. Thus, copper tetra-tert-butyl phthalocyanine was selected for a deeper study on its sensing performances at room temperature.

Firstly, experimental results revealed a reversible response with stable baseline in short-term. Among various metrological characteristics of a gas sensor, we were mainly interested in kinetics of response, repeatability, resolution, limit of detection, threshold and selectivity. Assessment of kinetics of sensor response was achieved by estimating response and recovery times. If toluene exhibited fast kinetics of adsorption as well as desorption with response and recovery times less than 3 minutes, xylenes showed a delayed sorption highlighted by response and recovery times of the sensor to 10 minutes. Benzene followed even slower kinetics of desorption. The monotonic variations of gas concentrations highlighted repeatable and reproducible response of sensors to each of three gases. The higher slope of calibration curve for xylenes was attributed to diffusion through the pores of ortho- and meta- isomers of xylenes at higher concentrations which remained negligible at low concentrations. Non-monotonic variations in gas concentrations highlighted negligible effect of gas exposure history in case of toluene. The resolution of sensor was estimated to 10 ppm for toluene. Limit of detection for benzene, toluene and xylenes were assessed to 2.15 ppm,

1.8 ppm and 0.75 ppm respectively although experimental measurements show a significant response for toluene concentration lower than 1 ppm. Selectivity of the sensor was determined by cross-sensitivity measurement with common atmospheric pollutants. If sensor exhibited no significant response to NO₂, CO and H₂S, exposure to ozone was prejudicial to the stability of the sensing layers. The interference of ozone can be addressed by integrating Indigo based Ozone chemical filter upstream the gas exposure fluidic line. Nevertheless, the selectivity level of such devices remains insufficient to the discriminated metrology of benzene, toluene and xylenes. This challenge remains to overcome.

To investigate the gas/material interactions, we considered adsorption of gas molecules on available active sites and diffusion within the sensor layer. The calibration curve of the sensor was fitted using a combination of Langmuir and Henry adsorption isotherms. A two-step adsorption model taking into account specific and non-specific interactions of the gas molecules with sensor surface was proposed and validated by experimental results. Diffusion within the sensing layers was investigated by experiments on samples with different thicknesses. Strong diffusion within the ttb-CuPc sensing layer was established and the role of tert-butyl groups on the increase in adsorption site number was confirmed by means of intercomparison with measurement achieved on CuPc layers with different thicknesses. Finally, a slow ageing of ttb-CuPc layer was established and attributed to irreversible chemisorption of molecular oxygen on macrocycles. This was observed on sensor responses in continuous working mode as well as on sensors stored under atmospheric air. To prevent long-term sensor drifts, storage under inert gas seems efficient.

References

1. Wheeler, S.E., et al., *Substituent Effects in the Benzene Dimer are Due to Direct Interactions of the Substituents with the Unsubstituted Benzene*. Journal of the American Chemical Society, 2008. **130**(33): p. 10854-10855.
2. Wheeler, S.E., *Local Nature of Substituent Effects in Stacking Interactions*. Journal of the American Chemical Society, 2011. **133**(26): p. 10262-10274.
3. Wheeler, S.E., *Understanding Substituent Effects in Noncovalent Interactions Involving Aromatic Rings*. Accounts of Chemical Research, 2012. **46**(4): p. 1029-1038.
4. Arendorf, J.R.T., *A study of some non-covalent functional group π -interactions*. Thesis dissertation, 2011. University College London.
5. Tsuzuki, S., et al., *Magnitude and Directionality of the Interaction Energy of the Aliphatic CH/ π Interaction: Significant Difference from Hydrogen Bond*. The Journal of Physical Chemistry A, 2006. **110**(33): p. 10163-10168.
6. Nishio, M., *The CH/[small pi] hydrogen bond in chemistry. Conformation, supramolecules, optical resolution and interactions involving carbohydrates*. Physical Chemistry Chemical Physics, 2011. **13**(31): p. 13873-13900.
7. Lee, L.-H., *Fundamentals of Adhesion*. 1991 Springer USA.
8. Atkin, P., Paula, J. D., *Physical Chemistry for the Life Sciences*. 2006, Oxford, UK: Oxford University Press. 2.
9. Banerjee, K., et al., *Adsorption kinetics of o-xylene by flyash*. Water Research, 1997. **31**(2): p. 249-261.
10. Mehio, N., et al., *Quantum Mechanical Basis for Kinetic Diameters of Small Gaseous Molecules*. The Journal of Physical Chemistry A, 2014. **118**(6): p. 1150-1154.

11. Breck, D.W., *Zeolite molecular sieves: structure, chemistry, and use*. 1984: R.E. Krieger.
12. Matteucci, S., et al., *Transport of Gases and Vapors in Glassy and Rubbery Polymers*, in *Materials Science of Membranes for Gas and Vapor Separation*. 2006, John Wiley & Sons, Ltd. p. 1-47.
13. Baertsch, C.D., et al., *Permeation of Aromatic Hydrocarbon Vapors through Silicalite–Zeolite Membranes*. *The Journal of Physical Chemistry*, 1996. **100**(18): p. 7676-7679.
14. Santos, K. A., et al., *Separation of xylene isomers through adsorption on microporous materials: A review*. *Brazilian Journal of petroleum and gas*, 2011. **5**(4): p. 14-20.
15. Yang, K., et al., *Adsorption of volatile organic compounds by metal–organic frameworks MIL-101: Influence of molecular size and shape*. *Journal of Hazardous Materials*, 2011. **195**: p. 124-131.
16. Archer, P.B.M., et al., *Kinetic factors in the response of organometallic semiconductor gas sensors*. *Sensors and Actuators*, 1989. **16**(4): p. 379-392.
17. Brunet, J., et al., *An optimised gas sensor microsystem for accurate and real-time measurement of nitrogen dioxide at ppb level*. *Sensors and Actuators B: Chemical*, 2008. **134**(2): p. 632-639.
18. Kılınç, N., et al., *Electrical and NO₂ sensing properties of liquid crystalline phthalocyanine thin films*. *Sensors and Actuators B: Chemical*, 2012. **173**: p. 203-210.
19. Schütze, A., et al., *Quantitative ozone measurement using a phthalocyanine thin-film sensor and dynamic signal evaluation*. *Sensors and Actuators B: Chemical*, 1995. **23**(2–3): p. 215-217.
20. *COST Action TD 1105 - EuNetAir*. <http://www.eunetair.it/>.

21. Brunet, J., et al., *Comparisons between NO₂ and ozone sensing properties of phthalocyanines and n-InP thin films in controlled and noncontrolled atmospheres.* Sensors Journal, IEEE, 2004. **4**(6): p. 735-742.
22. Brunet, J., et al., *Physical and chemical characterizations of nanometric indigo layers as efficient ozone filter for gas sensor devices.* Thin Solid Films, 2011. **520**(3): p. 971-977.
23. Cédric, R., et al., *Limite de détection de méthodes d'analyse et termes apparentés.* Techniques de l'ingénieur Qualité au laboratoire, 2014. **base documentaire: TIB497DUO**(ref. article : p262 (1-14).
24. Armbruster, D.A., et al., *Limit of Blank, Limit of Detection and Limit of Quantitation.* The Clinical Biochemist Reviews, 2008. **29**(Suppl 1): p. S49-S52.
25. Sadler, W.A., *Using the variance function to estimate limit of blank, limit of detection and their confidence intervals.* Ann Clin Biochem, 2015.
26. Gautschi, K., et al., *A new look at the limits of detection (LD), quantification (LQ) and power of definition (PD).* Eur J Clin Chem Clin Biochem, 1993. **31**(7): p. 433-40.
27. Armbruster, D.A., et al., *Limit of detection (LOD)/limit of quantitation (LOQ): comparison of the empirical and the statistical methods exemplified with GC-MS assays of abused drugs.* Clin Chem, 1994. **40**(7 Pt 1): p. 1233-1238.
28. Browne, R.W., et al., *Procedures for determination of detection limits: application to high-performance liquid chromatography analysis of fat-soluble vitamins in human serum.* Epidemiology, 2010. **21 Suppl 4**: p. S4-9.
29. Linnet, K., et al., *Partly nonparametric approach for determining the limit of detection.* Clin Chem, 2004. **50**(4): p. 732-740.
30. Dąbrowski, A., *Adsorption — from theory to practice.* Advances in Colloid and Interface Science, 2001. **93**(1–3): p. 135-224.

31. Everett, D.H., *Manual of Symbols and Terminology for Physicochemical Quantities and Units, Appendix II: Definitions, Terminology and Symbols in Colloid and Surface Chemistry*. Pure Appl. Chem., 1972. **31**(4): p. 577-638.
32. Steele, W., *Molecular interactions for physical adsorption*. Chemical Reviews, 1993. **93**(7): p. 2355-2378.
33. Langmuir, I., *The adsorption of gases on plane surfaces of glass, mica and platinum*. Journal of the American Chemical Society, 1918. **40**(9): p. 1361-1403.
34. Clayton, W., *Capillary and colloid chemistry*. By Prof. H. Freundlich. Translated by H. Stafford Hatfield, Journal of the Society of Chemical Industry, 1926. **45**(44): p. 797-798.
35. Loughlin, K., et al., *Adsorption Henry constants calculated from the entire isotherm*. Adsorption, 2013. **19**(6): p. 1189-1196.
36. Richardson, T.H., et al., *The NO₂ gas sensing properties of calixarene/porphyrin mixed LB films*. Colloids and Surfaces A: Physicochemical and Engineering Aspects, 2006. **284–285**: p. 320-325.
37. Ma, X., et al., *Effects of fluorination in the ring of zinc tetraphenylporphyrin on its gas-response to volatiles at room temperature*. Sensors and Actuators B: Chemical, 2006. **114**(2): p. 1035-1042.
38. Richardson, T.H., et al., *Development and optimization of porphyrin gas sensing LB films*. Advances in Colloid and Interface Science, 2005. **116**(1–3): p. 81-96.
39. Richardson, T.H., et al., *Taking advantage of optical and electrical properties of organic molecules for gas sensing applications*. Thin Solid Films, 2001. **393**(1–2): p. 259-266.

40. Macagnano, A., et al., *Sorption and condensation phenomena of volatile compounds on solid-state metalloporphyrin films*. Sensors and Actuators B: Chemical, 2007. **124**(1): p. 260-268.
41. Su, F., et al., *Adsorption of benzene, toluene, ethylbenzene and p-xylene by NaOCl-oxidized carbon nanotubes*. Colloids and Surfaces A: Physicochemical and Engineering Aspects, 2010. **353**(1): p. 83-91.
42. Capan, İ., et al., *The interaction between the gas sensing and surface morphology properties of LB thin films of porphyrins in terms of the adsorption kinetics*. Materials Chemistry and Physics, 2012. **136**(2–3): p. 1130-1136.
43. Shiue, A., et al., *Vapor adsorption characteristics of toluene in an activated carbon adsorbent-loaded nonwoven fabric media for chemical filters applied to cleanrooms*. Building and Environment, 2010. **45**(10): p. 2123-2131.
44. Yu, F., et al., *Kinetic and Thermodynamic Studies of Toluene, Ethylbenzene, and m-Xylene Adsorption from Aqueous Solutions onto KOH-Activated Multiwalled Carbon Nanotubes*. Journal of Agricultural and Food Chemistry, 2012. **60**(50): p. 12245-12253.
45. Oh, G.-Y., et al., *Adsorption of toluene on carbon nanofibers prepared by electrospinning*. Science of The Total Environment, 2008. **393**(2–3): p. 341-347.
46. László, K., et al., *Simultaneous adsorption of toluene and water vapor on a high surface area carbon*. Carbon, 2012. **50**(11): p. 4155-4162.
47. Fietzek, C., et al., *Soluble phthalocyanines as coatings for quartz-microbalances: specific and unspecific sorption of volatile organic compounds*. Sensors and Actuators B: Chemical, 1999. **57**(1–3): p. 88-98.
48. Fietzek, C., et al., *Reversible intercalation of volatile amines into stacks of soluble phthalocyanines*. Journal of Materials Chemistry, 2002. **12**(8): p. 2305-2311.

49. Bodenhöfer, K., et al., *Chiral Discrimination of Inhalation Anesthetics and Methyl Propionates by Thickness Shear Mode Resonators: New Insights into the Mechanisms of Enantioselectivity by Cyclodextrins*. *Analytical Chemistry*, 1997. **69**(19): p. 4017-4031.
50. Gopakumar, T.G., et al., *Porous Network Structure of Octacyano-Metal-Free Phthalocyanine on the Basal Plane of Highly Oriented Pyrolytic Graphite*. *The Journal of Physical Chemistry C*, 2008. **112**(20): p. 7698-7705.
51. Kanari, M., et al., *Improved Density and Mechanical Properties of a Porous Metal-Free Phthalocyanine Thin Film Isotropically Pressed with Pressure Exceeding the Yield Strength*. *Applied Physics Express*, 2011. **4**(11): p. 111603.
52. Hong, D., et al., *Structural templating and growth behavior of copper phthalocyanine thin films deposited on a polycrystalline perylenetetracarboxylic dianhydride layer*. *Journal of Applied Physics*, 2011. **109**(6): p. 063507(1-6).
53. Lawton, E.A., *The Thermal Stability of Copper Phthalocyanine*. *The Journal of Physical Chemistry*, 1958. **62**(3): p. 384-384.
54. Słota, R., et al., *UV Photostability of Metal Phthalocyanines in Organic Solvents*. *Inorganic Chemistry*, 2003. **42**(18): p. 5743-5750.
55. Krebs, F.C., *Stability and Degradation of Organic and Polymer Solar Cells*. 2012: Wiley.
56. Caronna, T., et al., *Decomposition of a phthalocyanine dye in various conditions under UV or visible light irradiation*. *Journal of Photochemistry and Photobiology A: Chemistry*, 2006. **184**(1-2): p. 135-140.
57. Huh, Y.J., et al., *Thermal Decomposition and Deformation of Dye and Polycarbonate in Compact Disc-Recordables*. *Japanese Journal of Applied Physics*, 1997. **36**(12R): p. 7233.

58. Hermenau, M., et al., *Comparison of different conditions for accelerated ageing of small molecule organic solar cells.* in *Organic Photonics IV* Brussels. 2010, SPIE proceeding, **7722**.
59. Park, J., et al., *Ambient induced degradation and chemically activated recovery in copper phthalocyanine thin film transistors.* Journal of Applied Physics, 2009. **106**(3): p. 034505 (1-5).
60. d'Alessandro, N., et al., *Rapid and Selective Oxidation of Metallosulphthalocyanines Prior to Their Usefulness as Precatalysts in Oxidation Reactions.* European Journal of Inorganic Chemistry, 2003. **2003**(9): p. 1807-1814.
61. Yan, X., et al., *An investigation on air stability of copper phthalocyanine-based organic thin-film transistors and device encapsulation.* Thin Solid Films, 2006. **515**(4): p. 2655-2658.

Chapter 5:

Ongoing activities and perspective

1. On-going activities focused on sensing performance improvements

The attractive sensing performances obtained with ttb-CuPc based QCM sensors and justified by all the experimental results reported in the previous chapters make these devices well suitable for the measurement of monocyclic aromatic hydrocarbons concentrations in occupational environments. However, to satisfy the environmental guidelines for non-occupational conditions defined in the sub-ppm range, further improvements are required especially lower limit of detection, higher resolution and better selectivity.

In order to perform sensing devices with higher resolution and lower limit of detection, our strategy is to benefit from a high number of active sites available for gas adsorption by the dispersion of macrocycles onto an extended surface. With high specific surface areas and the possibility to be functionalized with various active groups on their surface, nanocarbonaceous materials appear as relevant matrix for the development of such highly sensitive materials to gaseous species. Indeed, the structural backbone of carbon nanotube and ttb-CuPc offer the possibility to achieve non-covalent functionalization through π - π interactions. Moreover, even for a moderate functionalization rate of ttb-CuPc on CNTs, the π -conjugated structure of carbon nanotubes having extended benzene rings can provide a lot of interaction sites for BTX adsorption. Thus, carbon nanotube/ttb-CuPc hybrid materials have been synthesized, coated on quartz crystals and investigated as sensitive layer. Few preliminary results will be given.

As already stated, the selectivity is a metrological characteristic to improve because the discriminated measurement of benzene, toluene and xylenes remains unachievable. With this objective, our strategy is the development of a gas discrimination module which would be

implemented upstream the sensing device into a complete sensor-system. Two scenarios are considered:

- Gas discrimination module acting as a selective filtering unit and sensor-system response correlated to the concentration of one target analyte;
- Gas discrimination module acting as a gas retention matrix, each aromatic hydrocarbon being released at different temperatures by programmed thermo-desorption process and sensor-system response sequentially attributed to each target gas.

This last method takes the advantage of different activation energies of desorption of benzene, toluene and xylenes from the available interaction sites. No result will be given, only the strategy will be described.

All these objectives constitute one part of the on-going scientific activities of the *Chemical Sensor System and Micro-system* group of Institut Pascal. Works are still in progress with the financial support of the CNRS through the multidisciplinary exploratory projects ASTHMAA (Selective Analysis of Total MonoAromatic Hydrocarbons in Air, granted in 2015), the scientific support of the transdisciplinary COST Action TD 1105 – EuNetAir (2013-2016) and the interest of the European Sensor-System Cluster (ESSC).

2. Sensitivity enhancement: development of CNT/ttb-CuPc hybrid materials

2.1. Raw and functionalized carbon nanotubes: generalities

Carbon nanotubes (CNTs) belong to the family of synthetic carbon allotropes and are characterized by a network of sp^2 hybridized carbon atoms. It is one dimensional carbon superstructure with average diameter in a range of 0.6–5 nm (for SWNT) [1, 2] The structure of nanotubes has been first described as helical microtubules of graphitic carbon in 1991 by Iijima. They were accidentally synthesized by an arc discharge evaporation process originally designed for the production of fullerenes [1]. Since then, extensive researches have highlighted the structure and the properties of this highly remarkable carbon allotrope [3-8]. Single-walled carbon nanotubes, namely SWCNTs, are organized as a rolled graphene sheet with a cylindrical form (see Fig. 1a) [9]. Multi-walled carbon nanotubes (MWCNTs) are constituted by an array of single-wall nanotubes concentrically rolled (see Fig. 1b). Depending on the ways the graphene sheet is rolled up, a huge diversity of SWCNT structures can be constructed differing in length, diameter and roll-up angle. These structures can be better understood by considering the chiral vector C_h which corresponds to a cross-section of the nanotube perpendicular to the axis as schematically shown in the unrolled honeycomb lattice in Fig. 1a.

polymers and semiconductors [10]. The physical and chemical natures of carbon nanotubes, which can be considered as fully conjugated poly-aromatic macromolecules, impart the above mentioned diverse properties. While fundamental researches were focused on the intrinsic properties of isolated carbon nanotubes, applications involve their interactions with neighboring environment. These interactions can be because of non-covalent forces acting between the nanotube and molecular, ionic or macromolecular species. Due to their high polarizability and smooth surface, SWCNTs interact together by means of strong Van Der Waals interactions reaching ~ 500 eV per μm of NT's length [11]. Thus, carbon nanotubes are not usually isolated in liquid or solid phase but aggregate into bundles where several nanotubes are aligned parallel to each other.

In order to separate nanotubes from each other's, functionalization is an efficient treatment. Grafting of an organic moiety (surfactant, polymer or macromolecule) can be achieved through either covalent or non-covalent functionalization [12, 13]. Because of the establishment of new chemical bonds between carbonaceous matrix and the functional groups, covalent functionalization in most cases alters the intrinsic properties of CNTs such as conductivity and mechanical strength since it destroys the regular graphene-type structure. In contrast, noncovalent functionalization of CNTs with polymers or macromolecules is an effective way to disperse the nanotubes in aqueous and non-aqueous solvents without damaging their unique structure and thus preserving their intrinsic properties. High specific surface area of carbon nanotubes is another advantage especially in the context of gas sensing applications. It was reported earlier by Eswaramoorthy et al. about the high surface area of SWNT as $400 \text{ m}^2 \text{ g}^{-1}$ using BET N_2 absorption isotherms at 77 K [14]. Treatment with concentrated HCl or HNO_3 can further enhanced the surface area of SWNTs, making the interior cavity more accessible.

2.2. Non-Covalent functionalization of carbon nanotubes by phthalocyanines macrocycles

Considering the aromatic character and conjugated structure of phthalocyanines, the non-covalent functionalization of CNTs by these organic molecules can be performed. Moreover, previous researches were reported about such non-covalent functionalization of CNTs [15-18] for various applications including ammonia and VOCs detection. The enhancement in sensing performances with these hybrid materials was manifested. Taking into account previous studies and structure of the hybrid, the functionalization of CNTs by phthalocyanine macrocycles should greatly improve the distribution of adsorption sites for BTX. Thus, a higher sensitivity can be expected.

The non-covalent functionalization of CNTs by phthalocyanines is governed by π - π stacking as illustrated by Fig. 2. Phthalocyanine macrocycles can be stacked in a parallel configuration on the CNT surface. Such parallel stacking configuration was confirmed from theoretical studies [17] which took into account the highest non-covalent interaction energies. The non-covalent functionalization can be monitored by the variation in spectral band of UV-Vis [19] and Raman spectroscopy [20] of CNT/MPcs hybrid material from individual raw materials. The assumed interactions of BTX molecules on the surface of CNT/MPcs hybrid material are illustrated in Fig. 2. Nevertheless, in addition to interactions with phthalocyanine macrocycles, aromatic target molecule can also interact with benzene ring of the carbonaceous matrix through π - π interactions. As a consequence, even if the functionalization remains not complete (carbon nanotubes not completely decorated), a higher sensitivity is expected as compared to phthalocyanine or carbon nanotube considered separately. Sensing characteristics of ttb-CuPc based QCM sensor being clearly demonstrated in this work, the grafting of ttb-CuPc on carbonaceous matrix exhibiting a high SSA was performed to benefit from higher sensor responses.

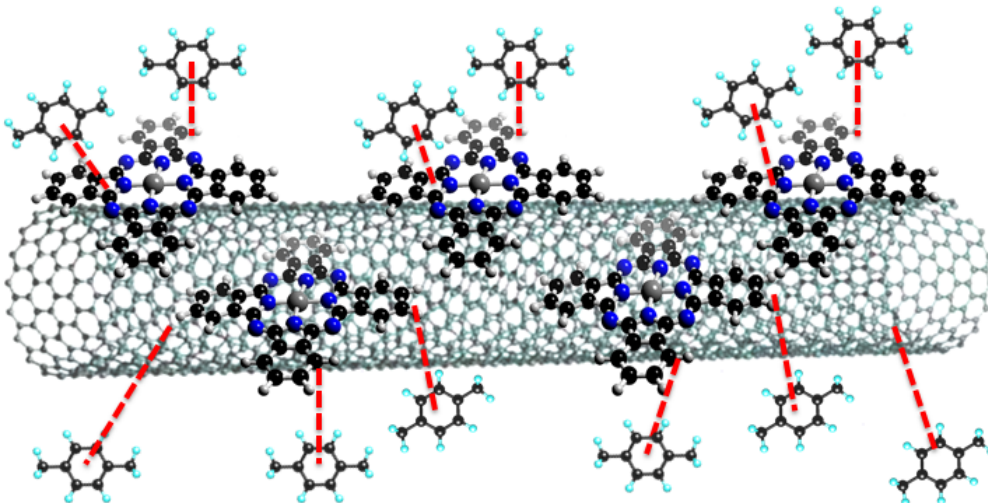


Fig. 2: Schematic illustration of interaction of BTX gases with non-covalent functionalized CNTs/ttb-CuPc.

2.3. Preliminary results of ttb-CuPc/CNT hybrid based QCM toward BTX

2.3.1. Sensor development

Functionalization of hybrid material was achieved by adding 1 mg of raw SWCNTs into 10 ml of ttb-CuPc dispersed into chloroform (0.005 mM). The resulting solution was then sonicated during 15 minutes at room temperature. Colorless or lightly colored supernatant so formed was separated. The extent of functionalization was monitored by UV-Vis absorption spectroscopy of the supernatant solution. For that, dispersion of hybrid material in chloroform was prepared for different concentration of SWCNT. The Q-band absorbance of ttb-CuPc with increasing ratio of SWCNT has been depicted in Fig. 3b. It can be noticed in the Fig 3b that with each addition of SWCNT into the ttb-CuPc solution, the Q-band absorbance of ttb-CuPc is decreasing. After the complete functionalization, further addition of SWCNT doesn't have any effect on total absorbance of the solution.

Sensitive layers of hybrid material were realized by the deposition of ttb-CuPc/SWCNT dispersed into chloroform on quartz crystal according to drop casting process. After deposition, quartz crystal was heated at 80°C to facilitate solvent evaporation.

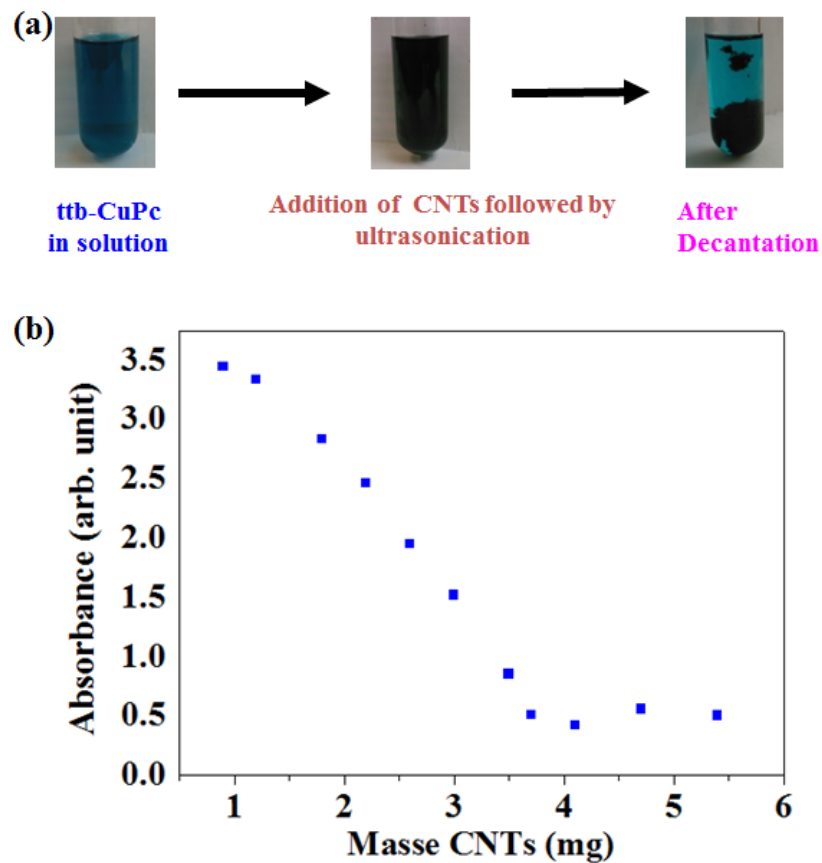


Fig.3: Functionalization of SWNT by ttb-CuPc: (a) addition of SWNT in ttb-CuPc solution in chloroform and (b) decrease in Q-band of resulting supernatant with each addition of SWNT.

2.3.2. Characterization of hybrid sensing material

In order to justify the functionalization of SWCNTs by ttb-CuPc, hybrid material was characterized using Thermo Gravimetric Analysis (TGA), Raman spectroscopy and Transmission Electron Microscopy (TEM).

TGA is an analytical technique which determines the change in physical or chemical properties of a material as a function of temperature. Thermal decomposition analysis of ttb-CuPc and hybrid material can put in obviousness the functionalization by the determination of the weight loss of hybrid material versus temperature because phthalocyanine decomposes between 400–490°C while SWCNTs remain weakly altered below 600°C. Experimental results from TGA characterization is shown in Fig. 4. It is evident from the graphs that weight loss in hybrid material is higher than SWCNT and lower than ttb-CuPc, which can be an indication of presence of ttb-CuPc in the hybrid.

To attest the functionalization, Transmission Electron Microscopy (TEM) was performed on hybrid material, micrograph being reported in Fig. 5. It can be noticed in the micrograph that ttb-CuPc are present like a small grains immobilized on SWNT surface. This is in agreement with the previous findings through adsorption and TGA studies.

The Raman spectra of hybrid material washed properly in chloroform, SWNT and ttb-CuPc was recorded at an excitation wavelength of 514.8 nm as shown in in Fig 6. The band positions at 1328 cm^{-1} (D-band) and 1590 cm^{-1} (G-band) in SWNT can correspond to defects in hexagonal framework and graphitic structure respectively. In hybrid material, SWNT characteristics peaks (D and G bands) are superimposed with ttb-CuPc peaks and form two novel peaks which match ideally with ttb-CuPc peaks. Also, D and G bands are slightly broadened because of superimposition. These results confirm the functionalization of SWNT with ttb-CuPc.

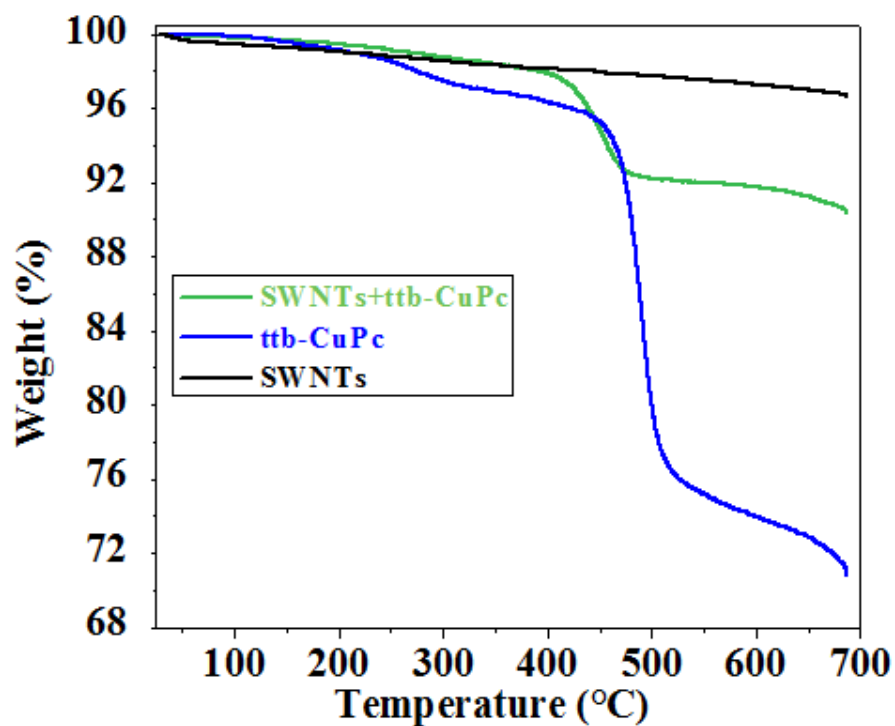


Fig. 4: Thermo Gravimetric Analysis of SWNT, ttb-CuPc and ttb-CuPc/SWCNT by comparison of weight loss of three materials

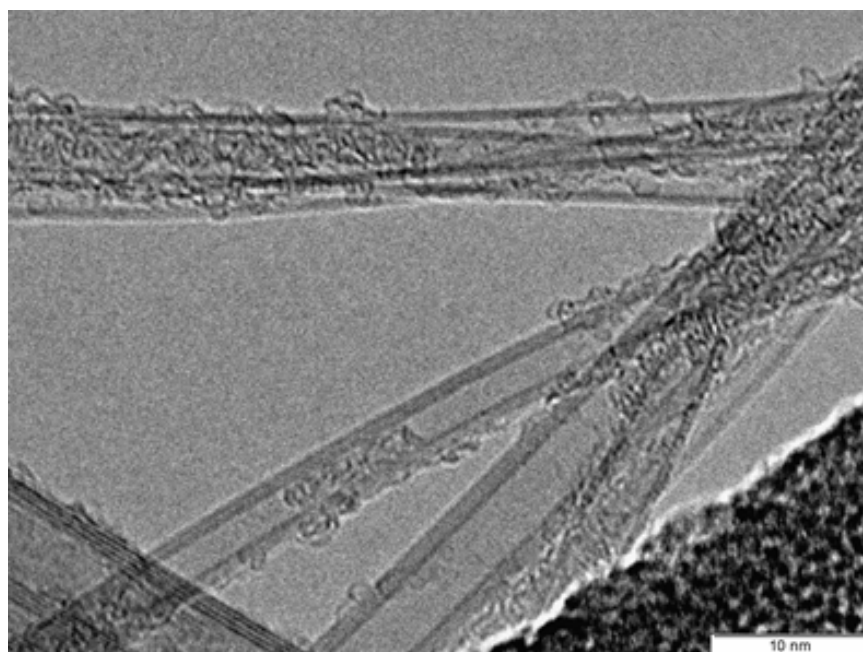


Fig. 5: TEM micrograph of ttb-CuPc/CNT hybrid.

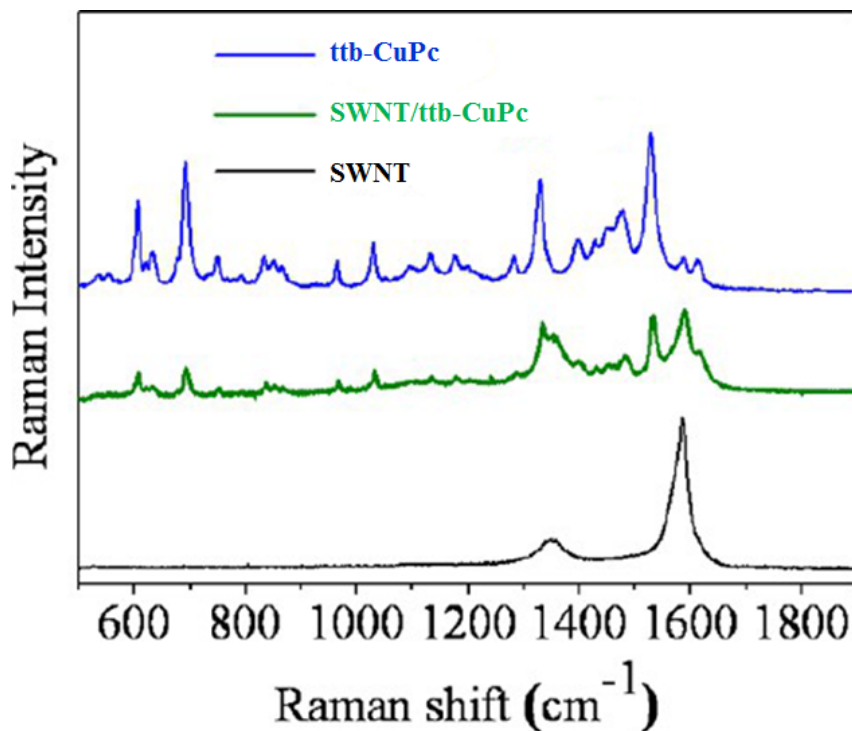


Fig. 6: Intercomparison of Raman spectra of ttb-CuPc, SWCNT and ttb-CuPc/SWCNT hybrid.

2.3.3. Sensing potentialities: case of toluene

The sensing layer previously characterized was tested toward different concentrations of toluene in a range of 60–1200 ppm at room temperature. The improvement in sensing performance of the hybrid layer was further highlighted from the individual constituting materials. The sensor responses towards toluene at different concentrations are depicted in Fig. 7. As shown, sensor exhibited a reversible response at all the studied concentrations. The frequency shifts of the sensor corresponding to 1200 ppm, 430 ppm, 200 ppm and 60 ppm were 100 Hz, 70 Hz, 40 Hz and 30 Hz respectively. Intercomparison of sensitivity of ttb-CuPc, ttb-CuPc/CNT and CNT was made and is shown in Fig. 8 in a toluene concentrations range from 26 to 1000 ppm. The higher sensitivity provided by ttb-CuPc/CNT hybrid material as compared to CNTs and ttb-CuPc considered separately is manifested at all concentrations. As an example, response measured at 430 ppm of toluene on hybrid sensitive layer is three-

times higher than obtained with ttb-CuPc layer and four-times higher than those measured on CNT layer. Based on their sensitivity S toward toluene, the sensing material can be classified as following, $S_{\text{CNT}} < S_{\text{ttb-CuPc}} < S_{\text{hybrid}}$ for all the studied concentrations. The expected higher sensitivity of hybrid is thus confirmed. Hybrid material provides a high number of adsorption site due to macrocycles dispersion onto a large specific surface area as well as extra adsorption sites intrinsic to the nanocarbonaceous matrix. Such preliminary results are encouraging to make a deep study of different metrological characteristics of ttb-CuPc/CNT hybrid towards BTX gases. These sensing properties will be investigated in detail in future.

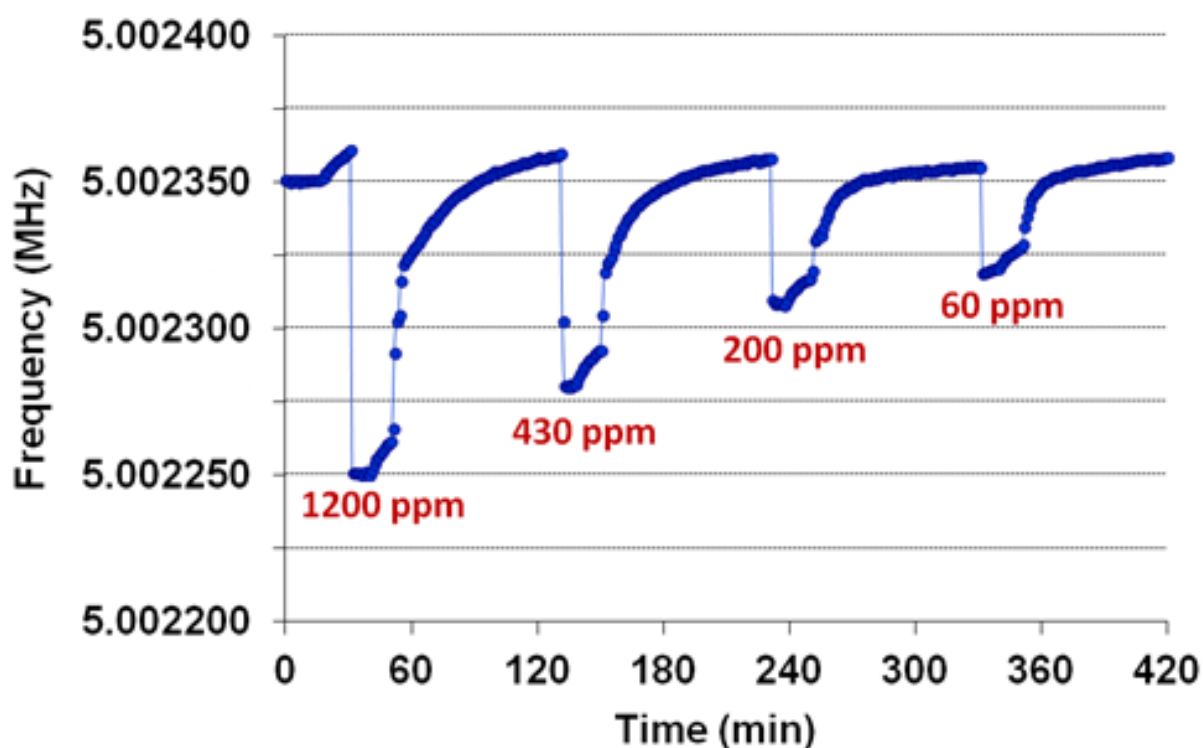


Fig: 7: CNT/ttb-CuPc hybrid based QCM sensor response to toluene at room temperature.

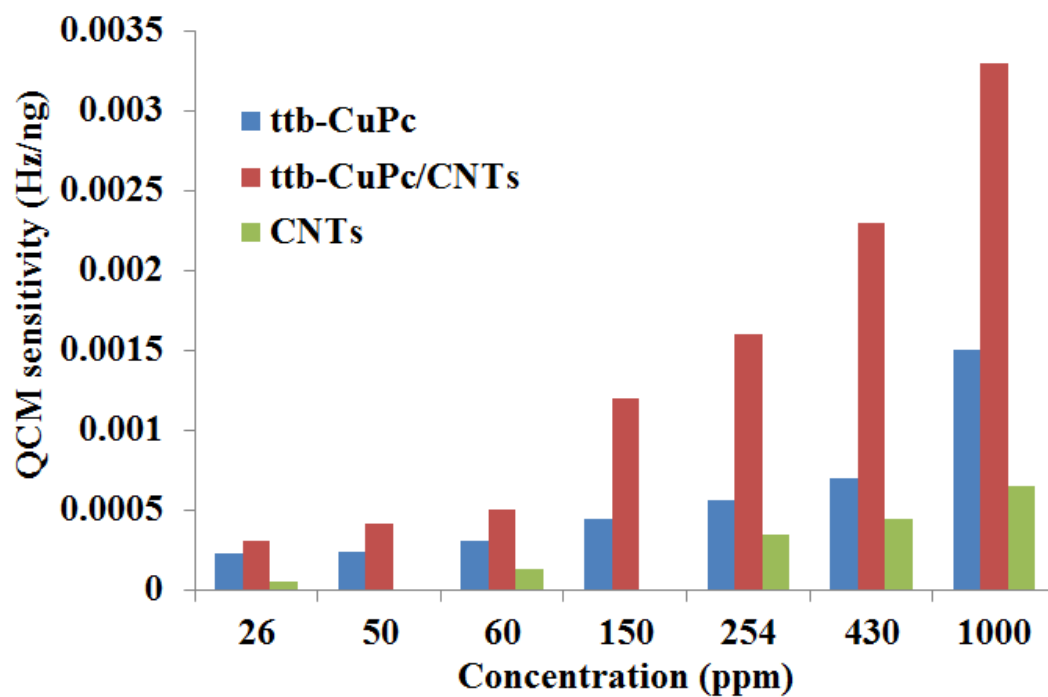


Fig. 8: Intercomparison of responses of QCM based sensors with CNTs, ttb-CuPc and ttb-CuPc/CNTs as sensitive material to toluene at room temperature.

3. Selectivity enhancement: strategy for discriminated measurements of BTX

3.1. Sensing strategy: general description

As previously discussed, the selectivity remains the main drawback of ttb-CuPc-based QCM sensors to achieve the discriminated measurement of each aromatic hydrocarbon. To overcome this problem, our approach consists in the pretreatment of gas sample upstream the sensor through a gas retention matrix to act as either selective chemical filter or a pre-concentrator unit.

In the first case, the sensor-system response will be attributed to the gaseous pollutant(s) which will not be removed from gas sample by the filter. The filtering efficiency will depend on the chemical properties of the material, the specific interactions involved with the different target gases as well as its porosity. To target the filtering selectivity toward a gas rather than another, the nature of the material is crucial. In the second case, the properties of gaseous retention of materials behaving as total BTX filter will be investigated. The material should act as a preconcentrator matrix (gas retention remaining reversible), each trapping pollutants being sequentially released by thermal treatments of material at different temperatures. Sensor localized downstream this preconcentrator unit will ensure the sequential measurements of pollutant concentration desorbed from the gas retention matrix. Such method is inspired by Temperature Programmed Desorption (TPD) process, temperature remaining constant in our case until the complete desorption of each pollutant from the retention matrix. The increase in temperature being step by step, we will speak about Sequential Thermal Desorption method (STD).

3.2.Relevance of TPD for BTX discrimination

Previous studies were reported about the use of TPD as thermal treatment to perform discriminated measurement of BTX concentrations or other VOCs [24-26]. Different gas retention matrix has been implemented and all these studies have highlighted the crucial impact of the pre-concentrating materials on the gas discrimination level reached. Thus, Morris et al. [24] used a commercial available poly-aromatic resin Tenax as a pre-concentrating material to adsorb mixture of gases and subsequent release by TPD. By adopting this method, they were able to measure a reliable and reproducible detection of 0.1 ppb of xylenes with 40 minutes as sampling time. Camara et al. reported micro-machined porous silicon filled with SWCNT based pre-concentrator unit applied for TPD of benzene [27]. Selective detection of 250 ppb benzene in humidity condition was shown. C. Pijolat et al. shown a similar approach in which gas pre-concentration was achieved by a silicon micro-machined pre-concentrator filled with 0.30 mg of commercial activated charcoal powder [28]. They demonstrated the selective detection of 1.3 ppm of benzene. F. Zheng et al. proposed a carbon nanotubes based pre-concentrator for discrimination of organic vapors including toluene vapors at 1300 ppm [29]. F. Bender et al. proposed a SAW micro-sensor integrated with a pre-concentrator unit for sub-ppm detection of BTX [30]. Adsorbing material in the preconcentrator unit was Tenax TA and signal discrimination was achieved by principle component analysis method with detection limit of 400 ppb, 114 ppb and 32 ppb for benzene, toluene and xylenes respectively.

3.3.Ongoing activities and expected results

As gas retention material, our attention is focused on the use of nanocarbonaceous matrix which physical (porosity, specific surface area) and chemical properties could be

modulated to interact more or less specifically with the mono-aromatic hydrocarbons considered. Firstly, to benefit from physical filtering properties, different nanocarbons with various pore sizes will be considered. Moreover, to modulate their filtering efficiency, fluorination treatments are planned. Indeed, recent work clearly established that the grafting of fluorine atoms on the pore surface provide a decrease in porous volume as well as in specific surface area. Thus, filtering potentialities of raw and fluorinated nanocarbonaceous matrix toward BTX will be determined. Materials exhibiting partial removal of BTX molecules from air sample will be then implemented upstream ttb-CuPc based QCM sensor and the selectivity of such sensor-system towards BTX will be assessed.

If the previous investigated materials act as strong diffusion barriers leading to the total obstruction of BTX molecules, the adsorption/desorption capability of such nanocarbons as well as their potentialities as pre-concentrating materials will be determined. If the desorption of BTX molecules from nanocarbons commonly occurs at high temperature (several hundred degrees Celsius), lower temperatures of desorption could be obtained consecutively to a moderated fluorination of these carbonaceous materials. Indeed, a decrease in the interaction forces involved between the carbonaceous matrix and the adsorbed aromatic hydrocarbons is expected, that should result in lower temperatures of BTX desorption than those measured on raw nanocarbons. Moreover, if each monoaromatic hydrocarbon desorbed at discriminated temperatures from the material, their selective quantification by the sensor should be possible without the use of chromatographic column but by sequential thermo-desorption. The expected response of sensor in such experimental conditions with our methodology can be illustrated by Fig.9. The proposed strategy remains easily embeddable in anticipation of the further development of a portable unit.

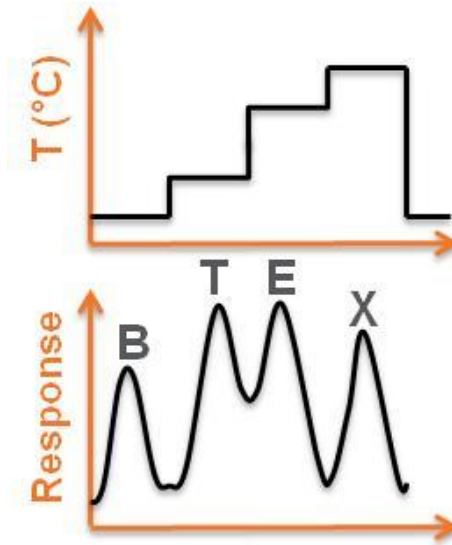


Fig.9: Hypothetical sensor response towards BTEX for sequential thermo-desorption of pollutant from pre-concentrating material.

Works on such scientific approach for selectivity enhancement are currently in progress in collaboration with the Institute of Chemistry from Clermont-Ferrand (ICCF) and the Institute of Science of Material of Mulhouse (IS2M) through an exploratory multidisciplinary project granted in 2015 by the CNRS.

References

1. Iijima, S., *Helical microtubules of graphitic carbon*. *Nature*, 1991. **354**(6348): p. 56-58.
2. Hirsch, A., *Functionalization of Single-Walled Carbon Nanotubes*. *Angewandte Chemie International Edition*, 2002. **41**(11): p. 1853-1859.
3. Dresselhaus, S., G. Dresselhaus, and P. Avouris, *Carbon Nanotubes: Synthesis, Structure, Properties, and Applications*. 2001: Springer.
4. Yamabe, T., et al., *The Science and Technology of Carbon Nanotubes*. 1999: Elsevier Science.
5. Bettinger, H.F., *Carbon Nanotubes—Basic Concepts and Physical Properties*. *ChemPhysChem*, 2004. **5**(12): p. 1914-1915.
6. Jorio, A., G. Dresselhaus, and M.S. Dresselhaus, *Carbon Nanotubes: Advanced Topics in the Synthesis, Structure, Properties and Applications*. 2007: Springer Berlin Heidelberg.
7. Saito, R., G. Dresselhaus, and S. Dresselhaus, *Physical Properties of Carbon Nanotubes*. 1998: Imperial College Press.
8. Meyyappan, M., *Carbon Nanotubes: Science and Applications*. 2004: Taylor & Francis.
9. Dresselhaus, M.S., et al., *Carbon fibers based on C₆₀ and their symmetry*. *Physical Review B*, 1992. **45**(11): p. 6234-6242.
10. Avouris, P., *Molecular Electronics with Carbon Nanotubes*. *Accounts of Chemical Research*, 2002. **35**(12): p. 1026-1034.
11. Girifalco, L.A., et al., *Carbon nanotubes, buckyballs, ropes, and a universal graphitic potential*. *Physical Review B*, 2000. **62**(19): p. 13104-13110.

12. Britz, D.A., et al., *Noncovalent interactions of molecules with single walled carbon nanotubes*. Chemical Society Reviews, 2006. **35**(7): p. 637-659.
13. Bilalis, P., et al., *Non-covalent functionalization of carbon nanotubes with polymers*. RSC Advances, 2014. **4**(6): p. 2911-2934.
14. Eswaramoorthy, M., et al., *A study of micropores in single-walled carbon nanotubes by the adsorption of gases and vapors*. Chemical Physics Letters, 1999. **304**(3–4): p. 207-210.
15. Wang, B., et al., *Copper phthalocyanine noncovalent functionalized single-walled carbon nanotube with enhanced NH₃ sensing performance*. Sensors and Actuators B: Chemical, 2014. **190**: p. 157-164.
16. Banimuslem, H., et al., *Copper phthalocyanine/single walled carbon nanotubes hybrid thin films for pentachlorophenol detection*. Sensors and Actuators B: Chemical, 2014. **190**: p. 990-998.
17. Correa, J.D., et al., *Optical response of carbon nanotubes functionalized with (free-base, Zn) porphyrins, and phthalocyanines: A DFT study*. Physical Review B, 2012. **86**(12): p. 125417.
18. Ndiaye, A., et al., *Noncovalent Functionalization of Single-Wall Carbon Nanotubes for the Elaboration of Gas Sensor Dedicated to BTX Type Gases: The Case of Toluene*. The Journal of Physical Chemistry C, 2013. **117**(39): p. 20217-20228.
19. Xu, H.-B., et al., *A novel donor–acceptor heterojunction from single-walled carbon nanotubes functionalized by erbium bisphthalocyanine*. Materials Chemistry and Physics, 2005. **94**(2–3): p. 342-346.
20. Graupner, R., *Raman spectroscopy of covalently functionalized single-wall carbon nanotubes*. Journal of Raman Spectroscopy, 2007. **38**(6): p. 673-683.

21. Demmin, R.A., et al., *Design parameters for temperature-programmed desorption from a packed bed*. Journal of Catalysis, 1984. **90**(1): p. 32-39.
22. Gorte, R.J., *Design parameters for temperature programmed desorption from porous catalysts*. Journal of Catalysis, 1982. **75**(1): p. 164-174.
23. Redhead, P.A., *Thermal desorption of gases*. Vacuum, 1962. **12**(4): p. 203-211.
24. Ljubov, M., et al., *Simple system for part-per-billion-level volatile organic compound analysis in groundwater and urban air*. Measurement Science and Technology, 2002. **13**(4): p. 603.
25. Brigo, L., et al., *Silver Nanoprism Arrays Coupled to Functional Hybrid Films for Localized Surface Plasmon Resonance-Based Detection of Aromatic Hydrocarbons*. ACS Applied Materials & Interfaces, 2014. **6**(10): p. 7773-7781.
26. Raimo A. Ketola, J.T.K., et al., *Detection of volatile organic compounds by temperature-programmed desorption combined with mass spectrometry and Fourier transform infrared spectroscopy*. Analytica Chimica Acta, 2006. **562**(2): p. 245.
27. Camara, E.H.M., et al. *A micro gas preconcentrator with improved performances for environmental monitoring*. in *Solid-State Sensors, Actuators and Microsystems Conference, 2009, IEEE*, p: 983-986.
28. Pijolat, C., et al., *Application of carbon nano-powders for a gas micro-preconcentrator*. Sensors and Actuators B: Chemical, 2007. **127**(1): p. 179-185.
29. Zheng, F., et al., *Single-Walled Carbon Nanotube Paper as a Sorbent for Organic Vapor Preconcentration*. Analytical Chemistry, 2006. **78**(7): p. 2442-2446.
30. Bender, F., et al., *Development of a preconcentration unit for a SAW sensor micro array and its use for indoor air quality monitoring*. Sensors and Actuators B: Chemical, 2003. **93**(1-3): p. 135-141.

Conclusion

Conclusion

The aim of this PhD thesis has been to develop a sensor microsystem especially dedicated to measurement of BTX concentration in atmosphere. Taking into account the physical and chemical properties of the target pollutant, sensing device based on organic macromolecular materials, phthalocyanines, associated to acoustic transducer, QCM, was developed to fulfill these objectives. Although sensor development and validation were the main goals of this work, investigations on the properties of layered samples through different characterization methods, the better understanding of interaction mechanisms involved between gases and materials and the formalization of the sensing mechanisms occurring at macroscopic and microscopic scale were also the final objectives.

The scientific objectives defined during this PhD thesis were achieved through many experimental involvements. The development of a sensor testing platform at Institut Pascal designed to sensor calibration under BTX vapor at room temperature was an important issue. Thus, a home-made test bench able to generate BTX vapors as low as 1 ppm and with synchronous acquisition of frequency with low signal noise level was especially developed. Despite the thermal stability of QCM claimed by the manufacturer, we have established that even low temperature variations in the sensor exposure chamber results in sensor signal drifts. To remove the contribution of thermal fluctuations on sensor response, a systematic temperature correction on each measured QCM frequency was systematically achieved. Using this approach surrounding temperature variations influence on sensor signal has been compensated by more than 70 %.

The establishment of the most relevant material leading to optimum sensing performances was the key point of this work. This was achieved through a systematic study on three different types of phthalocyanine: unsubstituted mono-macrocyclic, substituted

mono-macrocyclic and unsubstituted double-decker metallophthalocyanines. All QCM devices layered with these materials were tested towards BTX gases to assess their potentialities. Considered as a critical point, the structural stability of metallophthalocyanines substituted by bulky ligands during layering process was firstly confirmed by the similar positions of FT-IR peaks determined for powdered and layered materials.

QCM sensors characteristics are strongly different and depend on the type of phthalocyanines materials. If unsubstituted metallophthalocyanines associated to QCMs exhibit low magnitude as well as slow kinetics of response, high magnitude and fast kinetics of responses were highlighted for tert-butyl substituted mono-macrocyclic and double-decker metallophthalocyanines. In contrast, fluoro-substituted mono-macrocyclic phthalocyanines based QCM were found insensitive to BTX gases. Such variations in sensitivity were justified by i) the difference in macrocycle organizations into the layers as established by XRD and SEM characterizations and ii) aromatic interactions between phthalocyanines and BTX species. Studies made on the effect of layer thickness on sensor response revealed a predominant gas molecules adsorption localized at the surface of unsubstituted metallophthalocyanine layers whereas adsorption of BTX occurs in the entire volume of tetra tert-butyl metallophthalocyanines layers. Interactions between phthalocyanine macrocycles and BTX molecules were caused by non-covalent forces and known as aromatic interactions. The higher magnitude and faster kinetics of sensor response observed with tetra tert-butyl substituted metallophthalocyanines as compared to unsubstituted ones was correlated to the enhancement of dispersion forces involved in aromatic interactions. However, LuPc₂ and fluoro-substituted metallophthalocyanines based sensors responses are dominated by electrostatic forces based aromatic interactions.

From this systematic study, tert-butyl substituted metallophthalocyanines were identified as the best materials for sensor development dedicated to BTX detection as justified

by their high magnitude and fast kinetics of response. Although LuPc₂ exhibited slightly higher magnitude of QCM response, its slow kinetics and commercial non-availability are the main drawbacks. Therefore, ttb-CuPc was chosen as appropriate sensing material and deep assessment of sensors metrological characteristics have been performed. Among various metrological performances, reversibility, kinetics, repeatability, resolution, limit of detection, threshold and selectivity were especially quantified. ttb-CuPc based QCM sensors have exhibited an easy and fast reversibility at room temperature, response magnitude in the order of xylenes > toluene > benzene and a stable baseline signal for intermediate-period (36 hours) of continuous operation. Kinetics of response was determined from response and recovery times of sensors which were close to few minutes. Sensors exhibited a high repeatability and reproducibility illustrated by the negligible effects of gas-exposure history on response observed in the 30–500 ppm range. A resolution higher than 10 ppm and a detection limit lower than 1 ppm have been experimentally established. Cross-sensitivity measurements for common atmospheric pollutants showed the sensor insensitive to NO₂, CO and H₂S while ozone causes an irreversible destructuring of the sensing layer which could be prevented by the implementation of an indigo filter upstream the sensor.

Interactions of BTX gases on the sensing layers have been interpreted considering gas molecules adsorption on active interaction sites assisted by fast diffusion. Calibration curve of sensor toward toluene was precisely fitted by a two-step Langmuir-Henry adsorption model. At the lowest gas concentrations (< 200 ppm), gas molecules mainly adsorb on specific adsorption sites that can be described by Langmuir isotherm of adsorption while at the highest concentration (> 200 ppm), mainly non-specific Henry adsorption takes place. According to SEM pictures and intercomparison of sensor responses versus layer thickness, the easy diffusion of BTX molecules into the volume is highly probable. The higher linear dependence of ttb-CuPc based sensor response with layer thickness suggests that the diffused molecules of

BTX can reach adsorption sites distributed into the whole volume of the sensing layer. In contrast, the response of CuPc based sensors remaining constant whatever the layer thickness greater than 100 nm, the diffused gaseous pollutants not lead to adsorption, this remaining localized at the surface. At last, slow ageing of sensing layer was observed for sensors in continuous operation as well as stored in atmospheric air. Such effects can be prevented by the storage of sensors under nitrogen before their use.

If a partial selectivity was experimentally observed, discriminated measurements of benzene, toluene and xylenes are unsatisfied. This remains a real challenge to overcome. The development of selective retention matrix localized upstream the sensing devices in the fluid circuit could be a way of improvement. These works on this metrological problematics are in progress.

Résumé

Ce travail de thèse est consacré à enquêter sur les potentialités des matériaux de phtalocyanines de réaliser un capteur à microbalance à cristal de quartz (QCM) pour le benzène, toluène et les xylènes (BTX) la détection dans l'air. L'objectif est de développer un capteur microsystème capable de mesurer des concentrations BTX quantitativement ci-dessous les directives environnementales avec une précision suffisante. Pour atteindre ces objectifs, nos stratégies axées principalement sur des œuvres expérimentales englobant capteurs réalisation, caractérisation des matériaux de détection, développement des installations de gaz-test et le test de capteur pour différents gaz cibles. L'un des principaux objectifs est d'identifier le matériel de phtalocyanine le plus approprié pour le développement des capteurs. Après des études comparatives de détection, dispositif de QCM à base de phtalocyanine de tert-butyle et de cuivre se trouve que les caractéristiques métrologiques les plus sensibles et de détail sont encore étudiées. Les résultats montrent l'ampleur reproductible, réversible et de réponse élevé, les temps de réponse et de récupération faible, limite de détection de gamme sous-ppm, de hautes résolutions et la sélectivité combinée de gaz BTX chez les polluants atmosphériques communs. Une attention particulière est accordée à comprendre les interactions gaz / matérielles qui sont atteints par (a) XRD et MEB caractérisations de couches de détection, (b) la formalisation d'un modèle d'adsorption en deux étapes et (c) d'évaluer l'étendue de la diffusion de gaz cible dans la détection couche. Enfin, possible vieillissement de capteurs et de stockage approprié des conditions pour éviter un tel effet sont étudiés.

Summary

This PhD work is dedicated to investigate potentialities of phthalocyanines materials to realize a Quartz Crystal Microbalance (QCM) sensor for Benzene, Toluene and Xylenes (BTX) detection in air. The goal is to develop a sensor-microsystem capable of measuring BTX concentrations quantitatively below the environmental guidelines with sufficient accuracy. To achieve these objectives, our strategies mainly focused on experimental works encompassing sensors realization, sensing material characterizations, development of gas-testing facility and sensor testing for different target gases. One of the main aims is to identify most appropriate phthalocyanine material for sensor development. After comparative sensing studies, tert-butyl-copper phthalocyanine based QCM device is found as most sensitive and detail metrological characteristics are further investigated. Results show repeatable, reversible and high magnitude of response, low response and recovery times, sub-ppm range detection limit, high resolutions and combined selectivity of BTX gases among common atmospheric pollutants. Special focus is given to understand the gas/material interactions which are achieved by (a) XRD and SEM characterizations of sensing layers, (b) formalization of a two-step adsorption model and (c) assessing extent of diffusion of target gas in sensing layer. At last, possible ageing of sensor and suitable storage conditions to prevent such effect are investigated.

Key-words: Gas sensors, Microsystems, Organic macromolecular materials, phthalocyanines, QCM sensors, Air quality control, aromatic interactions